Lauma Laipniece

DENDRONIZĒTU NELINEĀRI OPTISKO AZOHROMOFORU SINTĒZE UN PĒTĪJUMI

Promocijas darbs

SYNTHESIS AND STUDIES OF DENDRONIZED NONLINEAR OPTICAL AZOCHROMOPHORES

Doctoral Thesis

RĪGAS TEHNISKĀ UNIVERSITĀTE
Materiālzinātnes un lietišķās ķīmijas fakultāte
Lietišķās ķīmijas institūts

RIGA TECHNICAL UNIVERSITY
Faculty of Materials Science and Applied Chemistry
Institute of Applied Chemistry

Lauma Laipniece
Doktora studiju programmas "Ķīmija" doktorante
Doctoral Student of the Study Programme "Chemistry"

DENDRONIZĒTU NELINEĀRI OPTISKO AZOHROMOFORU SINTĒZE UN PĒTĪJUMI
Promocijas darbs

SYNTHESIS AND STUDIES OF DENDRONIZED NONLINEAR OPTICAL AZOCHROMOPHORES
Doctoral Thesis

Zinātniskais vadītājs / Scientific supervisor
profesors *Dr. habil. chem.* / Professor *Dr. habil. chem.*
VALDIS KAMPARS

Zinātniskais vadītājs / Scientific supervisor
profesors *Dr. chem.* / Professor *Dr. chem.*
VALDIS KOKARS

NATIONAL DEVELOPMENT PLAN 2020

EUROPEAN UNION
European Social Fund

INVESTING IN YOUR FUTURE

PROMOCIJAS DARBS IZVIRZĪTS ZINĀTNES DOKTORA GRĀDA IEGŪŠANAI RĪGAS TEHNISKAJĀ UNIVERSITĀTĒ

Promocijas darbs zinātnes doktora (*Ph. D.*) grāda iegūšanai tiek publiski aizstāvēts 2023. gada 18. maijā plkst. 14 Rīgas Tehniskās universitātes Materiālzinātnes un lietišķās ķīmijas fakultātē, Paula Valdena ielā 3 272. auditorijā.

OFICIĀLIE RECENZENTI

Profesors *Dr. chem.* Māris Turks,
Rīgas Tehniskā universitāte

Vadošais pētnieks *Dr. phys.* Aivars Vembris,
Latvijas Universitātes Cietvielu fizikas institūts, Latvija

Vadošā pētniece *Dr. chem.* Aiva Plotniece,
Latvijas Organiskās sintēzes institūts, Latvija

APSTIPRINĀJUMS

Apstiprinu, ka esmu izstrādājusi šo promocijas darbu, kas iesniegts izskatīšanai Rīgas Tehniskajā universitātē zinātnes doktora (*Ph. D.*) grāda iegūšanai. Promocijas darbs zinātniskā grāda iegūšanai nav iesniegts nevienā citā universitātē.

Lauma Laipniece ....
                           (*paraksts*)
Datums: ....

Promocijas darbs ir sagatavots kā tematiski vienotu zinātnisko publikāciju kopa ar kopsavilkumu latviešu un angļu valodā. Promocijas darbs ietver četrus rakstus, kas publicēti zinātniskajos žurnālos, un divas publikācijas konferenču ziņojumu izdevumos (*proceedings*). Raksti zinātniskajos žurnālos, kā arī publikācijas konferenču ziņojumu izdevumos ir angļu valodā, to kopējais apjoms, ieskaitot pielikumus, ir 72 lpp.

SATURS

1. pielikums: L. Laipniece, V. Kampars, S. Belyakov, A. Bundulis, A. Tokmakovs, M. Rutkis. Utilization of amorphous phase forming trityl groups and Ar-Ar^F interactions in synthesis of NLO active azochromophores. *Dyes Pigm.*, **2022**, *204*, 110395.

2. pielikums: L. Laipniece, V. Kampars, S. Belyakov, A. Tokmakovs, E. Nitiss, M. Rutkis. Dendronized azochromophores with aromatic and perfluoroaromatic fragments: Synthesis and properties demonstrating Ar-Ar^F interactions. *Dyes Pigm.*, **2019**, *162*, 394–404.

3. pielikums: L. Laipniece, V. Kampars. Synthesis and Thermal Properties of Azobenzene Core Polyester Dendrimers with Trityl Groups at the Periphery. *Key Eng. Mater.*, **2018**, *762*, 171–175.

4. pielikums: L. Laipniece, V. Kampars. Synthesis, thermal and light absorption properties of push-pull azochromophores substituted with dendronizing phenyl and perfluorophenyl fragments. *Main Group Chem.*, **2015**, *14*, 43–58.

5. pielikums: K. Traskovskis, E. Zarins, L. Laipniece, A. Tokmakovs, V. Kokars, M. Rutkis. Structure-dependent tuning of electro-optic and thermoplastic properties in triphenyl groups containing molecular glasses. *Mat. Chem. Phys.*, **2015**, *155*, 232–240.

6. pielikums: A. Tokmakovs, M. Rutkis, K. Traskovskis, E. Zariņš, L. Laipniece, V. Kokars, V. Kampars. Nonlinear Optical Properties of Low Molecular Organic Glasses Formed by Triphenyl Modified Chromophores. *IOP Conference Series: Materials Science and Engineering*, **2012**, *38*, 012034.

LIETOTIE SAĪSINĀJUMI

ε	molārais ekstinkcijas koeficients
λ_{max}	absorbcijas maksimuma viļņa garums
AEŠH	augsti efektīvā šķidrumu hromatogrāfija
Ar-Ar^F	aromātiskie-perfluoraromātiskie fragmenti
d_{31}	nelineāri optiskais koeficients, kas noteikts, mērot otrās harmonikas ģenerācijas intensitāti p polarizētai gaismai, apstarojot paraugu ar s polarizētu gaismu
d_{33}	nelineāri optiskais koeficients, kas noteikts, mērot otrās harmonikas ģenerācijas intensitāti p polarizētai gaismai, apstarojot paraugu ar p polarizētu gaismu
$d_{33}(0)$	nelineāri optiskais koeficients d_{33} ekstrapolēts uz nulles frekvenci
DBU	1,8-diazabiciklo[5.4.0]undec-7-ēns
DCC	*N,N′*-dicikloheksilkarbodiimīds
DCM	dihlormetāns
DIAD	diizopropilazodikarboksilāts
DIPEA	diizopropiletilamīns
DMAP	4-(dimetilamino)piridīns
DMF	*N,N*-dimetilformamīds
DMSO	dimetilsulfoksīds
DSC	diferenciālā skenējošā kalorimetrija
EtOBz	etilbenzoāts
IPB	1,3-diokso-2-(piridīnij-1-il)-2,3-dihidro-1*H*-indēn-2-īds jeb 1,3-indāndionil-piridīnija betaīns
KMR	kodolu magnētiskā rezonanse
Ms	metānsulfonil- jeb mezil-
MS	masspektrometrija
n_{1064} un n_{532}	gaismas laušanas koeficienti norādītajā gaismas viļņa garumā
NLO	nelineārā optika / nelineāri optisks
PPTS	piridīnija p-toluolsulfonāts
SHI	otrās harmonikas ģenerācijas intensitāte
S_NAr	nukleofīlā aromātiskā aizvietošana
TBAB	tetrabutilamonija bromīds
THF	tetrahidrofurāns
THP	tetrahidro-2*H*-pirān-2-il-
Trt	trifenilmetil- jeb tritil-
T_d	termiskā stabilitāte – temperatūra, kad termogravimetriskajā analīzē parauga masa samazinājusies par 5 %
T_g	stiklošanās temperatūra
$T_{kuš}$	kušanas temperatūra
TGA	termogravimetriskā analīze
T_{SHI50}	temperatūra, pie kuras, paraugu sildot, SHI samazinās par 50 % no sākotnējās intensitātes

PROMOCIJAS DARBA VISPĀRĒJS RAKSTUROJUMS

Tēmas aktualitāte

Organisko nelineāri optisko (NLO) hromoforu sintēze un uz to bāzes veidoto materiālu īpašības pieder vienam no modernākajiem pētījumu virzieniem – elektrooptisko materiālu un informācijas nesēju izstrādei komunikāciju un fotonikas nozarēs. Jauni organiskie NLO materiāli, arī uz azohromoforu bāzes izstrādātie, ļautu izveidot vēl efektīvākas informācijas tehnoloģiju iekārtas, piemēram, elektooptiskos modulatorus, kas varētu būt potenciāli labāki par pašlaik esošajām šāda veida iekārtām uz neorganisko materiālu bāzes [1–3]. Organisko NLO materiālu galvenā sastāvdaļa ir polāra hromofora fragments, kas kovalenti saistīts polimēra virknē vai molekulāra hromofora veidā ir dopēts polimērā. Tas var būt arī kovalenti saistīts dendrimērā vai veidot organiskos molekulāros stiklus – cietus amorfus materiālus, kas veidoti no viena organiskā savienojuma molekulām. Polārais hromofors ir molekula vai tās daļa, ko veido elektronu donors un elektronu akceptors fragments, kas ar konjugētu π elektronu tiltiņu ir savstarpēji kovalenti saistīti, jeb D–π–A tipa hromofors, dēvēts arī par *push-pull* hromoforu. Organiskos NLO hromoforus var modificēt, lai panāktu uz to bāzes izgatavoto materiālu vieglāku apstrādi un nodrošinātu atbilstību piecām galvenajām prasībām: vairākas reizes augstāki NLO koeficienti nekā neorganiskajiem materiāliem, lieli gaismas laušanas koeficienti, lieliska optiskā caurlaidība, ilglaicīga necentrosimetriski orientēto dipolu stabilitāte un augsta fotoķīmiskā stabilitāte ierīces lietošanas apstākļos [1, 4, 5].

Otrās kārtas NLO efekts ir novērojams tikai materiālam ar necentrosimetriski orientētiem hromofora dipoliem, ko visbiežāk panāk, iedarbojoties uz materiālu ar optisko vai elektrisko lauku. Tomēr D–π–A tipa hromoforiem visbiežāk ir lieli dipolmomenti, un notiek dipolu relaksācija centrosimetriska sakārtojuma virzienā, samazinot vai dzēšot NLO efektu [1, 6]. Tādējādi, lai saglabātu polāro kārtību, amorfajam NLO materiālam ir jābūt ar pēc iespējas augstāku stiklošanās temperatūru (T_g), hromofori ir jāizolē cits no cita, lai samazinātu elektrisko dipolu atgrūšanos [1, 6], vai arī jāizmanto piemērotas starpmolekulāras mijiedarbības starp molekulu fragmentiem, lai iesaldētu hromoforu savstarpējo novietojumu pēc orientēšanas [1]. Cits šo moderno materiālu NLO koeficienta paaugstināšanas ceļš ir tādu NLO hromoforu veidošana, kuru summārie dipolmomenti nebūtu lieli pat pie ļoti augstiem hiperpolarizējamības raksturojumiem, ko var panākt, izmantojot divus hromoforus ar pretēji vērstiem fragmentu dipolmomentu vektoriem, bet vienādi vērstiem hiperpolarizējamības vektoriem. Šis ceļš var efektīvi samazināt visas molekulas dipolmomentu, molekulu atgrūšanos un tieksmi veidot centrosimetriski orientētas struktūras amorfā organiskā molekulārā stikla fāzē [7, 8].

Zināms, ka molekulu perfluoraromātiskie fragmenti spēcīgi mijiedarbojas ar aromātiskajiem fragmentiem kristālos, šķidrajos kristālos, supramolekulārajās nanošķiedrās, hidrogēlos un pat šķīdumos [9]. Aromātisko-perfluoraromātisko (Ar-Ar^F) fragmentu mijiedarbību var izmantot, lai iegūtu necentrosimetriski sakārtotas amorfas struktūras pēc orientēšanas un līdz ar to palielinātu to NLO īpašības [1, 4, 6, 10–13]. Dendrimēra un dendrona sintēzi izmanto, lai iegūtu struktūras ar telpiski izolētu hromoforu, kam piemīt liels dipolmoments, un uzlabotu materiāla termiskās īpašības [1, 4, 14, 15]. 1,2-Difenildiazēna jeb

azobenzola atvasinājumus ar dendroniem un dendrimēriem var kovalenti saistīt savā starpā dažādos veidos [16]: azobenzola fragmentu var kovalenti iekļaut dendrona vai dendrimēra kodolā, perifērijā vai viscaur dendrimēra zarojumā. Ar-Ar[F] mijiedarbību izmantošanu un dendronu ievadīšanu molekulā var summēt, izmantojot dendronus ar aromātisko un pentafluorfenilfragmentu, lai palielinātu organisko molekulāro stiklu NLO koeficientus un orientācijas stabilitāti [10–12].

NLO īpašības vairumā gadījumu ir pētītas dendrimēriem, kas satur D–π–A tipa azobenzola fragmentus visā dendrimēra zarojumā [17–21]. Apjomīgi pētījumi par D–π–A tipa azobenzola NLO dendrimēriem veikti profesora *Zhen Li* grupā [6, 13, 15, 22–33]. Viņi arī konstatējuši NLO īpašību pastiprināšanos azobenzola dendronos un dendrimēros, izmantojot Ar-Ar[F] mijiedarbības [13, 24–26]. D–π–A tipa azohromoforus saturoši NLO materiāli iepriekš nav pētīti, ja hromofors ir kovalenti saistīts dendrimēra vai dendrona kodolā.

Pētījuma mērķis un uzdevumi

Promocijas darba mērķis ir iegūt un raksturot jaunus, dendronizētus, organiskajiem NLO materiāliem izmantojamus D–π–A tipa azohromoforu atvasinājumus, izmantojot dendrona fragmentus ar apjomīgiem aromātiskiem un/vai perfluoraromātiskiem fragmentiem. Papildu mērķis ir sasniegt atbilstošas materiāla īpašības – stiklošanās temperatūru virs 100 °C [5] un NLO koeficienta d_{33} vērtību virs 25,2 pm·V^{-1}, kas pārspētu visefektīvāko no četriem visbiežāk lietotajiem neorganiskajiem kristāliem LiNbO$_3$ [34].

Darba mērķa īstenošanai definēti šādi uzdevumi:

1) veikt struktūras dizainu un sintezēt dendronizētus vienu vai vairākus azobenzola fragmentus saturošus savienojumus, kam piemīt organisko molekulāro stiklu īpašības;

2) raksturot sintezēto savienojumu un materiālu termiskās, optiskās un NLO īpašības;

3) izzināt sakarības starp sintezēto savienojumu ķīmisko struktūru un to fizikālajām īpašībām, akcentējot NLO īpašības.

Zinātniskā novitāte un galvenie rezultāti

Promocijas darbā izstrādātas trīs pieejas D–π–A tipa azohromoforu saturošu organisko NLO materiālu sintēzei. Pirmkārt, iegūti azobenzola kodola dendrimēri, no kuriem veidotajos NLO materiālos azohromoforu fragmenti cits no cita ir atdalīti ar dendrimēra zarojumu, nepieļaujot centrosimetrisko hromofora sakārtošanos pēc tā orientēšanas elektriskajā laukā. Otrkārt, izmantota fenilgrupas un pentafluorfenilgrupas saturošo dendronizējošo fragmentu Ar-Ar[F] mijiedarbība, lai stabilizētu amorfo fāzi organiskajam molekulārajam stiklam pēc tā hromoforu orientēšanas elektriskajā laukā. Treškārt, veikta vairāku kovalenti saistītu hromoforu saturoša organiskā molekulārā stikla summārā dipolmomenta samazināšana, vienlaikus palielinot molekulāro hiperpolarizējamību.

Promocijas darbā aprakstīti jauni dendronizēti hromofori, kuru sintēzē izmantoti 4-amino-4′-nitroazobenzols un 3,5-bis(2-hidroksietoksi)benzoskābes vai 3,5-dibenziloksibenzoskābes esteri un to atvasinājumi kā dendronizējošie fragmenti. Sintezēto savienojumu struktūrās

iekļautas arī telpiski apjomīgās tritilgrupas, kas veicina cietas amorfās fāzes veidošanu vienkomponenta organiskajam molekulārajam stiklam. Sintezēti azobenzola atvasinājumi ar vienu vai vairākām pentafluorfenilgrupām, kas spēj veidot iekšmolekulārus vai starpmolekulārus kompleksus ar aromātiskajiem fragmentiem, stabilizējot necentrosimetrisko kārtību pēc molekulu orientēšanas elektriskajā laukā un paaugstinot NLO parametrus. Ar rentgenstruktūranalīzes metodi pirmo reizi parādīta iekšmolekulāra Ar-Ar^F mijiedarbība liela dendronizēta NLO aktīva azohromofora kristālā, novērojama pentafluorfenilgrupas sadarbība ar azobenzola fragmentu. Pentafluorfenilfragmentus saturošo savienojumu optiskajās īpašībās novērota Ar-Ar^F mijiedarbība, kas sasaucas ar rentgenstruktūranalīzes rezultātiem. Sintezēti dendroni, kovalenti saistot azohromoforu ar indāndionilpiridīnija betaīnu vai citu azohromoforu ar pretēji vērstiem fragmentu dipolmomentiem.

Noteiktas visu sintezēto savienojumu stiklošanās, kušanas un sadalīšanās temperatūras un raksturota molekulas dendronu fragmentu un gala grupu ietekme uz savienojumu stiklošanās un sadalīšanās temperatūrām. Tika noteiktas sintezēto savienojumu NLO īpašības: NLO koeficienti d_{31} un d_{33}, kas noteikti, mērot otrās harmonikas ģenerācijas intensitāti (*SHI*) p polarizētai gaismai, apstarojot paraugu attiecīgi ar s vai p polarizētu gaismu, un NLO īpašību saglabāšanās, karsējot paraugu. Konstatēts, ka atsevišķu molekulas fragmentu savstarpējas mijiedarbības rezultātā NLO īpašības var tikt gan uzlabotas, ja tiek stabilizēta necentrosimetriskā hromoforu kārtība, gan būtiski pasliktinātas, kad tiek stabilizēta centrosimetriska hromoforu kārtība. Pētīto D–π–A tipa azohromofora fragmentu NLO īpašību un mijiedarbības veicinošo molekulas fragmentu sinerģijas dēļ tika iegūti 15 dendronizēto azohromoforu paraugi, no kuriem astoņu savienojumu paraugiem NLO koeficienti pārsniedz plaši izmantotā LiNbO$_3$ ($d_{33} = 25{,}2$ pm·V^{-1}) vērtību.

Darba struktūra un apjoms

Promocijas darbs sagatavots kā tematiski vienota zinātnisko publikāciju kopa par azobenzolu satorošu dendrimēru sintēzi un struktūras, optisko, termisko un NLO īpašību pētījumiem. Promocijas darbs apkopo sešas oriģinālpublikācijas *SCOPUS* un/vai *Web of Science* indeksētos zinātniskajos žurnālos un konferenču rakstu krājumos.

Darba aprobācija un publikācijas

Promocijas darba rezultāti publicēti čeros zinātniskajos rakstos un divos pilna teksta konferenču rakstos. Pētījumu rezultāti prezentēti 10 konferencēs, piedaloties ar 12 konferenču tēzēm.

Zinātniskās publikācijas
1. **L. Laipniece**, V. Kampars, S. Belyakov, A. Bundulis, A. Tokmakovs, M. Rutkis. Utilization of amorphous phase forming trityl groups and Ar-Ar^F interactions in synthesis of NLO active azochromophores. *Dyes Pigm.*, **2022**, *204*, 110395.

2. **L. Laipniece**, V. Kampars, S. Belyakov, A. Tokmakovs, E. Nitiss, M. Rutkis. Dendronized azochromophores with aromatic and perfluoroaromatic fragments: Synthesis and properties demonstrating Ar-Ar^F interactions. *Dyes Pigm.*, **2019**, *162*, 394–404.

3. **L. Laipniece**, V. Kampars. Synthesis and Thermal Properties of Azobenzene Core Polyester Dendrimers with Trityl Groups at the Periphery. *Key Eng. Mater.*, **2018**, *762*, 171–175.

4. **L. Laipniece**, V. Kampars. Synthesis, thermal and light absorption properties of push-pull azochromophores substituted with dendronizing phenyl and perfluorophenyl fragments. *Main Group Chem.*, **2015**, *14*, 43–58.

5. K. Traskovskis, E. Zarins, **L. Laipniece**, A. Tokmakovs, V. Kokars, M. Rutkis. Structure-dependent tuning of electro-optic and thermoplastic properties in triphenyl groups containing molecular glasses. *Mat. Chem. Phys.*, **2015**, *155*, 232–240.

6. A. Tokmakovs, M. Rutkis, K. Traskovskis, E. Zariņš, **L. Laipniece**, V. Kokars, V. Kampars. Nonlinear Optical Properties of Low Molecular Organic Glasses Formed by Triphenyl Modified Chromophores. *IOP Conference Series: Materials Science and Engineering*, **2012**, *38*, 012034.

Konferenču tēzes, kurās atspoguļoti darba rezultāti

1. **L. Laipniece**, V. Kampars, A. Tokmakovs, A. Bundulis, M. Rutkis. Structurally perfect glassy azobenzene core first generation dendrimer and its non-linear optical properties. In: *Materials Science and Applied Chemistry 2019 Programme and Abstracts book*, Latvia, Riga, 24 October, 2019. Riga: http://msac.rtu.lv/, 2019, pp. 38.

2. **L. Laipniece**, V. Kampars, A. Ozols, P. Augustovs. Synthesis of Dendronized Chromophores and Holographic Recording in the Chromophores Containing Samples. In: *Abstracts of the 32nd Scientific Conference*, Latvia, Riga, 17–19 February, 2016. Riga: Institute of Solid State Physics, University of Latvia, 2016, pp. 120.

3. **L. Laipniece**, V. Kampars. Synthesis of dendronized azobenzene 2,3,4,5,6-pentafluorobenzyl ether. In: *Abstracts of the Riga Technical University 56th International Scientific Conference*, Latvia, Riga, 14–16 October, 2015. Riga: RTU Press, 2015, pp. 18.

4. **L. Laipniece**, V. Kampars. Light Absorption and Thermal Properties of Dendronized Azochromophores with Benzyl and 2,3,4,5,6-Pentafluorobenzyl Fragments. In: *Developments in Optics and Communications 2013, Book of Abstracts*, Latvia, Riga, 10–12 April, 2013. Riga: University of Latvia, 2013, pp. 128–129.

5. Z. Kalniņa, A. Tokmakovs, I. Mihailovs, K. Traskovskis, **L. Laipniece**, M. Rutkis. Thermo-induced non-centrosymmetric crystal growth in glassy thin films of azobenzene chromophore. In: *Book of Abstracts of the 15-th International Conference-School Advanced Materials and Technologies*, Lithuania, Palanga, 27–31 August, 2013. Kaunas: 2013, pp. 117.

6. A. Tokmakovs, M. Rutkis, K. Traskovskis, E. Zarins, **L. Laipniece**, V. Kokars, V. Kampars. Nonlinear optical properties of low molecular organic glasses formed by

triphenyl modified chromophores. In: *Book of abstracts. International conference Functional materials and nanotechnologies 2012 (FM&NT-2012)*, Latvia, Riga, 17–20 April, 2012. Riga: 2012, pp. 196.

7. A. Tokmakovs, M. Rutkis, K. Traskovskis, E. Zarins, **L. Laipniece**, V. Kokars, V. Kampars. Properties of EO Active Molecular Glasses Based on Indandione and Azobenzene Chromophores. In: *Book of Abstracts of the 14-th International Conference-School. Advanced Materials and Technologies*; Lithuania, Palanga, 27–31 August, 2012. Palanga: 2012, pp. 96.

8. V. Kampars, P. Pastors, J. Kreicberga, **L. Laipniece**, I. Neibolte, M. Plotniece, K. Teivena, R. Kampare. Nonlinear Optical Chromophores with 1,3-Indanedione Moiety. In: *Riga Technical University 53rd International Scientific Conference: Dedicated to the 150th Anniversary and the 1st Congress of World Engineers and Riga Polytechnic Institute / RTU Alumni: Digest*; Latvia, Riga, 11–12 October, 2012. Riga: RTU, 2012, pp. 227.

9. **L. Laipniece**, V. Kampars. Azobenzene Core Dendrimers with Trityl Groups in the Periphery. In: *Riga Technical University 53rd International Scientific Conference: Dedicated to the 150th Anniversary and the 1st Congress of World Engineers and Riga Polytechnic Institute / RTU Alumni: Digest*, Latvia, Riga, 11–12 October, 2012. Riga: RTU, 2012, pp. 229.

10. **L. Laipniece**, V. Kampars. Synthesis of Dendronized Azochromophores with Benzyl and 2,3,4,5,6-Pentafluorobenzyl Fragments. In: *Riga Technical University 53rd International Scientific Conference: Dedicated to the 150th Anniversary and the 1st Congress of World Engineers and Riga Polytechnic Institute / RTU Alumni: Digest*, Latvia, Riga, 11–12 October, 2012. Riga: RTU, 2012, pp. 230.

11. **L. Laipniece**, V. Kampars. Synthesis of azobenzene derivatives for research of arene-perfluoroarene interactions. In: *Abstracts of the 52nd International Scientific Conference of Riga Technical University. Section: Material Science and Applied Chemistry*, Latvia, Riga, 13–15 October, 2011. Riga: RTU Publishing House, 2011, pp. 20.

12. V. Kampars, J. Kreicberga, P. Pastors, M. Roze, S. Gaidukovs, K. Balodis, M. Plotniece, J. Sirotkina, **L. Laipniece**, N. Kiričenko, K. Pīterāne, L. Vesjolaja, G. Bērziņa, B. Turovska, I. Muzikante, M. Rutks. Jaunu organisko hromoforu sintēze un to raksturojumi. No: *Apvienotais pasaules latviešu zinātnieku III un Letonikas IV kongress „Zinātne, sabiedrība un nacionālā identitāte". Sekcija „Tehniskās zinātnes". Tēžu krājums;* Latvija, Rīga, 24.–27. oktobris, 2011. Rīga: RTU Izdevniecība, 2011, 90. lpp.

PROMOCIJAS DARBA GALVENIE REZULTĀTI

1. Dendrimēri ar azobenzola kodolu

1.1. Dendrimēru uzbūve un sintēzes paņēmieni

Dendrimēri ir regulāri sazarotas makromolekulas ar skaidri definētu struktūru, kas nosaka molekulas sfērisku, tukšumus saturošu formu un raksturīgas fizikālās īpašības [35]. Dendrimēru iegūst vairākās secīgās reakcijās, lielākā daļa sintēzes paņēmienu saistīti ar pastāvīgu dendrimēra augšanas un funkcionālo grupu nomaiņas reakciju virkni, lai izvairītos no nekontrolējamas polimerizācijas. Dendrimēram ir trīs raksturīgi uzbūves elementi: centrālā daļa jeb kodols (▷), zarojums (✄) un gala grupas jeb periferija (A, B, X, Y, ●) (1. att.) [35]. Viena veida dažāda izmēra dendrimērus iedala paaudzēs *G1*, *G2*, *G3* utt. (angļu val. – *generation*), atbilstošā kontekstā dendrimēra kodols nereti iegūst nulles paaudzes *G0* apzīmējumu. Ir divas klasiskās dendrimēru sintēzes metodes: diverģentā un konverģentā [35, 36].
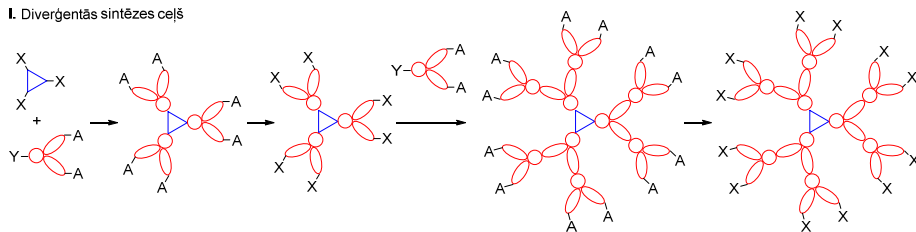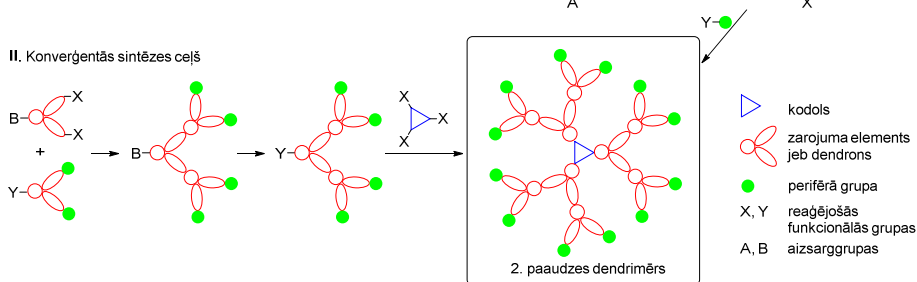
1. att. Shematisks otrās paaudzes (*G2*) dendrimēra struktūras un tā diverģentās (I) un konverģentās (II) sintēzes ceļu attēlojums [35].

Vēsturiski pirmā dendrimēru sintēzē tika izmantota diverģentā metode (1. att. I), kurā molekulu veido, sākot ar kodolu, pēc tam pievienojot vienu kārtu monomēru ar ķīmiski inertām periferijas grupām, ko vēlāk aktivizē nākamās kārtas pievienošanai. Šos divus soļus atkārto [35]. Dendrimēra periferiju var funkcionalizēt ar kādām īpašām funkcionālajām grupām vai struktūrām, ko izvēlas atkarībā no plānotajiem pētījumiem vai lietojuma. Periferо grupu skaits ar katru dendrimēra paaudzi pieaug eksponenciāli, tādēļ potenciāla problēma, nepilnīgi reaģējot periferijas funkcionālajām grupām, ir struktūras defektu parādīšanās lielu paaudžu

dendrimēriem. Turklāt reakcijas veiksmīgai norisei nepieciešamais reaģentu pārākums var apgrūtināt produktu attīrīšanu [37].

Konverģentajā metodē dendrimēra sintēzi sāk ar periferiju un beidz ar kodolu (1. att. II). Ārējos slāņus pakāpeniski savieno, iegūstot sazarotas struktūras, ko dēvē par dendroniem. Kad dendroni sasnieguši izvēlēto paaudzi, tos pievieno piemērotam kodolam un iegūst dizainētās paaudzes dendrimēru [35]. Konverģentajā sintēzē ir maza blakusreakciju varbūtība katrā solī, un dendrona augšanā nepieciešamais reaģējošo grupu skaits ir viegli kontrolējams, tāpēc monodispersu dendrimēru sintēze iespējama ar lielāku precizitāti, jo katrā solī attīrīšana ir vienkāršāka nekā diverģentās sintēzes gadījumā [35, 36]. Konverģentās metodes lielākais trūkums ir stēriska kodola funkcionālās grupas aizsegšana lielākās paaudzēs, kas rada ļoti zemus dendrimēru galaproduktu iznākumus [37].

Konverģentās vai diverģentās sintēzes izmantošanu nosaka izvēlētais dendrimēra zarojuma un sintēzes reakcijas veids, periferijas un kodola funkcionālo grupu stabilitāte un iespējamās blakusreakcijas. Kombinējot un pilnveidojot šīs klasiskās sintēzes stratēģijas, ir radītas arī paātrinātās jeb eksponenciālās lielu dendrimēru sintēzei piemērotas stratēģijas, izmantojot mazāku kopējo reakciju skaitu un iegūstot lielākus iznākumus [36, 38].

1.2. Dendrimēru ar azobenzola kodolu sintēze

Iepriekšējos pētījumos tika sintezēti dendrimēri ar azobenzola kodolu līdz trešajai paaudzei, diverģentās sintēzes ceļā veidojot poliestera zarojumu ar gala hidroksigrupām vai tetrahidropiranilgrupām (THP-grupām) [39]. Iegūtajiem dendrimēriem ar THP-grupām tika noteikta otrās kārtas hiperpolarizējamība šķīdumā [40]. Minētie dendrimēri tika iegūti viskozu vasku veidā, kuru stiklošanās temperatūras ir 15–27 °C [39], un tos nevarēja lietot cietu amorfu kārtiņu veidošanai NLO materiāliem. Tritilgrupu (Trt-grupu) ievadīšana organiskos hromoforus saturošajās molekulās sekmē visa savienojuma spēju veidot cietas amorfas kārtiņas [41], tāpēc tika veikta tādas dendrona zarojumu veidojošās molekulas sintēze, kas periferijā satur Trt-grupas.

Iepriekš tika sintezēti 3,5-bis(2-hidroksietoksi)benzoskābes atvasinājumi **3a** ar THP-aizsarggrupām [39] (2. att.). Pēc analogas shēmas tika veikta dendrona **3b** ar gala Trt-grupām sintēze (2. att.). Vispirms metil-3,5-dihidroksibenzoāts (**1**) tika alkilēts ar 2-(tritiloksi)etilhlorīdu DMF šķīdumā NaH bāzes klātbūtnē, iegūstot savienojumu **2c**, tomēr reakcija notika lēni un ar mazu iznākumu. Visticamāk, stēriski apjomīgā tritilgrupa traucē nukleofīlās aizvietošanās reakciju –CH_2Cl fragmentā. Tādēļ tika izmantots cits sintēzes ceļš, un no savienojuma **2a** tika iegūts metil-3,5-bis(2-hidroksietoksi)benzoāts (**2b**), kuru funkcionalizējot ar Trt-grupām, iegūst savienojumu **2c**. Hidrolizējot savienojuma **2c** estera grupu, tika iegūta nepieciešamā tritilētā skābe **3b**.
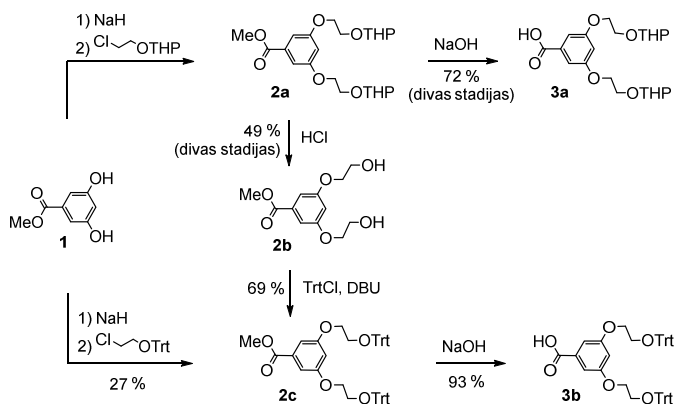
2. att. 3,5-Dihidroksibenzoskābes atvasinājumu sintēze.

Izmantojot diverģentās sintēzes metodi, dendrimēru periferās hidroksigrupas tika funkcionalizētas par Trt-grupām. Kodola **G0-OH** un pirmās paaudzes dendrimēra **G1-OH** reakcijā ar tritilhlorīdu piridīnā trietilamīna klātbūtnē attiecīgi tika iegūti produkti **G0-Trt** un **G1-Trt** (3. att.). Savienojums **G0-Trt** attīrīts, to kristalizējot, un iegūts ar vidēju iznākumu un augstu mērķa savienojuma jeb pamatvielas saturu. Paraugu pamatvielas satura analīze veikta ar augstas efektivitātes šķidrumu hromatogrāfiju (AEŠH). Nulles paaudzes savienojums **G0-Trt** sintezēts, lai optisko un termisko īpašību pētījumos novērotu tā devēto "dendrimēra efektu", kas rodas, pievienojot kodolam dendrimēra zarojumus vairākās paaudzēs. Dendrimērs **G1-Trt** tika attīrīts, izmantojot kolonnas hromatogrāfiju, kur tika novērota Trt-grupu hidrolīze uz silikagela, rezultātā iegūstot tikai 37 % iznākumu un 50 % pamatvielas saturu. Dendrimēra **G1-Trt** paraugā bez mērķa savienojuma arī ir līdzīgas struktūras azosavienojums, kam notikusi vienas Trt-grupas hidrolīze. Analogā veidā no dendrimēra **G2-OH** ar tritilhlorīdu piridīnā trietilamīna klātbūtnē sintezēts dendrimērs **G2-Trt**, bet iegūtais paraugs ir piecu vielu (kopā 70–75 %), kurām ir ļoti līdzīgas struktūras, maisījums. Izolētais maisījums, kas apzīmēts ar **G2-Trt**, satur gan pamatvielu, gan dendrimēru tipa azosavienojumus ar mazāku Trt-grupu skaitu, kas varētu veidoties nepilnīgas hidroksigrupu funkcionalizēšanas dēļ. Vidēji visā dendrimēra **G2-Trt** paraugā pietrūkst vienas Trt-grupas. Funkcionālo grupu attiecība maisījumā esošajām vielām noteikta ar ^{1}H KMR spektrometriju. Trešās paaudzes dendrimēra ar periferām Trt-grupām diverģentajā sintēzē tika iegūts paraugs, kas ir ļoti polidisperss vidēji ar sešu no 16 Trt-grupām iztrūkumu, tādēļ iegūtā parauga optiskās un termiskās īpašības promocijas darbā netiks apskatītas.
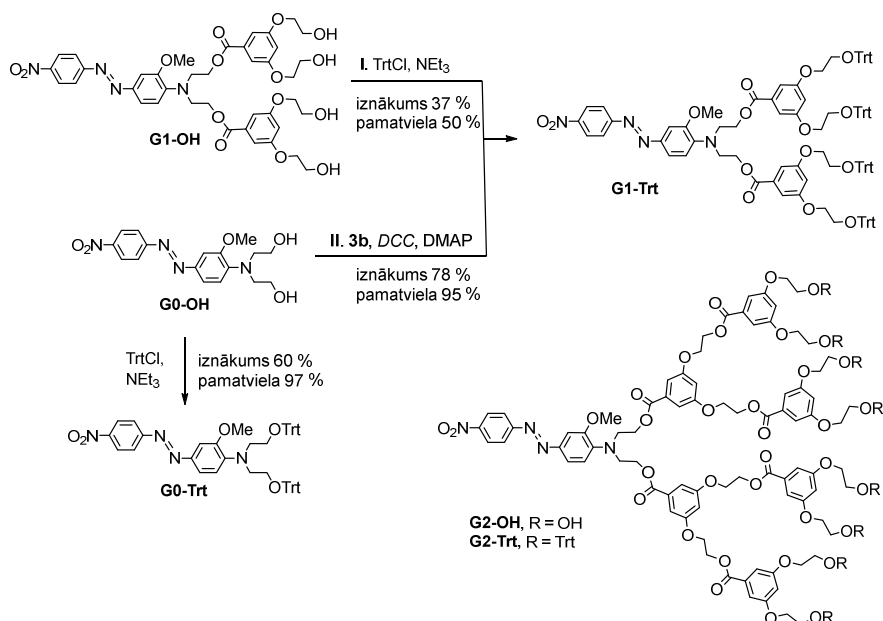
3. att. Savienojuma **G0-Trt** sintēze un dendrimēru **G1-Trt** diverģentā (I) un konverģentā (II) sintēze. Otrās paaudzes dendrimēru struktūras.

Tika secināts, ka diverģentās sintēzes metodei ir būtisks trūkums – palielinoties gala grupu skaitam, ir grūti nodrošināt to pilnīgu funkcionalizēšanu. Tāpēc dendrimēru ar Trt-grupām perifērijā sintēzi daudz efektīvāk varētu veikt, izmantojot konverģento dendrimēru sintēzes metodi. Skābes **3b** esterificēšanas ar azosavienojumu **G0-OH** reakcijā tika iegūts dendrimērs **G1-Trt** (3. att. II), kas tika attīrīts, izmantojot frakcionētu izgulsnēšanu. Izmantojot konverģentās sintēzes paņēmienu, dendrimērs **G1-Trt** tika sintezēts vienā stadijā ar labu iznākumu (78 %) un augstu pamatvielas saturu (95 %), kas noteikts, izmantojot AEŠH un ^{1}H KMR spektrometriju. Jāatzīmē, ka šī metode ir daudz efektīvāka par iepriekš izmantoto diverģentās sintēzes metodi, kad tas pats dendrimērs **G1-Trt** tika iegūts ar kopējo iznākumu 37 %. Šajā darbā aprakstītie dendrimēri **G1-Trt** un **G2-Trt**, kas iegūti diverģentās sintēzes ceļā, sastāv no vairākām individuālām vielām – pamatvielas un līdzīgas struktūras azosavienojumiem, kas visi satur aktīvo azohromoforu un izolējošo dendrimēra zarojumu, atšķiras tikai precīza perifēro hidroksi- un Trt-grupu attiecība un novietojums. Interesējošās īpašības nosaka visos materiālos esošais azohromofors, tāpēc sintezētie produkti ir izmantojami kā materiāli to turpmākiem optisko, termisko un NLO īpašību pētījumiem.

1.3. Dendrimēru ar azobenzola kodolu īpašības

Sintezētajiem produktiem **G0-Trt**, **G1-Trt**, **G2-Trt** un to prekursoriem **G0-OH**, **G1-OH**, **G2-OH** acetonā gaismas absorbcijas maksimumi (λ_{max}) un molārie ekstinkcijas koeficienti (ε) atbilst zemākās frekvences lādiņa pārejas joslai (1. tab.). Savienojumu **G0-OH** un **G0-Trt**

absorbcijas maksimumi acetonā ir batohromi nobīdīti attiecībā pret pirmās un otrās paaudzes dendrimēriem (1. tab., 1., 4. rinda), jo trūkst dendrimēra zarojuma un tā veidotās lokālās vides, kas iespaido azohromofora absorbcijas spektru gan ar elektrostatisko mijiedarbību, gan telpiski ierobežojot šķīdinātāja molekulu piekļuvi kodola azohromoforam. Savukārt, analizējot vienas paaudzes dendrimēru ar abām gala grupām datus (1. tab., salīdzinot 2. ar 5. un 3. ar 6. rindu), netika novērota gala grupu ietekme uz absorbcijas maksimumu, kas liecina par to relatīvi tālu novietojumu no azohromofora fragmenta.

1. tabula

Sintezēto dendrimēru un to sintēzē izmantoto izejvielu optiskās un termiskās īpašības

Nr. p. k.	Dendrimērs	λ_{max},[a] nm	ε,[a] $M^{-1} \cdot cm^{-1}$	T_g, °C	$T_{kuš}$, °C	T_d, °C
1.	G0-OH	494	28 200	–	114	245
2.	G1-OH	467	23 400	53	129	289
3.	G2-OH	472	24 500	64	102	300
4.	G0-Trt	490	26 000	73	198	288
5.	G1-Trt	470	22 000	83	–	286
6.	G2-Trt	471	24 500	85	–	294

[a] 30 µmol·L⁻¹ acetona šķīdumā.

Tika pētītas arī sintezēto produktu **G0-Trt**, **G1-Trt**, **G2-Trt** un to prekursoru **G0-OH**, **G1-OH**, **G2-OH** termiskās īpašības, izmantojot diferenciālo skenējošo kalorimetriju (*DSC*) un termogravimetrisko analīzi (TGA). Termiskā stabilitāte (T_d) noteikta 5 % masas zuduma temperatūrā, kas pirmās un otrās paaudzes dendrimēriem ir lielāka par 285 °C (1. tab.). Azosavienojums **G0-OH** ir kristālisks ar kušanas temperatūru ($T_{kuš}$) 114 °C, stiklošanās temperatūra (T_g) netika novērota arī otrajā karsēšanas etapā pēc straujas izkausētā parauga atdzesēšanas. Azosavienojums **G0-OH** ir arī termiski nestabilākais savienojums no aprakstītajiem, bet Trt-grupu vai dendrimēra zarojuma pievienošana palielina termisko stabilitāti. Dendrimēri ar Trt-grupām **G1-Trt**, **G2-Trt** ir amorfi, jo tiem ir novērojama T_g, bet nav novērojama $T_{kuš}$. Dendrimēri **G1-OH**, **G2-OH** ar hidroksigrupām ir kristāliski, tomēr, izkausētos paraugus strauji atdzesējot, veidojas amorfā cietā fāze un atkārtotā karsēšanā var noteikt T_g. Dendrimēru T_g un T_d palielinās, pieaugot dendrimēra paaudzei sērijas ietvaros, dendrimēriem ar gala Trt-grupām T_g sasniedzot 85 °C. Dendrimēru **G1-Trt** optiskās un termiskās īpašības ir praktiski vienādas neatkarīgi no strukturāli līdzīgo azosavienojumu piejaukuma pakāpes jeb gala Trt- un hidroksigrupu attiecības, tādēļ 1. tabulā parādīti tikai konverģenti iegūtā dendrimēra dati.

Diverģenti un konverģenti sintezētajam dendrimēram **G1-Trt** konstatētas atšķirīgas NLO īpašības, tāpēc radās nepieciešamība atšķirīgi apzīmēt abos sintēzes ceļos iegūtos produktus, sasaistot ar parauga sastāvu. Iespējams, atšķirības noteica izmaiņas periferijas Trt- un hidroksigrupu savstarpējā attiecībā. Konverģentās sintēzes ceļā iegūtais dendrimēra materiāls apzīmēts ar **G1-Trt-a**, un tas satur pamatvielu jeb mērķa savienojumu ar visām četrām Trt-grupām. Savukārt diverģentās sintēzes ceļā iegūtais dendrimēra materiāls apzīmēts ar **G1-Trt-b**, un tas satur divus līdzīgas struktūras azosavienojumus līdzīgās proporcijās, kur

vienam ir visas četras Trt-grupas, savukārt otram trīs Trt-grupas un viena hidroksigrupa, kas vidēji dod 3,5 Trt-grupas un pusi hidroksigrupas. Dendrimēra materiāla paraugs **G2-Trt** satur vidēji septiņas Trt-grupas un vienu hidroksigrupu.

NLO īpašības ir mērītas trijiem dendrimēru materiāliem **G1-Trt-a**, **G1-Trt-b** un **G2-Trt**, nosakot otrās harmonikas ģenerācijas intensitāti (*SHI*) šo materiālu plānām amorfām elektriskajā laukā orientētām kārtiņām *Maker fringe* eksperimentā (sadarbības partneri LU Cietvielu fizikas institūtā *Dr. phys.* Mārtiņa Rutka vadībā). Iegūtas lielas NLO koeficienta d_{33} vērtības (2. tab.), kas ir skaidrojamas ar alkoksiaizvietotāju esamību azohromofora donorajā daļā. Visiem paraugiem ir plašas absorbcijas joslas, un absorbcijas maksimums ir novērojams tuvu 500 nm, turklāt absorbcijas joslā ietilpst otrā harmoniskā viļņa garums 532 nm, kas nodrošina NLO efektivitātes rezonanses uzlabošanos. NLO koeficienti ir atkarīgi no frekvences, tāpēc tās ietekmes mazināšanai veikta ekstrapolācija uz nulles frekvenci ($d_{33}(0)$) saskaņā ar divu līmeņu modeli [42]. Amorfā stiklveida kārtiņā dendrimēru materiāliem **G1-Trt-a**, **G1-Trt-b** un **G2-Trt** ir par 14–18 nm batohromi nobīdīti gaismas absorbcijas maksimumi, salīdzinot ar maksimumu acetona šķīdumā, kas liecina par hromofora fragmentu agregāciju cietajā fāzē [43].

2. tabula

Dendrimēru materiālu plāno amorfo kārtiņu NLO īpašības

Nr. p. k.	Dendrimēru materiāls	Trt- un hidroksigrupu attiecība	d_{33},[a] pm·V^{-1}	$d_{33}(0)$,[b] pm·V^{-1}	T_{SHI50},[c] °C	λ_{max},[d] nm
1.	**G1-Trt-a**	4 Trt / 0 OH	73	12	53	485
2.	**G1-Trt-b**	3,5 Trt / 0,5 OH	125	16	74	488
3.	**G2-Trt**	7 Trt / 1 OH	167	23	74	488

[a] NLO koeficients noteikts pie 532 nm;

[b] NLO koeficients ekstrapolēts uz nulles frekvenci;

[c] temperatūra, pie kuras *SHI* ir 50 % no sākotnējās intensitātes, paraugu sildot;

[d] absorbcijas maksimums mērīts plānai amorfai kārtiņai uz kvarca stikliņa.

Salīdzinot diverģentās sintēzes ceļā iegūtos dendrimēru materiālus **G1-Trt-b** un **G2-Trt** (2. tab., 2. un 3. rindas), redzams, ka otrās paaudzes dendrimēra materiālam **G2-Trt** ir augstākas NLO koeficienta d_{33} vērtības nekā pirmās paaudzes dendrimēra materiālam **G1-Trt-b**. To varētu skaidrot ar labāku azohromofora izolēšanu dendrimēra zarojumā, lielāku brīvību novietoties paralēli orientējošam elektriskajam laukam, neskatoties uz hromofora koncentrācijas samazināšanos molekulas sastāvā, pieaugot dendrona apjomam molekulā. Salīdzināti arī dendrimēru materiāli **G1-Trt-a** un **G1-Trt-b** ar atšķirīgu gala grupu attiecību (2. tab., 1. un 2. rindas). Dendrimēra materiāls **G1-Trt-a** ar četrām Trt-grupām uzrāda tikai 58 % no NLO koeficienta d_{33} vērtības, salīdzinot ar materiāla **G1-Trt-b** paraugu, kam Trt/OH grupu attiecība ir 3,5/0,5. Atšķirību nevar skaidrot vienīgi ar aktīvā hromofora masas daļas samazināšanos pilnīgākā dendrimēra struktūrā, bet atšķirību varētu skaidrot ar sinerģiju, visiem molekulas fragmentiem savstarpēji mijiedarbojoties. Konverģentās sintēzes paņēmiena izmantošanas mērķis bija ne tikai gala produkta iznākuma palielināšana, bet arī ķīmiski tīrāka jeb mērķa struktūru vairāk saturoša materiāla iegūšana, kam būtu jādarbojas efektīvāk nekā

iepriekš iegūtajam paraugam, kas ir tikai daļēji funkcionalizēts ar Trt-grupām. Pretēji gaidītajam visas NLO īpašības konverģenti iegūtajam dendrimēra materiāla paraugam **G1-Trt-a** (2. tab,, 1. rinda) bija vājākas nekā diverģenti iegūtajam paraugam **G1-Trt-b** (2. tab., 2. rinda).

Temperatūra T_{SHI50} ir noteikta NLO eksperimentā, kad, vienlaikus veicot parauga sildīšanu un *SHI* mērīšanu, novēro amorfā materiāla *SHI* samazināšanos uz pusi. Diverģenti iegūto dendrimēru materiālu **G1-Trt-b** un **G2-Trt** (2. tab., 2. un 3. rindas) T_{SHI50} vērtības ir par 8–9 °C mazākas nekā šo materiālu T_g vērtības, ko var skaidrot ar atšķirīgo molekulu sakārtojumu orientētā NLO aktīvā kārtiņā, atļaujot brīvākas hromofora fragmenta kustības nekā no šķīduma izgulsnētā amorfā paraugā. Savukārt dendrimēra paraugam **G1-Trt-a** (2. tab., 1. rinda), kas satur četras Trt-grupas, T_{SHI50} vērtība ir par 30 °C zemāka nekā atbilstošā T_g vērtība, un pat visa NLO aktivitāte ir zudusi pirms T_g sasniegšanas. Iespējams, amorfās fāzes struktūra pēc orientēšanas elektriskajā laukā ievērojami atšķiras no izkususās amorfās fāzes *DSC* mērījumos, kā rezultātā samazinās nepieciešamais enerģijas daudzums molekulārajām kustībām un viegli notiek dezorientācija. Dendrimēra materiāla paraugam **G1-Trt-b** ar Trt/OH grupu attiecību 3,5/0,5 T_{SHI50} vērtība ir par 20 °C augstāka nekā materiālam **G1-Trt-a** ar četrām Trt-grupām, ko varētu skaidrot ar amorfās fāzes stabilizēšanos, izmantojot brīvās hidroksigrupas un ūdeņraža saites. Līdzīgus secinājumus izdarījuši profesora *Zhen Li* grupas zinātnieki [44]. Iepriekš minētais amorfo fāzi stabilizējošais efekts, visticamāk, ir noteicošais arī lielu NLO koeficientu d_{33} vērtībām. Sintezēto dendrimēru materiālu NLO koeficienti d_{33} ievērojami pārsniedz plaši izmantotā LiNbO$_3$ kristālu NLO koeficientu vērtības (d_{33} = 25,2 pm·V^{-1} [34]), izmantojot to pašu lāzera starojuma viļņa garumu – 1064 nm. Tomēr ekstrapolētie koeficienti d_{33}(0) ir mazāki par LiNbO$_3$ kristālu koeficientu vērtību, bet pārsniedz divu citu no biežāk lietotajiem neorganiskajiem kristāliem KTiOPO$_4$ (d_{33} = 14,6 pm·V^{-1}) un LiB$_3$O$_5$ (d_{33} = 0,04 pm·V^{-1}) NLO koeficientu vērtības [34].

Oriģinālpublikācijas par šajā nodaļā aprakstītajiem pētījumiem – 1. un 3. pielikumā.

2. Dendronizēti monoazohromofori

Iepriekšējā nodaļā aprakstītie dendrimēri veidoja materiālus, kas lielākoties sastāvēja no vairākiem azosavienojumiem ar līdzīgu struktūru, tāpēc tika nolemts pārbaudīt aktīvā hromofora fragmentu izolēšanas koncepciju, izmantojot 1. nodaļā aprakstītā Trt-grupas saturošā dendrona pievienošanu azobenzola molekulas vienā pusē. Dendronizētā azohromofora molekulas otrā pusē ievadījām pentafluorfenilfragmentu, kas, iesaistoties Ar-Ar^F starpmolekulārajās mijiedarbībās, varētu ierobežot molekulu kustīgumu amorfajā fāzē, paaugstinot T_g vērtību un uzlabojot NLO parametrus. Tika sintezēti arī dendronizētie azohromofori, kuros Trt-grupas saturošā dendrona vietā ir THP- vai hidroksigrupas saturošs dendrons, lai, salīdzinot optiskās un termiskās īpašības, izprastu molekulas dažādo fragmentu ietekmi uz materiālu īpašībām.

Lai uzlabotu NLO parametrus, tika sintezēti dendronizētie azohromofori, izmantojot dendronus ar divām benzilgrupām vai divām (pentafluorfenil)metilgrupām, kas savstarpēji mijiedarbotos, stabilizējot elektriskajā laukā orientētu plāno kārtiņu. Tika pievienoti atšķirīgi dendroni azohromofora donorajā vai akceptorajā daļā. Optisko, termisko un NLO īpašību salīdzināšanai tika sintezēti arī simetriskie azohromofori tādā izpratnē, ka azobenzola akceptora un donora daļas saistītas ar vienādiem dendronu fragmentiem. Pētījumu sākumposmā Trt-grupas saturošais dendrons un (pentafluorfenil)metilgrupas saturošais dendrons azohromofora donorajā pusē uzrādīja labas termiskās un NLO īpašības, tāpēc tika izlemts sintezēt arī tādu azohromoforu, kas apvieno šos abus fragmentus.

## 2.1. Dendronizētu azohromoforu sintēze

2-Amino-5-nitrofenols (**4**) kalpo kā izejviela visiem šajā nodaļā aprakstītajiem azosavienojumiem. Diazotējot aminofenolu **4**, tika iegūts diazonija betaīns **5** (4. att.), kas ir fotojutīga oranža kristāliska viela. Azosavienojums **6** ar nelielu iznākumu tika iegūts azosametināšanas reakcijā starp betaīnu **5** un *N*-metilanilīnu, kaut gan tika testēti vairāki azosametināšanas reakcijas apstākļi. Taču tālāku azosavienojuma **6** alkilēšanu ar 2-hloretanolu, lai iegūtu produktu **7**, realizēt neizdevās, notiekot izejvielas **6** sabrukšanai bāziskā vidē.

Azosavienojuma **7** iegūšanai tika izvēlēts cits sintēzes ceļš. Alkilējot savienojuma **4** fenolātu, tika iegūts 2-(2-hloretoksi)-4-nitroanilīns (**8**) ar 44 % iznākumu (4. att.). Diazotējot savienojumu **8** un tālākā azosametināšanas reakcijā ar savienojumu **9**, tika iegūts nepieciešamais divas hidroksigrupas saturošais azosavienojums **7**. Simetriski dendronizētie azohromofori **10a–c** tika sintezēti no azosavienojuma **7** un dendronizējošajiem fragmentiem **3a,b** esterificēšanas reakcijā, izmantojot DCC un DMAP [45, 46]. Hidroksigrupas saturošais azohromofors **10c** tika iegūts, nošķeļot THP grupas savienojumam **10a**.

Savienojumi **14a–c** ar pentafluorfenilgrupu molekulas akceptorajā daļā sintezēti atbilstoši 5. attēlā redzamajai shēmai. Alkilējot savienojumu **4** ar mezilatvasinājumu **11**, tika iegūts savienojums **12**, to tālāk diazotējot un azosametinot ar anilīna atvasinājumu **9**, tika iegūts azohromofors **13**. Dendronizējošo skābju pievienošana savienojumam **13** un THP grupu noņemšana veikta līdzīgi iepriekš aprakstītajiem savienojumiem **10a–c**, iegūstot azohromoforus **14a–c**.
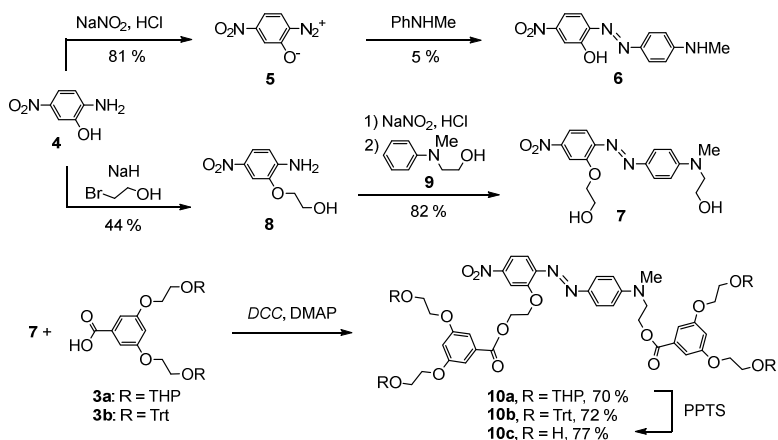
4. att. Simetriski dendronizēto azobenzolu **10a–c** sintēzes shēma.
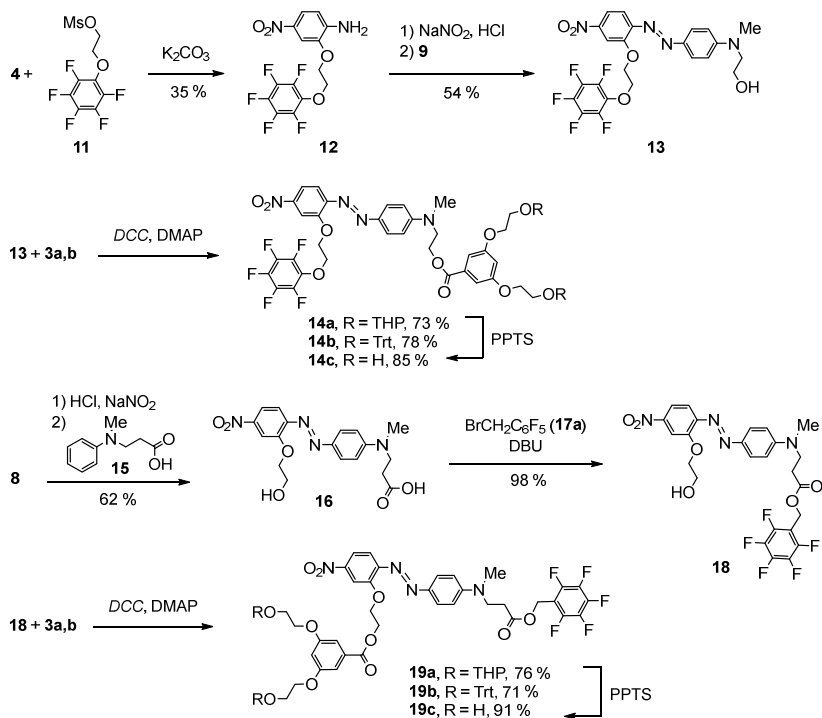
5. att. Azohromoforu **14a–c** un **19a–c** sintēzes shēma.

Savienojumu **19a–c** sintēzei fluoraromātiskā fragmenta un azohromofora kovalenta savienošana vispirms tika veikta ar estera saites palīdzību (5. att.). Anilīna atvasinājums **8** pēc diazotēšanas stājās azosametināšanas reakcijā ar savienojumu **15**, veidojot azobenzolu **16**.

Azobenzolam **16**, kas molekulas vienā galā satur skābes, otrā spirta grupu, bija jāveido divas jaunas estera saites. Vispirms, izmantojot DBU metodi [47], savienojums **16** tika apstrādāts ar bromīdu **17a** un kvantitatīvi tika iegūts benzilētais starpprodukts **18**. Galaprodukti **19a–c** tika iegūti, lietojot tādas pašas metodes kā savienojumu **10a–c** un **14a–c** iegūšanā.

Savienojumi **24a–c**, kuriem fluoraromātiskais fragments kovalenti saistīts ar benzilētera tipa saiti azohromofora donorajā daļā, sintezēti pēc 6. attēlā redzamās shēmas. Betaīna **5** azosametināšanas reakcija ar anilīna atvasinājumu **9** deva azosavienojumu **20**. Alkilējot savienojumu **20**, tika iegūts azosavienojums **21a**, no kura tālāk sintezēti aizejošās grupas saturošie mezilāts **21b** un trihloracetimidāts **21c**.
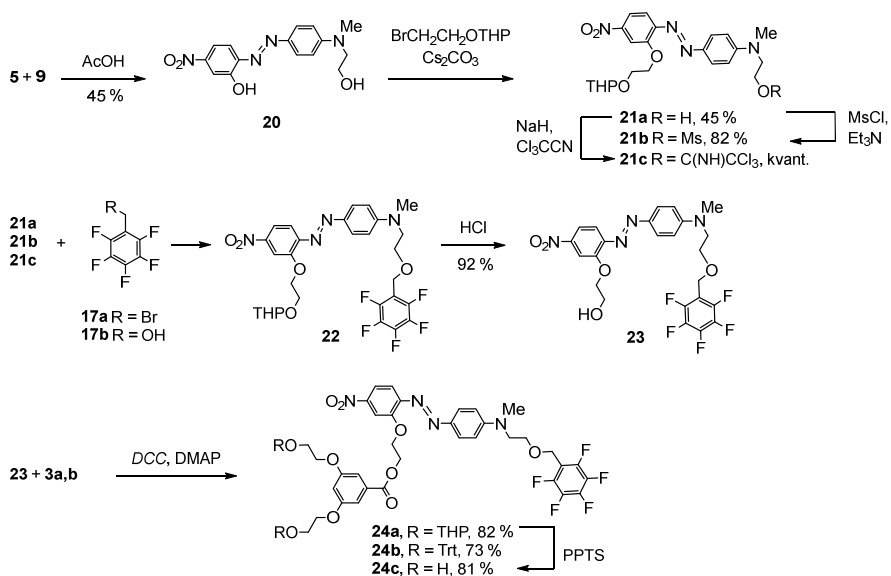
6. att. Azosavienojumu **24a–c** sintēzes shēma.

Reakcijas apstākļi savienojuma **22** sintēzes mēģinājumiem apkopoti 3. tabulā. Vispirms no azobenzola atvasinājumiem **21a,b** Viljamsona ēteru sintēzes reakcijās ar dažādiem (pentafluorfenil)metilatvasinājumiem **17a,b** tika mēģināts iegūt savienojumu **22** (3. tab., 1.–3. rinda). Tomēr tikai trešā eksperimenta AEŠH-MS analīze uzrādīja savienojuma **22** rašanās zīmes. Tā kā iespējamas arī nevēlamas blakusreakcijas kā fluora atoma nukleofilā aromātiskā aizvietošana (S_NAr) [48], tad tika mēģināts mainīt reakciju apstākļus (4.–6. eksperiments), tomēr mērķa produkts **22** neveidojās.

Reakcijas apstākļu variācijas savienojuma **22** iegūšanas eksperimentiem

Nr. p. k.	Reaģenti	Reakcijas apstākļi	Literatūra	Rezultāts
1.	**21a**, **17a**	NaH, THF, 60 °C, 1 d.		S_NAr blakusreakcija, produkts nav novērots
2.	**21b**, **17b**	NaH, DMF, ist. temp., 2 d.		S_NAr blakusreakcija, produkts nav novērots
3.	**21a**, **17a**	NaN(SiMe$_3$)$_2$, DMF, 70 °C, 1 d.		S_NAr blakusreakcija, savienojuma **22** zīmes
4.	**21c**, **17b**	BF$_3$·Et$_2$O, CHCl$_3$, cikloheksāns, ist. temp., 1 d.	[49]	produkts nav novērots
5.	**21c**, **17b**	HOSO$_2$CH$_3$, CHCl$_3$, cikloheksāns, ist. temp., 1 d.	[50]	produkts nav novērots
6.	**21a**, **17a**	Ag$_2$O, *DCM*, ist. temp., 3 d.	[51]	blakusreakcija, produkts nav novērots
7.	**21a**, **17b**	DIAD, PPh$_3$, *DCM*, ist. temp., 1 d.		savienojuma **22** zīmes
8.	**21a**, **17a**	TBAB, KOH, KI, THF, 70 °C, 1 d.	[52]	savienojuma **22** zīmes
9.	**21a**, **17a**	TBAB, KOH, *DCM*, H$_2$O, ist. temp., 1 d.	[53]	savienojums **22**, 60 %

Veicot sintēzi septītajā un astotajā eksperimentā uzrādītajos apstākļos, konstatētas savienojuma **22** zīmes, izmantojot AEŠH-MS. Tomēr savienojumu **22** ar 60 % iznākumu izdevās iegūt devītajā eksperimentā, piemērojot atbilstošus reakcijas apstākļus [53]. Eksperimenta būtiskākā atšķirība no visiem pārējiem ir reaģentu lielais pārākums pret savienojumu **21a**: 20 ekvivalenti savienojuma **17a** un 40 ekvivalenti KOH. Bromīds **17a** pēc reakcijas paliek reakcijas maisījumā un to var hromatogrāfējot atdalīt un lietot atkārtoti. Tika konstatēts, ka būtiska nozīme ir reaģentu lielajam stehiometriskajam pārākumam. Izmantojot savienojumus **17a** un **21a** molārajās attiecībās 1,2:1, reakcija norisinās, tomēr arī pēc divām dienām vēl ir novērojama izejvielu klātbūtne plānslāņa hromatogrāfijā. THP-aizsarggrupas noņemšana savienojumam **22** noris sālsskābes šķīdumā, un savienojums **23** iegūts ar 92 % iznākumu. No savienojuma **23** ar jau iepriekš lietotajām metodēm iegūti mērķa savienojumi **24a–c**.

Benzilgrupas un (pentafluorfenil)metilgrupas saturošo dendronizēto azohromoforu **34**, **36–39** sintēzē var noteikt trīs posmus: 1) dendronizējošo fragmentu sintēze; 2) azohromofora sintēze; 3) dendronizējošo fragmentu un azohromofora kovalenta saistīšana vienā savienojumā. Atbilstoši 7. attēlā dotajai shēmai, vispirms tika lietota zināma dendrimēra sintēzes metode [35], kur savienojums **1** tika alkilēts ar benzilbromīdu (**25**) fāžu pārneses katalīzes apstākļos un tika iegūts esteris **26**. Estera **26** hidrolīze bāziskos apstākļos deva skābi **27** ar 92 % iznākumu.

Fluorētā dendrona **30** sintēze tika realizēta atšķirīgi no dendrona **27** sintēzes, jo fluoraromātiskie savienojumi ir nestabili izteikti sārmainos šķīdumos [48]. 3,5-Dihidroksibenzoskābe (**28**) reaģēja ar 1-(brommetil)-2,3,4,5,6-pentafluorbenzolu (**17a**), veidojot pilnībā alkilētu esteri **29**, kas, hidrolizēts vārošā H$_2$SO$_4$/dioksāna šķīdumā, veidoja dendronizējošo skābi **30** (7. att.).
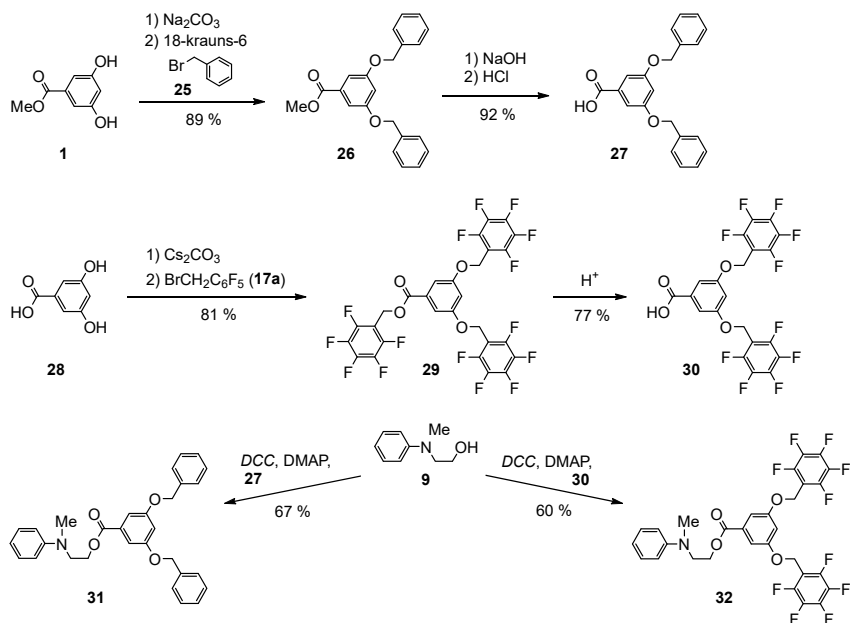
7. att. Dendronizējošo skābju un hromoforu prekursoru sintēze.

Asimetrisko azohromoforu **34**, **36** un **37** sintēzes pirmais solis bija hromofora prekursora **9** dendronizēšana (7. att.). Anilīna atvasinājums **9** reaģēja ar katru no dendronizējošajām skābēm **27** un **30**, izmantojot *DCC* un DMAP. Iegūtie esteri **31** un **32** azosametināšanas reakcijās ar diazotētu anilīna atvasinājumu **8** tālāk veidoja attiecīgos monodendronizētos azohromoforus **33** un **35** (8. att.). Asimetriskie hromofori **34** un **36** ar atšķirīgiem dendroniem katrā molekulas pusē iegūti no azosavienojumiem **33** un **35**, izmantojot *DCC* un DMAP ar attiecīgajām dendronizējošām skābēm **30** un **27**. Tika sintezēts arī dendronizētais azohromofors **37** no azosavienojuma **35** un skābes **3b**, izmantojot iepriekš minēto karbodiimīdu metodi (8. att.). Savienojums **37** tika attīrīts, pārgulsnējot no *DCM* šķīduma ar metanolu, lai saglabātu skābā vidē hidrolītiski nestabilās Trt-grupas.
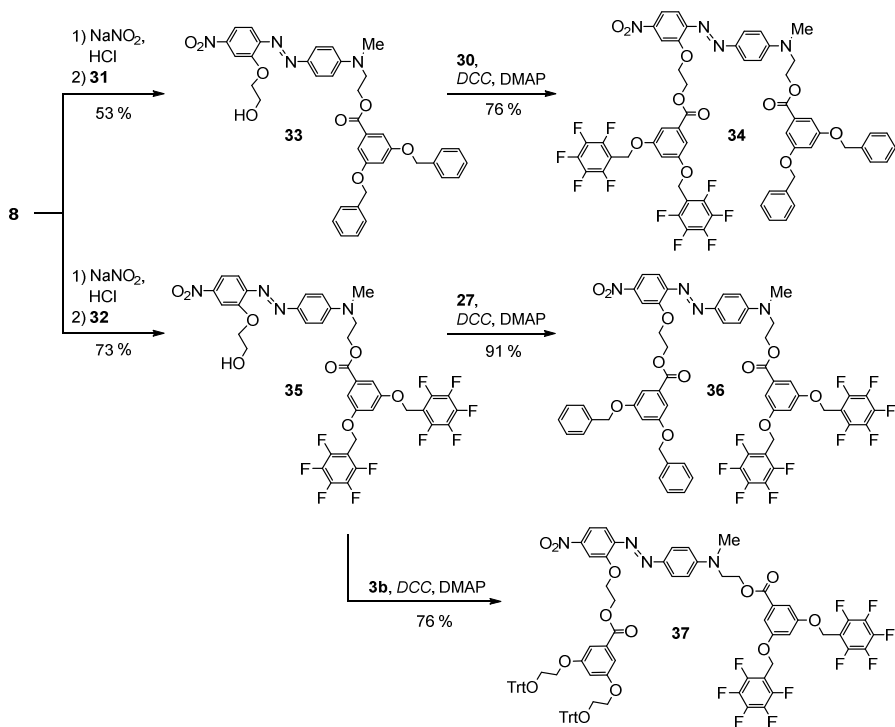
8. att. Nesimetrisko dendronizēto azohromoforu sintēze.

Azosavienojuma **7** esterificēšanā ar skābi **27** vai **30** tika iegūti simetriskie azohromofori **38** un **39** ar vienādiem dendronizējošiem fragmentiem molekulā (9. att.).
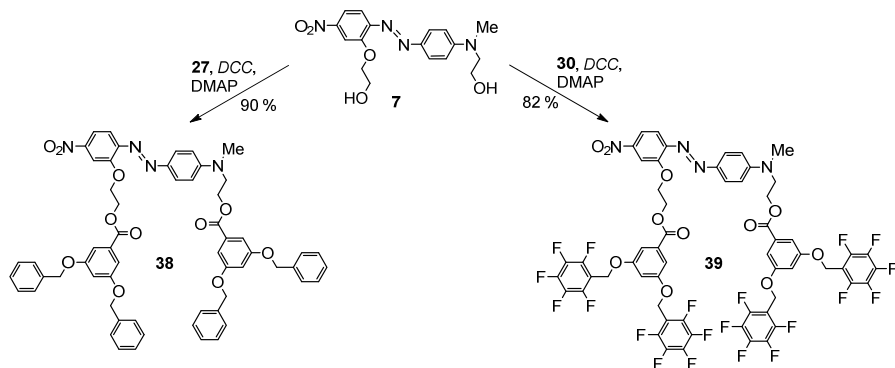
9. att. Simetrisko dendronizēto azohromoforu sintēze.

2.2. Ar-Ar^F mijiedarbību konstatēšana

Dendrimēriem, kas satur azobenzolu visā zarojumā, profesora *Zhen Li* grupā pētīta Ar-Ar^F mijiedarbību ietekme uz struktūras topoloģijām un NLO īpašībām [24, 25]. Balstoties ^{19}F KMR spektros un kvantu ķīmiskajos aprēķinos, tika secināts, ka pentafluorfenilfragments piedalās Ar-Ar^F iekšmolekulārās mijiedarbībās ar azobenzola fragmenta donoro daļu [24, 25, 54, 55]. Tomēr literatūrā azobenzola dendrimēru un organisko molekulāro stiklu rentgenstruktūranalīzes rezultāti iepriekš nebija publicēti.

Lēnām ietvaicējot dendronizētā azohromofora **36** *DCM*/etilacetāta šķīdumu, tika iegūti tā monokristāli. Rentgenstruktūranalīzē (*Dr. sc. phys.* Sergejs Beļakovs) šajos monokristālos tika novērota iekšmolekulāra pentafluorfenilfragmenta Ar-Ar^F mijiedarbība ar azobenzola fragmenta akceptoro daļu. 10. attēlā redzamas divas savienojuma **36** molekulas, kas veido triklīnās singonijas normālās simetrijas kristālrežģi. Abu šo molekulu benzilgrupas un pentafluorfenilgrupas saturošo dendronu visi trīs aromātiskie gredzeni starpmolekulāri saistās, izmantojot Ar-Ar^F un aromātiskās π-π mijiedarbības, bet viens no pentafluorfenilfragmentiem, iekšmolekulāri mijiedarbojas ar azobenzola akceptoro daļu un azogrupu. Kristālisko struktūru stabilizē arī starpmolekulāras CH···F un CH···O mijiedarbības. Tomēr kristālā ir vērojama viena molekulas fragmenta nesakārtotība, un šķīdinātāja molekulas arī tiek ieslēgtas. Iespējams, nesakārtotības dēļ nav izdevies iegūt citu dendronizēto azosavienojumu monokristālus.
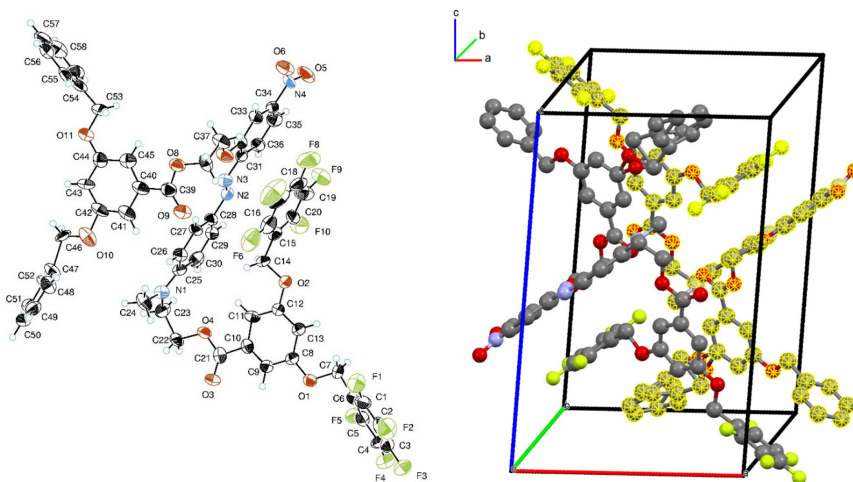
10. att. Molekulas **36** *ORTEP* shēma ar termiskajiem elipsoīdiem 50 % varbūtībā (pa kreisi), divu savienojuma **36** molekulu (viena ir iezīmēta) novietojums kristālrežģī (pa labi).

2.3. Termiskās īpašības

Tika noteiktas un analizētas sintezēto savienojumu termiskās īpašības, meklējot sakarības starp sintezēto molekulu struktūras elementiem un to stiklošanās, kušanas un sadalīšanās temperatūrām, izmantojot *DSC* un TGA eksperimentos iegūtos datus, kas apkopoti 4. tabulā. Ja vienā savienojuma molekulā ir iekļauti dažādi strukturāli atšķirīgi fragmenti, šāda savienojuma T_g vērtība ir atkarīga no visu dažādo iekļauto fragmentu īpašībām [56]. Pentafluorfenilfragmentu pievienošanas mērķis sintezēto azohromoforu struktūrā bija ar starpmolekulāru Ar-Ar^F mijiedarbību palīdzību stabilizēt orientēto molekulu novietojumu amorfajā kārtiņā NLO mērījumiem. Līdzīgi kā literatūrā aprakstīts fenil- un pentafluorfenilgrupas saturošiem NLO aktīviem organiskajiem molekulārajiem stikliem [10], to varētu novērot kā T_g un T_{SHI50} vērtību palielināšanos, salīdzinot ar analogiem savienojumiem, kuriem pentafluorfenilfragmentu vietā ir fenilgrupas.

Tika novērots, ka THP grupu klātbūtne izteikti pazemina T_g vērtības. Nevienam no savienojumiem **10a**, **14a**, **19a** un **24a** T_g vērtību nebija iespējams novērot iekārtas darbības diapazonā (15–1000 °C). Visiem pārējiem pētītajiem savienojumiem T_g vērtības ir augstākas par 20 °C. Vismazākajam azohromoforam **7** T_g vērtība ir viszemākā (37 °C), ko var paaugstināt, funkcionalizējot azohromofora struktūru ar dendroniem un pentafluorfenilgrupas saturošiem fragmentiem. Dendrona ar terminālām hidroksigrupām (savienojumos **14c**, **19c** un **24c**) un dendrona ar benzilgrupām (savienojumos **33** un **38**) pievienošana azobenzola kodolam dod aptuveni vienādu un nebūtisku T_g vērtības palielinājumu par 0–9 °C. Savukārt divu dendronu ar terminālām hidroksigrupām izmantošana savienojumā **10c** dod salīdzinoši augstu T_g vērtību (60 °C). Ievērojami T_g vērtību palielina Trt-grupas saturošais dendrons savienojumos **14b**, **19b** un **24b**, savukārt divu šādu dendronu klātbūtne savienojumā **10b** dod T_g vērtības palielinājumu par 41 °C.

Ar-Ar^F mijiedarbību pētīšanai tika sagatavoti divi bināri ekvimolāri azosavienojumu maisījumi (**34** + **36**) un (**38** + **39**) no savienojumiem **34** un **36** un no savienojumiem **38** un **39** ar nolūku salīdzināt to termiskās un NLO īpašības ar azohromoforu **34**, **36**, **38**, **39** plānajām kārtiņām. Maisījumi (**34** + **36**) un (**38** + **39**) uzrādīja identiskas T_g vērtības (55 °C), kas bija aptuveni to sastāvdaļu vidējais rādītājs. Tika gaidīts, ka abas maisījuma sastāvdaļas mijiedarbosies un T_g vērtība būs lielāka par atsevišķo komponentu T_g vērtībām, kā aprakstīts literatūrā [10], taču efekts netika novērots. Benzilgrupas saturošais dendrons nav noteicošais, jo visaugstākās T_g vērtības starp azohromoforiem **33–39** ir novērojamas savienojumiem **35**, **37** un **39**, kuriem (pentafluorfenil)metilgrupas saturošais dendrons ir pievienots azohromofora donorajā daļā. To var izskaidrot ar Ar-Ar^F mijiedarbību starp pentafluorfenilfragmentiem un azobenzolu benzilfragmentu vietā, ko skaidri parāda savienojuma **36** kristāla struktūra. Vislielākā T_g vērtība novērojama, apvienojot Trt-grupas saturošo dendronu ar (pentafluorfenil)metilgrupas saturošo dendronu azohromofora donorajā daļā savienojumā **37**, kura struktūras dizains veikts, balstoties iepriekš iegūtajās savienojumu **10b**, **36** un **39** T_g vērtībās.

Promocijas darbā iegūtajiem savienojumiem ir novērotas zemākas T_g vērtības nekā nepieciešams esošo elektrooptisko ierīču izgatavošanā [57], tomēr materiāliem ar līdzīgām T_g

vērtībām ir potenciāls izmantošanai zemās temperatūrās. Augsta T_g vērtība nepieciešama materiāliem, ko izmanto istabas vai augstākās temperatūrās, savukārt materiāli ar zemu T_g var būt piemēroti izmantošanai Arktikā vai Antarktikā valdošajās temperatūrās [22].

Kristālisko fāzi veido visi savienojumi, kas satur hidroksigrupas, pentafluorfeniloksigrupas un benzilgrupas vai (pentafluorfenil)metilgrupas saturošos dendronus. Kristālisko dabu, visticamāk, nosaka iespēja veidoties stabilizējošām ūdeņraža saitēm, kā arī Ar-Ar^F un CH···F mijiedarbībām. Pentafluorfeniloksigrupai piemīt spēcīga tieksme sakārtoties, kā rezultātā savienojums **14a** ir vienīgais kristāliskais THP-grupas saturošais savienojums, pārējie istabas temperatūrā ir amorfi un mīksti. Otrās sildīšanas ciklā *DSC* analīzē savienojumiem **7** un **14c** novērojama spontāna kristalizēšanās, pēdējam ir arī visaugstākā novērotā $T_{kuš}$ vērtība (193 °C), iespējams, summējoties ūdeņraža saišu un Ar-Ar^F mijiedarbību ietekmei. Lielākā daļa no Trt-grupas saturošajiem savienojumiem ir amorfas cietas vielas, bet savienojumi **14b** un **37** ir iegūti arī kristāliski. Starp T_g un $T_{kuš}$ vērtībām nav korelācijas, kas liecina par ievērojamām telpiskās struktūras variācijām augstākās temperatūrās.

4. tabula

Sintezēto azohromoforu termiskās un optiskās īpašības

Savieno-jums	T_g, °C	$T_{kuš}$, °C	T_d, °C	Absorbcija CHCl₃[a]		Absorbcija EtOBz[a]	
				λ_{max}, nm	ε, M^{-1}·cm^{-1}	λ_{max}, nm	ε, M^{-1}·cm^{-1}
7	37	146	264	489	35 200	499	24 500
10a	—[b]	—[b]	269	478	29 600	484	26 100
10b	78	—[b]	285	478	25 400	483	27 300
10c	60	150	268	479	26 400	485	—[c]
14a	—[b]	112	239	481	27 700	483	25 500
14b	66	138	247	479	31 900	483	29 400
14c	45	193	242	480	30 500	483	25 100
19a	—[b]	—[b]	264	476	25 600	478	29 500
19b	55	—[b]	282	474	29 700	481	26 600
19c	41	100	265	475	30 200	481	28 800
24a	—[b]	—[b]	266	483	29 700	485	22 300
24b	63	—[b]	274	484	32 300	486	28 800
24c	37	105	267	483	32 700	486	31 300
33	44	132, 156[d]	260	483	30 000	482	30 200
34	53	147	282	479	28 900	481	30 800
35	60	166	287	482	32 900	486	29 800
36	58	119	284	480	26 600	487	31 600
37	79	103	277	480	29 300	486	36 800
38	46	130, 152[d]	288	479	26 800	482	29 800
39	60	103	286	476	32 100	484	31 500

[a] šķīduma koncentrācija 20 µmol·L^{-1};
[b] nav novērota;
[c] neizšķīst pilnībā;
[d] novēroti divi endotermiski maksimumi pirmajā sildīšanas ciklā.

Termiskā stabilitāte novērtēta, izmantojot sadalīšanās temperatūru (T_d), kad termogravimetrijas līknē ir novērojams masas zudums par 5 %. Visi sintezētie savienojumi ir stabili vismaz līdz 239 °C, augstākā T_d vērtība (288 °C) novērojama savienojumam **38**. Trt-grupa palielina molekulas termisko stabilitāti, un Trt-grupu saturošo vielu **10b**, **14b**, **19b** un **24b** T_d vērtības ir lielākas nekā to struktūras analogiem ar THP- un hidroksigrupām, kurām ir vienāda ietekme uz termisko stabilitāti. Augstu (282–288 °C) sadalīšanās temperatūru savienojumiem **34**, **36**, **38** un **39** nodrošina molekulas abās pusēs pievienotie (pentafluorfenil)metilgrupas un benzilgrupas saturošie dendroni. Pentafluorfeniloksifragmentu saturošajiem savienojumiem **14a–c** ir viszemākās T_d vērtības, salīdzinot ar pārējām savienojumu grupām.

Organisko molekulāro stiklu iegūšanai no sintezētajiem azobenzola atvasinājumiem nav piemēroti savienojumi, kas satur THP-grupas mazo T_g vērtību dēļ un hidroksi-, pentafluorfeniloksi- funkcionālās grupas, jo savienojumi neveido amorfu plāno kārtiņu, bet pēc šķīdinātāja iztvaicēšanas kristalizējas. Savukārt Trt- un (pentafluorfenil)metilgrupas saturošie dendroni ir piemēroti azobenzola hromoforu saturošo organisko molekulāro stiklu sintēzei, jo spēj veidot stabilas amorfas kārtiņas.

2.4. Optiskās īpašības

Lai sintezētajiem pentafluorfenilfragmentus saturošajiem azohromoforiem pētītu iespējamās iekšmolekulārās un starpmolekulārās mijiedarbības, tika reģistrēti gaismas absorbcijas spektri CHCl$_3$ un etilbenzoāta (EtOBz) šķīdumos (4. tab.). CHCl$_3$ un EtOBz šķīdinātājiem ir ļoti tuvas empīrisko polaritātes parametru vērtības [58], bet atšķirīgas iespējas mijiedarboties ar izšķīdušo hromoforu saturošo vielu. Pentafluorfenilgrupas un azobenzola fragmentu iekšmolekulārā Ar-Ar^F mijiedarbība mainītu azobenzola hromofora absorbcijas maksimuma viļņa garumu un intensitāti CHCl$_3$ šķīdumā attiecībā pret EtOBz šķīdumu, kurā pentafluorfenilgrupa varētu veidot Ar-Ar^F vai π-π mijiedarbības ar šķīdinātāja EtOBz molekulām.

Spektros novēroti gaismas absorbcijas maksimumi (λ_{max}) un intensitāte zemākās frekvences lādiņa pārneses joslai. Absorbcijas joslas redzamās gaismas diapazonā izskatās ļoti līdzīgas visiem pilnībā dendronizētajiem azohromoforiem, visievērojamākās atšķirības ir 250–350 nm diapazonā. Šī spektra daļa atbilst dendronizējošiem un fluorētos gredzenus saturošajiem fragmentiem, kas pētītajiem savienojumiem ir atšķirīgi (11. att.).

Azohromofora **7** absorbcijas maksimums (λ_{max}) ir batohromi nobīdīts abos šķīdinātājos, salīdzinot ar pārējiem savienojumiem (4. tab.), jo hromofora **7** molekulai nav kovalenti pievienoti dendronu fragmenti, kas varētu telpiski mijiedarboties ar azohromoforu un šķīdinātāja molekulām, kā tas ir pārējo pētīto savienojumu gadījumā.
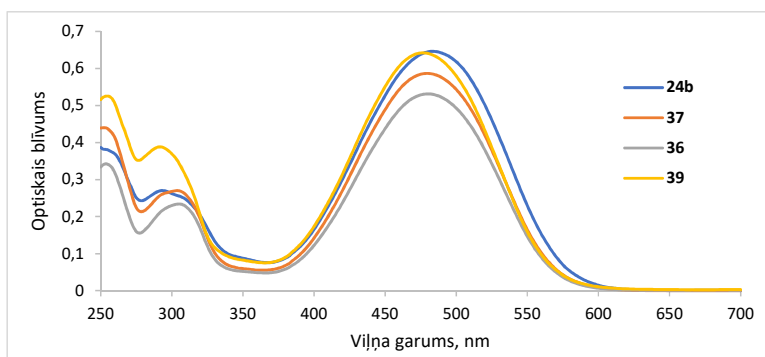
11. att. Dendronizēto azohromoforu **24b**, **36**, **37**, **39** absorbcijas spektri CHCl$_3$ šķīdumā ar parauga koncentrāciju 20 µmol·L^{-1}.

Zemākās frekvences lādiņa pārneses joslas absorbcijas maksimumi abos šķīdinātājos neatšķiras par vairāk nekā 3 nm katrā hromoforu sērijā **10a–c**, **14a–c**, **19a–c** vai **24a–c**. Tas nozīmē, ka dendronizējošā fragmenta terminālās grupas būtiski neietekmē hromofora absorbcijas enerģiju, to nosaka tikai kodola azohromofors, kas visos analizētajos savienojumos ir vienlīdz labi pieejams šķīdinātāja molekulām. Absorbcijas intensitāte mainās katrā hromoforu sērijā, lai gan molārie ekstinkcijas koeficienti (ε) ir vienas kārtas, kas atbilst viena un tā paša azohromofora esamībai molekulā (4. tab.).

Savienojumiem **19b,c**, **36**, **37** un **39** novērota vislielākā garāko viļņu λ_{max} nobīde, salīdzinot spektrus abos šķīdinātājos, tiem piemīt 6–8 nm hipsohroma nobīde CHCl$_3$ šķīdumā attiecībā pret EtOBz šķīdumu (4. tab.). To var skaidrot ar pentafluorfenilfragmentu kovalentu saistību pietiekami garā virknē vai caur dendrona fragmentu pie azohromofora donorās daļas un rezultējošo Ar-Ar^F mijiedarbību ar azohromofora akceptoro daļu, kad tās elektroni caur telpu tiek atvilkti un palielinās absorbcijai nepieciešamais enerģijas daudzums. Līdzīgi kā novērots savienojuma **36** monokristālā, visticamāk, iekšmolekulāras Ar-Ar^F vai π-π mijiedarbības var veidoties CHCl$_3$ šķīdumā, savukārt EtOBz šīs mijiedarbības izjūk. Savienojumu grupa **19a–c** izceļas ar hipsohromi nobīdītiem λ_{max} attiecībā pret pārējiem 4. tabulā redzamajiem savienojumiem abos šķīdinātājos, ko var izskaidrot ar (2-karboksietil)aminofragmentu pie azobenzola donorās daļas, kas vājina donoro spēku.

Cietas vielas gaismas absorbcijas spektri mērīti tikai to savienojumu plānajām kārtiņām, kurām veikti NLO mērījumi (5. tab.). Visiem savienojumiem spektros novērota batohroma nobīde cietā stāvoklī, salīdzinot ar spektriem CHCl$_3$ šķīdumos. Batohromā nobīde cietā stāvoklī, salīdzinot ar spektriem EtOBz šķīdumos, ir mazāka, savukārt savienojuma **37** spektrā novērota hipsohroma nobīde cietā stāvoklī, salīdzinot ar spektru EtOBz šķīdumā, kas, visticamāk, ir saistīts ar atšķirīgu savienojuma **37** molekulu sakārtošanos amorfajā kārtiņā, kas varētu būt saistīts ar azosavienojuma **37** NLO īpašībām. Maisījumu (**34 + 36**) un (**38 + 39**) absorbcijas maksimumi ir identiski komponentam, kura λ_{max} ir garākos viļņos. Netika novērots sagaidāmais mijiedarbības efekts divu savienojumu maisījumiem (**34 + 36**) un (**38 + 39**).

2.5. Nelineārās optiskās īpašības

NLO īpašības tika pārbaudītas savienojumiem **34**, **36–39** un abiem maisījumiem (**34 + 36**), (**38 + 39**), kas satur dendronus ar divām benzil- un/vai divām (pentafluorfenil)metilgrupām (sadarbības partneri LU Cietvielu fizikas institūtā *Dr. phys.* Mārtiņa Rutka vadībā). NLO īpašības mērītas arī Trt-grupas saturošajiem savienojumiem **10b** un **24b**. NLO īpašības netika pārbaudītas savienojumiem ar THP- un hidroksigrupām, jo tie neveido stabilas amorfas kārtiņas.

Otrās kārtas NLO koeficienti d_{33}, d_{31} un $d_{33}(0)$ izmantoti, lai raksturotu NLO īpašības organiskajiem molekulārajiem stikliem, kas iegūti no sintezētajiem savienojumiem. Plāno kārtiņu NLO koeficientu d_{33} un d_{31} novērtēšanai nepieciešams noteikt materiāla gaismas laušanas koeficientus n_{1064} un n_{532} pie pamata un otrās harmonikas viļņa garuma, kas apkopoti 5. tabulā. Tiek pieņemts, ka elektriskajā laukā orientētu organisko molekulāro stiklu plānajām kārtiņām piemīt $C_{\infty v}$ simetrija un materiālu var raksturot ar trim no nulles atšķirīgiem NLO koeficientiem – d_{33}, d_{31} un d_{15}. Saskaņā ar Kleinmana simetriju [59] tiek pieņemts, ka $d_{31} = d_{15}$. Tātad organisko molekulāro stiklu plāno kārtiņu raksturošanai pietiek ar diviem NLO koeficientiem, ko nosaka, iedarbojoties uz paraugu ar polarizētu lāzera starojumu.

Visi pētītie paraugi ir NLO aktīvi (5. tab.). Efektīvā hromofora fragmenta daļa molekulā (N) aprēķināta no molmasas, par efektīvo hromoforu pieņemot vienkāršotu metilatvasinājumu 4′-(dimetilamino)-2-metoksi-4-nitroazobenzolu. NLO koeficienti ir atkarīgi no aktīvā hromofora daļas, molekulārās hiperpolarizējamības un polārās kārtības. NLO koeficientu d_{33}/d_{31} attiecība parāda polāro kārtību orientētās hromoforu kārtiņās. Visiem vienu hromoforu saturošajiem paraugiem **10b**, **24b**, **34**, **36–39** šī attiecība ir 3,2 līdz 3,9 un liecina par augstu polāro kārtību [60]. Abi maisījumi (**34 + 36**) un (**38 + 39**) uzrāda ievērojami zemāku attiecību 2,2 un 2,0, kas liecina par sliktu hromoforu molekulu sakārtošanos, kā rezultātā rodas zemas NLO koeficientu d_{33} un $d_{33}(0)$ vērtības. Abu molekulu starpmolekulārās mijiedarbības šajos maisījumos var izpausties tādā veidā, lai veicinātu sistēmā esošo hromoforu centrosimetrisko sakārtošanos. Tā rezultātā samazinās arī attiecīgie NLO koeficienti. Iegūtie rezultāti ir pretēji literatūras datiem, kur komplementāru hromoforu maisījumam, kas satur vienus un tos pašus dendronus, ir vairāk nekā divas reizes lielāka elektrooptiskā koeficienta r_{33} vērtība nekā atsevišķiem komponentiem [10].

Dendronizētie azohromofori **10b**, **24b** ar Trt-grupām un dendronizētie azohromofori **36**, **39** ar (pentafluorfenil)metilgrupām, kas saistītas ar azohromofora donoro daļu, uzrādīja relatīvi labākus NLO koeficientus, kas pārsniedz LiNbO₃ koeficienta d_{33} vērtību. Tādēļ pētījumu nobeigumā tika sintezēts abus atšķirīgos dendronus saturošais azohromofors **37**. Pretēji gaidītajam, savienojuma **37** NLO koeficientu vērtības bija ļoti zemas. Tas skaidrojams ar savienojuma **37** lielākās daļas molekulu atrašanos centrosimetriskā sakārtojumā pat pēc orientēšanas, un tas samazināja NLO koeficienta vērtību. Arī pentafluorfenilgrupu un tritilgrupu starpmolekulārā Ar-Ar^F mijiedarbība stiklveida kārtiņā, visticamāk, notika, veicinot centrosimetrisko sakārtošanos.

Sintezēto organisko molekulāro stiklu amorfo plāno kārtiņu NLO īpašības

Paraugs	d_{33},[a] pm·V⁻¹	d_{31},[a] pm·V⁻¹	$d_{33}(0)$,[b] pm·V⁻¹	d_{33}/d_{31}	N,[c] %	T_{SHI50},[d] °C	n_{1064}[e]	n_{532}[e]	λ_{max}, nm kārtiņa
10b	38	—[f]	5,7	—[f]	17	90	1,60	2,04	495
24b	43	11	5,1	3,9	24	66	1,63	1,69	490
34	10	2,8	1,1	3,6	22	51	1,63	1,72	492
36	35	11	3,9	3,2	22	59	1,61	1,67	496
(34 + 36)	19	8,5	1,6	2,2	22	50	1,64[g]	1,72[g]	497
37	14	3,8	1,9	3,7	19	78	1,62	1,80	482
38	20	5,4	2,1	3,7	26	46	1,65	1,70	498
39	26	7,2	3,3	3,6	19	54	1,60	1,69	489
(38 + 39)	20	10	1,7	2,0	22	54	1,63[f]	1,70[f]	498

[a] NLO koeficienti noteikti pie 532 nm;

[b] NLO koeficents ekstrapolēts uz nulles frekvenci;

[c] efektīvā hromofora fragmenta daļa molekulā;

[d] temperatūra, pie kuras otrās harmonikas intensitāte ir 50 % no sākotnējās intensitātes;

[e] gaismas laušanas koeficients norādītajā viļņa garumā;

[f] nav noteikts;

[g] aprēķināts pēc Krāmera–Kroniga absorbcijas spektru transformācijas [61].

Savienojumam **24b** piemīt lielākā NLO koeficienta d_{33} vērtība un otra lielākā koeficienta $d_{33}(0)$ vērtība. Salīdzinot savienojuma **24b** un savienojumu **36**, **37** un **39** struktūru, var izvirzīt hipotēzi, ka viens pentafluorfenilfragments, kas saistīts īsā virknē, nespēj veidot iekšmolekulāru saiti ar azobenzolu, kā tas ir iespējams savienojumā **36**. Tas nozīmē, ka šajā gadījumā pentafluorfenilfragments, visticamāk, iesaistās Ar-Ar^F mijiedarbībā ar blakus esošo molekulu, palīdzot stabilizēt elektriskajā laukā orientēto hromoforu kārtību, kas veicina lielāku NLO koeficientu vērtību sasniegšanu.

Lai novērtētu hromoforu kārtības pēc orientēšanas elektriskajā laukā termisko stabilitāti plānās kārtiņās, tika izmantots *SHI* mērījums. Temperatūra T_{SHI50} (5. tab. un 12. att.) raksturo stāvokli, kad, sildot paraugu, sākotnējā *SHI* vērtība ir samazinājusies uz pusi un tā lielākoties labi saskan ar T_g mērījumiem. Atšķirības starp T_g un T_{SHI50} vērtībām varētu rasties no atšķirīga hromoforu molekulu sakārtojuma kausētā molekulārajā stiklā *DSC* eksperimenta laikā un orientētā organiskā molekulārā stikla kārtiņā, kas izlieta no šķīduma un kurā nevar izslēgt iesprostotu šķīdinātāja molekulu klātbūtni starp dendronu fragmentiem. Trijiem savienojumiem **10b**, **24b** un **36** T_{SHI50} vērtība ir nedaudz lielāka par T_g vērtību, un šiem savienojumiem izmērītas arī lielākās NLO koeficientu vērtības. Visticamāk, šiem savienojumiem ir atbilstoša molekulārā struktūra, kas nodrošina un veicina iekšmolekulāras un starpmolekulāras Ar-Ar^F un/vai π-π mijiedarbības, kas stabilizē orientēto necentrosimetrisko hromoforu kārtību plānās kārtiņās.
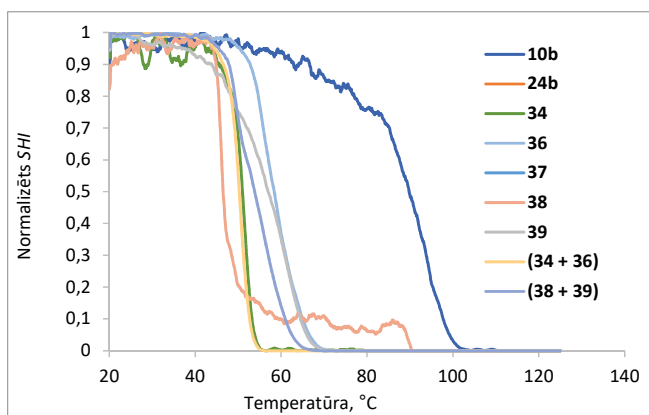
12. att. *SHI* signāla samazināšanās sildot NLO aktīvu amorfo molekulāro stiklu paraugus.

Oriģinālpublikācijas par šajā nodaļā aprakstītajiem pētījumiem – 1., 2. un 4. pielikumā, atsevišķi darba fragmenti publicēti konferences rakstā 6. pielikumā.

3. Poliazohromoforu organiskie molekulārie stikli

Tika pārbaudīta arī trešā pieeja NLO aktīvu savienojumu sintēzei, lai iegūtu stabilus organiskos molekulāros stiklus, kuru pamatā ir dažādas struktūras hromofori ar atšķirīgiem dipolmomentu virzieniem. Tika sintezēti dendroni, kas satur trīs hromoforus: divus vienādus D–π–A tipa azobenzola atvasinājumus un trešo atšķirīgas struktūras azobenzolu vai 1,3-indāndionilpiridīnija betaīnu (IPB). Pamatstāvoklī neitrāliem hromoforiem kā azobenzolam molekulārās hiperpolarizējamības un dipolmomenta vektoru virzieni sakrīt, bet pamatstāvoklī betaīna tipa hromoforiem kā IPB molekulārās hiperpolarizējamības un dipolmomenta vektoru virzieni ir pretēji [8]. Ja vienā molekulā vai materiālā kombinē pamatstāvoklī neitrālu un betaīna tipa hromoforu, molekulas robežās fragmenti orientētos, summārajam dipolmomentam pēc iespējas samazinoties, bet molekulārajai hiperpolarizējamībai summējoties [7, 8], un tā rezultātā NLO pētījumos pieaugtu orientēšanas efektivitāte un orientētās molekulu kārtības saglabāšanās laikā.

3.1. Poliazohromoforu dendronu sintēze

Sintezējamā dendrona struktūrā tika iekļauts azobenzola fragments un Trt-grupas. No azobenzola **40** ar divām identiskām hidroksigrupām tika iegūts atvasinājums **43**, kurā viena no hidroksigrupām pārvērsta par tritiloksi-, bet otra aktivēta ar mezilgrupu. Lai iegūtu tādu azobenzola molekulu, ir divi iespējamie ceļi: vai nu vispirms ievest mezilgrupu un pēc tam tritilgrupu, vai arī vispirms ievest tritilgrupu un pēc tam mezilgrupu. Tika izmēģinātas abas pieejas, ņemot izejvielas ekvimolāri. Kā sagaidāms, reakcijas beigās tika iegūts trīs vielu maisījums: izejviela, monoaizvietots produkts un diaizvietots produkts. Veiksmīgu preparatīvās hromatogrāfijas attīrīšanas procedūru izdevās realizēt tritilprodukta **41** gadījumā, tāpēc nepieciešamais azobenzols **43** tika sintezēts pēc 13. attēlā redzamās shēmas, iegūstot gandrīz kvantitatīvus iznākumus.
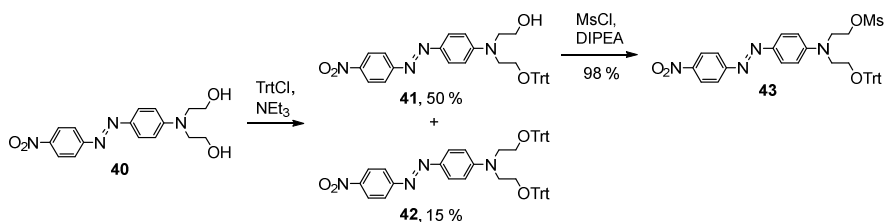
13. att. Azohromofora **40** abu hidroksigrupu funkcionalizēšana.

Alkilējot 3,5-dihidroksibenzoātu (**1**) ar azobenzola mezilatvasinājumu **43**, tika iegūts dendrons **D1Me**, kas satur divus vienādus azohromoforus (14. att.). Dendrons **D1Me** tika hidrolizēts ar NaOH DMF šķīdumā, starpprodukts nātrija sāls tika pārvērsts par skābi **D1OH**, izmantojot pietiekamas buferkapacitātes $HPO_4^{2-}/H_2PO_4^-$ buferšķīdumu ar aptuvenu pH vērtību 5, lai izvairītos no Trt-grupu hidrolīzes stipri skābā vidē.
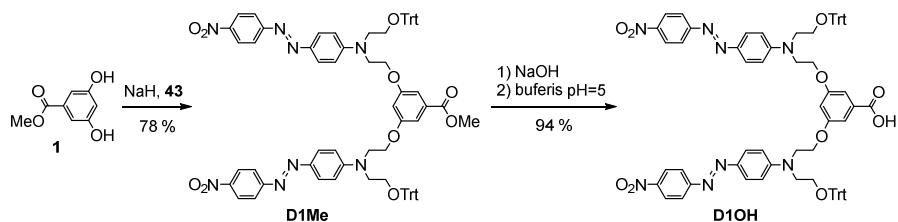
14. att. Dendronu **D1Me** un **D1OH** sintēzes.

Esterificējot karboksilgrupu saturošo azodendronu **D1OH,** iespējams tam kovalenti pievienot jaunus atšķirīgas struktūras hromoforus. Šādā veidā tika pievienots D–π–A tipa azobenzols **45**, kas tika iegūts, azosametinot betaīnu **5** ar *N,N*-dimetilanilīnu (**44**) etiķskābē (15. att.). Otrs pievienojamais hromofors ir 1,3-indāndionilpiridīnija betaīns **48**, kas tika iegūts, kondensējot izejvielas **46** un **47**.
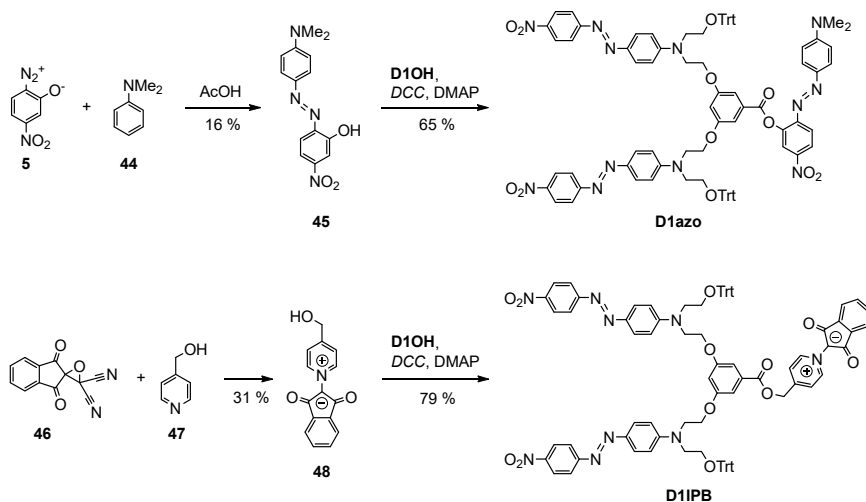
15. att. Dendronu **D1azo** un **D1IPB** sintēzes.

Esterificēšanas reakcija tika veikta, izmantojot *DCC*/DMAP metodi, un tika iegūti poliazohromofori dendroni **D1azo** un **D1IPB** (15. att.). Dendroni **D1azo** un **D1IPB** tika attīrīti, hromatogrāfējot tos Al₂O₃ kolonnā, lai procesa gaitā nenotiktu Trt-grupu atšķelšanās, kas iepriekš tika novērota hromatogrāfijas procesā uz silikagela.

3.2. Poliazohromoforu dendronu īpašības

Lai noskaidrotu sintezēto dendronu **D1Me**, **D1OH**, **D1azo**, **D1IPB** un to izejvielu hromoforu **45**, **48** fāžu pārejas, tika veikta termiskā analīze, izmantojot *DSC* un TGA (6. tab.). Hromofori **45** un **48** ir kristāliskas vielas, kas neveido amorfo fāzi un kūstot sadalās. Turpretī azohromofors **42**, kas reprezentē dendronu vienādos azohromofora zarus, tika iegūts gan

amorfā, gan kristāliskā formā. Otrās sildīšanas *DSC* līknē tam novērojamas sekojošas pārejas, T_g pie 81 °C, kam seko spontāna kristalizēšanās pie 166 °C, kušana pie 244 °C un sadalīšanās pie 286 °C, kas noteikta 5 % masas zuduma temperatūrā. T_g izdevās novērot tikai dendroniem **D1Me** un **D1IPB**. DSC līknes T_g raksturīgais pakāpiens bija mazāk izteikts kā 1. nodaļā aprakstītajiem azobenzola dendrimēriem un 2. nodaļā aprakstītajiem dendronizētajiem monoazohromoforiem, pat izmantojot līdzīgu parauga masu. Visi dendroni **D1Me**, **D1OH**, **D1azo** un **D1IPB** ir cietas, vismaz daļēji kristāliskas vielas, kas labi veido amorfo fāzi, ko var novērot, uzlejot caurspīdīgu un viendabīgu plāno kārtiņu. Sintezētajiem dendroniem **D1Me** un **D1IPB** ir konstatētas vislielākās T_g vērtības no visiem promocijas darbā aplūkotajiem savienojumiem, kas sasniedz un dendrona **D1IPB** gadījumā pat pārsniedz elektrooptisko ierīču izgatavošanā nepieciešamo 100 °C temperatūru [5]. Savukārt sintezēto savienojumu **D1Me**, **D1OH**, **D1azo** un **D1IPB** termiskā stabilitāte ir 240–267 °C robežās, kas ir mazāka kā iepriekšējās nodaļās aprakstītajiem savienojumiem.

6. tabula

Sintezēto produktu termiskās un optiskās īpašības

Savieno-jums	T_g, °C	$T_{kuš}$, °C	T_d, °C	λ_{max},[a] nm	ε, M^{-1}·cm^{-1}
42	81	244	286	488	25 200
45	—[b]	—[b]	264	509	45 400
48	—[b]	—[b]	240	409	43 800
D1Me	100	207	260	472	62 600
D1OH	—[b]	148	254	474	66 500
D1azo	—[b]	223	267	475	94 500
D1IPB	113	179	242	429	91 400

[a] CHCl$_3$ šķīdumā ar koncentrāciju 10 µmol·L^{-1};
[b] nav novērota.

Sintezētajiem poliazohromoforajiem dendroniem **D1Me**, **D1OH**, **D1azo**, **D1IPB** un hromoforiem **42**, **45**, **48** reģistrēti gaismas absorbcijas spektri CHCl$_3$ šķīdumā (6. tab.). Absorbcijas joslas intensitāte ir proporcionāla hromoforu skaitam molekulā [62], tātad, saskaitot vienkāršo izejvielu hromoforu ε vērtības, jāiegūst galaprodukta dendrona ε skaitliskā vērtība. Izmantojot šādu vienkāršu summēšanas novērtējumu, dendronu ε vērtība aptuveni atbilst aprēķinātajam.

Salīdzinot savienojumu **D1Me**, **48** un **D1IPB** spektrus CHCl$_3$, var redzēt, ka dendrona **D1IPB** absorbcijas josla pēc savas būtības ir divu joslu pārklāšanās, kas veidojas, summējot savienojumu **D1Me** un **48** spektrus (16. att.). Tomēr piridīnija betaīnam **48**, kas satur brīvo hidroksigrupu, spektra garāko viļņu absorbcijas maksimums ir hipsohromi nobīdīts attiecībā pret ar estera saiti saistīta betaīna fragmenta spektra absorbcijas maksimumu dendrona **D1IPB** sastāvā.
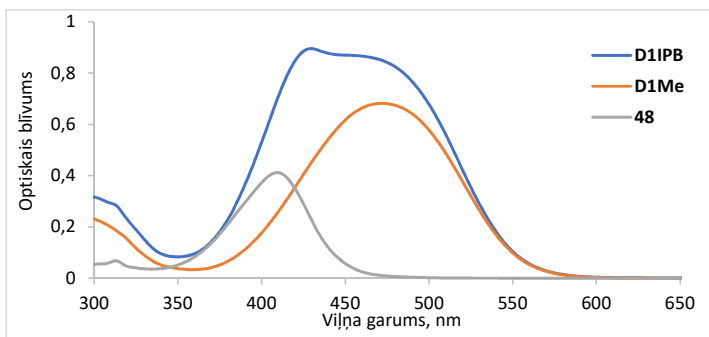
16. att. Dendrona **D1IPB** un tā sastāvdaļu spektri CHCl₃ ar 10 μmol·L⁻¹ koncentrāciju.

Savienojuma **D1IPB** spektri ir savdabīgi, un to forma ir atkarīga no izmantotā šķīdinātāja (17. att.). Dendrona **D1IPB** molekulā ir iesaistīti divi atšķirīgi hromofori: azobenzols, kam vērojama garo viļņu absorbcijas joslas batohroma nobīde, pieaugot šķīdinātāja polaritātei, un IPB, kam novērojama hipsohroma nobīde, pieaugot šķīdinātāja polaritātei. Šķīdinātāja polaritātei pieaugot, absorbcijas joslas batohromu nobīdi novēro, ja ierosinātais stāvoklis ir polārāks par pamata stāvokli, pretējā gadījumā novēro hipsohromu nobīdi [58]. Ņemot vērā to, ka abu veidu hromofori ir savienoti, izmantojot σ-saites, ievērojama elektronu blīvuma savstarpēja nobīde nav sagaidāma, līdz ar to, hromoforu joslām kombinējoties, dažādas polaritātes šķīdinātājos spektri būtiski atšķiras (17. att.). Nepolārajā šķīdinātājā toluolā, kur atsevišķo hromoforu λ_{max} vērtību atšķirība ir vismazākā, savienojuma **D1IPB** absorbcijas josla ir visšaurākā, un vērojams maksimums absorbcijas joslas īso viļņu pusē. Polārā šķīdinātājā kā DMSO, kur atsevišķo hromoforu λ_{max} vērtību atšķirība ir vislielākā, savienojuma **D1IPB** absorbcijas josla ir visplatākā, un vērojams maksimums absorbcijas joslas garo viļņu pusē. Vidēji polāros šķīdinātājos novērojamā aina visvairāk līdzinās diviem absorbcijas maksimumiem vai vienai platai absorbcijas joslai.
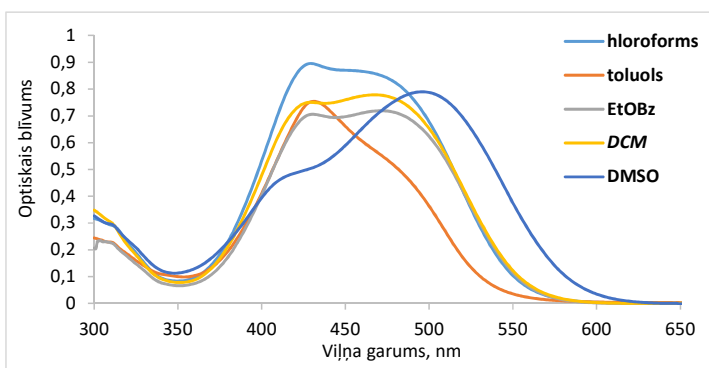
17. att. Dendrona **D1IPB** solvatohromija.

NLO īpašības pētītas sintezētajiem dažādus hromoforus saturošajiem dendroniem **D1azo** un **D1IPB** un azohromoforam **42**, nosakot elektriskajā laukā orientētām kārtiņām NLO

koeficientu d_{33}, orientēšanas termisko stabilitāti T_{SHI50} un aprēķinot $d_{33}(0)$ (7. tab.) (sadarbības partneri LU Cietvielu fizikas institūtā *Dr. phys.* Mārtiņa Rutka vadībā).

Vienkāršais tritilētais azohromofors **42** izrāda īpatnēju uzvedību karsēšanas laikā. Tā orientētai amorfai kārtiņai ir novērojama niecīga *SHI* vērtība, kas, paraugu karsējot apmēram 45 °C temperatūrā, izzūd, bet, turpinot karsēšanu, spontāni sākas kristalizēšanās. Veidojas azohromofora **42** necentrosimetriski sakārtoti kristāli, un pieaug *SHI*, maksimumu sasniedzot 127 °C temperatūrā. Tāda pati parādība novērojama, karsējot iepriekš neorientētu amorfo kārtiņu, taču tad azohromofora **42** kristalizēšanās sākas zemākā temperatūrā, maksimumu sasniedzot 111 °C temperatūrā. Tomēr izveidotās polikristāliskās kārtiņas ir necaurspīdīgas un neder praktiskajam lietojumam. Plēvītei, kas izveidota, savienojumu **42** iejaucot 10 % no masas poli(metilmetakrilātā) (PMMA), piemīt NLO aktivitāte, tomēr T_{SHI50} ir tikai 45 °C, kas ir gandrīz divreiz mazāka nekā savienojuma **42** T_g un apmēram trīsreiz mazāka nekā PMMA T_g. Tādēļ šīs parādības skaidrojums ir savienojuma **42** īpatnības, ko novēro jau tā plānajā kārtiņā.

7. tabula

Sintezēto organisko molekulāro stiklu plāno kārtiņu optiskās un NLO īpašības

Savienojums	$d_{33},$[a] pm·V^{-1}	$d_{33}(0),$[b] pm·V^{-1}	$T_{SHI50},$ °C	$\lambda_{max},$[d] nm
42[c]	26	3,3	45	487
D1azo	103	12	92	493
D1IPB	92	10	91	492

[a] NLO koeficients noteikts pie 532 nm;

[b] NLO koeficients ekstrapolēts uz nulles frekvenci;

[c] 10 % iejaukts PMMA matricā;

[d] absorbcijas maksimums mērīts plānai amorfai kārtiņai uz kvarca stikliņa.

Multihromoforus saturošie dendroni **D1azo** un **D1IPB** uzrāda mērenu NLO aktivitāti ar koeficienta d_{33} vērtībām apmēram 100 pm·V^{-1}, kas četras reizes pārsniedz LiNbO$_3$ koeficienta d_{33} vērtību. Tomēr šo savienojumu koeficienta d_{33} vērtības ir vidējs lielums starp dendrimēriem, kas aprakstīti 1. nodaļā, un abās azohromofora molekulas daļās dendronizētajiem savienojumiem, kas aprakstīti 2. nodaļā. Dendroniem **D1azo** un **D1IPB** ir visaugstākās T_{SHI50} vērtības starp darbā aplūkotajiem savienojumiem. Tomēr, atšķirībā no dendrona **D1IPB** T_g vērtības, tā T_{SHI50} vērtība nepārsniedz elektrooptisko ierīču darbībā nepieciešamo 100 °C temperatūru. Sintezēto dendronu struktūra ir piemērota NLO materiālu veidošanai tālākiem pētījumiem. Atšķirīgo hromoforu un telpiski izolējošo Trt-grupu mijiedarbība amorfajā stiklveida stāvoklī elektriskajā laukā veicina attiecīgā materiāla necentrosimetrisku orientāciju. Struktūras centrā esošais 3,5-dihidroksibenzoskābes fragments lieliski darbojas kā iekšmolekulāra izolējoša grupa, kas veicina necentrosimetriskās hromoforu kārtības saglabāšanos. Dendronam pievienotie azosavienojums un IPB ir atšķirīgi pēc struktūras, taču tiem nav atšķirīgas ietekmes uz dendronu **D1azo** un **D1IPB** NLO īpašībām, ko nosaka visa telpiskā dendrona struktūra kopumā, dodot augstas T_{SHI50} un d_{33} vērtības.

Šajā nodaļā aprakstītie pētījumi atrodami publikācijā 5. pielikumā.

SECINĀJUMI

1. (Pentafluorfenil)metilgrupu kovalenti saistīt pie hromofora fragmenta ir efektīvāk, izmantojot estera, nevis ētera saites. Esterificēšanas reakcijas lietošana ļauj izvairīties no spēcīgu nukleofīlu reaģentu izmantošanas, jo spēcīgs nukleofīls aizvietošanās reakcijā varētu aizvietot pentafluorfenilgrupas fluora atomus.

2. Ar rentgenstruktūranalīzes metodi pirmo reizi parādīta Ar-Ar^F mijiedarbība liela dendronizēta NLO aktīva azohromofora kristālā: pentafluorfenilfragments iekšmolekulāri mijiedarbojas ar azobenzola hromofora akceptoro daļu un azogrupu.

3. Tritilgrupu un (pentafluorfenil)metilgrupu izmantošana azohromoforu struktūrā paaugstina amorfās fāzes veidošanas spēju, kā arī stiklošanās un sadalīšanās temperatūras. Savukārt tetrahidropiranilgrupas klātbūtne samazina stiklošanās temperatūru zem 20 °C, bet hidroksigrupas un pentafluorfeniloksigrupas saturoši savienojumi neveido amorfu plāno kārtiņu.

4. Ja azohromofora donorā daļa ir kovalenti saistīta ar vienu pentafluorfenilgrupu pietiekami garā virknē vai ar divus pentafluorfenilfragmentus saturošu dendronu, novērojama relatīvi lielāka batohromā nobīde etilbenzoāta šķīdumā, salīdzinot ar CHCl$_3$ šķīdumu, ko var skaidrot ar iekšmolekulārām Ar-Ar^F vai π-π mijiedarbībām CHCl$_3$ šķīdumā.

5. Pat tad, ja azohromofora molekulā ietilpstošie fragmenti un funkcionālās grupas sinerģijas rezultātā nodrošina labas T_g un T_{SHI50} vērtības, tas nenozīmē, ka iespējamās Ar-Ar^F vai π-π mijiedarbības veicinās necentrosimetriskas kārtības izveidošanos elektriskajā laukā un lielus NLO koeficientus. Mijiedarboties spējīgo fragmentu savstarpējais novietojums var veicināt centrosimetriska azohromoforu sakārtojuma saglabāšanos organiskajā molekulārajā stiklā arī pēc orientēšanas.

6. Dendrona struktūrā savienojot trīs hromoforus un divas tritilgrupas, izdodas iegūt materiālu ar NLO koeficienta d_{33} vērtībām apmēram 100 pm·V^{-1} un visaugstākajām T_{SHI50} vērtībām (virs 90 °C) starp promocijas darbā pētītajiem savienojumiem.

PATEICĪBAS

Paldies maniem pirmajiem zinātniskā darba vadītājiem profesoram *Dr. habil. chem.* Valdim Kamparam un asoc. profesorei *Dr. chem.* Janai Kreicbergai par ievadīšanu interesantās azobenzola un dendrimēru sintēzes virzienā! Liels paldies profesoram *Dr. chem.* Valdim Kokaram par uzņemšanos vadīt manu promocijas darbu pēc *Dr. habil. chem.* Valda Kampara pēkšņās aiziešanas!

Paldies Lietišķās ķīmijas institūta kolektīvam par morālu un praktisku atbalstu darba sagatavošanā, it sevišķi Rūtai Kamparei par KMR spektru uzņemšanu, Kristīnei Lazdovičai par infrasarkano spektru iegūšanu un Ilzei Māliņai par elementu analīzes veikšanu! Izsaku pateicību Latvijas Universitātes Cietvielu fizikas institūta Organisko materiālu laboratorijas kolektīvam *Dr. phys.* Mārtiņa Rutka vadībā par ieguldījumu NLO mērījumu veikšanā. Paldies Latvijas Organiskās sintēzes institūta vadošajam pētniekam *Dr. phys.* Sergejam Beļakovam par kristālu rentgenstruktūranalīzes veikšanu!

LITERATŪRAS SARAKSTS

[1]   L. R. Dalton, P. A. Sullivan, D. H. Bale, *Chem. Rev.* **2010**, *110*, 25–55.

[2]   F. Ullah, N. Deng, F. Qiu, *PhotoniX* **2021**, *2*, 13.

[3]   J. Liu, W. Wu, *Symmetry (Basel).* **2022**, *14*, 882.

[4]   S.-H. Jang, A. K.-Y. Jen, *Chem. Asian J.* **2009**, *4*, 20–31.

[5]   J. Liu, C. Ouyang, F. Huo, W. He, A. Cao, *Dyes Pigm.* **2020**, *181*, 108509.

[6]   W. Wu, J. Qin, Z. Li, *Polymer (Guildf).* **2013**, *54*, 4351–4382.

[7]   Y. Liao, S. Bhattacharjee, K. A. Firestone, B. E. Eichinger, R. Paranji, C. A. Anderson, B. H. Robinson, P. J. Reid, L. R. Dalton, *J. Am. Chem. Soc.* **2006**, *128*, 6847–6853.

[8]   M. Rutkis, A. Tokmakovs, E. Jecs, J. Kreicberga, V. Kampars, V. Kokars, *Opt. Mater. (Amst).* **2010**, *32*, 796–802.

[9]   L. M. Salonen, M. Ellermann, F. Diederich, *Angew. Chemie – Int. Ed.* **2011**, *50*, 4808–4842.

[10] T.-D. Kim, J.-W. Kang, J. Luo, S.-H. Jang, J.-W. Ka, N. Tucker, J. B. Benedict, L. R. Dalton, T. Gray, R. M. Overney, et al., *J. Am. Chem. Soc.* **2007**, *129*, 488–489.

[11] X.-H. Zhou, J. Luo, S. Huang, T.-D. Kim, Z. Shi, Y.-J. Cheng, S.-H. Jang, D. B. Knorr Jr., R. M. Overney, A. K.-Y. Jen, *Adv. Mater.* **2009**, *21*, 1976–1981.

[12] T.-D. Kim, J. Luo, A. K.-Y. Jen, *Bull. Korean Chem. Soc.* **2009**, *30*, 882–886.

[13] W. Wu, G. Yu, Y. Liu, C. Ye, J. Qin, Z. Li, *Chem. – A Eur. J.* **2013**, *19*, 630–641.

[14] H. Ma, A. K.-Y. Jen, *Adv. Mater.* **2001**, *13*, 1201–1205.

[15] W. Wu, C. Li, G. Yu, Y. Liu, C. Ye, J. Qin, Z. Li, *Chem. Eur. J.* **2012**, *18*, 11019–11028.

[16] R. Deloncle, A.-M. Caminade, *J. Photochem. Photobiol. C Photochem. Rev.* **2010**, *11*, 25–45.

[17] S. Yokoyama, T. Nakahama, A. Otomo, S. Mashiko, *Chem. Lett.* **1997**, *26*, 1137–1138.

[18] S. Yokoyama, T. Nakahama, A. Otomo, S. Mashiko, *J. Am. Chem. Soc.* **2000**, *122*, 3174–3181.

[19] Y. Yamaguchi, Y. Yokomichi, S. Yokoyama, S. Mashiko, *J. Mol. Struct. THEOCHEM* **2002**, *578*, 35–45.

[20] Y. Yamaguchi, Y. Yokomichi, S. Yokoyama, S. Mashiko, *J. Mol. Struct. THEOCHEM* **2001**, *545*, 187–196.

[21] W. Zhang, J. Xie, W. Shi, X. Deng, Z. Cao, Q. Shen, *Eur. Polym. J.* **2008**, *44*, 872–880.

[22] W. Wu, L. Huang, C. Song, G. Yu, C. Ye, Y. Liu, J. Qin, Q. Li, Z. Li, *Chem. Sci.* **2012**, *3*, 1256–1261.

[23] W. Wu, Q. Huang, G. Xu, C. Wang, C. Ye, J. Qin, Z. Li, *J. Mater. Chem. C* **2013**, *1*, 3226–3234.

[24] R. Tang, S. Zhou, W. Xiang, Y. Xie, H. Chen, Q. Peng, G. Yu, B. Liu, H. Zeng, Q. Li, et al., *J. Mater. Chem. C* **2015**, *3*, 4545–4552.

[25] W. Wu, G. Xu, C. Li, G. Yu, Y. Liu, C. Ye, J. Qin, Z. Li, *Chem. Eur. J.* **2013**, *19*, 6874–6888.

[26] Z. Li, W. Wu, Q. Li, G. Yu, L. Xiao, Y. Liu, C. Ye, J. Qin, Z. Li, *Angew. Chemie - Int. Ed.* **2010**, *49*, 2763–2767.

[27] Z. Li, Q. Li, J. Qin, *Polym. Chem.* **2011**, *2*, 2723–2740.

[28] R. Tang, Z. Li, *Chem. Rec.* **2017**, *17*, 71–89.

[29] W. Wu, C. Wang, R. Tang, Y. Fu, C. Ye, J. Qin, Z. Li, *J. Mater. Chem. C* **2013**, *1*, 717–728.

[30] W. Wu, C. Wang, Q. Li, C. Ye, J. Qin, Z. Li, *Sci. Rep.* **2014**, *4*, 6101.

[31] W. Wu, C. Ye, J. Qin, Z. Li, *ACS Appl. Mater. Interfaces* **2013**, *5*, 7033–7041.

[32] Z. Li, G. Yu, W. Wu, Y. Liu, C. Ye, J. Qin, Z. Li, *Macromolecules* **2009**, *42*, 3864–3868.

[33] W. Wu, Z. Xu, Z. Li, *Polym. Chem.* **2014**, *5*, 6667–6670.

[34] D. N. Nikogosyan, *Nonlinear Optical Crystals: A Complete Survey*, Springer-Verlag, New York, **2005**.

[35] J. M. J. Frechet, D. A. Tomalia, Eds., *Dendrimers and Other Dendritic Polymers*, John Wiley & Sons, Ld: Chichester, **2001**.

[36] O. A. Matthews, A. N. Shipway, J. F. Stoddart, *Prog. Polym. Sci.* **1998**, *23*, 1–56.

[37] H.-F. Chow, T. K. K. Mong, M. F. Nongrum, C. Wan, *Tetrahedron* **1998**, *54*, 8543–8660.

[38] P. Patel, V. Patel, P. M. Patel, *J. Indian Chem. Soc.* **2022**, *99*, 100514.

[39] L. Laipniece, J. Kreicberga, V. Kampars, *Sci. Proc. RTU Mater. Sci. Appl. Chem.* **2008**, *16*, 88–99.

[40] G. Seniutinas, L. Laipniece, J. Kreicberga, V. Kampars, J. Gražulevičius, R. Petruškevičius, R. Tomašiūnas, *J. Opt. A Pure Appl. Opt.* **2009**, *11*, 034003.

[41] K. Traskovskis, I. Mihailovs, A. Tokmakovs, A. Jurgis, V. Kokars, M. Rutkis, *J. Mater. Chem.* **2012**, *22*, 11268.

[42] J. L. Oudar, D. S. Chemla, *J. Chem. Phys.* **1977**, *66*, 2664–2668.

[43] F. Cuétara-Guadarrama, M. Vonlanthen, K. Sorroza-Martínez, I. González-Méndez, E. Rivera, *Dyes Pigm.* **2021**, *194*, 109551.

[44] R. L. Tang, S. M. Zhou, Z. Y. Cheng, H. Chen, L. Deng, Q. Peng, Z. Li, *CCS Chem.* **2020**, *2*, 1040–1048.

[45] A. Hassner, V. Alexanian, *Tetrahedron Lett.* **1978**, *19*, 4475–4478.

[46] B. Neises, W. Steglich, *Angew. Chemie Int. Ed. English* **1978**, *17*, 522–524.

[47] N. Ono, T. Yamada, T. Saito, K. Tanaka, A. Kaji, *Bull. Chem. Soc. Jpn.* **1978**, *51*, 2401–2404.

[48] G. M. Brooke, *J. Fluor. Chem.* **1997**, *86*, 1–76.

[49] A. Armstrong, I. Brackenridge, R. F. W. Jackson, J. M. Kirk, *Tetrahedron Lett.* **1988**, *29*, 2483–2486.

[50] A. Nakazato, K. Sakagami, A. Yasuhara, H. Ohta, R. Yoshikawa, M. Itoh, M. Nakamura, S. Chaki, *J. Med. Chem.* **2004**, *47*, 4570–4587.

[51] Y. Xiang, B. Hirth, J. L. Kane, J. Liao, K. Noson, C. Yee, *Inhibitors of Sphingosine Kinase 1*, **2010**, WO2010033701 (A2).

[52] P. Hotchkiss, S. Marder, A. Giordano, T. D. Anthopoulos, *Electronic Devices Comprising Novel Phosphonic Acid Surface Modifiers*, **2010**, WO2010115854A1.

[53] C. S. Chiu, M. Saha, A. Abushamaa, R. W. Giese, *Anal. Chem.* **1993**, *65*, 3071–3075.

[54] W. Wu, Q. Huang, C. Zhong, C. Ye, J. Qin, Z. Li, *Polymer (Guildf).* **2013**, *54*, 5655–5664.

[55] Z. Li, P. Chen, Y. Xie, Z. Li, J. Qin, *Adv. Electron. Mater.* **2017**, 1700138.

[56] K. L. Wooley, C. J. Hawker, J. M. Pochan, J. M. J. Frechet, *Macromolecules* **1993**, *26*, 1514–1519.

[57] L. R. Dalton, P. A. Sullivan, D. H. Bale, S. Hammond, B. C. Olbricht, H. Rommel, B. Eichinger, B. Robinson, in *Tutorials in Complex Photonic Media*, SPIE, Bellingham, USA, **2007**, pp. 525–574.

[58] C. Reichardt, *Solvents and Solvent Effects in Organic Chemistry*, WILEY-VCH Verlag GmbH & Co. KGaA, Weinheim, **2003**.

[59] W. N. Herman, L. M. Hayden, *J. Opt. Soc. Am. B* **1995**, *12*, 416–427.

[60] R. Alicante, *Photoinduced Modifications of the Nonlinear Optical Response in Liquid Crystalline Azopolymers*, Springer Berlin Heidelberg, Berlin, Heidelberg, **2013**.

[61] K. Ohta, H. Ishida, *Appl. Spectrosc.* **1988**, *42*, 952–957.

[62] A.-M. Caminade, R. Laurent, J.-P. Majoral, *Adv. Drug Deliv. Rev.* **2005**, *57*, 2130–2146.

DOCTORAL THESIS PROPOSED TO RIGA TECHNICAL UNIVERSITY FOR THE PROMOTION TO THE SCIENTIFIC DEGREE OF DOCTOR OF SCIENCE

To be granted the scientific degree of Doctor of Science (Ph. D.), the present Doctoral Thesis has been submitted for the defence at the open meeting of RTU Promotion Council on May 18, 2023 at 14:00 at the Faculty of Materials Science and Applied Chemistry of Riga Technical University, 3 Paula Valdena Street, Room 272.

OFFICIAL REVIEWERS

Professor Dr. chem. Māris Turks,
Riga Technical University

Senior Researcher Dr. phys. Aivars Vembris
Institute of Solid State Physics, University of Latvia, Latvia

Senior Researcher Dr. chem. Aiva Plotniece
Latvian Institute of Organic Synthesis, Latvia

DECLARATION OF ACADEMIC INTEGRITY

I hereby declare that the Doctoral Thesis submitted for the review to Riga Technical University for the promotion to the scientific degree of Doctor of Science (Ph. D.) is my own. I confirm that this Doctoral Thesis had not been submitted to any other university for the promotion to a scientific degree.

Lauma Laipniece ....
                    (signature)
Date: ....

The Doctoral Thesis has been prepared as a collection of thematically related scientific publications complemented by summaries in both Latvian and English. The Doctoral Thesis includes four scientific publications and two publications in conference proceedings. The publications have been written in English, with the total volume of 72 pages, including supplementary data.

CONTENTS

Appendix 1:   L. Laipniece, V. Kampars, S. Belyakov, A. Bundulis, A. Tokmakovs, M. Rutkis. Utilization of amorphous phase forming trityl groups and Ar-Ar^F interactions in synthesis of NLO active azochromophores. *Dyes Pigm.*, **2022**, *204*, 110395.

Appendix 2:   L. Laipniece, V. Kampars, S. Belyakov, A. Tokmakovs, E. Nitiss, M. Rutkis. Dendronized azochromophores with aromatic and perfluoroaromatic fragments: Synthesis and properties demonstrating Ar-Ar^F interactions. *Dyes Pigm.*, **2019**, *162*, 394–404.

Appendix 3:   L. Laipniece, V. Kampars. Synthesis and Thermal Properties of Azobenzene Core Polyester Dendrimers with Trityl Groups at the Periphery. *Key Eng. Mater.*, **2018**, *762*, 171–175.

Appendix 4:   L. Laipniece, V. Kampars. Synthesis, thermal and light absorption properties of push-pull azochromophores substituted with dendronizing phenyl and perfluorophenyl fragments. *Main Group Chem.*, **2015**, *14*, 43–58.

Appendix 5: K. Traskovskis, E. Zarins, L. Laipniece, A. Tokmakovs, V. Kokars, M. Rutkis. Structure-dependent tuning of electro-optic and thermoplastic properties in triphenyl groups containing molecular glasses. *Mat. Chem. Phys.*, **2015**, *155*, 232–240.

Appendix 6: A. Tokmakovs, M. Rutkis, K. Traskovskis, E. Zariņš, L. Laipniece, V. Kokars, V. Kampars. Nonlinear Optical Properties of Low Molecular Organic Glasses Formed by Triphenyl Modified Chromophores. *IOP Conference Series: Materials Science and Engineering*, **2012**, *38*, 012034.

ABBREVIATIONS

ε	molar extinction coefficient
λ_{max}	wavelength of absorption maximum
Ar-Ar^F	aromatic-perfluoroaromatic fragments
d_{31}	nonlinear optical coefficient determined from the second harmonic generation intensity for p polarized light by irradiating the sample with s polarized light
d_{33}	nonlinear optical coefficient determined from the second harmonic generation intensity for p polarized light by irradiating the sample with p polarized light
$d_{33}(0)$	nonlinear optical coefficient d_{33} extrapolated to zero frequency
DBU	1,8-diazabicyclo[5.4.0]undec-7-ene
DCC	N,N'-dicyclohexylcarbodiimide
DCM	dichloromethane
DIAD	diisopropylazodicarboxylate
DIPEA	diisopropylethylamine
DMAP	4-(dimethylamino)pyridine
DMF	N,N-dimethylformamide
DMSO	dimethyl sulfoxide
DSC	differential scanning calorimetry
EtOBz	ethyl benzoate
HPLC	high performance liquid chromatography
IPB	1,3-dioxo-2-(pyridinium-1-yl)-2,3-dihydro-1H-indene-2-ide or 1,3-indane-dionylpyridinium betaine
mp	melting point
Ms	methanesulphonyl or mesyl
MS	mass spectrometry
n_{1064} and n_{532}	light refraction indices at the specified wavelength
NLO	nonlinear optics/nonlinear optical
NMR	nuclear magnetic resonance
PPTS	pyridinium p-toluenesulphonate
SHI	second harmonic generation intensity
S_NAr	nucleophilic aromatic substitution
TBAB	tetrabutylammonium bromide
THF	tetrahydrofuran
THP	tetrahydro-2H-pyran-2-yl
Trt	triphenylmethyl or trityl
T_d	thermal decomposition temperature – temperature at which the mass of the sample has decreased by 5 % in the thermogravimetric analysis
T_g	glass transition temperature
TGA	thermogravimetric analysis
T_{SHI50}	temperature at which the SHI decreases by 50 % of the initial intensity while heating the sample

GENERAL OVERVIEW OF THE THESIS

Introduction

The synthesis of organic nonlinear optical (NLO) chromophores and the properties of materials based on them belong to one of the modern research directions for the development of electro-optical materials and information carriers in the communication and photonics industries. New organic NLO materials, including those based on azochromophores, would allow for the creation of even more efficient information technology devices, such as electro-optical modulators, which could be potentially better than the existing devices of this type based on inorganic materials [1]–[3]. The main component of organic NLO materials is a polar chromophore fragment, which is covalently bound in a polymer chain or doped in a polymer as a molecular chromophore. It can also be covalently bound in a dendrimer structure or form organic molecular glasses – solid amorphous materials formed from molecules of a single organic compound. Polar chromophore is a molecule or a part of it, which is composed from an electron donor and an electron acceptor fragment that are covalently bound together by a conjugated π electron bridge, or D–π–A type chromophore, also known as a push-pull chromophore. Organic NLO chromophores could be modified to achieve easier processing of materials based on them and to ensure compliance with five main requirements at device application conditions: several times higher NLO coefficients than inorganic materials, high light refraction indices, excellent optical transparency, long-term stability of non-centrosymmetrically oriented dipoles, and high photochemical stability [1], [4], [5].

The second order NLO effect is observed only in a material with noncentrosymmetrically oriented chromophore dipoles, which is most often achieved by optical or electrical field poling. However, D–π–A type chromophores most often have large dipoles, and relaxation of dipoles takes place in the direction of centrosymmetric arrangement, reducing or erasing the NLO effect [1], [6]. Thus, in order to maintain the polar order, the amorphous NLO material must have the highest possible glass transition temperature (T_g), the chromophores must be isolated from each other to reduce the repulsion of electrical dipoles [1], [6], or appropriate intermolecular interactions between the fragments of molecules must be used to freeze the orientation of the chromophores after poling [1]. Another way of increasing the NLO coefficient of these modern materials is the formation of NLO chromophores whose summed dipole moments would not be large even at very high hyperpolarization characteristics, which can be achieved by using two chromophores with oppositely directed dipole moment vectors, but equally directed hyperpolarizability vectors. This way can effectively reduce the dipole moment of the entire molecule, the repulsion of molecules and the tendency to form centrosymmetrically oriented structures in the amorphous organic molecular glass phase [7], [8].

Perfluoroaromatic fragments are known to interact strongly with aromatic fragments of molecules in crystals, liquid crystals, supramolecular nanofibers, hydrogels, and even solutions [9]. The interactions of aromatic-perfluoroaromatic (Ar-Ar^F) fragments can be used to obtain noncentrosymmetrically arranged amorphous structures after orientation and thus increase their NLO properties [1], [4], [6], [10]–[13]. The synthesis of dendrimer and dendron

is used to obtain structures with spatially isolated chromophore having a large dipole moment and to improve the thermal properties of the material [1], [4], [14], [15]. Derivatives of 1,2-diphenyldiazene or azobenzene can be covalently linked to dendrons and dendrimers in different ways [16]: the azobenzene fragment can be covalently incorporated into the core, periphery, or entire branching of the dendron or dendrimer. The use of Ar-Ar[F] interactions and the introduction of dendrons into the molecule can be summed up using dendrons with aromatic and pentafluorophenyl fragments to increase the NLO coefficients and orientation stability of organic molecular glasses [10]–[12].

The NLO properties have been studied in most cases for dendrimers containing azobenzene fragments of D–π–A type along the entire branching of the dendrimer [17]–[21]. Extensive studies on azobenzene NLO dendrimers of D–π–A type have been conducted in prof. Zhen Li group [6], [13], [15], [22]–[33]. They also found an enhancement of NLO properties in azobenzene dendrons and dendrimers using Ar-Ar[F] interactions [13], [29]–[31]. NLO materials containing azochromophores of D–π–A type have not previously been studied if the chromophore is covalently bound in the core of a dendrimer or dendron.

Aims and Objectives

The aim of the Doctoral Thesis is to obtain and characterize new dendronized D–π–A type azochromophore derivatives, suitable for organic NLO materials, using dendron fragments with large aromatic and/or perfluoroaromatic fragments. Additional aim is to achieve the appropriate material properties – a glass transition temperature above 100 °C [5] and a NLO coefficient d_{33} value above 25.2 pm·V^{-1}, which would surpass the most efficient of the four most commonly used inorganic crystals, LiNbO$_3$ [34].

For the implementation of the aim of the Doctoral Thesis, the following objectives are set:

1) to carry out structural design and synthesize dendronized compounds containing one or more azobenzene fragments, which would have the properties of organic molecular glasses;

2) to characterize the thermal, optical, and NLO properties of synthesized compounds and materials;

3) to find out the relationships between the chemical structure of synthesized compounds and their physical properties, emphasizing the NLO properties.

Scientific Novelty and Main Results

In the Doctoral Thesis, three approaches are developed to the synthesis of organic NLO materials containing D–π–A type azochromophore. First, azobenzene core dendrimers are obtained, which formed NLO materials, where azochromophore fragments are separated from each other by the branching of the dendrimer, preventing the arrangement of the centrosymmetric chromophore order after orientation in the electric field. Second, the Ar-Ar[F] interaction of the dendronizing fragments containing phenyl group and pentafluorophenyl group has been used to stabilize the amorphous phase of organic molecular glass after orientation of its chromophores in the electric field. Third, the reduction of the total dipole

moment has been carried out for organic molecular glass containing several covalently bound chromophores, while increasing the molecular hyperpolarizability.

The Thesis describes the synthesis of new dendronized chromophores based on 4-amino-4′-nitroazobenzene and esters of 3,5-bis(2-hydroxyethoxy)benzoic acid or 3,5-dibenzyloxybenzoic acid and their derivatives as dendronizing fragments. The structures of synthesized compounds also include spatially voluminous trityl groups, which contribute to the formation of a solid amorphous phase for one-component organic molecular glass. Azobenzene derivatives with one or more pentafluorophenyl groups capable of forming intra- or intermolecular complexes with aromatic fragments have also been synthesized, stabilizing the noncentrosymmetric order of molecules after poling in an electric field and increasing NLO parameters. The X-ray analysis shows for the first time the intramolecular Ar-Ar^F interaction in the crystal of a large dendronized NLO active azochromophore, a stacking is observed of the pentafluorophenyl group with the azobenzene fragment. In the optical properties of the compounds containing pentafluorophenyl fragments, an Ar-Ar^F interaction was observed, which corresponds to the results of X-ray structural analysis. Dendrons are synthesized by covalently binding azochromophore to indanedionylpyridinium betaine or another azochromophore with oppositely directed fragment dipole moments.

The glass transition, melting and decomposition temperatures of all synthesized compounds were studied and the influence of dendron fragments and end groups of the molecule on the glass transition and decomposition temperatures of the compounds was characterized. The NLO properties of the synthesized compounds were determined: NLO coefficients d_{31} and d_{33}, which are determined by measuring the second harmonic generation intensity (SHI) for p polarized light by irradiating the sample with s or p polarized light, respectively, and the stability of NLO properties when heating the sample. It was found that as a result of the interaction of individual fragments of the molecule, the NLO properties can be both improved by stabilization of the noncentrosymmetric chromophore order and significantly impaired when the centrosymmetric chromophore order is stabilized. Due to the synergy of NLO properties of the investigated D–π–A type azochromophore and of the interacting molecular fragments, we obtained fifteen samples of dendronized azochromophores, of which the NLO coefficients of eight samples exceed the value of the widely used LiNbO$_3$ ($d_{33} = 25.2$ pm·V^{-1}).

Structure and Volume of the Thesis

The Doctoral Thesis has been prepared as a collection of thematically related scientific publications dedicated to the synthesis of azobenzene containing dendrimers and studies of their structure, optical, thermal, and NLO properties. The Doctoral Thesis includes six original publications in SCOPUS and/or Web of Science indexed scientific journals and conference proceedings.

Publications and Approbation of the Thesis

The results of the Doctoral Thesis are reported in 4 scientific publications and 2 full-text conference proceedings. The results of the research were presented at 10 conferences with 12 conference abstracts.

Scientific publications:

7. **L. Laipniece**, V.Kampars, S.Belyakov, A.Bundulis, A.Tokmakovs, M.Rutkis. Utilization of amorphous phase forming trityl groups and Ar-Ar^F interactions in synthesis of NLO active azochromophores. *Dyes Pigm.*, **2022**, *204*, 110395.

8. **L. Laipniece**, V. Kampars, S. Belyakov, A. Tokmakovs, E. Nitiss, M. Rutkis. Dendronized azochromophores with aromatic and perfluoroaromatic fragments: Synthesis and properties demonstrating Ar-Ar^F interactions. *Dyes Pigm.*, **2019**, *162*, 394–404.

9. **L. Laipniece**, V. Kampars. Synthesis and Thermal Properties of Azobenzene Core Polyester Dendrimers with Trityl Groups at the Periphery. *Key Eng. Mater.*, **2018**, *762*, 171–175.

10. **L. Laipniece**, V. Kampars. Synthesis, thermal and light absorption properties of push-pull azochromophores substituted with dendronizing phenyl and perfluorophenyl fragments. *Main Group Chem.*, **2015**, *14*, 43–58.

11. K. Traskovskis, E. Zarins, **L. Laipniece**, A.Tokmakovs, V.Kokars, M.Rutkis. Structure-dependent tuning of electro-optic and thermoplastic properties in triphenyl groups containing molecular glasses. *Mat. Chem. Phys.*, **2015**, *155*, 232–240.

12. A. Tokmakovs, M. Rutkis, K. Traskovskis, E. Zariņš, **L. Laipniece**, V. Kokars, V. Kampars. Nonlinear Optical Properties of Low Molecular Organic Glasses Formed by Triphenyl Modified Chromophores. *IOP Conference Series: Materials Science and Engineering*, **2012**, *38*, 012034.

Results of the Thesis have been presented in the following conference abstracts:

14. **L. Laipniece**, V. Kampars, A. Tokmakovs, A. Bundulis, M. Rutkis. Structurally perfect glassy azobenzene core first generation dendrimer and its non-linear optical properties. In: *Materials Science and Applied Chemistry 2019 Programme and Abstracts book*, Latvia, Riga, 24 October 2019. Riga: http://msac.rtu.lv/, 2019, p. 38.

15. **L. Laipniece**, V. Kampars, A. Ozols, P. Augustovs. Synthesis of Dendronized Chromophores and Holographic Recording in the Chromophores Containing Samples. In: *Abstracts of the 32nd Scientific Conference*, Latvia, Riga, 17–19 February 2016. Riga: Institute of Solid State Physics, University of Latvia, 2016, p. 120.

16. **L. Laipniece**, V. Kampars. Synthesis of dendronized azobenzene 2,3,4,5,6-pentafluorobenzyl ether. In: *Abstracts of the Riga Technical University 56th International Scientific Conference*, Latvia, Riga, 14–16 October 2015. Riga: RTU Press, 2015, p. 18.

17. **L. Laipniece**, V. Kampars. Light Absorption and Thermal Properties of Dendronized Azochromophores with Benzyl and 2,3,4,5,6-Pentafluorobenzyl Fragments. In: *Developments in Optics and Communications 2013, Book of Abstracts*, Latvia, Riga, 10–12 April 2013. Riga: University of Latvia, 2013, pp. 128–129.

18. Z. Kalniņa, A. Tokmakovs, I. Mihailovs, K. Traskovskis, **L. Laipniece**, M. Rutkis. Thermo-induced non-centrosymmetric crystal growth in glassy thin films of azobenzene chromophore. In: *Book of Abstracts of the 15th International Conference-School Advanced Materials and Technologies*, Lithuania, Palanga, 27–31 August 2013. Kaunas: 2013, p. 117.

19. A. Tokmakovs, M. Rutkis, K. Traskovskis, E. Zarins, **L. Laipniece**, V. Kokars, V. Kampars. Nonlinear optical properties of low molecular organic glasses formed by triphenyl modified chromophores. In: *Book of abstracts. International conference Functional materials and nanotechnologies 2012 (FM&NT-2012)*, Latvia, Riga, 17–20 April 2012. Riga: 2012, p. 196.

20. A. Tokmakovs, M. Rutkis, K. Traskovskis, E. Zarins, **L. Laipniece**, V. Kokars, V. Kampars. Properties of EO Active Molecular Glasses Based on Indandione and Azobenzene Chromophores. In: *Book of Abstracts of the 14th International Conference-School. Advanced Materials and Technologies*; Lithuania, Palanga, 27–31 August 2012. Palanga: 2012, p. 96.

21. V. Kampars, P. Pastors, J. Kreicberga, **L. Laipniece**, I. Neibolte, M. Plotniece, K. Teivena, R. Kampare. Nonlinear Optical Chromophores with 1,3-Indanedione Moiety. In: *Riga Technical University 53rd International Scientific Conference: Dedicated to the 150th Anniversary and the 1st Congress of World Engineers and Riga Polytechnical Institute/RTU Alumni: Digest*; Latvia, Riga, 11–12 October 2012. Riga: RTU, 2012, p. 227.

22. **L. Laipniece**, V. Kampars. Azobenzene Core Dendrimers with Trityl Groups in the Periphery. In: *Riga Technical University 53rd International Scientific Conference: Dedicated to the 150th Anniversary and the 1st Congress of World Engineers and Riga Polytechnical Institute/RTU Alumni: Digest*, Latvia, Riga, 11–12 October 2012. Riga: RTU, 2012, p. 229.

23. **L. Laipniece**, V. Kampars. Synthesis of Dendronized Azochromophores with Benzyl and 2,3,4,5,6-Pentafluorobenzyl Fragments. In: *Riga Technical University 53rd International Scientific Conference: Dedicated to the 150th Anniversary and the 1st Congress of World Engineers and Riga Polytechnical Institute/RTU Alumni: Digest*, Latvia, Riga, 11–12 October 2012. Riga: RTU, 2012, p. 230.

24. **L. Laipniece**, V. Kampars. Synthesis of azobenzene derivatives for research of arene-perfluoroarene interactions. In: *Abstracts of the 52nd International Scientific Conference of Riga Technical University. Section: Material Science and Applied Chemistry*, Latvia, Riga, 13–15 October 2011. Riga: RTU Publishing House, 2011, p. 20.

25. V. Kampars, J. Kreicberga, P. Pastors, M. Roze, S. Gaidukovs, K. Balodis, M. Plotniece, J. Sirotkina, **L. Laipniece**, N. Kiričenko, K. Pīterāne, L. Vesjolaja, G. Bērziņa,

B. Turovska, I. Muzikante, M. Rutks. Jaunu organisko hromoforu sintēze un to raksturojumi. No: *Apvienotais pasaules latviešu zinātnieku III un Letonikas IV kongress "Zinātne, sabiedrība un nacionālā identitāte". Sekcija "Tehniskās zinātnes". Tēžu krājums;* Latvija, Rīga, 24.–27. oktobris, 2011. Rīga: RTU Izdevniecība, 2011, 90. lpp.

MAIN RESULTS OF THE THESIS

1. Dendrimers with Azobenzene in the Core

1.1. Structure and Synthesis Methods of Dendrimers

Dendrimers are regularly branched macromolecules with a well-defined structure that determines the spherical, void-containing shape and inherent physical properties of the molecule [35]. The dendrimer is obtained in several sequential reactions; most synthesis techniques involve a constant series of reactions of dendrimer growth and replacement of functional groups in order to avoid uncontrollable polymerization. The dendrimer has three characteristic structural elements: the central part or core ($\triangleright$), branching ($\propto$), and the end groups or periphery (A, B, X, Y, ●) (Fig. 1) [35]. Dendrimers of different sizes of one type are divided into generations G1, G2, G3, etc., in the appropriate context, the core of the dendrimer often acquires the zero-generation G0 designation. There are two classical methods of dendrimer synthesis: divergent and convergent [35], [36].
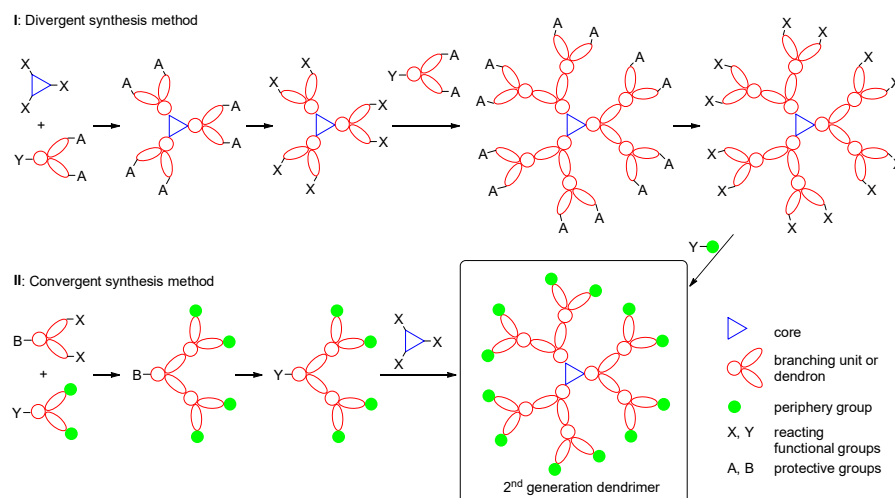
Fig. 1. Schematic representation of the structure of the second generation (G2) dendrimer and its divergent (I) and convergent (II) synthesis methods [35].

Historically, the divergent method was the first to be used in dendrimer synthesis (Fig. 1 I), where the molecule is formed starting with the core by adding a single layer of monomers with chemically inert periphery groups, which are afterwards activated to add the next layer. These two steps are repeated [35]. Any special functional groups or structures can be added to the periphery of the dendrimer, which are chosen depending on the intended research or application. The number of peripheral groups increases exponentially with each generation of dendrimer, so a potential problem is the formation of structural defects in large generations of

dendrimers, due to incomplete reactions of peripheral functional groups. In addition, the necessary excess of reagents for the success of the reaction may interfere in the purification of products [37].

In the convergent method, the synthesis of the dendrimer begins with the periphery and ends with the core (Fig. 1 II). The outer layers are gradually connected, acquiring branched structures called dendrons. When the dendrons reach the selected generation, they are attached to a suitable core and a dendrimer of the designed generation is obtained [35]. Convergent synthesis has a low probability of side reactions at each step, and the number of reactive groups required for dendron growth is easily controlled, so synthesis of monodisperse dendrimers with greater accuracy is possible, since purification at each step is simpler than in divergent synthesis [35], [36]. The greatest disadvantage of the convergent method is the steric hindrance of the core functional group in larger generations, which leads to very low yields of target dendrimer products [37].

The use of convergent or divergent synthesis is determined by the selected type of dendrimer branching and synthesis reaction, the stability of the functional groups of the periphery and core, and possible side reactions. By combining and refining these classical synthesis strategies, accelerated or exponential strategies suitable for the synthesis of large dendrimers have also been created, using a smaller total number of reactions and obtaining higher yields [36], [38].

1.2. Synthesis of Dendrimers with Azobenzene Core

In previous studies, we had synthesized azobenzene core dendrimers up to the third generation, forming a polyester branching by divergent synthesis with end hydroxy or tetrahydropyranyl (THP) groups [39]. We determined second-order hyperpolarizability in solution for obtained dendrimers with THP groups [40]. These dendrimers were obtained in the form of viscous waxes with glass transition temperature of 15–27 °C [39] and they could not be used to form solid amorphous films for NLO materials. Since the introduction of trityl (Trt) groups into molecules containing organic chromophores contributes to the ability of the entire compound to form solid amorphous films [41], we performed the synthesis of a dendritic branching unit that would have Trt groups at the periphery.

We had previously synthesized a 3,5-bis(2-hydroxyethoxy)benzoic acid derivative **3a** with THP end groups [39] (Fig. 2). According to analogous scheme, we performed a synthesis of dendron **3b** with Trt end groups (Fig. 2). We alkylated methyl 3,5-dihydroxybenzoate (**1**) with 2-(trityloxy)ethyl chloride in DMF solution with NaH base and obtained the compound **2c**, however, the reaction proceeded slowly and with a low yield. Most likely, the sterically large trityl group interferes with the nucleophilic substitution reaction in the –CH$_2$Cl fragment. Therefore, we used a different synthesis route, and compound **2a** was used to obtain methyl 3,5-bis(2-hydroxyethoxy)benzoate (**2b**), which was functionalized with Trt groups to produce the compound **2c**. By hydrolysing the ester group of compound **2c**, we obtained the necessary tritylated acid **3b**.
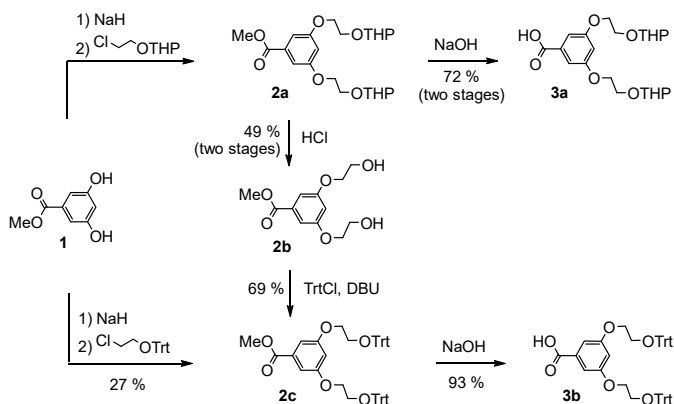
Fig. 2. Synthesis of derivatives of 3,5-dihydroxybenzoic acid.

Using divergent synthesis method, we functionalized peripheral hydroxy groups of dendrimers as Trt groups. In the reaction of the core **G0-OH** and the first-generation dendrimer **G1-OH** with trityl chloride in pyridine in the presence of triethylamine, we obtained the products **G0-Trt** and **G1-Trt**, respectively (Fig. 3). The compound **G0-Trt** was purified by crystallization and obtained with a medium yield and a high content of the target compound or principal substance. The analysis of the principal substance content of the samples was carried out by high performance liquid chromatography (HPLC). The zero-generation compound **G0-Trt** was synthesized to observe the so denoted "dendrimer effect" in the study of optical and thermal properties, which occurs by adding dendrimer branches to the core over several generations. We purified dendrimer **G1-Trt** using column chromatography, where we observed hydrolysis of the Trt groups on silica gel, as a result, we obtained only 37 % yield and the content of the principal substance was 50 %. In the dendrimer **G1-Trt** sample, without the target compound, there is also an azo compound of a similar structure that has hydrolysed one Trt group. Dendrimer **G2-Trt** was synthesized in analogous way from dendrimer **G2-OH** with trityl chloride in pyridine in the presence of triethylamine, but the resulting sample is a mixture of five substances (70–75 % in total) that have very similar structures. The isolated mixture, which we mark as **G2-Trt,** consists of both a principal substance and dendrimeric azo compounds with a smaller number of Trt groups probably due to the incomplete functionalization of hydroxy groups. One Trt group is missing on average throughout the dendrimer **G2-Trt** sample. The ratio of functional groups in the mixture is determined by the ^{1}H NMR spectrometry. The divergent synthesis of a third-generation dendrimer with peripheral Trt groups yielded a sample that is highly polydisperse with an average absence of six out of sixteen Trt groups, therefore the optical and thermal properties of the resulting sample will not be considered in the Doctoral Thesis.
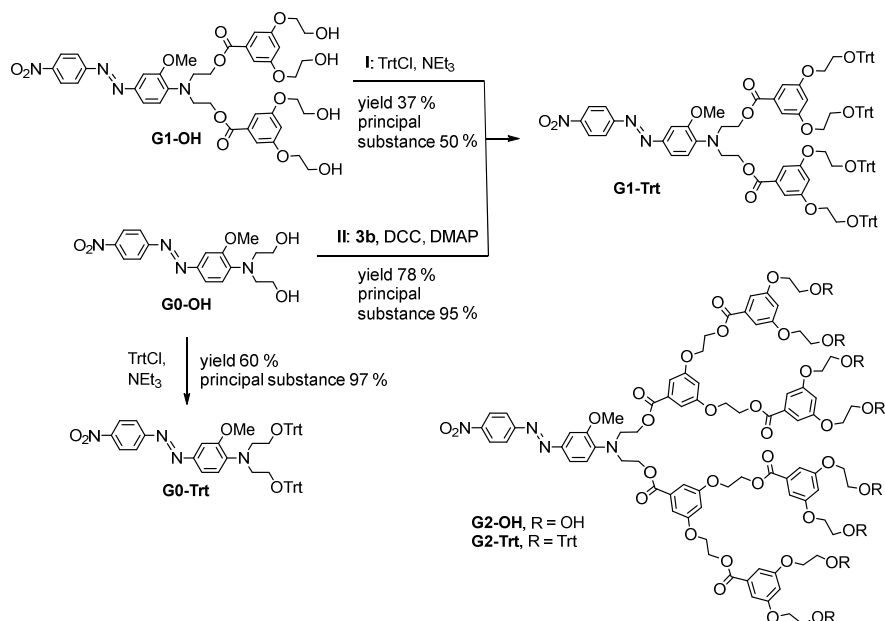
Fig. 3. Synthesis of compound **G0-Trt** and is divergent (I) and convergent (II) synthesis of dendrimer **G1-Trt**. Dendrimer structures of the second generation.

We concluded that the method of divergent synthesis has a significant drawback – with an increase in the number of end groups, it is difficult to ensure their complete functionalization. Therefore, the synthesis of dendrimers with Trt groups on the periphery could be carried out much more efficiently using the convergent method of dendrimer synthesis. In the esterification reaction of acid **3b** with the azo compound **G0-OH**, we obtained the dendrimer **G1-Trt** (Fig. 3 II), which we purified using fractional precipitation. Using the convergent synthesis technique, we synthesized dendrimer **G1-Trt** in one stage with a good yield (78 %) and a high content (95 %) of the principal substance, which is determined by HPLC and ^{1}H NMR spectrometry. It should be noted that this method is much more effective than the previously used divergent synthesis method, when we obtained the same dendrimer **G1-Trt** with a total yield of 37 %. The dendrimers **G1-Trt** and **G2-Trt** described in this work, obtained by divergent synthesis method, consist of several individual substances – principal substance and azo compounds of similar structure, all of which contain active azochromophore and insulating dendrimer branching, differing only in the exact peripheral hydroxy and Trt group ratio and position. Since the properties of interest are determined by the azo chromophore present in all materials, the synthesized products as materials are suited for further studies of their optical, thermal, and NLO properties.

1.3. Properties of Dendrimers with Azobenzene Core

For the synthesized products **G0-Trt**, **G1-Trt, G2-Trt** and their precursors **G0-OH**, **G1-OH, G2-OH**, the light absorption maxima (λ_{max}) and molar extinction coefficients (ε) in acetone correspond to the lowest frequency charge transfer transition band (Table 1). The absorption peaks of the compounds **G0-OH** and **G0-Trt** in acetone are batochromically shifted relative to the first and second generation dendrimers due to the lack of dendrimer branching and the local environment formed by it, which influences the absorption spectrum of the azohromophore both by electrostatic interactions and by spatially limiting the access of solvent molecules to the core azochromophore. On the other hand, when analyzing the data of dendrimers of the same generation with both end groups (Table 1, comparing rows 2 with 5 and 3 with 6), we do not observe the effect of the end groups on the absorption band, which indicates their relatively far position from the azochromophore fragment.

Table 1

Optical and Thermal Properties of Synthesized Dendrimers and their Starting Materials

Entry	Dendrimer	λ_{max},[a] nm	ε,[a] $M^{-1}{\cdot}cm^{-1}$	T_g, °C	mp, °C	T_d, °C
1	**G0-OH**	494	28 200	–	114	245
2	**G1-OH**	467	23 400	53	129	289
3	**G2-OH**	472	24 500	64	102	300
4	**G0-Trt**	490	26 000	73	198	288
5	**G1-Trt**	470	22 000	83	–	286
6	**G2-Trt**	471	24 500	85	–	294

[a] 30 μmol·L^{-1} in acetone solution.

We also studied the thermal properties of the synthesized products **G0-Trt**, **G1-Trt**, **G2-Trt** and their precursors **G0-OH**, **G1-OH, G2-OH** using differential scanning calorimetry (DSC) and thermogravimetric analysis (TGA). Thermal stability (T_d) is determined at a temperature of 5 % loss of mass, which is higher than 285 °C for first and second generation dendrimers (Table 1). The azo compound **G0-OH** is crystalline with a melting point (mp) of 114 °C, but glass transition temperature (T_g) was not observed even in the second stage of heating after rapid cooling of the molten sample. The azo compound **G0-OH** is also the most thermally unstable compound of those described, but the addition of Trt groups or dendrimer branching increases thermal stability. Dendrimers with Trt groups **G1-Trt**, **G2-Trt** are amorphous because they have a registered T_g but no mp was observed. Dendrimers **G1-OH, G2-OH** with hydroxy groups are crystalline, however, when molten samples are rapidly cooled, amorphous solid phase is formed and T_g can be detected at repeated heating. The T_g and T_d of the dendrimers increase with increasing dendrimer generation within the series, with the T_g of dendrimers with Trt end groups reaching 85 °C. The optical and thermal properties of dendrimers **G1-Trt** are practically the same, regardless of the degree of admixture of structurally similar azo compounds, or the ratio of the peripheral Trt and hydroxy groups, therefore Table 1 contains only data of dendrimer from convergent synthesis.

The NLO properties were different for the dendrimer **G1-Trt** obtained in divergent and convergent synthesis, so it was necessary to label differently products obtained by both synthetic strategies relating to the sample composition. Possibly differences were determined by the changes in the ratio of peripheral Trt and hydroxy groups. We denote the dendrimeric material obtained by convergent synthesis method as **G1-Trt-a,** and it contains the target compound with all four Trt groups. On the other hand, we denote the dendrimeric material obtained by divergent synthesis as **G1-Trt-b,** and it contains two azo compounds of similar structure in similar proportions, where one has all four Trt groups and the other has three Trt groups and one hydroxy group, which gives an average of 3.5 Trt groups and half hydroxy group. A sample of dendrimeric material **G2-Trt** contains an average of seven Trt groups and one hydroxy group.

NLO properties have been measured for three dendrimeric materials **G1-Trt-a**, **G1-Trt-b** and **G2-Trt** by determining the intensity of second harmonic generation (SHI) for thin amorphous poled films of these materials in the *Maker fringe* experiment (partners at the Institute of Solid State Physics, University of Latvia, under the leadership of Dr. phys. Mārtiņš Rutkis). High values of the NLO coefficient d_{33} were obtained (Table 2), which is explained by the presence of alkoxy substituents in the donor part of the azochromophore. All samples have wide absorption bands and an absorption maximum close to 500 nm, in addition, absorption band includes the second harmonic wavelength of 532 nm, which contributes to resonance enhancement of NLO efficiency. Since NLO coefficients depend on frequency, extrapolation to zero frequency ($d_{33}(0)$) according to the two-level model was performed to reduce its influence [42]. In the amorphous glassy film, the light absorption maxima for dendrimeric materials **G1-Trt-a**, **G1-Trt-b** and **G2-Trt** are bathochromically shifted by 14–18 nm compared to maxima in acetone solution, indicating aggregation of chromophore fragments in the solid phase [43].

Table 2

NLO Properties of Thin Amorphous Films of Dendrimer Materials

Entry	Dendrimeric material	Ratio of Trt and hydroxy groups	d_{33},[a] pm·V^{-1}	$d_{33}(0)$,[b] pm·V^{-1}	T_{SHI50},[c] °C	λ_{max},[d] nm
1	**G1-Trt-a**	4 Trt/0 OH	73	12	53	485
2	**G1-Trt-b**	3.5 Trt/0.5 OH	125	16	74	488
3	**G2-Trt**	7 Trt/1 OH	167	23	74	488

[a] NLO coefficient determined at 532 nm.

[b] NLO coefficient extrapolated to zero frequency.

[c] Temperature at which SHI is 50% of the initial intensity when the sample is heated.

[d] Absorption maxima measured for a thin amorphous film on a quartz glass.

Comparing the dendrimeric materials **G1-Trt-b** and **G2-Trt** obtained by divergent synthesis (Table 2, entries 2 and 3), it can be seen that the second-generation dendrimeric material **G2-Trt** has higher NLO coefficient d_{33} values than the first-generation dendrimeric material **G1-Trt-b**. This could be explained by better isolation of the azochromophore in the dendrimer branching, greater freedom to position itself parallel to the orienting electric field,

despite the decrease in the concentration of the chromophore in the molecule as the amount of dendron in the molecule increases. Dendrimeric materials **G1-Trt-a** and **G1-Trt-b** with different ratio of end groups were also compared (Table 2, entries 1 and 2). The dendrimeric material **G1-Trt-a** with four Trt groups shows only 58 % value of the NLO coefficient d_{33} comparing to the material **G1-Trt-b** with a Trt/OH group ratio of 3.5/0.5. The difference cannot be explained solely by the decrease in the mass fraction of the active chromophore in a more complete dendrimer structure, but the difference could be explained by the synergy of all fragments of the molecule interacting with each other. The purpose of using the convergent synthesis technique was not only to increase the yield of the final product, but also to obtain a chemically purer material or a material containing more of the target structure, this material should work more efficiently than the previously obtained sample, which is only partially functionalized with Trt groups. Contrary to expectations, all NLO properties of the convergently obtained sample of dendrimeric material **G1-Trt-a** (Table 2, entry 1) were weaker than those of the divergently obtained sample **G1-Trt-b** (Table 2, entry 2).

The temperature T_{SHI50} is determined in the NLO experiment, when simultaneously heating the sample and measuring the SHI, a halving of the SHI of the amorphous material is observed. The T_{SHI50} values of the divergently obtained dendrimeric materials **G1-Trt-b** and **G2-Trt** (Table 2, entries 2 and 3) are 8–9 °C lower than their T_g values, which can be explained by the different arrangement of molecules in the oriented NLO active film, allowing freer movements of the chromophore fragment than in an amorphous sample precipitated from solution. On the other hand, for the dendrimer sample **G1-Trt-a** (Table 2, entry 1) containing four Trt groups, T_{SHI50} value is 30 °C lower than corresponding T_g value, and even all NLO activity has disappeared before reaching T_g. Perhaps, the structure of the amorphous phase after orientation in the electric field is significantly different from the molten amorphous phase in DSC measurements, which results in a decrease in the amount of energy required for molecular motions and easy disorientation. The dendrimer material sample **G1-Trt-b** with a Trt/OH group ratio of 3.5/0.5 has a 20 °C higher T_{SHI50} value than the material **G1-Trt-a** with four Trt groups, which could be explained by the stabilization of the amorphous phase by free hydroxy groups and hydrogen bonds. Similar conclusions were made in Prof. Zhen Li group [44]. The above-mentioned stabilizing effect of the amorphous phase is most likely also the determining factor for high NLO coefficient d_{33} values. The NLO coefficients d_{33} of the synthesized dendrimer materials significantly exceed the values of the widely used $LiNbO_3$ crystal NLO coefficient values ($d_{33} = 25.2$ pm·V^{-1} [34]) using the same laser radiation wavelength of 1064 nm. However, the extrapolated coefficients $d_{33}(0)$ are smaller than the value of $LiNbO_3$ crystal coefficient but exceeds the NLO coefficient values of two other commonly used inorganic crystals $KTiOPO_4$ ($d_{33} = 14.6$ pm·V^{-1}) and LiB_3O_5 ($d_{33} = 0.04$ pm·V^{-1}) [34].

Original publications of the studies described in this chapter can be found in Appendices 1 and 3.

2. Dendronized Monoazochromophores

Since the dendrimers described in the previous chapter formed materials that mostly consisted of several azo compounds with similar structure, we decided to test the concept of isolating fragments of the active chromophore using addition of the dendron containing Trt groups described in Chapter 1 to one side of the azobenzene molecule. On the other side of the dendronized azochromophore molecule, we introduced pentafluorophenyl fragment, which, by engaging in intermolecular Ar-Ar^F interactions, could limit the mobility of molecules in the amorphous phase, raising T_g value and improving NLO parameters. We also synthesized dendronized azochromophores, in which the dendron containing Trt groups is replaced by a dendron containing THP or hydroxy groups, in order to understand the influence of the different fragments of the molecule on the material properties by comparing the optical and thermal properties.

With the aim of improving NLO parameters, we synthesized dendronized azochromophores using dendrons with two benzyl groups or two (pentafluorophenyl)methyl groups, which would interact with each other stabilizing the poled thin film. We added different dendrons in the donor or acceptor part of the azochromophore. To compare optical, thermal, and NLO properties, we also synthesized symmetrical azochromophores in a way that the same dendron fragments are connected to the azobenzene acceptor and donor parts. In the early stages of the studies, the dendron containing Trt group and the dendron containing (pentafluorophenyl)methyl group on the donor side of the azochromophore showed good thermal and NLO properties, so we chose to synthesize also an azochromophore that combines these two fragments.

2.1. Synthesis of Dendronized Azochromophores

2-Amino-5-nitrophenol (**4**) serves as starting material for all azo compounds described in this chapter. In diazotization reaction of aminophenol **4** (Fig. 4), we obtained diazonium betaine **5**, which is a photosensitive orange crystalline substance. We obtained azo compound **6** in the azo coupling reaction between betaine **5** and *N*-methylaniline with a low yield, although several azo coupling reaction conditions were tested. However, further alkylation of azo compound **6** with 2-chloroethanol to obtain product **7** failed to be realized, starting material **6** decomposed in basic environment.

We chose a different synthesis path for azo compound **7**. By alkylation of the compound **4** phenolate, we obtained 2-(2-chloroethoxy)-4-nitroaniline (**8**) with a 44 % yield (Fig. 4). The required two hydroxy groups containing azo compound **7** was obtained by diazoting compound **8** and executing azo coupling reaction with compound **9**. We synthesized symmetrically dendronized azochromophores **10a–c** from azocompound **7** and dendronizing fragments **3a,b** in esterification reaction using DCC and DMAP [45], [46]. We obtained hydroxy-containing azochromophore **10c** by deprotection of THP groups of compound **10a**.

Compounds **14a–c** with the pentafluorophenyl group in the acceptor part of the molecule are synthesized according to the scheme shown in Fig. 5. By alkylating compound **4** with mesyl derivative **11**, we obtained compound **12**, which was further diazotized and azo coupled with

aniline derivative **9** to obtain azochromophore **13**. The addition of dendronizing acids to compound **13** and the removal of THP groups were carried out in a similar way to the compounds **10a–c** described above, obtaining azochromophores **14a–c**.
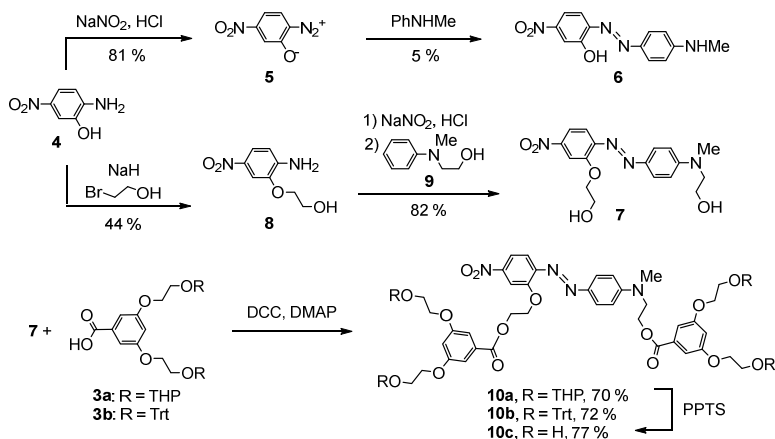

Fig. 4. Synthesis of symmetrically dendronized azobenzenes **10a–c**.
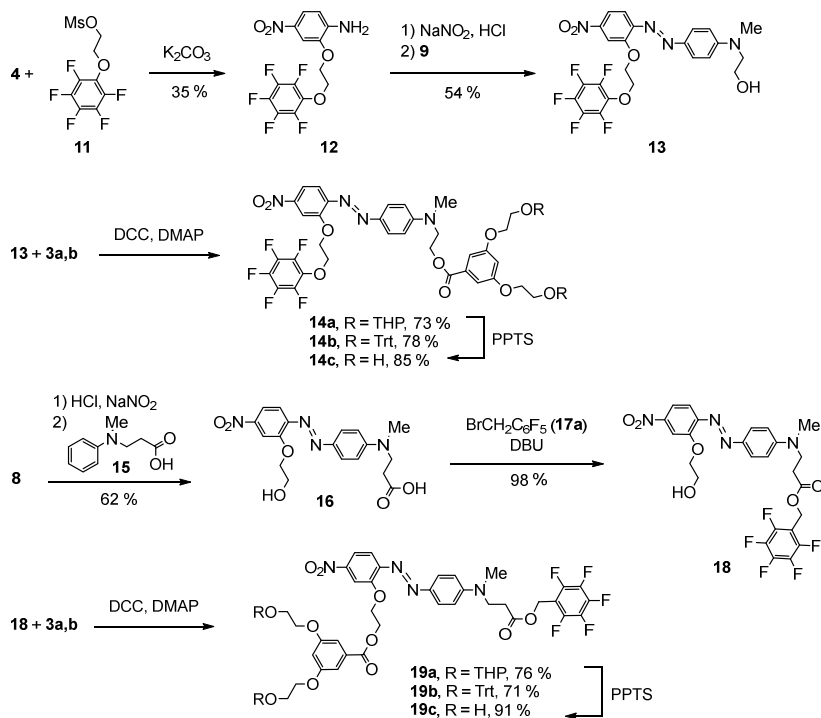

Fig. 5. Synthesis of azochromophores **14a–c** and **19a–c**.

For the synthesis of compounds **19a–c**, we first performed covalent bonding of the fluoroaromatic fragment and the azochromophore by means of an ester bond (Fig. 5). Aniline derivative **8** after diazotization entered into an azo coupling reaction with compound **15**, forming azobenzene **16**. Azobenzene **16**, which contains acid functionality at one end of the molecule and an alcohol group at the other, had to form two new ester bonds. First, using the DBU method [47], we treated compound **16** with bromide **17a** and quantitatively obtained the benzylated intermediate **18**. We obtained the target products **19a–c** using the same methods as in obtaining compounds **10a–c** and **14a–c**.

Compounds **24a–c** in which the fluoroaromatic fragment is covalently bound to the donor part of the azochromophore using benzylether type bond are synthesized according to the scheme shown in Fig. 6. Betaine **5** in azo coupling reaction with aniline derivative **9** gave azo compound **20**. By alkylating compound **20**, we obtained azocompound **21a**, from which the leaving group containing mesylate **21b** and trichloroacetimidate **21c** were further synthesized.
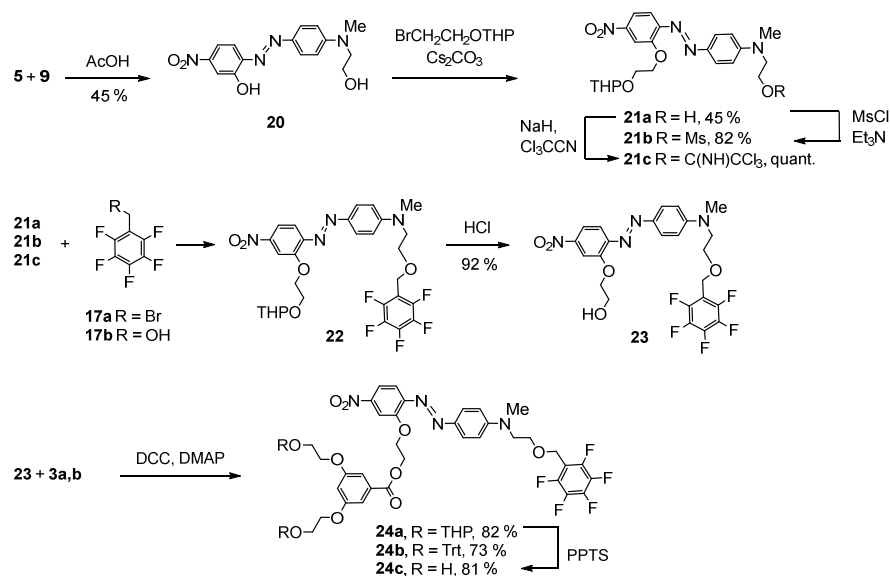
Fig. 6. Synthesis of azocompounds **24a–c**.

The reaction conditions for the synthesis attempts of compound **22** are summarized in Table 3. First, using Williamson's ether synthesis reactions, we tried to obtain compound **22** from azobenzene derivatives **21a,b** and various (pentafluorophenyl)methyl derivatives **17a,b** (Table 3, entries 1–3). However, the HPLC-MS analysis showed signs of the compound **22** only in the third experiment. Since undesirable side reactions such as nucleophilic aromatic substitution of the fluorine atom [48] are also possible, we tried to change the reaction conditions (Experiments 4–6), but even then the target product **22** did not form.

Table 3

Variations in Reaction Conditions for the Experiments of Obtaining the Compound **22**.

Entry	Reagents	Reaction conditions	Reference	Result
1	**21a**, **17a**	NaH, THF, 60 °C, 1 d.		S_NAr side reaction, product not observed
2	**21b**, **17b**	NaH, DMF, r. t., 2 d.		S_NAr side reaction, product not observed
3	**21a**, **17a**	NaN(SiMe$_3$)$_2$, DMF, 70 °C, 1 d.		S_NAr side reaction, signs of compound **22**
4	**21c**, **17b**	BF$_3$·Et$_2$O, CHCl$_3$, cyclohexane, r. t., 1 d.	[49]	product not observed
5	**21c**, **17b**	HOSO$_2$CH$_3$, CHCl$_3$, cyclohexane, r. t., 1 d.	[50]	product not observed
6	**21a**, **17a**	Ag$_2$O, DCM, r. t., 3 d.	[51]	side reaction, product not observed
7	**21a**, **17b**	DIAD, PPh$_3$, DCM, r. t., 1 d.		signs of compound **22**
8	**21a**, **17a**	TBAB, KOH, KI, THF, 70 °C, 1 d.	[52]	signs of compound **22**
9	**21a**, **17a**	TBAB, KOH, DCM, H$_2$O, r. t., 1 d.	[53]	compound **22**, 60 %

When the synthesis was performed under the conditions presented in Experiments 7 and 8, signs of the compound **22** was found by HPLC-MS. However, the compound **22** with 60 % yield was obtained in Experiment 9 by applying the appropriate reaction conditions [53]. The most significant difference of the experiment from all others is the high excess of the reagents to the compound **21a**: 20 equivalents of the compound **17a** and 40 equivalents of KOH. Bromide **17a** remains in the reaction mixture after the reaction and may be separated by chromatography and reused. We found that the high stoichiometric excess of reagents is of fundamental importance. Using compounds **17a** and **21a** in molar ratio 1.2:1, the reaction occurs, however, even after two days, the presence of starting materials was still observed in thin-layer chromatography. Removing the THP protective group from the compound **22** proceeded in hydrochloric acid solution, and the compound **23** was obtained with 92 % yield. Target compounds **24a–c** were obtained from compound **23** by previously applied methods.

In the synthesis of dendronized azochromophores **34**, **36–39** containing benzyl and (pentafluorophenyl)methyl groups, three stages can be distinguished: 1) synthesis of dendronizing fragments, 2) synthesis of azochromophore, 3) covalent binding of dendronizing fragments and azochromophore in a single compound. According to the scheme given in Fig. 7, we began with a known method of dendrimer synthesis [35], where compound **1** was alkylated with benzyl bromide (**25**) in phase transfer catalysis conditions and ester **26** was obtained. The hydrolysis of ester **26** under basic conditions gave acid **27** with 92 % yield.

The synthesis of fluorinated dendron **30** was realized differently from the synthesis of dendron **27** due to the instability of fluoroaromatic compounds in highly alkaline solutions [48]. 3,5-Dihydroxybenzoic acid (**28**) reacted with 1-(bromomethyl)-2,3,4,5,6-pentafluorobenzene (**17a**) to obtain a fully alkylated ester **29**, which was hydrolysed in boiling H$_2$SO$_4$/dioxane solution to form dendronizing acid **30** (Fig. 7).
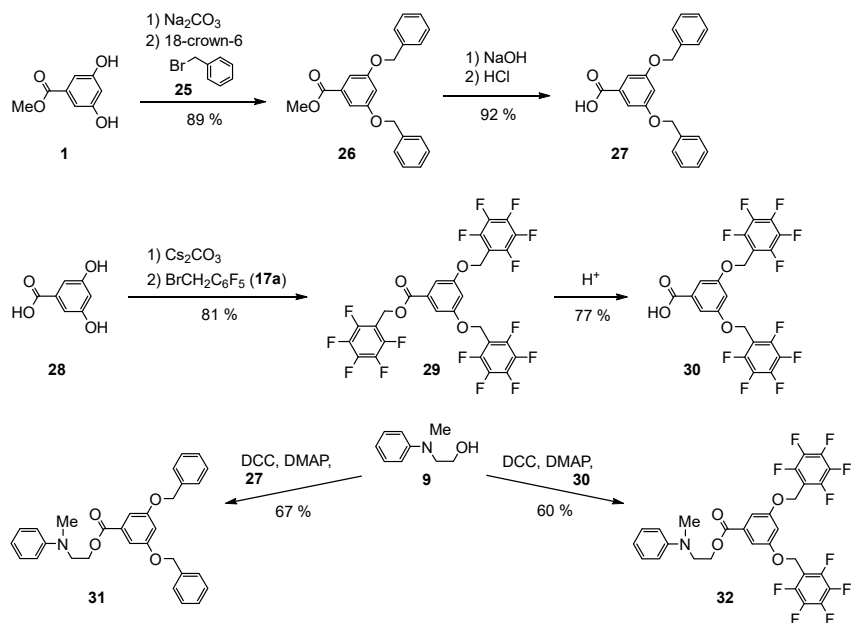
Fig. 7. Synthesis of precursors of dendronizing acids and chromophores.

The first step in the synthesis of asymmetric azochromophores **34**, **36**, and **37** was the dendronization of the chromophore precursor **9** (Fig. 7). Aniline derivative **9** reacted with each of the two dendronizing acids **27** and **30** using DCC and DMAP. The resulting esters **31** and **32** in the azo coupling reactions with aniline derivative **8** further formed the corresponding monodendronized azochromophores **33** and **35** (Fig. 8). Asymmetric chromophores **34** and **36** with different dendrons on each side of the molecule are derived from azo compounds **33** and **35** using DCC and DMAP with the corresponding dendronizing acids **30** and **27**. We also synthesized dendronized azochromophore **37** from azocompound **35** and acid **3b** using the carbodiimide method mentioned above (Fig. 8). Compound **37** was purified by precipitation from a DCM solution with methanol to preserve the hydrolytically unstable Trt groups in an acidic environment.
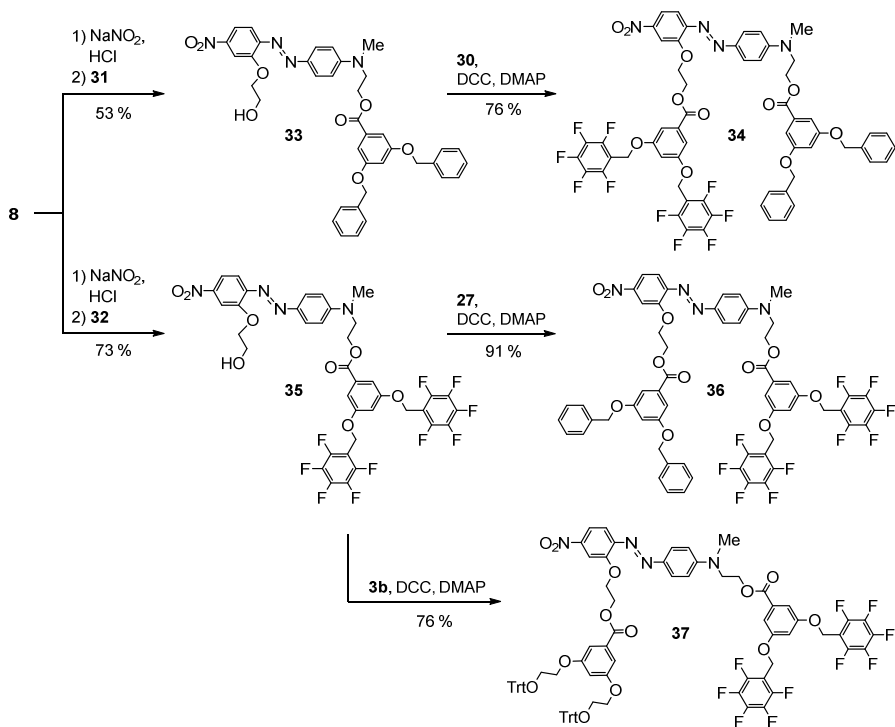
Fig. 8. Synthesis of nonsymmetrical dendronized azochromophores.

Synthesis of symmetrical azochromophores **38** and **39** with equal dendronizing fragments in the molecule was performed by esterification of azocompound **7** with acid **27** or **30** (Fig. 9).
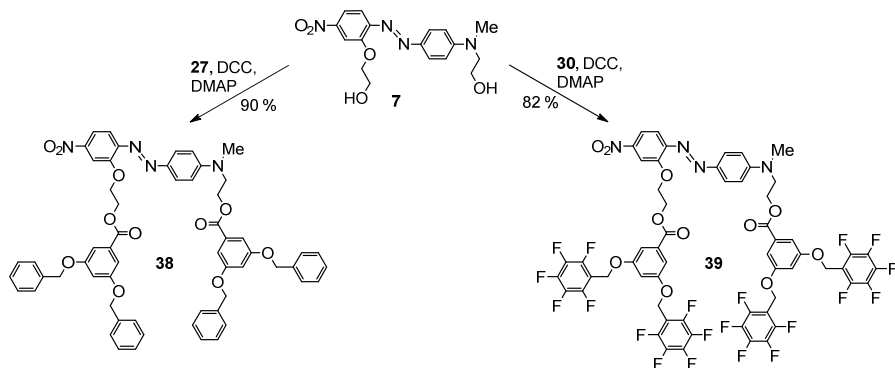

Fig. 9. Synthesis of symmetrical dendronized azochromophores.

2.2. Detection of Ar-Ar^F Interactions

For dendrimers containing azobenzene throughout the branching, Prof. Zhen Li studied the effect of Ar-Ar^F interactions on structure topologies and NLO properties [29], [30]. Based on ^{19}F NMR spectra and quantum chemical calculations, it was concluded that pentafluorophenyl fragment participates in intramolecular Ar-Ar^F interactions with the donor part of the azobenzene fragment [29], [30], [54], [55]. However, the results of X-ray analysis of azobenzene dendrimers and organic molecular glasses had not previously been published in the literature.

By slowly evaporating a DCM/ethyl acetate solution of dendronized azochromophore **36**, we obtained its monocrystals. In X-ray analysis (Dr. sc. phys. Sergey Belyakov) in these monocrystals, the intramolecular Ar-Ar^F interaction of the pentafluorophenyl fragment with the acceptor part of the azobenzene fragment was observed. Figure 10 shows two molecules of the compound **36** that form the crystal lattice of triclinic normal crystal system. The two dendrons of both these molecules containing benzyl and pentafluorphenyl rings bind intermolecularly through the Ar-Ar^F and aromatic π-π interactions, while one of the pentafluorophenyl fragments interacts intramolecularly with the acceptor part of azobenzene and the azo group. The crystalline structure is also stabilized by intermolecular CH···F and CH···O interactions. However, in the crystal, a partial fragment disorder of the molecule is observed, and the solvent molecules are also disordered. It may not have been possible to obtain monocrystals of other dendronized azo compounds due to the disorder.
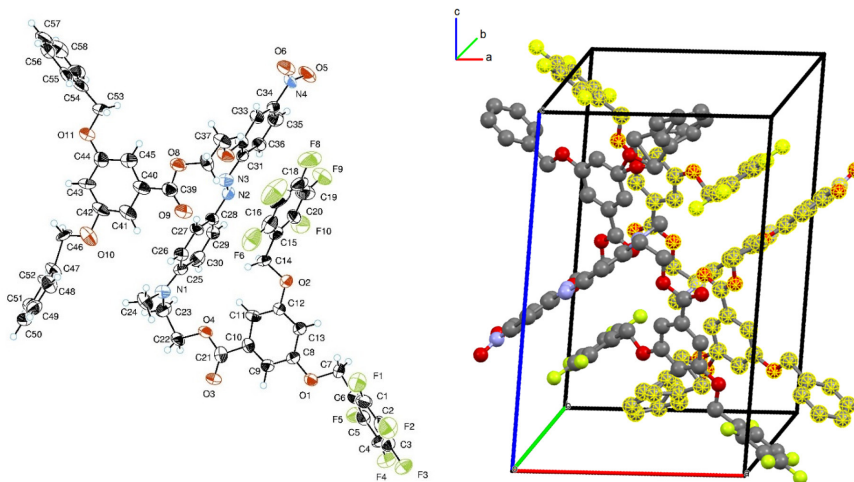

Fig. 10. The ORTEP drawing of the molecule **36** with thermal ellipsoids in 50 % probability (left) and the position of two molecules of the compound **36** (one is marked) in the crystal lattice (right).

2.3. Thermal Properties

We determined and analyzed the thermal properties of the synthesized compounds, looking for relationships between the structural elements of the synthesized molecules and their glass transition, melting, and decomposition temperatures. We used the data obtained from the DSC and TGA experiments, which are summarized in Table 4. If various structurally different fragments are included in the same molecule, T_g value of such a compound depends on the properties of all the various fragments included [56]. The purpose of adding pentafluorophenyl fragments to the structure of synthesized azochromophores was to stabilize the position of the oriented molecules by means of intermolecular Ar-Ar^F interactions in the amorphous film for NLO measurements. Similar to what is described in the literature for NLO active organic molecular glasses containing phenyl and pentafluorophenyl groups [10], this could be observed as an increase in T_g and T_{SHI50} values compared to analogous compounds that have phenyl groups instead of pentafluorophenyl fragments.

We observed that the presence of THP groups strongly lowers T_g values. It was not possible to observe T_g values for any of the compounds **10a**, **14a**, **19a**, and **24a** within the operating range of the equipment (15–1000 °C). For all other compounds studied, T_g value is higher than 20 °C. The smallest azochromophore **7** has the lowest T_g value (37 °C), which can be elevated by functionalization of the structure of the azochromophore with dendrons and fragments containing pentafluorophenyl group. The addition of a dendron with terminal hydroxy groups (in compounds **14c**, **19c**, and **24c**) and a dendron with benzyl groups (in compounds **33** and **38**) to the core azobenzene gives approximately the same and insignificant increase in T_g value by 0–9 °C. In turn, the use of two dendrons with terminal hydroxy groups in the compound **10c** gives a relatively high T_g value of 60 °C. Significantly T_g value is increased by the Trt group containing dendron in compounds **14b**, **19b**, and **24b**, but the presence of two such dendrons in compound **10b** gives an increase of T_g value by 41 °C.

Two binary equimolar blends of azo compounds (**34+36**) and (**38+39**) were prepared: from compounds **34** and **36**, and from compounds **38** and **39**. These blends were used for the study of Ar-Ar^F interactions to compare their thermal and NLO properties with thin films of azohromophores **34**, **36**, **38**, **39**. The blends (**34+36**) and (**38+39**) showed identical T_g values (55 °C), which was approximately the average of their constituents. We expected that the two components of the mixture would interact and T_g value would be greater than T_g values of the individual components as described in the literature [10], but no such effect was observed. The dendron containing the benzyl group is not determinative, since the highest T_g values between azochromophores **33–39** are observed for compounds **35**, **37**, and **39**, to which the dendron containing the (pentafluorophenyl)methyl group is attached to the donor part of the azochromophore. This can be explained by the Ar-Ar^F interaction between pentafluorophenyl fragments and azobenzene instead of benzyl fragments, which is clearly shown by the crystal structure of the compound **36**. The highest T_g value is observed by combining the dendron containing Trt groups with the dendron containing the (pentafluorophenyl)methyl group in the donor part of the azochromophore in compound **37**, the structure design of which was carried out on the basis of the beforehand obtained T_g values of compounds **10b**, **36**, and **39**.

The compounds obtained in the Thesis have lower T_g values than is required for the design of existing electro-optical devices [57]; however, materials with similar T_g value have a potential for use at low temperatures. High T_g value is required for materials used at room or higher temperature, while materials with low T_g value may be suitable for use at temperatures prevailing in the Arctic or Antarctic [27].

Table 4

Thermal and Optical Properties of Synthesized Azochromophores.

Compound	T_g, °C	mp, °C	T_d, °C	Absorption in CHCl₃[a]		Absorption in EtOBz[a]	
				λ_{max}, nm	ε, $M^{-1}\cdot cm^{-1}$	λ_{max}, nm	ε, $M^{-1}\cdot cm^{-1}$
7	37	146	264	489	35 200	499	24 500
10a	_[b]	_[b]	269	478	29 600	484	26 100
10b	78	_[b]	285	478	25 400	483	27 300
10c	60	150	268	479	26 400	485	_[c]
14a	_[b]	112	239	481	27 700	483	25 500
14b	66	138	247	479	31 900	483	29 400
14c	45	193	242	480	30 500	483	25 100
19a	_[b]	_[b]	264	476	25 600	478	29 500
19b	55	_[b]	282	474	29 700	481	26 600
19c	41	100	265	475	30 200	481	28 800
24a	_[b]	_[b]	266	483	29 700	485	22 300
24b	63	_[b]	274	484	32 300	486	28 800
24c	37	105	267	483	32 700	486	31 300
33	44	132, 156[d]	260	483	30 000	482	30 200
34	53	147	282	479	28 900	481	30 800
35	60	166	287	482	32 900	486	29 800
36	58	119	284	480	26 600	487	31 600
37	79	103	277	480	29 300	486	36 800
38	46	130, 152[d]	288	479	26 800	482	29 800
39	60	103	286	476	32 100	484	31 500

[a] Concentration of the solution 20 µmol·L⁻¹.
[b] Not observed.
[c] Does not dissolve completely.
[d] Two endothermic peaks are observed in the first heating cycle.

The crystalline phase is formed by all compounds containing hydroxy group, pentafluorophenyloxy group, and dendrons containing benzyl or (pentafluorophenyl)methyl groups. The crystalline nature is most likely determined by the possibility of the formation of stabilizing hydrogen bonds, as well as the Ar-Ar^F and CH···F interactions. The pentafluorophenyloxy group has a strong tendency to order in crystalline state, as a result of which the compound **14a** is the only crystalline compound containing the THP group, the rest are amorphous and soft at room temperature. In the second heating cycle, spontaneous crystallization is observed in DSC analysis for compounds **7** and **14c**, the latter also having the highest observed mp of 193 °C, possibly summing up the effects of hydrogen bonds and Ar-Ar^F

interactions. Most of the compounds with the Trt group are amorphous solids, but compounds **14b** and **37** are also obtained crystalline. There is no correlation between T_g value and *mp*, indicating significant variations in spatial structure at higher temperatures.

Thermal stability is estimated using the decomposition temperature (T_d), when a mass loss of 5 % is observed in the thermogravimetry curve. All synthesized compounds are stable to at least 239 °C, the highest T_d value of 288 °C is observed for compound **38**. The Trt group increases the thermal stability of the molecule, and the substances **10b**, **14b**, **19b**, and **24b** with the Trt group have greater T_d values than their structural analogues with OH and THP groups, which have the same effect on thermal stability. Compounds **34**, **36**, **38**, and **39** have high T_d values (282–288 °C) due to (pentafluorophenyl)methyl and benzyl groups containing dendrons on both sides of the molecules. Pentafluorophenyloxy fragment containing compounds **14a–c** have the lowest T_d compared to other groups of compounds.

For the use as organic molecular glasses from the synthesized azobenzene derivatives, compounds containing THP groups are not suitable due to the small T_g values, and the hydroxy, pentafluorophenyloxy functional groups are not suitable, since the compounds do not form an amorphous thin film but crystallize after evaporation of the solvent. In turn, dendrons containing Trt and (pentafluorophenyl)methyl groups are suitable for the synthesis of organic molecular glasses containing azobenzene chromophores due to their ability to form stable amorphous films.

2.4. Optical Properties

In order to study possible intramolecular and intermolecular interactions with synthesized pentafluorophenyl fragments of azochromophores, light absorption spectra were recorded in $CHCl_3$ and ethyl benzoate (EtOBz) solutions (Table 4). The $CHCl_3$ and EtOBz solvents have very close values of empirical polarity parameters [58], but different possibilities for interaction with the dissolved chromophore-containing substance. The Ar-Ar^F intramolecular interaction of the pentafluorophenyl group and the azobenzene fragments would change the wavelength and intensity of the absorption peak of azobenzene chromophore in $CHCl_3$ solution relative to the EtOBz solution in which the pentafluorophenyl group could form Ar-Ar^F or π-π interactions with solvent EtOBz molecules.

The spectra show maxima of light absorption (λ_{max}) and the intensity of the lower frequency charge transfer band. Absorption bands in the visible light range look very similar to all fully dendronized azochromophores, the most noticeable differences are in the range of 250–350 nm, this part of the spectrum corresponds to dendronizing and fluorinated ring containing fragments, which are different for the studied compounds (Fig. 11).

The absorption band (λ_{max}) of azohromophore **7** has batochromic shift in both solvents compared to the other compounds (Table 4), since the chromophore **7** molecule does not have covalently attached dendron fragments that could spatially interact with azochromophore and solvent molecules, as in the case of the other compounds studied.
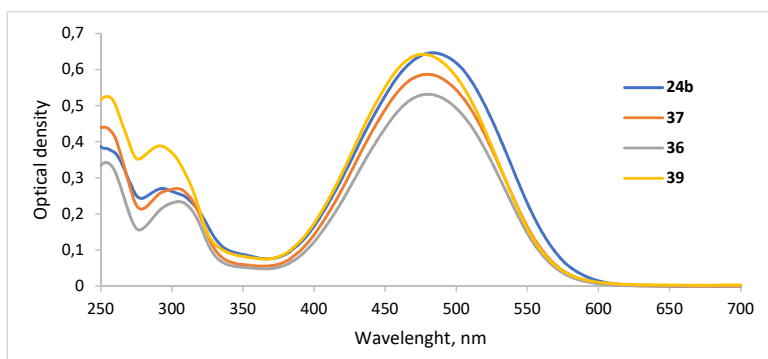
Fig. 11. Absorption spectra of dendronized azochromophores **24b**, **36**, **37**, **39** in CHCl₃ solution with a sample concentration of 20 µmol·L⁻¹.

The absorption peaks of the lower frequency charge transfer band in the two solvents does not differ by more than 3 nm in each series of chromophores **10a–c**, **14a–c**, **19a–c,** or **24a–c**. This means, that the terminal groups of the dendronizing fragment do not significantly affect the absorption energy of the chromophore, it is determined only by the core azochromophore, which is equally accessible to solvent molecules in all analyzed compounds. The intensity of absorption varies with each series of chromophores, although the molar extinction coefficients (ε) are in the same order, corresponding to the presence of the same azochromophore in the molecule (Table 4).

The greatest λ_{max} shift was observed for compounds **19b,c**, **36**, **37**, and **39** when comparing spectra in both solvents, they exhibit a 6–8 nm hipsochromic shift in CHCl₃ solution relative to EtOBz solution (Table 4). This can be explained by the covalent bonding of pentafluorophenyl fragments in a sufficiently long chain or through the dendron fragment to the donor part of the azochromophore and the resulting Ar-Ar^F interaction with acceptor part of azochromophore, when its electrons are pulled through space and the amount of energy required for absorption increases. Similar to what has been observed in the monocrystal of compound **36**, it is more likely that intramolecular Ar-Ar^F or π-π interactions can form in a solution of CHCl₃, but in EtOBz these interactions break down. The group of compounds **19a–c** is distinguished by hipsochromic shift of λ_{max} relative to the other compounds shown in Table 4 in both solvents, which can be explained by the (2-carboxyethyl)amino fragment at the donor part of the azobenzene, which weakens the donor strength.

The light absorption spectra of a solid are measured only for thin films of compounds that have undergone NLO measurements (Table 5). All compounds have observable batochromic shift in the solid state compared to spectra in CHCl₃ solutions. The batochromic shift in the solid state relative to the EtOBz solution is less, while a hipsochromic shift in the solid state was observed in the spectrum of the compound **37** relative to the spectrum in EtOBz solution, which is most likely due to the different arrangement of the molecules of the compound **37** in the amorphous film, which could be related to the NLO properties of the azo compound **37**. The absorption maxima for blends (**34+36**) and (**38+39**) are identical to a component whose

λ_{max} is present in longer wavelength. The expected effect of interactions between two compounds in blends (**34+36**) and (**38+39**) could not be observed.

2.5. Nonlinear Optical Properties

NLO properties were tested for compounds **34**, **36–39**, and both blends (**34+36**), (**38+39**) containing dendrons with two benzyl and/or two (pentafluorophenyl)methyl groups (partners at the Institute of Solid State Physics, University of Latvia, under the leadership of Dr. phys. Mārtiņš Rutkis). Similarly, NLO properties have also been measured for Trt group containing compounds **10b** and **24b**. NLO properties were not tested for compounds with THP and hydroxy groups because they do not form stable amorphous films.

The second-order NLO coefficients d_{33}, d_{31}, and $d_{33}(0)$ are used to characterize the NLO properties of the organic molecular glasses, which were obtained from synthesized compounds. For the evaluation of the NLO coefficients d_{33} and d_{31} of thin films, it is necessary to determine the refractive indices n_{1064} and n_{532} of the material at the fundamental and second harmonic wavelength, which are reported in Table 5. The poled thin films of organic molecular glass are assumed to have $C_{\infty v}$ symmetry, and the material can be characterized by three non-zero NLO coefficients – d_{33}, d_{31}, and d_{15}. However, according to Kleinman's symmetry [59], it is assumed that $d_{31} = d_{15}$. So, two NLO coefficients are sufficient for the characterization of thin films of organic molecular glasses, which are determined when the sample is exposed to polarized laser radiation.

All samples studied are NLO active (Table 5). The loading density of the effective chromophore fragment in the molecule (N) is calculated from the molar mass by assuming the simplified methyl derivative 4′-(dimethylamino)-2-methoxy-4-nitroazobenzene as the effective chromophore. NLO coefficients depend on the loading density of the effective chromophore, molecular hyperpolarizability, and polar order. The ratio of NLO coefficients d_{33}/d_{31} shows the polar order in oriented chromophore films. For all samples containing a single chromophore, **10b**, **24b**, **34**, **36–39**, this ratio is 3.2 to 3.9 and indicates a high polar order [60]. Both blends (**34+36**) and (**38+39**) show significantly lower ratios of 2.2 and 2.0, indicating poor arrangement of chromophore molecules, resulting in low values of NLO coefficients d_{33} and $d_{33}(0)$. The intermolecular interaction of the two molecules in these blends can manifest itself in such a way as to contribute to the centrosymmetric arrangement of the chromophores present in the system. As a result, the corresponding NLO coefficients are also reduced. The results obtained are contrary to literature data, where a mixture of complementary chromophores containing the same dendrons has more than twice the value of the electro-optical coefficient r_{33} than the individual components [10].

Dendronized azochromophores **10b**, **24b** with Trt groups and dendronized azochromophores **36**, **39** with (pentafluorophenyl)methyl groups connected to the donor part of the azochromophore showed relatively better NLO coefficients above coefficient d_{33} value of LiNbO₃. Therefore, at the end of the studies, we synthesized azochromophore **37**, which contains the two different dendrons. However, contrary to expectations, the values of the NLO coefficients of the compound **37** were very low. We explain this by the presence of the majority

of the molecules of the compound **37** in centrosymmetric arrangement even after poling, which reduced the value of the NLO coefficient. Also, the intermolecular Ar-Ar^F interactions of pentafluorophenyl and trityl groups in the glassy film were likely to occur by promoting centrosymmetric arrangement.

Table 5

Amorphous Thin Film NLO Properties of Synthesized Organic Molecular Glasses

Sample	d_{33},[a] pm·V^{-1}	d_{31},[a] pm·V^{-1}	$d_{33}(0)$,[b] pm·V^{-1}	d_{33}/d_{31}	N,[c] %	T_{SHI50},[d] °C	n_{1064}[e]	n_{532}[e]	λ_{max}, nm film
10b	38	_[f]	5.7	_[f]	17	90	1.60	2.04	495
24b	43	11	5.1	3.9	24	66	1.63	1.69	490
34	10	2.8	1.1	3.6	22	51	1.63	1.72	492
36	35	11	3.9	3.2	22	59	1.61	1.67	496
(34+36)	19	8.5	1.6	2.2	22	50	1.64[g]	1.72[g]	497
37	14	3.8	1.9	3.7	19	78	1.62	1.80	482
38	20	5.4	2.1	3.7	26	46	1.65	1.70	498
39	26	7.2	3.3	3.6	19	54	1.60	1.69	489
(38+39)	20	10	1.7	2.0	22	54	1.63[f]	1.70[f]	498

[a] LO coefficients determined at 532 nm.

[b] NLO coefficient extrapolated to zero frequency.

[c] Loading density of the effective chromophore moiety.

[d] Temperature at which the intensity of the second harmonic is 50 % of the initial intensity.

[e] Refractive index of light at the specified wavelength.

[f] Not determined.

[g] Calculated from the Kramers-Kronig transformation of absorption spectrum [61].

Compound **24b** has the highest NLO coefficient d_{33} value and the second highest coefficient $d_{33}(0)$ value. Comparing the structure of compound **24b** and compounds **36**, **37**, and **39**, one can hypothesize that a single pentafluorophenyl fragment bound in a short chain is not capable of forming an intramolecular bond with azobenzene, as is possible in compound **36**. That is, in this case, pentafluorophenyl fragment is more likely to engage in the Ar-Ar^F interaction with an adjacent molecule, aiding to stabilize the poled order of chromophores, which contributes to the achievement of higher NLO coefficient values.

To assess the thermal stability of the poled order of chromophores in thin films, we used the SHI measurement. The temperature T_{SHI50} (Table 5 and Fig. 12) describes a condition in which the initial SHI value has been halved when the sample is heated, and it agrees mostly well with the T_g measurements. The differences between T_g and T_{SHI50} values could result from a different arrangement of chromophore molecules in molten molecular glass during the DSC experiment and in a poled film of organic molecular glass cast from the solution in which the presence of trapped solvent molecules between dendron fragments cannot be excluded. Compounds **10b**, **24b**, and **36** have T_{SHI50} value slightly higher than T_g value and these compounds also have shown the highest NLO coefficient values. Most likely, these compounds have an appropriate molecular structure that provides and promotes intramolecular and

intermolecular Ar-Ar^F and/or π-π interactions that stabilize the poled order of noncentrosymmetric chromophores in thin films.
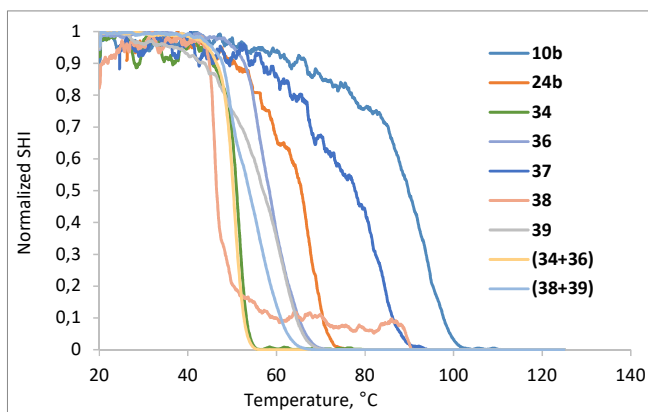

Fig. 12. Decrease in SHI signal when heating samples of NLO active amorphous molecular glasses.

Original publications on the studies described in this chapter can be found in Appendices 1, 2, and 4, and individual excerpts of the work are published in conference proceedings in Appendix 6.

3. Organic Molecular Glasses of Polyazochromophores

We also examined a third approach to the synthesis of NLO active compounds to achieve stable organic molecular glasses based on chromophores of different structures with different dipole moment directions. We synthesized dendrons containing three chromophores: two identical D–π–A type azobenzene derivatives and a third azobenzene of different structure or 1,3-indanedionylpyridinium betaine (IPB). Directions of the molecular hyperpolarizability and dipole moment vectors coincide for in the ground state neutral chromophores such as azobenzene, while betaine type chromophores such as IPB have opposite directions of the vectors of molecular hyperpolarizability and dipole moment in the ground state [8]. If a neutral and betaine-type chromophore are combined into a single molecule or material, the fragments within the molecule would orient themselves by minimizing the resulting dipole moment as much as possible, while the molecular hyperpolarizability would be summed up [7], [8], resulting in increased poling efficiency and the preservation of poled order in NLO studies.

3.1. Synthesis of Polyazochromophore Dendrons

We included the azobenzene fragment and the Trt groups in the structure of the synthesizable dendron. From azobenzene **40** with two identical hydroxy groups, we obtained a derivative **43**, in which one of the hydroxy groups was converted to trityloxy, and the other was activated with a mesyl group. To obtain such an azobenzene molecule, there are two possible paths: first to bring in a mesyl group, and then a trityl group, or to bring in a trityl group first, and then a mesyl group. We tried both approaches taking equimolar quantities of starting materials. As expected, at the end of the reaction we obtained a mixture of three substances: starting material, monosubstituted product, and disubstituted product. A successful preparative chromatography purification procedure was realized in the case of trityl product **41**, so we synthesized the necessary azobenzene **43** in almost quantitative yield according to scheme in Fig. 13.
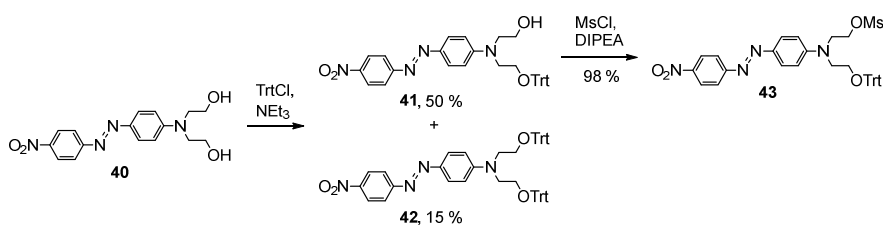
Fig. 13. Functionalization of both hydroxy groups of azochromophore **40**.

By alkylating 3,5-dihydroxybenzoate (**1**) with azobenzene mesyl derivative **43**, we obtained dendron **D1Me**, which contains two identical azochromophores (Fig. 14). We hydrolysed the dendron **D1Me** with NaOH in DMF solution, turned the intermediate sodium salt into acid **D1OH** using a $HPO_4^{2-}/H_2PO_4^-$ buffer of sufficient buffer capacity with a pH value of approximately 5 to avoid hydrolysis of the Trt groups in a strongly acidic environment.

Fig. 14. Syntheses of dendrons **D1Me** and **D1OH**.

By esterifying the carboxyl-containing azodendron **D1OH**, it is possible to covalently add new chromophores of a different structure to it. In this way, we added D–π–A type azobenzene **45**, which we obtained by azo coupling of betaine **5** with *N,N*-dimethylaniline (**44**) in acetic acid (Fig. 15). The second chromophore to be added is 1,3-indanedionylpyridinium betaine **48**, which we obtained by condensing starting materials **46** and **47**.
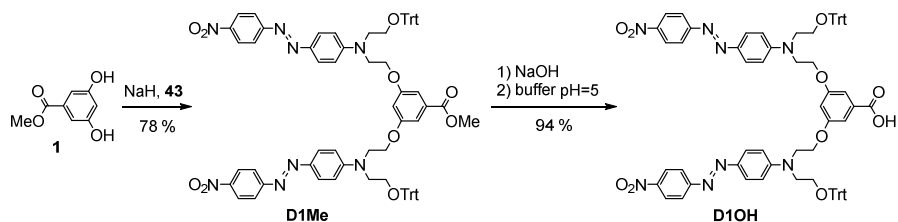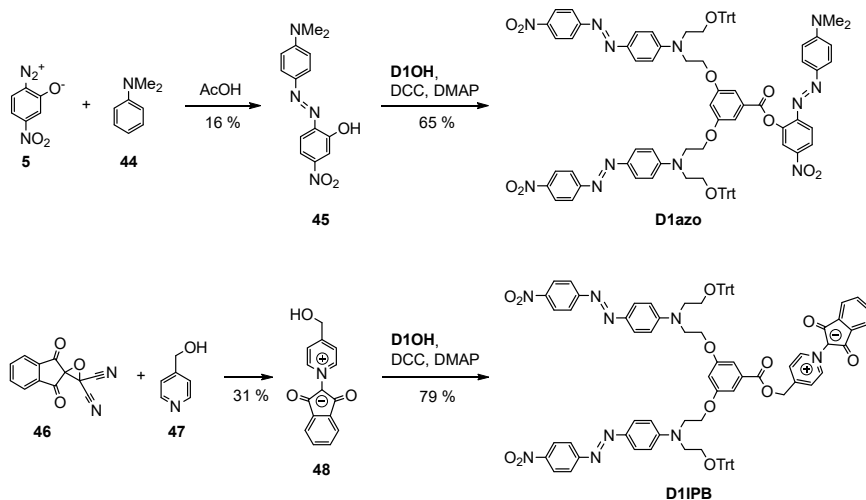

Fig. 15. Syntheses of dendrons **D1azo** and **D1IPB**.

We performed the esterification reaction using the DCC/DMAP method and obtained polyazochromophoric dendrons **D1azo** and **D1IPB** (Fig. 15). We purified the dendrons **D1azo** and **D1IPB** by Al_2O_3 column chromatography so that to avoid cleavage of the Trt groups during the process, which was previously observed during chromatography on silica.

3.2. Properties of Polyazochromophore Dendrons

To find out the phase transitions of the synthesized dendrons **D1Me, D1OH**, **D1azo, D1IPB** and their starting materials chromophores **45** and **48**, we conducted a thermal analysis using DSC and TGA (Table 6). Chromophores **45** and **48** are crystalline substances that do not form the amorphous phase and decompose as they melt. In contrast, we obtained the azochromophore

42, representing the equal azochromophore branches of the dendrons, in both amorphous and crystalline form. In the DSC curve of the second heating, it shows the following transitions, T_g at 81 °C, followed by spontaneous crystallization at 166 °C, melting at 244 °C and decomposition at 286 °C determined at 5 % mass loss temperature. T_g could be observed only for dendrons **D1Me** and **D1IPB**. The characteristic T_g step of the DSC curve was less pronounced than that of the azobenzene dendrimers described in Chapter 1 and the dendronized monoazochromophores described in Chapter 2, even using a similar sample mass. All dendrons **D1Me**, **D1OH, D1azo**, and **D1IPB** are solid, at least semi-crystalline substances that well form the amorphous phase, which can be observed by casting a transparent and homogeneous thin film. Synthesized dendrons **D1Me** and **D1IPB** have been found to have the highest T_g values of all the compounds considered in the Thesis, which reach and in the case of dendron **D1IPB** even exceed the temperature of 100 °C required for the manufacture of electro-optical devices [5]. On the other hand, the thermal stability of the synthesized compounds **D1Me**, **D1OH, D1azo**, and **D1IPB** is in the range of 240–267 °C, which is less than that of the compounds described in the previous chapters.

Table 6

Thermal and Optical Properties of Synthesized Products

Compound	T_g, °C	mp, °C	T_d, °C	λ_{max},[a] nm	ε, M^{-1}·cm^{-1}
42	81	244	286	488	25 200
45	_[b]	_[b]	264	509	45 400
48	_[b]	_[b]	240	409	43 800
D1Me	100	207	260	472	62 600
D1OH	_[b]	148	254	474	66 500
D1azo	_[b]	223	267	475	94 500
D1IPB	113	179	242	429	91 400

[a] CHCl$_3$ solution with a concentration of 10 μmol·L^{-1}.
[b] Not observed.

Light absorption spectra in CHCl$_3$ solutions were recorded for the synthesized polyazochromophoric dendrons **D1Me, D1OH, D1azo, D1IPB** and chromophores **42**, **45**, **48** (Table 6). The intensity of the absorption band is proportional to the number of chromophores in the molecule [62], so by adding up the ε values of the chromophores of the simple starting materials, the numerical value of ε of the final product dendron must be obtained. Using such a simple summation estimate, the dendron ε value approximates the calculated one.

Comparing the spectra of the compounds **D1Me**, **48**, and **D1IPB** in CHCl$_3$, it can be seen that the absorption band of the dendron **D1IPB** is by its nature an overlap of two bands, which is formed by summing the spectra of the compounds **D1Me** and **48** (Fig. 16). However, for pyridine betaine **48**, which contains the free hydroxy group, the absorption maximum of the longest wavelength of the spectrum is hypsochromic shifted relative to the absorption maximum of the spectrum for ester-bonded betaine fragment in the composition of the dendron **D1IPB**.
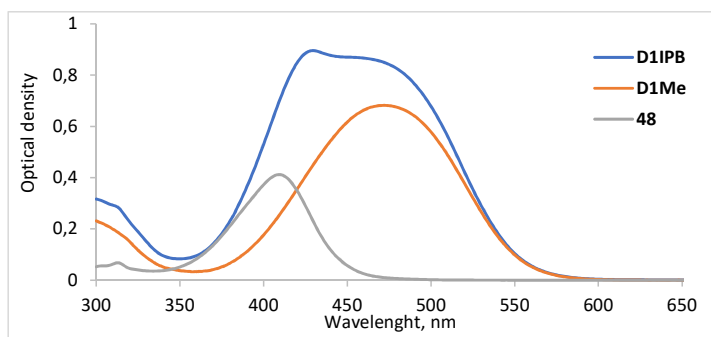
Fig. 16. Spectra of dendron **D1IPB** and its components in CHCl$_3$ with 10 µmol·L^{-1} concentration.

The spectra of the compound **D1IPB** are peculiar and their shape depends on the solvent used (Fig. 17). Two distinct chromophores are involved in the dendron **D1IPB** molecule: azobenzene, which exhibits a batochromic shift of the long-wave absorption band with increasing solvent polarity, and IPB, which exhibits a hipsochromic shift as the solvent polarity increases. As the polarity of the solvent increases, a bathochromic shift of the absorption band is observed if the excited state is more polar than the ground state, otherwise a hypsochromic shift is observed [58]. Since the two types of chromophores are connected using σ-bonds, a significant shift in electron density between them is not expected, so that when the chromophore bands combine, the spectra differ significantly in solvents of different polarity (Fig. 17). In the non-polar solvent toluene, where the difference in λ_{max} values of the individual chromophores is smallest, the absorption band of dendron **D1IPB** is the narrowest and the maximum is observed on the short-wave side of the absorption band. In a polar solvent like DMSO, where the difference in the λ_{max} values of the individual chromophores is greatest, the absorption band of the compound **D1IPB** is the widest and a maximum on the long-wave side of the absorption band is observed. In moderately polar solvents, the observed picture is most similar to two absorption maxima or one wide absorption band.
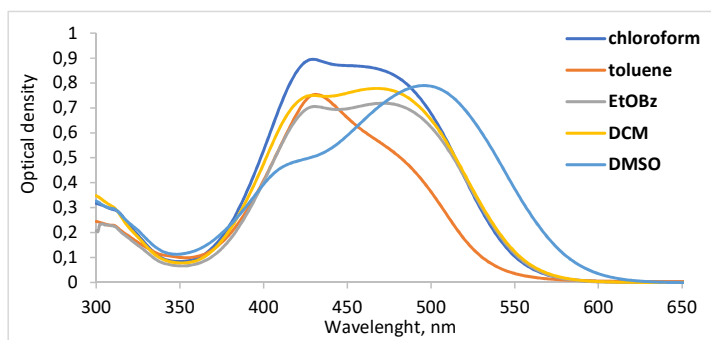

Fig. 17. Solvatochromism of dendron **D1IPB**.

NLO properties have been studied for synthesized dendrons **D1azo** and **D1IPB** containing various chromophores and azochromophore **42**, determining the NLO coefficient d_{33}, the thermal stability T_{SHI50}, and calculating $d_{33}(0)$ for electric field poled films (Table 7) (partners at the Institute of Solid State Physics, University of Latvia, under the leadership of Dr. phys. Mārtiņš Rutkis).

The simple tritylated azochromophore **42** exhibits a peculiar behavior during heating. Its poled amorphous film exhibits a minute SHI value, which disappears when the sample is heated at about 45 °C, but crystallization spontaneously begins as the heating continues. Noncentrosymmetrically arranged crystals of azochromopore **42** are formed, and SHI rises, peaking at 127 °C. The same phenomenon is observed when heating a previously unpoled amorphous film, but then the crystallization of azochromofore **42** begins at a lower temperature, reaching a maximum at 111 °C. However, the formed polycrystalline films are opaque and are not suitable for practical use. The film formed by mixing 10 wt% of compound **42** in poly(methyl methacrylate) (PMMA) is NLO active; however, T_{SHI50} is only 45 °C, which is almost half the T_g of compound **42** and about three times lower than T_g of PMMA. Therefore, the explanation for this phenomenon is the peculiarities of the compound **42**, which is observed in its thin film.

Table 7

Optical and NLO Properties of Thin Films of Synthesized Organic Molecular Glasses

Compound	d_{33},[a] pm·V^{-1}	$d_{33}(0)$,[b] pm·V^{-1}	T_{SHI50}, °C	λ_{max},[d] nm
42[c]	26	3,3	45	487
D1azo	103	12	92	493
D1IPB	92	10	91	492

[a] NLO coefficient determined at 532 nm.

[b] NLO coefficient extrapolated to zero frequency.

[c] 10 wt% in the PMMA matrix.

[d] Absorption maxima measured for a thin amorphous film on a quartz glass.

Multichromophore-containing dendrons **D1azo** and **D1IPB** show moderate NLO activity with coefficient d_{33} values of about 100 pm·V^{-1}, which is four times the value of the coefficient d_{33} of the LiNbO$_3$. However, the coefficients d_{33} of these compounds have average values between the dendrimers described in Chapter 1 and at both sides of the azochromophore dendronised compounds described in Chapter 2. Dendrons **D1azo** and **D1IPB** have the highest T_{SHI50} values among the compounds considered in the Thesis. However, unlike the T_g value of the dendron **D1IPB**, its T_{SHI50} value does not exceed the temperature of 100 °C required for the operation of electro-optical devices. The structure of synthesized dendrons is suitable for the design of NLO materials for further research. The interaction of different chromophores and spatially insulating Trt groups in the amorphous glassy state promotes a non-centrosymmetric orientation of the poled material. The 3,5-dihydroxybenzoic acid fragment at the center of the structure works perfectly as an intramolecular insulating group, which contributes to the

preservation of the order of noncentrosymmetric chromophores. The azo compound and IPB attached to the dendron are different in structure, but they do not have a different effect on the NLO properties of the dendrons **D1azo** and **D1IPB**. NLO properties are determined by the entire spatial structure of the dendron giving high values of T_{SHI50} and d_{33}.

The studies described in this chapter can be found in publication in Appendix 5.

CONCLUSIONS

7. It is more efficient to bind the (pentafluorophenyl)methyl group covalently to the chromophore fragment by ester rather than ether bonds. The use of an esterification reaction avoids the use of strong nucleophilic reagents, since a strong nucleophile could replace fluorine atoms of the pentafluorophenyl group in the substitution reaction.

8. Ar-Ar^F interaction in a large dendronized NLO active azochromophore crystal was demonstrated for the first time by X-ray diffraction method: the pentafluorophenyl fragment interacts intramolecularly with the azobenzene acceptor part and the azo group.

9. The use of trityl and (pentafluorophenyl)methyl groups in the structure of azochromophores increases the ability to form an amorphous phase, as well as the temperatures of glass transition and decomposition. The presence of tetrahydropyranyl groups, on the other hand, reduce the glass transition temperature below 20 °C, while compounds containing the hydroxy group and pentafluorophenyloxy group do not form an amorphous thin layer.

10. If the donor part of the azochromophore is covalently bound to one pentafluorophenyl group in a sufficiently long chain or to a dendron containing two pentafluorophenyl fragments, a relatively larger batochromic shift in the ethyl benzoate solution is observed compared to the CHCl$_3$ solution, which can be explained by intramolecular Ar-Ar^F or π-π interactions in CHCl$_3$ solution.

11. Even if the fragments contained in the azochromophore molecule and the functional groups provide good values of T_g and T_{SHI50} as a result of synergy, this does not mean that possible Ar-Ar^F or π-π interactions will contribute to the formation of a non-centrosymmetric order in the electric field and large NLO coefficients. The mutual position of the interacting fragments can contribute to the preservation of the centrosymmetric order of azochromophores in organic molecular glass, even after poling.

12. By connecting three chromophores and two trityl groups in the structure of the dendron, it is possible to obtain a material with NLO coefficient d_{33} values of about 100 pm·V^{-1} and the highest values of T_{SHI50} (above 90 °C) among the compounds studied in the Doctoral Thesis.

ACKNOWLEDGEMENTS

REFERENCES

[1] L. R. Dalton, P. A. Sullivan, D. H. Bale, *Chem. Rev.* **2010**, *110*, 25–55.

[2] F. Ullah, N. Deng, F. Qiu, *PhotoniX* **2021**, *2*, 13.

[3] J. Liu, W. Wu, *Symmetry (Basel).* **2022**, *14*, 882.

[4] S.-H. Jang, A. K.-Y. Jen, *Chem. Asian J.* **2009**, *4*, 20–31.

[5] J. Liu, C. Ouyang, F. Huo, W. He, A. Cao, *Dyes Pigm.* **2020**, *181*, 108509.

[6] W. Wu, J. Qin, Z. Li, *Polymer (Guildf).* **2013**, *54*, 4351–4382.

[7] Y. Liao, S. Bhattacharjee, K. A. Firestone, B. E. Eichinger, R. Paranji, C. A. Anderson, B. H. Robinson, P. J. Reid, L. R. Dalton, *J. Am. Chem. Soc.* **2006**, *128*, 6847–6853.

[8] M. Rutkis, A. Tokmakovs, E. Jecs, J. Kreicberga, V. Kampars, V. Kokars, *Opt. Mater. (Amst).* **2010**, *32*, 796–802.

[9] L. M. Salonen, M. Ellermann, F. Diederich, *Angew. Chemie – Int. Ed.* **2011**, *50*, 4808–4842.

[10] T.-D. Kim, J.-W. Kang, J. Luo, S.-H. Jang, J.-W. Ka, N. Tucker, J. B. Benedict, L. R. Dalton, T. Gray, R. M. Overney, et al., *J. Am. Chem. Soc.* **2007**, *129*, 488–489.

[11] X.-H. Zhou, J. Luo, S. Huang, T.-D. Kim, Z. Shi, Y.-J. Cheng, S.-H. Jang, D. B. Knorr Jr., R. M. Overney, A. K.-Y. Jen, *Adv. Mater.* **2009**, *21*, 1976–1981.

[12] T.-D. Kim, J. Luo, A. K.-Y. Jen, *Bull. Korean Chem. Soc.* **2009**, *30*, 882–886.

[13] W. Wu, G. Yu, Y. Liu, C. Ye, J. Qin, Z. Li, *Chem. – A Eur. J.* **2013**, *19*, 630–641.

[14] H. Ma, A. K.-Y. Jen, *Adv. Mater.* **2001**, *13*, 1201–1205.

[15] W. Wu, C. Li, G. Yu, Y. Liu, C. Ye, J. Qin, Z. Li, *Chem. Eur. J.* **2012**, *18*, 11019–11028.

[16] R. Deloncle, A.-M. Caminade, *J. Photochem. Photobiol. C Photochem. Rev.* **2010**, *11*, 25–45.

[17] S. Yokoyama, T. Nakahama, A. Otomo, S. Mashiko, *Chem. Lett.* **1997**, *26*, 1137–1138.

[18] S. Yokoyama, T. Nakahama, A. Otomo, S. Mashiko, *J. Am. Chem. Soc.* **2000**, *122*, 3174–3181.

[19] Y. Yamaguchi, Y. Yokomichi, S. Yokoyama, S. Mashiko, *J. Mol. Struct. THEOCHEM* **2002**, *578*, 35–45.

[20] Y. Yamaguchi, Y. Yokomichi, S. Yokoyama, S. Mashiko, *J. Mol. Struct. THEOCHEM* **2001**, *545*, 187–196.

[21] W. Zhang, J. Xie, W. Shi, X. Deng, Z. Cao, Q. Shen, *Eur. Polym. J.* **2008**, *44*, 872–880.

[22] W. Wu, L. Huang, C. Song, G. Yu, C. Ye, Y. Liu, J. Qin, Q. Li, Z. Li, *Chem. Sci.* **2012**, *3*, 1256–1261.

[23] W. Wu, Q. Huang, G. Xu, C. Wang, C. Ye, J. Qin, Z. Li, *J. Mater. Chem. C* **2013**, *1*, 3226–3234.

[24] R. Tang, S. Zhou, W. Xiang, Y. Xie, H. Chen, Q. Peng, G. Yu, B. Liu, H. Zeng, Q. Li, et al., *J. Mater. Chem. C* **2015**, *3*, 4545–4552.

[25] W. Wu, G. Xu, C. Li, G. Yu, Y. Liu, C. Ye, J. Qin, Z. Li, *Chem. Eur. J.* **2013**, *19*, 6874–6888.

[26] Z. Li, W. Wu, Q. Li, G. Yu, L. Xiao, Y. Liu, C. Ye, J. Qin, Z. Li, *Angew. Chemie – Int. Ed.* **2010**, *49*, 2763–2767.

[27] Z. Li, Q. Li, J. Qin, *Polym. Chem.* **2011**, *2*, 2723–2740.

[28] R. Tang, Z. Li, *Chem. Rec.* **2017**, *17*, 71–89.

[29] W. Wu, C. Wang, R. Tang, Y. Fu, C. Ye, J. Qin, Z. Li, *J. Mater. Chem. C* **2013**, *1*, 717–728.

[30] W. Wu, C. Wang, Q. Li, C. Ye, J. Qin, Z. Li, *Sci. Rep.* **2014**, *4*, 6101.

[31] W. Wu, C. Ye, J. Qin, Z. Li, *ACS Appl. Mater. Interfaces* **2013**, *5*, 7033–7041.

[32] Z. Li, G. Yu, W. Wu, Y. Liu, C. Ye, J. Qin, Z. Li, *Macromolecules* **2009**, *42*, 3864–3868.

[33] W. Wu, Z. Xu, Z. Li, *Polym. Chem.* **2014**, *5*, 6667–6670.

[34] D. N. Nikogosyan, *Nonlinear Optical Crystals: A Complete Survey*, Springer-Verlag, New York, **2005**.

[35] J. M. J. Frechet, D. A. Tomalia, Eds. , *Dendrimers and Other Dendritic Polymers*, John Wiley & Sons, Ld: Chichester, **2001**.

[36] O. A. Matthews, A. N. Shipway, J. F. Stoddart, *Prog. Polym. Sci.* **1998**, *23*, 1–56.

[37] H.-F. Chow, T. K. K. Mong, M. F. Nongrum, C. Wan, *Tetrahedron* **1998**, *54*, 8543–8660.

[38] P. Patel, V. Patel, P. M. Patel, *J. Indian Chem. Soc.* **2022**, *99*, 100514.

[39] L. Laipniece, J. Kreicberga, V. Kampars, *Sci. Proc. RTU Mater. Sci. Appl. Chem.* **2008**, *16*, 88–99.

[40] G. Seniutinas, L. Laipniece, J. Kreicberga, V. Kampars, J. Gražulevičius, R. Petruškevičius, R. Tomašiūnas, *J. Opt. A Pure Appl. Opt.* **2009**, *11*, 034003.

[41] K. Traskovskis, I. Mihailovs, A. Tokmakovs, A. Jurgis, V. Kokars, M. Rutkis, *J. Mater. Chem.* **2012**, *22*, 11268.

[42] J. L. Oudar, D. S. Chemla, *J. Chem. Phys.* **1977**, *66*, 2664–2668.

[43] F. Cuétara-Guadarrama, M. Vonlanthen, K. Sorroza-Martínez, I. González-Méndez, E. Rivera, *Dyes Pigm.* **2021**, *194*, 109551.

[44] R. L. Tang, S. M. Zhou, Z. Y. Cheng, H. Chen, L. Deng, Q. Peng, Z. Li, *CCS Chem.* **2020**, *2*, 1040–1048.

[45] A. Hassner, V. Alexanian, *Tetrahedron Lett.* **1978**, *19*, 4475–4478.

[46] B. Neises, W. Steglich, *Angew. Chemie Int. Ed. English* **1978**, *17*, 522–524.

[47] N. Ono, T. Yamada, T. Saito, K. Tanaka, A. Kaji, *Bull. Chem. Soc. Jpn.* **1978**, *51*, 2401–2404.

[48] G. M. Brooke, *J. Fluor. Chem.* **1997**, *86*, 1–76.

[49] A. Armstrong, I. Brackenridge, R. F. W. Jackson, J. M. Kirk, *Tetrahedron Lett.* **1988**, *29*, 2483–2486.

[50] A. Nakazato, K. Sakagami, A. Yasuhara, H. Ohta, R. Yoshikawa, M. Itoh, M. Nakamura, S. Chaki, *J. Med. Chem.* **2004**, *47*, 4570–4587.

[51] Y. Xiang, B. Hirth, J. L. Kane, J. Liao, K. Noson, C. Yee, *Inhibitors of Sphingosine Kinase 1*, **2010**, WO2010033701 (A2).

[52] P. Hotchkiss, S. Marder, A. Giordano, T. D. Anthopoulos, *Electronic Devices Comprising Novel Phosphonic Acid Surface Modifiers*, **2010**, WO2010115854A1.

[53] C. S. Chiu, M. Saha, A. Abushamaa, R. W. Giese, *Anal. Chem.* **1993**, *65*, 3071–3075.

[54] W. Wu, Q. Huang, C. Zhong, C. Ye, J. Qin, Z. Li, *Polymer (Guildf).* **2013**, *54*, 5655–5664.

[55] Z. Li, P. Chen, Y. Xie, Z. Li, J. Qin, *Adv. Electron. Mater.* **2017**, 1700138.

[56] K. L. Wooley, C. J. Hawker, J. M. Pochan, J. M. J. Frechet, *Macromolecules* **1993**, *26*, 1514–1519.

[57] L. R. Dalton, P. A. Sullivan, D. H. Bale, S. Hammond, B. C. Olbricht, H. Rommel, B. Eichinger, B. Robinson, in *Tutorials in Complex Photonic Media*, SPIE, Bellingham, USA, **2007**, pp. 525–574.

[58] C. Reichardt, *Solvents and Solvent Effects in Organic Chemistry*, WILEY-VCH Verlag GmbH & Co. KGaA, Weinheim, **2003**.

[59] W. N. Herman, L. M. Hayden, *J. Opt. Soc. Am. B* **1995**, *12*, 416–427.

[60] R. Alicante, *Photoinduced Modifications of the Nonlinear Optical Response in Liquid Crystalline Azopolymers*, Springer Berlin Heidelberg, Berlin, Heidelberg, **2013**.

[61] K. Ohta, H. Ishida, *Appl. Spectrosc.* **1988**, *42*, 952–957.

[62] A.-M. Caminade, R. Laurent, J.-P. Majoral, *Adv. Drug Deliv. Rev.* **2005**, *57*, 2130–2146.

PIELIKUMI / APPENDICES

L. Laipniece, V. Kampars, S. Belyakov, A. Bundulis, A. Tokmakovs, M. Rutkis. Utilization of amorphous phase forming trityl groups and Ar-ArF interactions in synthesis of NLO active azochromophores. *Dyes Pigm.*, **2022**, *204*, 110395.
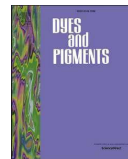
Publikācijas pielikums pieejams bez maksas *Science Direct* mājaslapā
The Supporting Information is available free of charge on the *Science Direct* website

Grafiskais kopsavilkums / graphical abstract
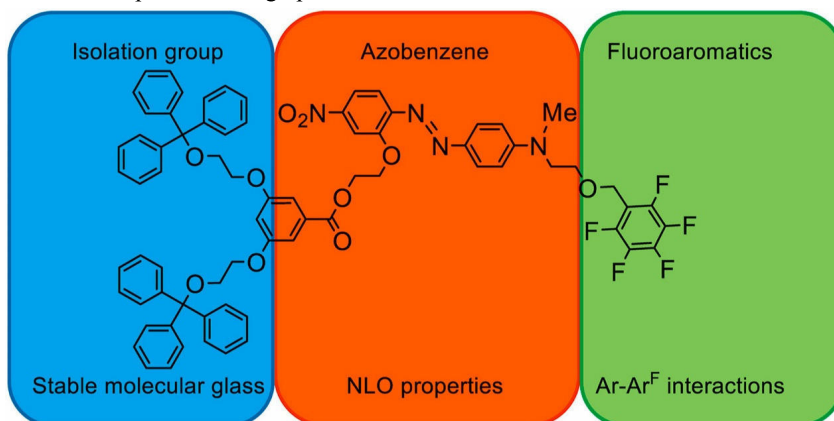
Utilization of amorphous phase forming trityl groups and Ar-Ar^F interactions in synthesis of NLO active azochromophores

Lauma Laipniece [a,*], Valdis Kampars [a,1], Sergey Belyakov [a,b], Arturs Bundulis [c], Andrejs Tokmakovs [c], Martins Rutkis [c]

[a] Faculty of Materials Science and Applied Chemistry, Riga Technical University, P. Valdena 3/7, Riga, LV-1048, Latvia
[b] Latvian Institute of Organic Synthesis, Aizkraukles 21, Riga, LV-1006, Latvia
[c] Institute of Solid State Physics, University of Latvia, Kengaraga 8, Riga, LV-1063, Latvia

ARTICLE INFO

ABSTRACT

New NLO active organic molecular glasses were synthesized based on *push-pull* azobenzene, which was dendronized with 3,5-bis[2-(trityloxy)ethoxy]benzoic acid and pentafluorophenyl groups were added to enchance thermal and NLO properties *via* Ar-Ar^F interactions. The configuration, where pentafluorophenyl groups containing dendronizing fragment was attached to donor part of azochromophore, was very promising in our recent research, therefore trityl groups containing dendron was added to acceptor part to rise the glass transition temperature of amorphous compound. Effect of one or two pentafluorophenyl groups was investigated and about three times better NLO parameters were obtained when using one pentafluorophenyl group, as it has greater possibility of NLO properties enchanting Ar-Ar^F interactions with neighboring molecules. New convergent method was used to synthesize azobenzene core dendrimer fully functionalized with trityl end groups. Thermal, optical, and NLO properties were compared to previously reported results of dendrimer samples containing both hydroxyl and trityl groups. Full set of trityl end groups resulted in decreased NLO parameters and stability of poled order. Glass transition temperatures of all synthesized molecular glasses were 63–83 °C, and thermal destruction temperatures of all synthesized compounds were at least 250 °C. NLO coefficient d_{33} values were 14–73 pm·V^{-1}.

1. Introduction

Organic nonlinear optical (NLO) materials are studied and developed to perform better than inorganic materials in applications for high speed and effective data transmission, high speed electro-optical modulators, ultrafast optical switches, signal processing, and optical data storage [1–8]. Organic NLO materials consist of a chromophore denoting the NLO effect of the material. Hosting polymer or crosslinking monomers may also be present in the NLO material and responsible for the bulk physical properties, but the active chromophore becomes diluted reducing overall NLO response [3]. More efficient materials could be composed of a single component, a NLO active organic molecular glass. Structure of the organic molecular glasses can be modified to meet five main requirements at device application conditions: large NLO coefficients, high refractive indices, good optical transparency, excellent temporal stability of non-centrosymmetrically aligned dipoles, and

excellent photochemical stability [1–3,6,9–11].

An organic NLO active chromophore is usually strongly polar "acceptor – conjugated π bridge – donor" (D-π-A) type compound, which molecules are ordered with antiparallel dipoles in crystals and thin amorphous films because electrostatic repulsion prohibits parallel or non-centrosymmetric arrangement. The final material must contain non-centrosymmetrically aligned chromophores to be able to demonstrate a second order NLO effect [1,2,9,11–14]. Non-centrosymmetric arrangement is forced upon molecules by external electric field poling in many cases. Nevertheless strongly dipolar chromophore units relax back to more favorable centrosymmetric alignment even below the glass transition temperature (T_g) of the material, thus reducing the second order NLO effect [2,9,12]. There are many approaches to overcome this problem: T_g must be as high as possible [1,6,15]; self-assembly of molecules utilizing strong interaction forces between functional groups [2,9,10,12]; isolation of active chromophore as

---

* Corresponding author.
E-mail address: lauma.laipniece@rtu.lv (L. Laipniece).
[1] Deceased

host-guest system [16–19]; site isolation in dendrimer [2,10,20,21]; use of isolation chromophores [22,23]; or use of different chromophores in one material with opposite dipole moments, but parallel hyperpolarizability vectors [15,24].

Dendrimer synthesis and small dendron addition to chromophores are used to isolate in space the chromophore with large dipole moment and improve thermal and chemical properties of the material [2,10,20, 21,25]. Trityl groups are known isolation groups, which also rise T_g [26–29]. Aromatic-perfluoroaromatic (Ar-Ar^F) groups have favorable inter-ring interactions leading to self-assembly of the molecules [30–36]. Both Ar-Ar^F self-assembly and dendron or dendrimer synthesis have been employed to obtain noncentrosymmetrically ordered amorphous materials and to increase orientation stability and NLO response of the materials [10,12,23,37–46]. One of chromophores to include in NLO active materials is azobenzene, which, in general, is thermally and optically stable but *push-pull* type azobenzenes exhibit also NLO properties [13,16,47,48]. *Push-pull* azobenzene containing dendrimers are synthesized to research their NLO properties mostly when azobenzene is incorporated in the branching structure of dendrimer [9,12,21,23,37, 45,49–58]. Azobenzene core dendrimers have been synthesized mostly to investigate their *cis-trans* isomerization [59–67]. Azochromophores of *push-pull* type were incorporated in dendrimer or dendron cores for investigation of NLO properties only in our previous works [27,28, 68–74].

We have previously synthesized compounds 1–3 (Fig. 1) with added Trt groups containing dendron fragment at either donor or acceptor, or both sides of azochromophore [27], and the most promising compound 1 showed T_g of 78 °C and NLO coefficient d_{33} value of 38 pm·V^{-1} [28]. To research influence of Ar-Ar^F interactions on physical properties of dendronized azochromophores, we have synthesized compound 2 with pentafluorophenyloxy moiety connected to azobenzene acceptor part and compound 3 with (pentafluorophenyl)methyl ester connected to azobenzene donor part [27]. However the thermal properties were unsatisfactory: pentafluorophenyloxy group induces crystallinity, (pentafluorophenyl)methyl ester function increases thermal stability, but lowers T_g and we proposed a hypothesis that (pentafluorophenyl)methyl ether groups could give better properties to azochromophore molecular glass. We have also synthesized compounds 4, 5 (Fig. 1) with two (pentafluorophenyl)methyl ether groups containing dendron with T_g of 58–60 °C and NLO coefficient d_{33} values of 26–35 pm·V^{-1}. We have discovered in comparison with analogs without fluoroaromatic fragments at acceptor side, that connection of pentafluorophenyl fragment to donor part of azochromophore is most successful [74]. The effect of Trt groups on physical properties was investigated by synthesis of azobenzene core dendrimers. We have attempted to synthesize azobenzene core dendrimer 6 with both dendronizing fragments connected to donor

part of the azobenzene molecule (Fig. 1) [73], but in series with next two generations we failed to obtain flawless structure. The used synthesis and purification method led to imperfect sample of several compounds with partially free hydroxyl groups, although showing expected high T_g of 82 °C [73] and NLO coefficient d_{33} value of 125 pm·V^{-1} [75].

In this work, our aim is to synthesize azochromophores with one or two (pentafluorophenyl)methyl ether moieties connected to donor part of the chromophore and Trt groups containing dendron connected to acceptor part of the chromophore to investigate and compare structure influence on thermal, optical, and NLO properties. We revised the synthesis method of compound 6 and obtained it as a pure sample which is fully functionalized with trityl groups. We have measured optical, thermal, and NLO properties and compared obtained results to results of previous sample of imperfect dendrimer.

2. Experimental details

2.1. Reagents and general procedures

Solvents were dried by standard procedures. Commercially obtained reagents were used without further purification. Following starting materials were prepared according to the literature: 3-nitrobenzene-6-diazoniumolate (7) [27], 2-[methyl(phenyl)amino]ethan-1-ol (8) [27], 3,5-bis[2-(tetrahydro-2*H*-pyran-2-yloxy)ethoxy]benzoic acid (14a) [68], 3,5-bis[2-(trityloxy)ethoxy]benzoic acid (14b) [27], 4'-[*N*-(2-{3, 5-bis[(pentafluorophenyl)methoxy]benzoyloxy}ethyl)--*N*-methylamino)-2-(2-hydroxyethoxy)-4-nitroazobenzene (16) [74], and 4-[*N*,*N*-bis(2-hydroxyethyl)amino)-3-methoxy-4'-nitroazobenzene (19) [68]. Purity of all compounds was checked by TLC method on Merck F$_{254}$ silica plates. The spots were visualized when necessary in UV light. Chromatographic separations were carried out on silica gel (ROTH Kieselgel 60, 60–200 μm). Melting points were taken on a Stuart SMP10 apparatus. The UV–Vis spectra were recorded using Perkin Elmer Lambda 35 spectrometer, and IR spectra were recorded by Perkin Elmer Spectrum 100 FT-IR spectrometer using UATR accessory. ^{1}H and ^{13}C NMR spectra were obtained on a Varian Mercury BB 200 MHz and Bruker Avance 300 MHz spectrometers against solvent residue as internal reference, spin coupling constants are shown in Hz. The elemental analysis was carried out on automatic analyzers Carlo Erba EA 1106 and Euro Vector EA 3000. Reaction mixture analysis was carried out on HPLC-MS system consisting of Waters Alliance 2695 chromatograph equipped with XTerra® MS C18 5 μm 2.1 × 100 mm column, Waters 2996 PDA detector, and Waters EMD 1000 (ESI) masspectrometer. Thermogravimetric (TG) analysis and differential scanning calorimetry (DSC) were accomplished on Perkin Elmer STA 6000 apparatus. All the samples were heated at 10 °C/min from 20 to 200 °C under nitrogen for
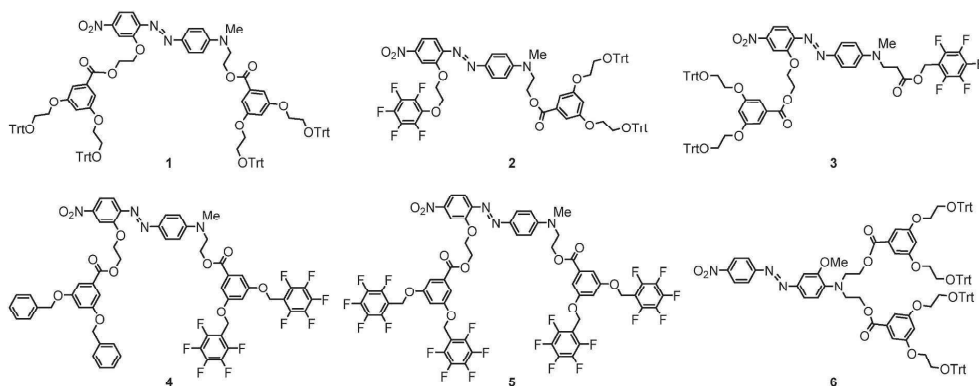

Fig. 1. Structures of previously synthesized dendronized azochromophores.

the first scan, then cooled to 17 °C, and heated at 10 °C/min from 17 to 500 °C for the second scan. Thermal destruction temperature (T_d) was measured where TG curve shows 5% weight loss. All measurements and experiments were performed twice and the average value was calculated.

2.2. X-ray analysis

Crystals of compound **18** were grown from CH_2Cl_2/MeOH solution. Single crystals of compound **18** ($C_{51}H_{46}Cl_2O_6$) were investigated on a Rigaku XtaLAB Synergy Dualflex diffractometer equipped with HyPix detector. The crystal was kept at 173(1) K during data collection. Program Olex2 [76] was used, the structure was solved with the ShelXT [77] structure solution program using Intrinsic Phasing and refined with the olex2.refine [78] refinement package using Levenberg-Marquardt minimization. For further details, see crystallographic data for this compound deposited with the Cambridge Crystallographic Data Centre as Supplementary Publications of CCDC 2035030 number. Copies of the data can be obtained, free of charge, on application to CCDC, 12 Union Road, Cambridge CB2 1EZ, UK.

Crystal data of compound **18**: triclinic, space group $P\bar{1}$ (no. 2), $a = 8.8620(2)$ Å, $b = 14.4393(3)$ Å, $c = 17.2972(5)$ Å, $\alpha = 107.065(2)°$, $\beta = 92.079(2)°$, $\gamma = 98.479(2)°$, $V = 2085.37(9)$ Å³, $Z = 2$, $T = 173(1)$ K, μ(Cu Kα) = 1.212 mm⁻¹, Dcalc = 1.2475 g/cm³, 32801 reflections measured ($2\Theta \leq 155.0°$), 8809 unique ($R_{int} = 0.0482$, $R_{sigma} = 0.0484$) which were used in all calculations. The final R_1 was 0.0653 ($I \geq 2\sigma(I)$) and wR_2 was 0.2046 (all data).

2.3. Thin film preparation and NLO measurements

The glassy thin films used for measurements of NLO properties were prepared from chromophore solution in CHCl₃ (analytical grade) with a typical concentration of 10 mg/mL. Thin films were prepared from solution using solvent casting method. The prepared samples were dried at room temperature for 3 days. The thickness of the obtained films was measured with Dektak 150 profilometer and was in the range of 0.6–1.7 μm.

Due to large absorption coefficients of the materials, absorption spectra were measured for specially prepared 20–40 nm thin samples. The prepared CHCl₃ solution was spin-coated on glass or quartz slides with a Laurell WS-400B-6NPP/LITE spin-coater with total spinning time of 2.4 s, acceleration 800 rpm/s and rotation speed of 900 rpm. After spin-coating the samples were dried at room temperature for 3 days. These samples were used only for absorption spectra measurements. The thickness of these thin films was determined by a Dektak 150 profilometer and white light interferometer Zygo NewView 7100.

The Corona discharge poling, measurements of refractive index and second harmonic intensity (SHI), and calculations of NLO properties were accomplished using previously reported experimental setup and mathematical models [28,74].

2.4. Syntheses

2-(2-Bromoethoxy)tetrahydro-2*H*-pyran. 2-Bromoethanol (28.4 mL, 0.40 mol) was dissolved in dry CH_2Cl_2 (50 mL) and catalyst pyridinium 4-methylbenzenesulphonate (2.00 g, 0.008 mol) was added. The mixture was cooled in an ice bath and a solution of 3,4-dihydro-2*H*-pyran (40 mL, 0.44 mol) in dry CH_2Cl_2 (35 mL) was added dropwise. Resulting solution was let for a day at room temperature. The reaction mixture was washed with cool satd. NaHCO₃ solution (3 × 40 mL) and cool brine (3 × 40 mL), dried over Na₂SO₄, filtered, concentrated, and distilled in vacuum at 89–90 °C/8 mmHg (lit. [79] 98–102 °C/23 mmHg), yield 46.53 g (56%) of yellowish liquid. ¹H NMR (300 MHz, CDCl₃) δ, ppm: 4.6 (t, *J* = 2.8, 1H, 3H, OC*H*H), 3.51–3.38 (m, 3H, CH₂Br, OC*H*H), 1.82–1.45 (m, 6H, THP).

4-[*N*-(2-Hydroxyethyl)-*N*-methylamino]-2′-hydroxy-4′-

nitroazobenzene (9). Betaine **7** (3.48 g, 0.021 mol) and aniline **8** (3.18 g, 0.021 mol) were dissolved in AcOH (15 mL), resulting mixture was stirred overnight at room temperature in the dark, then temperature was raised to 40 °C and the mixture was stirred 1 h. Water was added, and the flask was put in refrigerator overnight. Precipitate was filtered, washed with water, and recrystallized from toluene. Yield 3.01 g (45%) of brown crystalline solid, m.p. 181–183 °C. Anal. calcd. for $C_{15}H_{16}N_4O_4$: C 56.96; H 5.10; N 17.71. Found: C 57.01; H 4.84; N 17.25. IR (cm⁻¹) 3340.6, 2946.8, 2918.1, 1603.6, 1513.7, 1339.1, 1315.0, 1266.4, 1161.5, 1073.9, 1064.9, 1040.5, 819.7. MS ESI+ *m/z* calcd. for $C_{15}H_{17}N_4O_4$ 317.1 [M+H]⁺, found 317.4 [M+H]⁺. ¹H NMR (200 MHz, CDCl₃) δ, 7.90–7.73 (m, 5H, Ar), 6.77 (d, *J* = 9.0, 2H, Ar), 3.86 (t, *J* = 5.6, 2H, CH₂), 3.61 (t, *J* = 5.6, 2H, NCH₂), 3.12 (s, 3H, NCH₃), 1.62 (br. s, 2H, OH).

4-[*N*-(2-Hydroxyethyl)-*N*-methylamino]-2′-[2-(tetrahydro-2*H*-pyran-2-yloxy)ethoxy]-4′-nitroazobenzene (10a). Azobenzene **9** (0.60 g, 1.9 mmol) was suspended in 10 mL of abs. MeCN under Ar, Cs₂CO₃ (0.33 g, 1.0 mmol) and 2-(2-bromoethoxy)tetrahydro-2*H*-pyran (0.44 g, 2.1 mmol) were added. Reaction mixture was refluxed for 12 h, then precipitate was filtered off, mixture of CH_2Cl_2 and water was added. Organics was separated and washed with water three times, dried over Na₂SO₄ and filtered. CH_2Cl_2 solution was brought on short column of silica gel, byproducts were eluted off with CH_2Cl_2, and product was eluted with EtOAc. Deep red oil was afforded on evaporation, which crystallized. Yield 0.38 g (45%) of violet crystalline solid, m. p. 125–128 °C. Anal. calcd. for $C_{22}H_{28}N_4O_6$: C 59.45; H 6.35; N 12.60. Found: C 59.50; H 6.35; N 12.29. IR (cm⁻¹) 3075.9, 2943.5, 2911.1, 2865.3, 1595.8, 1519.2, 1455.2, 1427.8, 1336.0, 1303.6, 1260.1, 1208.9, 1142.7, 1104.3, 1086.1, 1074.0, 1028.2, 978.1, 959.4, 905.2. MS ESI+ *m/z* calcd. for $C_{22}H_{29}N_4O_6$ 445.2 [M+H]⁺, found 445.1 [M+H]⁺. ¹H NMR (200 MHz, CDCl₃) δ, ppm: 7.94 (d, *J* = 2.2, 1H, Ar), 7.88–7.78 (m, 3H, Ar), 7.60 (d, *J* = 8.4, 1H, Ar), 6.73 (d, *J* = 9.2, 2H, Ar), 4.76–4.68 (m, 1H, acetal H), 4.38 (t, *J* = 4.8, 2H, CH₂OAr), 4.09 (dt, *J* = 4.4, 11.6, 1H, OCH*H*), 3.92–3.79 (m, 4H, HOC*H*₂, OC*H*H), 3.58 (t, *J* = 5.6, 2H, NCH₂), 3.51–3.39 (m, 1H, OCH*H*), 3.09 (s, 3H, NCH₃), 1.82–1.38 (m, 6H, THP).

4-{*N*-[2-(Methanesulfonyloxy)ethyl]-*N*-methylamino}-2′-[2-(tetrahydro-2*H*-pyran-2-yloxy)ethoxy]-4′-nitroazobenzene (10b). Azocompound (**10a**) (0.51 g, 1.1 mmol) was dissolved in dry CH_2Cl_2 (5 mL) and NEt₃ (0.24 g, 2.3 mmol) was added. Solution was cooled to −15 °C and methanesulfonyl chloride (0.13 g, 1.2 mmol) was added dropwise while stirring. Reaction mixture was stirred for 4 h, and then washed once with satd. NaHCO₃ solution and three times with water. Solution was dried over Na₂SO₄, filtered, and evaporated. A red oil, which crystallizes was obtained. The crude product was purified by silica gel chromatography, eluted with EtOAc/CH_2Cl_2 (gradient 0–25%). Yield 0.49 g (82%) of red crystalline solid, m.p. 111–114 °C. Anal. calcd. for $C_{23}H_{30}N_4O_8S$: C 52.86; H 5.79; N 10.72. Found: C 53.03; H 5.61; N 10.62. IR (cm⁻¹) 2943.5, 1599.1, 1515.0, 1460.2, 1421.4, 1377.0, 1330.0, 1308.7, 1238.2, 1167.4, 1146.8, 1127.5, 1079.2, 1033.3, 987.5, 968.5, 912.3. MS ESI+ *m/z* calcd. for $C_{23}H_{31}N_4O_8S$ 523.2 [M+H]⁺, found 523.1 [M+H]⁺. ¹H NMR (200 MHz, CDCl₃) δ, ppm: 7.94 (d, *J* = 2.2, 1H, Ar), 7.90–7.77 (m, 3H, Ar), 7.61 (d, *J* = 8.8, 1H, Ar), 6.73 (d, *J* = 9.2, 2H, Ar), 4.76–4.68 (m, 1H, acetal H), 4.44–4.32 (m, 4H, SOCH₂, CH₂OAr), 4.10 (dt, *J* = 4.5, 11.6, 1H, OCH*H*), 3.92–3.75 (m, 4H, NCH₂, OC*H*H), 3.52–3.40 (m, 1H, OCH*H*), 3.10 (s, 3H, NCH₃), 2.91 (s, 3H, SCH₃), 1.82–1.38 (m, 6H, THP).

4-{*N*-[2-(2,2,2-Trichloroacetimidoyl)oxyethyl]-*N*-methyl-amino}-2′-[2-(tetrahydro-2*H*-pyran-2-yloxy)ethoxy]-4′-nitro-azobenzene (10c). A solution of compound **10a** (0.29 g, 0.66 mmol) in abs. THF (1.5 mL) was added to a suspension of NaH (2.5 mg, 0.06 mmol, 60% in mineral oil) in abs. THF (1.0 mL). Resulting mixture was cooled in an ice bath, then Cl₃CCN (66 μL, 0.66 mmol) was added. The ice bath was removed, and the mixture stirred for 2 h, then 1% solution of MeOH in hexane (1 mL) was added. Precipitate was filtered off and mother liquor was evaporated to afford 0.35 g (100%) of crude product

as red oil, which was used in the next step without further purification. MS ESI+ m/z calcd. for $C_{24}H_{29}Cl_3N_5O_6$ 588.1, 590.1, 592.1 $[M+H]^+$, found 588.1, 590.0, 592.1 $[M+H]^+$.

4-(*N*-{2-[(Pentafluorophenyl)methoxy] ethyl}-*N*-methyl-amino)-2'-[2-(tetrahydro-2*H*-pyran-2-yloxy)ethoxy] -4'-nitro-azobenzene (12). Azocompound **10a** (0.30 g, 0.68 mmol), TBAB (1.29 g, 4.0 mmol) and bromide **11b** (3.55 g, 13.6 mmol) were dissolved in CH$_2$Cl$_2$ (80 mL). Solution of KOH (1.56 g, 28 mmol) in dest. H$_2$O (29 mL) was added after 5 min. Reaction mixture was vigourously stirred for 24 h at room temperature. Aqueous and organic layers were separated, and the organic solution was washed with water three times. Solution was dried over Na$_2$SO$_4$, filtered, and evaporated. Crude product was purified by silica gel chromatography, eluted with EtOAc/CH$_2$Cl$_2$ (gradient 0–10%). Bromide **11b** (2.20 g, 62%) was recovered after recrystallization from petroleum ether in freezer. Yield 0.25 g (60%) of red solid, m. p. 68–73 °C. Anal. calcd. for $C_{29}H_{29}F_5N_4O_6$: C 55.77; H 4.68; N 8.97. Found: C 55.85; H 4.71; N 8.48. IR (cm^{-1}) 2925.9, 2875.5, 1737.7, 1656.6, 1598.6, 1514.4, 1503.6, 1373.5, 1326.9, 1305.5, 1258.4, 1238.5, 1141.4, 1134.0, 1079.6, 1052.3, 1037.4, 967.2, 956.0, 935.7. MS ESI+ m/z calcd. for $C_{29}H_{30}F_5N_4O_6$ 625.2 $[M+H]^+$, found 625.4 $[M+H]^+$. ^{1}H NMR (300 MHz, DMSO-d_6) δ, ppm: 8.03 (d, J = 2.3, 1H, Ar), 7.91 (dd, J = 8.9, 2.3, 1H, Ar), 7.76 (d, J = 9.0, 2H, Ar), 7.61 (d, J = 8.8, 1H, Ar), 6.81 (d, J = 9.3, 2H, Ar), 4.75 (t, J = 2.9, 1H, acetal H), 4.60 (s, 2H, CH$_2$C$_6$F$_5$), 4.46 (t, J = 4.3, 2H, CH$_2$OAr), 4.00 (dt, J = 8.8, 4.2, 1H, OCHH), 3.86–3.74 (m, 2H, OCHH), 3.68 (s, 4H, NCH$_2$CH$_2$O), 3.47–3.37 (m, 1H, OCHH), 3.04 (s, 3H, NCH$_3$), 1.77–1.08 (m, 6H, THP).

4-(*N*-{2-[(Pentafluorophenyl)methoxy] ethyl}-*N*-methyl-amino)-2'-(2-hydroxyethoxy)-4'-nitroazobenzene (13). Compound **12** (0.30 g, 0.48 mmol) was dissolved in CH$_2$Cl$_2$ (4 mL), MeOH (10 mL) and conc. HCl (40 μL, 0.48 mmol) were added. Reaction mixture was stirred for 2 h, then satd. NaHCO$_3$ solution (20 mL) was added, layers were separated, and organic solution was washed with water three times. The solution was dried over Na$_2$SO$_4$, filtered, and evaporated. Crude product was purified by silica gel chromatography, eluted with EtOAc/CH$_2$Cl$_2$ (gradient 1–20%). Yield 0.24 g (92%) of deep red crystalline solid, m.p. 131–135 °C. Anal. calcd. for $C_{24}H_{21}F_5N_4O_5 \cdot H_2O$: C 51.62; H 4.15; N 10.03. Found: C 52.06; H 4.09; N 9.50. IR (cm^{-1}) 3391.5, 2945.1, 2923.2, 1656.4, 1599.9, 1523.8, 1504.6, 1334.2, 1307.3, 1256.0, 1153.7, 1140.1, 1128.1, 1100.6, 1082.9, 1039.0, 964.6, 935.9. MS ESI+ m/z calcd. for $C_{24}H_{22}F_5N_4O_5$ 541.1 $[M+H]^+$, found 541.3 $[M+H]^+$. ^{1}H NMR (300 MHz, DMSO-d_6) δ, ppm: 8.01 (d, J = 2.4, 1H, Ar), 7.91 (dd, J = 8.8, 2.4, 1H, Ar), 7.78 (d, J = 9.2, 2H, Ar), 7.62 (d, J = 8.9, 1H, Ar), 6.83 (d, J = 9.2, 2H, Ar), 4.97 (t, J = 5.3, 1H, OH), 4.61 (s, 2H, CH$_2$C$_6$F$_5$), 4.32 (t, J = 5.1, 2H, CH$_2$OAr), 3.82 (q, J = 5.3, 2H, CH$_2$OH), 3.69 (s, 4H, NCH$_2$CH$_2$O), 3.05 (s, 3H, NCH$_3$).

4-(*N*-{2-[(Pentafluorophenyl)methoxy] ethyl}-*N*-methyl-amino)-2'-(2-{3,5-bis [2-(tetrahydro-2*H*-pyran-2-yloxy)ethoxy] benzoyloxy}ethoxy)-4'-nitroazobenzene (15a). Compound **13** (0.220 g, 0.41 mmol) and acid **14a** (0.200 g, 0.49 mmol) were dissolved in dry CH$_2$Cl$_2$ (6 mL) and DMAP (5.5 mg, 0.044 mmol) was added while stirring in an ice bath, then a solution of DCC (101 mg, 0.21 mmol) in dry CH$_2$Cl$_2$ (2 mL) was added dropwise over 30 min. Reaction mixture was stirred for 24 h at room temperature, then a drop of MeOH was added to quench excess acid. Flask was put in a freezer for all *N,N'*-dicyclohexylurea to crystallize, then filtered, and evaporated. The crude product was purified by silica gel flash-chromatography, eluted with EtOAc/CH$_2$Cl$_2$ (3%). Yield 0.31 g (82%) of deep red very viscous oil. Anal. calcd. for $C_{45}H_{49}F_5N_4O_{12}$: C 57.94; H 5.29; N 6.01. Found: C 57.56; H 5.60; N 5.67. IR (cm^{-1}) 2943.0, 2872.5, 1721.0, 1656.9, 1597.7, 1518.3, 1504.9, 1444.2, 1374.3, 1337.1, 1307.9, 1220.5, 1171.9, 1139.2, 1123.6, 1087.4, 1072.3, 1033.6, 966.7, 936.3. MS ESI+ m/z calcd. for $C_{45}H_{50}F_5N_4O_{12}$ 933.3 $[M+H]^+$, found 933.6 $[M+H]^+$. ^{1}H NMR (300 MHz, CDCl$_3$) δ, ppm: 8.00–7.75 (m, 4H, Ar), 7.68 (d, J = 8.8, 1H, Ar), 7.19 (d, J = 2.3, 2H, Ar), 6.77–6.54 (m, 3H, Ar), 4.83–4.70 (m, 2H, acetal H), 4.70–4.50 (m, 6H, esterOCH$_2$CH$_2$OAr, CH$_2$C$_6$F$_5$), 4.18–4.03 (m, 4H, dendronArOCH$_2$), 3.99 (dt, J = 11.0, 4.3, 2H, OCHH),

3.90–3.57 (m, 8H, OCHH, NCH$_2$CH$_2$O), 3.56–3.43 (m, 2H, OCHH), 3.08 (s, 3H, NCH$_3$), 1.93–1.35 (m, 12H, THP). ^{13}C NMR (75 MHz, CDCl$_3$) δ, ppm: 166.2, 160.0, 155.0, 152.0, 148.1, 147.5, 145.6 (d, J = 249), 144.6, 141.4 (d, J = 255), 137.5 (d, J = 254), 131.6, 126.3, 117.7, 117.5, 111.6, 110.9, 108.3, 107.4, 99.0, 68.8, 68.3, 67.8, 65.7, 63.4, 62.2, 60.1, 52.3, 39.8, 30.5, 25.5, 19.4.

4-(*N*-{2-[(Pentafluorophenyl)methoxy] ethyl}-*N*-methyl-amino)-2'-(2-(3,5-bis [2-(trityloxy)ethoxy] benzoyloxy}ethoxy)-4'-nitroazobenzene (15b). Compound **15b** was obtained using the same method as for synthesis of compound **15a**, starting materials were compound **7** (0.103 g, 0.19 mmol), acid **14b** (0.15 g, 0.21 mmol), DMAP (3.0 mg, 0.02 mmol), and DCC (43 mg, 0.21 mmol). The crude product was purified by precipitation from EtOAc/MeOH. Yield 0.174 g (73%) of deep red amorphous solid. Anal. calcd. for $C_{73}H_{61}F_5N_4O_{10}$: C 70.18; H 4.92; N 4.48. Found: C 69.77; H 5.00; N 4.24. IR (cm^{-1}) 3060.6, 2926.4, 1720.7, 1656.0, 1597.8, 1519.2, 1505.3, 1446.8, 1374.4, 1337.7, 1308.1, 1219.5, 1169.4, 1142.4, 1089.7, 1001.3, 936.2. ^{1}H NMR (300 MHz, CDCl$_3$) δ, ppm: 7.98 (d, J = 2.3, 1H, Ar), 7.93 (dd, J = 8.8, 2.3, 1H, Ar), 7.86 (d, J = 9.2, 2H, Ar), 7.72 (d, J = 8.8, 1H, Ar), 7.57–7.42 (m, 12H, Trt), 7.37–7.15 (m, 20H, Ar, Trt), 6.75 (t, J = 2.3, 1H, Ar), 6.65 (d, J = 9.2, 2H, Ar), 4.81 (t, J = 4.8, 2H, OCH$_2$), 4.67–4.50 (m, 4H, CH$_2$C$_6$F$_5$, OCH$_2$), 4.14 (t, J = 4.9, 4H, OCH$_2$), 3.68 (t, J = 5.3, 2H, OCH$_2$), 3.59 (t, J = 5.2, 2H, NCH$_2$), 3.43 (t, J = 4.9, 4H, OCH$_2$), 3.04 (s, 3H, NCH$_3$). ^{13}C NMR (75 MHz, CDCl$_3$) δ, ppm: 166.4, 160.2, 155.0, 152.1, 148.2, 147.7, 144.7, 144.0, 131.7, 128.9, 128.0, 127.2, 126.3, 117.7, 117.6, 111.6, 111.0, 108.3, 107.5, 86.9, 68.8, 68.3, 68.0, 63.4, 62.7, 60.2, 52.2, 39.7.

4-(*N*-{2-[(Pentafluorophenyl)methoxy] ethyl}-*N*-methyl-amino)-2'-{2-[3,5-bis(2-hydroxyethoxy)benzoyloxy] ethoxy}-4'-nitroazobenzene (15c). Compound **15c** was obtained using the same method as for synthesis of compound **13**, starting materials were compound **15a** (0.20 g, 0.21 mmol) in CH$_2$Cl$_2$ (4 mL), MeOH (10 mL), and conc. HCl (20 μL, 0.24 mmol). Crude product was purified by silica gel chromatography, eluted with EtOAc/heptane (gradient 30–60%). Yield 0.13 g (81%) of deep red crystalline solid, m.p. 105 °C. Anal. calcd. for $C_{35}H_{33}F_5N_4O_{10}$: C, 54.98; H, 4.35; N, 7.33. Found: C 55.00; H 4.49; N 7.26. IR (cm^{-1}) 3480.2, 2934.3, 2874.3, 1716.7, 1655.0, 1601.6, 1517.2, 1503.2, 1335.4, 1236.5, 1174.2, 1142.5, 1119.3, 1085.2, 1085.2, 1055.3, 1018.1, 988.6, 929.3. MS ESI+ m/z calcd. for $C_{35}H_{34}F_5N_4O_{10}$ 765.2 $[M+H]^+$, found 765.6 $[M+H]^+$. ^{1}H NMR (300 MHz, CDCl$_3$) δ, ppm: 7.99 (d, J = 1.9, 1H, Ar), 7.94–7.76 (m, 3H, Ar), 7.68 (d, J = 8.8, 1H, Ar), 7.15 (d, J = 2.0 Hz, 2H, Ar), 6.74–6.55 (m, 3H, Ar), 4.86–4.69 (m, 2H, OCH$_2$), 4.69–4.45 (m, 4H, CH$_2$C$_6$F$_5$, OCH$_2$), 4.06–3.94 (m, 4H, OCH$_2$), 3.94–3.80 (m, 4H, OCH$_2$), 3.79–3.55 (m, 4H, NCH$_2$CH$_2$O), 3.09 (s, 3H, NCH$_3$), 2.15 (br. s, 2H, OH). ^{13}C NMR (75 MHz, CDCl$_3$) δ, ppm: 166.1, 159.8, 155.1, 152.2, 148.1, 147.6, 145.6 (d, J = 249), 144.6, 141.4 (d, J = 255), 137.5 (d, J = 254), 131.8, 126.3, 117.8, 117.6, 111.6, 111.1, 108.4, 106.8, 69.7, 68.8, 68.3, 63.8, 61.3, 60.2, 52.2, 39.8.

4'-[*N*-(2-{3,5-bis [(pentafluorophenyl)methoxy] benzoyloxy} ethyl)-*N*-methylamino) -2-(2-{3,5-bis [2-(trityloxy)ethoxy] benzoyloxy}ethoxy)-4-nitroazobenzene (17). Compound **17** was obtained using the same method as for synthesis of compound **15a**, starting materials were compound **16** (100 mg, 0.117 mmol), acid **14b** (93 mg, 0.129 mmol), DMAP (1.5 mg, 0.012 mmol), and DCC (36 mg, 0.178 mmol). The crude product was purified by precipitation from CH$_2$Cl$_2$/MeOH. Yield 0.139 g (76%) of deep red amorphous solid. Anal. calcd. for $C_{87}H_{66}F_{10}N_4O_{13}$: C 66.75; H 4.25; N 3.58. Found: C 67.22; H 4.69; N 3.49. IR (cm^{-1}) 3031.4, 2949.1, 1720.3, 1658.5, 1597.2, 1521.3, 1506.8, 1446.7, 1375.0, 1339.3, 1309.9, 1220.9, 1145.9, 1090.4, 1056.4, 974.6, 939.7. ^{1}H NMR (300 MHz, CDCl$_3$) δ, ppm: 8.05–7.79 (m, 4H, Ar), 7.62 (d, J = 8.8, 1H, Ar), 7.57–7.39 (m, 12H, Trt), 7.39–7.07 (m, 22H, Ar, Trt), 6.83 (d, J = 9.1, 2H, Ar), 6.77–6.56 (m, 2H, Ar), 4.91 (s, 4H, CH$_2$C$_6$F$_5$), 4.82 (t, J = 4.5, 2H, OCH$_2$), 4.57 (t, J = 4.5, 2H, OCH$_2$), 4.48 (t, J = 5.2, 2H, NCH$_2$CH$_2$O), 4.12 (t, J = 4.7, 4H, OCH$_2$), 3.79 (t, J = 5.0, 2H, NCH$_2$), 3.44 (t, J = 4.9, 4H, CH$_2$OTrt), 3.08 (s, 3H, NCH$_3$). ^{13}C NMR (75 MHz, CDCl$_3$) δ, ppm: 166.3, 165.9, 160.1, 159.2,

155.1, 152.6, 148.3, 146.8, 145.8 (d, $J = 252$), 144.5, 144.0, 141.9 (d, $J = 250$), 137.6 (d, $J = 252$), 132.0, 131.7, 128.9, 128.1, 128.0, 127.4, 127.2, 126.3, 117.3, 117.0, 111.7, 110.4, 109.7 (t, $J = 17$), 108.6, 108.3, 108.2, 107.4, 86.9, 68.5, 68.0, 63.2, 62.7, 62.5, 57.7, 50.1, 38.2.

4-[N,N-bis-(2-{3,5-bis[2-(trityloxy)ethoxy] benzoyloxy}ethyl) amino]-3-methoxy-4′-nitroazobenzene (6). Compound **6** was obtained using the same method as for synthesis of compound **15a**, starting materials were azobenzene **19** (35 mg, 98 μmol), acid **14b** (150 mg, 210 μmol), DMAP (3.0 mg, 25 μmol), and DCC (43 mg, 210 μmol). The crude product was purified by precipitation from CH$_2$Cl$_2$ (2 mL) solution with MeOH (3 mL), the precipitation was repeated second time. Yield 137 mg (78%) of red solid. Anal. calcd. for C$_{115}$H$_{100}$N$_4$O$_{15}$: C 77.68; H 5.67; N 3.15. Found: C 77.75; H 5.71; N 3.35. ^{1}H NMR (300 MHz, CDCl$_3$) δ, ppm: 8.16 (d, $J = 9.0$, 2H, Ar), 7.75 (d, $J = 8.9$, 2H, Ar), 7.54–7.28 (m, 26H, Trt, Ar), 7.28–6.97 (m, 41H, Trt, Ar), 6.59 (t, $J = 2.1$, 2H, Ar), 4.44 (t, $J = 5.6$, 4H, NCH$_2$CH$_2$O), 4.01 (t, $J = 4.7$, 8H, OCH$_2$), 3.88–3.59 (m, 7H, NCH$_2$, NCH$_3$), 3.31 (t, $J = 4.7$, 8H, CH$_2$OTrt). ^{13}C NMR (75 MHz, CDCl$_3$) δ, ppm: 166.3, 160.1, 156.3, 152.4, 148.0, 147.5, 144.0, 143.7, 131.8, 128.8, 128.0, 127.2, 124.8, 123.1, 122.4, 119.1, 108.2, 107.2, 103.2, 86.8, 67.9, 62.9, 62.7, 55.8, 51.4.

3. Results and discussion

3.1. Synthesis

We synthesized azochromophore **9** from freshly synthesized betaine **7** and 2-[methyl(phenyl)amino]ethan-1-ol (**8**) in acetic acid (Fig. 2). Compound **10a** was obtained in Williamson ether synthesis from azobenzene **9** and 2-(2-bromoethoxy)tetrahydro-2H-pyran in 45% yield. Active mesylate **10b** was obtained straightforwardly from compound **10a** with mesyl chloride in presence of NEt$_3$ in 82% yield. Active trichloroacetimidate **10c** was obtained from compound **10a** with Cl$_3$CCN quantitatively and readily used in the next step.

Synthesis of pentafluorobenzyl ether **12** appeared to be the most time consuming. We carried out series of reactions to obtain compound **12** in Williamson ether synthesis (Table 1, experiments No. 1–3). Traces of compound **12** were found by HPLC-MS analysis only in experiment 3. Usually, azobenzene was found partially unreacted after reaction in experiments 1–3 but fluoroaromatic compound could not be found. We concluded that formation of desired product is far less favorable than nucleophilic substitution of aromatic fluorine atoms [80], because reaction of compound **10a** with benzyl bromide in conditions of experiment 2 gave azo according ether.

We conduced also experiments 4–6 in non-nucleophilic conditions, but the desired product was not obtained. We resumed that experiments 4 and 5 were unsuccessful because reactions of trichloroacetimidates from tertiary [81] and secondary [82] alcohols are described in literature, but we used primary alcohol. Small amount of compound **12** could be detected in HPLC-MS analysis of experiment 6 along with many other

Table 1
Reaction conditions to obtain ether **12**.

Entry	Reagents	Reaction conditions
1	**10b, 11a**	NaH, DMF, r.t., 2 d.
2	**10a, 11b**	NaH, THF, 60 °C, 1 d.
3	**10a, 11b**	NaN(SiMe$_3$)$_2$, DMF, 70 °C, 1 d.
4	**10b, 11a**	BF$_3$·Et$_2$O, CHCl$_3$, cyclohexane, r.t., 1 d. [81]
5	**10b, 11a**	HOSO$_2$CH$_3$, CHCl$_3$, cyclohexane, r.t., 1 d. [82]
6	**10a, 11b**	Ag$_2$O, CH$_2$Cl$_2$, r.t., 3 d. [83]
7	**10a, 11a**	DIAD, PPh$_3$, CH$_2$Cl$_2$, r.t., 1 d.
8	**10a, 11b**	TBAB, KOH, KI, THF, 70 °C, 1 d. [84]
9	**10a, 11b**	TBAB, KOH, CH$_2$Cl$_2$, H$_2$O, r.t., 1 d. [85]

unidentified peaks, but the purification was unsuccessful. Mitsunobu reaction (No. 7) gave only traces of product **12**.

Similar reaction conditions to No. 8 [84] and 9 [85] were found in literature to obtain ether of general formula RCH$_2$CH$_2$OCH$_2$C$_6$F$_5$. Experiment No. 8 gave only trace amount of product **12**. Finally experiment No. 9 was successful and compound **12** was obtained in 60% yield. The main difference between experiment No. 9 and other experiments was ratio of reactants – 20 times excess of bromide **11b** comparing to azobenzene **10a**, because method was previously used in derivatization for GC-MS analysis [85]. Most of the starting material **11b** was recovered and reused on the second run. The synthesis was also performed using only 1.2 equiv. of the bromide **11b**, but the reaction was less efficient, it was run for twice the time and only 41% yield of product **12** was obtained.

Protection group removal went easily and compound **13** was obtained in 92% yield (Fig. 2). Compound **13** reacted with dendronizing acids **14a,b** using *N,N′*-dicyclohexylcarbodiimide (DCC) and 4-(dimethylamino)pyridine (DMAP) [86,87]; we obtained dendronized azochromophores **15a,b** in good yields (Fig. 3). Third dendronized azochromophore **15c** was obtained from compound **15a** removing THP protection groups in good yield using HCl.

We synthesized dendronized azochromophore **17** from our published azochromophore **16** [74] and acid **14b** using the same reagents DCC and DMAP. Product **17** was obtained in good yield (Fig. 4). The compound
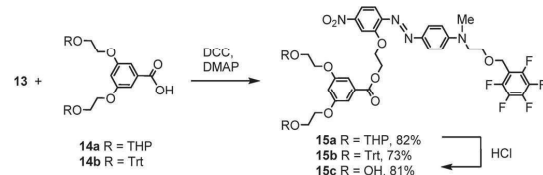
Fig. 3. Scheme of the dendronized azochromophore synthesis. DCC - *N,N′*-dicyclohexylcarbodiimide, DMAP - 4-(dimethylamino)pyridine, Trt - trityl.
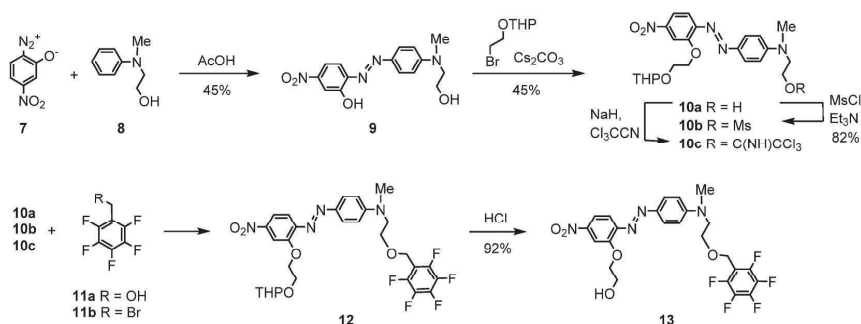
Fig. 2. Scheme of the azochromophore synthesis. Ms – methanesulfonyl, THP – tetrahydropyranyl.
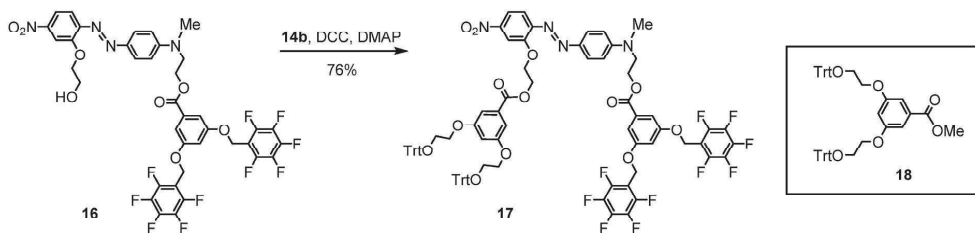
Fig. 4. The synthesis scheme of azochromophore **17**.

17 was purified by precipitation from CH$_2$Cl$_2$ with MeOH to preserve Trt groups, it formed both amorphous chunks and small crystals, but unexpectedly comparatively big crystals formed in mother liquor, which were analyzed with HPLC and NMR to find out that these crystals contained compound **17** and methyl ester **18**, which was formed from excess acid **14b** when reaction was quenched with MeOH.

The synthesis of dendrimer **6** was accomplished using the known method with DCC and DMAP; title compound was obtained in good yield from azocompound **19** and acid **14b** (Fig. 5). We purified the crude product by fractional precipitation from CH$_2$Cl$_2$ with MeOH to keep all Trt end groups, which are not stable on silica gel and were partially removed in previous experiments, when we attempted to synthesize this compound in slightly different way [73].

3.2. Characterization

Structures of synthesized intermediate compounds were proven using ^{1}H NMR spectra and HPLC-MS results. Dendronized azochromophores **6**, **15a–c**, **17** have also ^{13}C NMR spectra. Low resolution mass spectrometry connected to HPLC was used to verify molecular mass of intermediates and compounds **15a,b**, but it was not possible for compounds having greater molecular mass than 1090 g/mol.

Successful addition of (pentafluorophenyl)methyl group in synthesis of compound **12** is indicated by correct molecular mass and appearance of a new peak in ^{1}H NMR spectrum for two benzyl type protons at about 4.6 ppm for compound **12**, which is found in the same place for compounds **13** and **15a–c**. Pentafluorophenyl fragment is seen also in ^{13}C NMR spectra of products **15a,c** as three doublets for CF groups with $^1J_{CF}$ = 249–255 Hz. Compound **15b** shows only benzyl CH$_2$ fragment both in ^{1}H and ^{13}C NMR spectra, but signals for CF are not resolved from baseline. Compounds with THP groups **10a,b**, **12**, and **15a** have characteristic peaks for THP group: acetal proton is found at 4.72–4.75 ppm and wide multiplet in strongest fields for 6H of THP group, and several signals for OCH fragments at 3.4–4.0 ppm, which arises from chair form of THP group and diasterotopic nature of CH$_2$OTHP protons.

Spectra of compound **17** are compared to its precursor **16**, and show
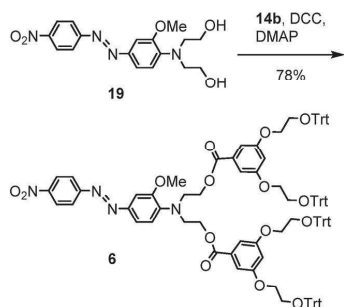
all needed fragments, even all four carbons of pentafluorophenyl rings are visible in ^{13}C NMR spectrum. Purity of azochromophore **6** was analyzed with HPLC and structure was approved using ^{1}H and ^{13}C NMR spectra. Elemental composition is matching theoretical calculation far better than previously obtained imperfect dendrimer [73].

We investigated accidently obtained crystals containing both compounds **17** and **18**, but X-ray analysis showed only compound **18**, and HPLC analysis revealed that molar proportion of compounds **18** and **17** is 18:1. We previously reported that compound **18** is amorphous [27], but now we succeeded to grow crystals of pure compound **18** from CH$_2$Cl$_2$/MeOH. Compound **18** crystallized as CH$_2$Cl$_2$ solvate in triclinic crystal system, space group $P\overline{1}$ (see Fig. 6). Compound **17** formed crystals of insufficient quality for X-ray structure analysis. We tried to grow crystals of several proportions between compound **17** and ester **18** for elaboration purposes of molecular configuration of compound **17** to observe potential Ar-Ar^F interactions. We discovered that pure compound **17** is precipitating from solution of equimolar proportions of compounds **18** and **17**, but small crystals of insufficient quality for X-ray analysis are forming in various proportions from solutions of varying and increasing part of ester **18**, but good crystals are formed only in 18:1 ratio. Crystal of both compounds probably is solid solution of compound **17** in crystals of compound **18**.

3.3. Thermal and optical properties

The dendronized azochromophores **6**, **15a–c**, **17** are red colored: compound **15a** is very viscous oil, compounds **15b** and **6** are amorphous solids, and compounds **15c** and **17** are crystalline solids with very similar melting points of 105 and 103 °C, respectively. Thermal properties were investigated using differential scanning calorimetry (DSC) and thermogravimetry (TG) (Table 2, supporting information Figs. S2 and S3). Glass transition temperature (T$_g$) was not observed for

Fig. 5. The synthesis scheme of azobenzene core dendrimer **6**.
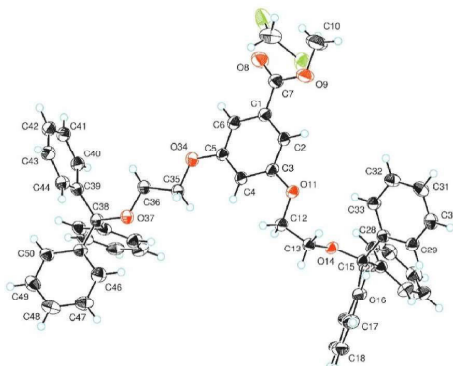
Fig. 6. Molecular structure of molecule **18** with atoms represented by thermal vibration ellipsoids of 50% probability.

Table 2
Thermal and linear optical properties of the synthesized azocompounds **6**, **15a–c**, **17**.

Compound	T_g, °C	mp, °C	T_d, °C	λ_{max}, nm CHCl$_3$	ε, M^{-1}·cm^{-1} CHCl$_3$	λ_{max}, nm EtOBz	ε, M^{-1}·cm^{-1} EtOBz	λ_{max}, nm DMF	ε, M^{-1}·cm^{-1} DMF	λ_{max}, nm thin film
6	83	–	286	463.2	21700	472.1	23100	479.8	22500	485
15a	–	–	253	482.6	29700	484.9	22300	495.8	22400	
15b	63	–	274	483.6	32300	485.7	28800	496.3	31600	490
15c	37	105	267	483.0	37700	485.7	31300	494.1	34400	
17	79	103	277	479.7	29300	485.9	36800	497.1	21000	482

compound **15a** because it is below room temperature. Compound **15b** with Trt groups has higher T_g for 26 °C than compound **15c** with OH groups and higher T_g than compound **3**, where ester linkage was used for attachment of pentafluorophenyl containing fragment. Thermal characteristics of compound **6** were almost the same as for previously reported imperfect sample [73]. Compounds **17** and **6** have the highest T_g and also the highest thermal stabilities up to 277 °C. Nevertheless T_g of compounds **6**, **15b**, **17** are low compared to widely expected [1,6,15], but such materials with low T_g could perform better than materials with high T_g in Arctic or Antarctic climate zones [9].

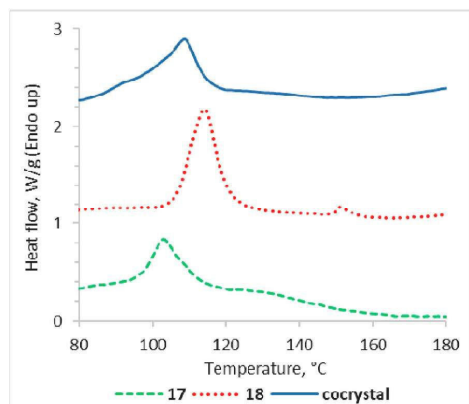Cocrystals of compounds **17** and **18** showed thermal properties more similar to ester **18**, the T_g and T_d were almost identical: 53 and 295 °C for ester **18**, 54 and 293 °C for cocrystal, respectively. This showed that spatial structure of cocrystal is determined by ester **18**. The differences were observed in melting points (see Fig. 7). Pure compound **18** had the highest melting point of 114 °C and a second peak at 151 °C, but the cocrystal showed melting in between of both constituents at 109 °C.

UV–Vis spectra were recorded in CHCl$_3$, EtOBz, and DMF to compare different interactions with pentafluorophenyl rings. Absorption maxima of compounds **15a–c** were almost identical in CHCl$_3$, and in EtOBz; this meant that the end groups of dendronizing fragment do not notably affect absorption energy of this chromophore and is determined by core azochromophore as it is accessible to solvent molecules. Minimal solvatochromism was observed on average of 2.4 nm with batochromic shift in EtOBz compared with CHCl$_3$. Compounds **15a–c** and **17** had very close absorption maxima in EtOBz, this could be due to the same core azochromophore and similar solvation environment in EtOBz, where solvent molecules engage in Ar-Ar^F interactions with pentafluorophenyl groups and free all azochromophore accessible to EtOBz. Solvation is different in CHCl$_3$ (Fig. 8), where intramolecular Ar-Ar^F interactions in compound **17** may be formed, and absorption maximum of compound **17** is close to compounds **4** and **5** with solvatochromism of 6.2 nm. Molar absorptivity in CHCl$_3$ is higher for compounds **15a–c**, but lower

Fig. 8. Light absorption spectra of fluorinated products in CHCl$_3$ solution (20 µmol/L).

for compounds **17** and **6** compared to EtOBz solution. DMF, as the most polar solvent from chosen solvents, causes batochromic shift of all compounds by 7.7–11.2 nm compared to EtOBz solutions.

Light absorption spectrum of compound **6** was recorded also in acetone (Fig. 9) for comparison purposes with previously synthesized imperfect dendrimer; and it was almost identical to previously reported: light absorption maximum of lowest frequency charge transfer transition band in acetone is 469.7 nm with molar absorptivity 22000 M^{-1}·cm^{-1}, which is slightly lower, due to complete dendrimer branches and therefore decreased mass fraction of the chromophore fragment compared to incomplete dendrimer. Absorption band of amorphous thin film on quartz glass (Fig. 9) showed bathochromic shift compared to

Fig. 7. DSC curves of pure compounds **17** and **18** and their cocrystal showing melting.
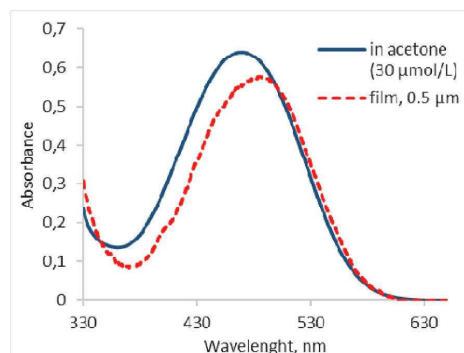
Fig. 9. Light absorption spectra of dendrimer **6** in acetone solution and of thin film on quartz glass.

solution and its maximum was 485 nm, indicating aggregate formation in solid state [13].

3.4. Nonlinear optical properties

NLO properties were tested for Trt groups containing chromophores **6**, **15b**, **17**, the other compounds did not form stable amorphous films at room temperature. Second harmonic intensity (SHI) in a Maker fringe experiment was measured for solvent cast amorphous films of pure synthesized compounds and the second order NLO coefficients d_{33}, d_{31}, and $d_{33}(0)$ were calculated to characterize the NLO properties. Fig. 10 shows Maker fringe for sample of compound **6** and standard x-cut quartz crystal. The corona poling procedure using corona triode was employed to break centrosymmetric ordering inside previously prepared glassy films. Refractive indices were measured or calculated at fundamental and second harmonic wavelengths (n_{1064} and n_{532} in Table 3) to evaluate NLO coefficients d_{33} and d_{31} of poled thin films. All compounds have wide absorption bands overlapping with second harmonic wavelength at 532 nm, which brings about resonance enhancement of NLO efficiency. As the NLO coefficients are frequency dependent, extrapolation to zero frequency ($d_{33}(0)$) was made according to two-level model [88] to subdue this interference.

All prepared thin films showed NLO activity (Table 3). Response of NLO properties is mostly dependent on molecular hyperpolarizability, extent of polar order, and chromophore content. Ratio of NLO coefficients d_{33}/d_{31} show polar order of poled chromophore films. This ratio is 3.5–4.0 for poled amorphous films of compounds **6**, **15b**, **17** and it indicates high polar order [91]. Chromophore loading density (N) was calculated from molar mass and the active chromophore was assumed as methoxy and methylamino derivative of core azobenzene in places of bulky substituents. Dendrimer **6** has biggest dendrimer branches and therefore N is the smallest, but nevertheless its NLO coefficients d_{33}, d_{31}, and $d_{33}(0)$ are the highest, which is related with alkoxy substituent on the donor part of the azochromophore. Compound **17** had the lowest NLO coefficient values, and this led to assumption that molecules of compound **17** for the most part after poling stayed ordered in centrosymmetric fashion leading to decreased NLO coefficients. Intermolecular Ar-Ar^F interactions of pentafluorophenyl and trityl groups between molecules in glassy film more likely occurred in a way favoring centrosymmetric ordering. Crystals of dendron ester fragment **18** and crystals of compound **4** share the same crystal system with centrosymmetric arrangement of molecules, so despite the unavailable single crystals of compound **17**, but considering its good incorporation in crystals of compound **18**, we suggest that compound **17** also may form centrosymmetric crystals strongly retaining that tendency in amorphous film.

Positive effect of increased NLO coefficients of compound **15b** compared to compounds **4**, **5**, and **17** could arise from shorter linkage between azobenzene and pentafluorphenyl ring and resulting inability of intramolecular bond formation between said two parts as in compound **4** [74]. What this means is that pentafluorophenyl ring most likely engage in Ar-Ar^F interactions with neighboring molecule, aiding to poling efficiency and higher NLO coefficients.

We used the SHI measurement for estimation of thermal stability of polar order of chromophores in thin films. The temperature T_{SHI50} (Table 3 and Fig. 11), when the initial SHI has been reduced by half, is in good agreement with T_g measurements only for compounds **15b** and **17**. Compound **6** has considerably lower T_{SHI50} than T_g and even all NLO activity has faded before reaching of T_g. Probably the amorphous phase structure after poling is considerably different from melted amorphous phase in DSC measurements leading to decreased energy need for molecular movements and disorientation [28]. Peaks in SHI decay curve could be caused by increased NLO effect of partially disoriented or rotated molecules. There were speculations about possible crystallization as the cause for peak and plateau in T_{SHI} curve of compound **6**, but it was discarded as no changes in DSC curve could be observed in all three measurement rounds: first heating, cooling and second heating for T_g determination. Newly synthesized compound **6** performed poorly compared to previous sample having both Trt and OH groups, which T_{SHI50} was 74 °C [75], the reason could be stabilization of amorphous phase of previous sample utilizing free OH groups and H-bonds.

4. Conclusions

Successful synthesis of (pentafluorophenyl)methyl ether **12** could be performed in relatively mild phase transfer catalysis, but high reagent excess is needed to complete the reaction. When strong bases are used in (pentafluorophenyl)methyl ether synthesis, the starting materials engage in side reactions and no product could be isolated. DCC and DMAP ensured syntheses produce dendronized azochromophores **15a–c** and **17** and azobenzene core dendrimer **6** with trityl groups at periphery.

Dendronized azochromophores **15a–c** with (pentafluorophenyl) methyl ether have good thermal stability, but molecular glass forming abilities depend on dendronizing part end groups: THP groups in compound **15a** give soft material, trityl groups in compound **15b** denote glassy material with T_g 63 °C, but OH groups in compound **15c** determine crystalline material with mp 105 °C.

We reached our aim for synthesis of compound **15b**: it has slightly higher NLO coefficients and polar order than earlier synthesized compound **1** and even compounds **4** and **5** with more pentafluorophenyl
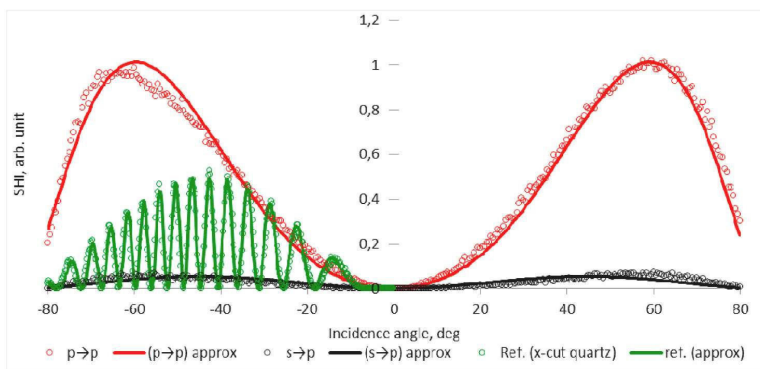

Fig. 10. Experimental Maker fringe SHI results for sample **6** and x-cut quartz crystal indicated by points. The fit indicated by lines is done according to Herman-Hayden approach [89].

Table 3
Properties of thin films of synthesized compounds **6, 15b, 17**.

Sample	d_{33},[a] $pm \cdot V^{-1}$	d_{31},[a] $pm \cdot V^{-1}$	$d_{33}(0)$,[b] $pm \cdot V^{-1}$	d_{33}/d_{31}	N,[c] %	T_{SHI50},[d] °C	n_{1064}[e]	n_{532}[e]
6	73	20.8	11.6	3.5	17	52.5	1.62	1.80
15b	43	10.7	5.1	4.0	24	65.8	1.63	1.69[f]
17	14	3.8	1.9	3.7	19	78.3	1.62	1.80

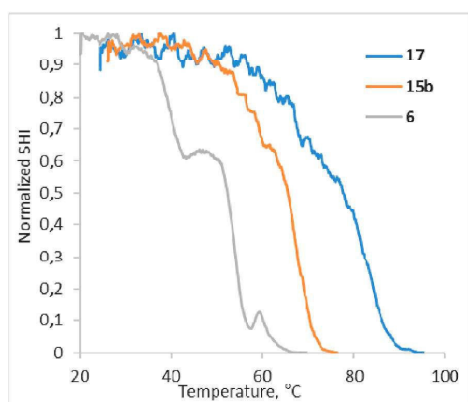[a] NLO coefficients measured at 532 nm.
[b] NLO coefficient extrapolated to zero frequency.
[c] Loading density of the effective chromophore moiety within molecule.
[d] Temperature, at which SHI is 50% from initial intensity.
[e] Refractive index at indicated wavelength.
[f] Estimated from Kramers-Kronig transformation of absorption spectra [90].

Fig. 11. Heat induced decay of SHI in poled amorphous films of synthesized compounds.

rings, possibly manifesting intermolecular $Ar \text{-} Ar^F$ bonding ensured stabilization of amorphous molecular glass. But T_g of compound **15b** is lower than for compound **1**, because T_g is more defined by trityl groups than $Ar \text{-} Ar^F$ interactions. On contrary our expectations were fulfilled only partially by compound **17** with bulky trityl groups containing substituent at acceptor side and two pentafluorophenyl rings connected to donor side of the molecule: the T_g was higher than of previously investigated compounds **1–5** and T_{SHI50} was higher than of compounds **2–5**, but it showed poor NLO coefficients.

First generation dendrimer containing azobenzene in the core and dendrons attached to donor side of molecule was synthesized in one step. The reason for reviewing of synthesis procedure and preparation of perfect sample of dendrimer **6** was hypothesis, that perfect uniform material will perform better than previously obtained without complete set of trityl end groups. But contrary to anticipated, all NLO properties were worse. The conclusion is that combination of both trityl and OH groups and possibly uneven distribution of them provide favorable structural arrangements to gain higher NLO coefficients and their thermal stability.

CRediT authorship contribution statement

Lauma Laipniece: Investigation, Formal analysis, Conceptualization, Writing – original draft, Writing – review & editing, Visualization. **Valdis Kampars:** Conceptualization, Writing – review & editing, Supervision. **Sergey Belyakov:** Investigation, Formal analysis. **Arturs Bundulis:** Investigation, Formal analysis, Writing – review & editing. **Andrejs Tokmakovs:** Methodology, Formal analysis. **Martins Rutkis:** Conceptualization, Supervision.

Declaration of competing interest

The authors declare that they have no known competing financial interests or personal relationships that could have appeared to influence the work reported in this paper.

Appendix A. Supplementary data

Supplementary data to this article can be found online at https://doi.org/10.1016/j.dyepig.2022.110395.

References

[1] Dalton LR, Sullivan PA, Bale DH, Hammond S, Olbricht BC, Rommel H, et al. Organic photonic materials. Bellingham, USA: Tutorials in Complex Photonic Media; 2007. p. 525–74. https://doi.org/10.1117/3.832717.ch16. SPIE.
[2] Dalton LR, Sullivan PA, Bale DH. Electric field poled organic electro-optic materials: state of the art and future prospects. Chem Rev 2010;110:25–55. https://doi.org/10.1021/cr9000429.
[3] Xu H, Liu F, Elder DL, Johnson LE, de Coene Y, Clays K, et al. Ultrahigh electro-optic coefficients, high index of refraction, and long-term stability from diels–alder cross-linkable binary molecular glasses. Chem Mater 2020;32:1408–21. https://doi.org/10.1021/acs.chemmater.9b03725.
[4] Chen P, Zhang H, Han M, Cheng Z, Peng Q, Li Q, et al. Janus molecules: large second-order nonlinear optical performance, good temporal stability, excellent thermal stability and spherical structure with optimized dendrimer structure. Mater Chem Front 2018;2:1374–82. https://doi.org/10.1039/c8qm00128f.
[5] Yang H, Cheng Z, Liu C, Wu W, Zhang K, Xu S, et al. A second-order nonlinear optical dendronized hyperbranched polymer containing isolation chromophores : achieving good optical nonlinearity and stability simultaneously. Sci China Chem 2018;61. https://doi.org/10.1007/s11426-017-9207-4. doi:doi:10.1007/s11426-017-9207-4.
[6] Liu J, Ouyang C, Huo F, He W, Cao A. Progress in the enhancement of electro-optic coefficients and orientation stability for organic second-order nonlinear optical materials. Dyes Pigments 2020;181:108509. https://doi.org/10.1016/j.dyepig.2020.108509.
[7] Liu J, Huo F, He W. Construction of a simple crosslinking system and its influence on the poling efficiency and oriental stability of organic electro-optic materials. RSC Adv 2020;10:6482–90. https://doi.org/10.1039/c9ra10813k.
[8] Liu J, Gao W, Liu X, Zhen Z. Benefits of the use of auxiliary donors in the design and preparation of NLO chromophores. Mater Lett 2015;143:333–5. https://doi.org/10.1016/j.matlet.2014.12.112.
[9] Li Z, Li Q, Qin J. Some new design strategies for second-order nonlinear optical polymers and dendrimers. Polym Chem 2011;2:2723–40. https://doi.org/10.1039/c1py00205h.
[10] Jang S-H, Jen AK-Y. Electro-optic (E-O) molecular glasses. Chem Asian J 2009;4:20–31. https://doi.org/10.1002/asia.200800179.
[11] Cho MJ, Choi DH, Sullivan PA, Akelaitis AJP, Dalton LR. Recent progress in second-order nonlinear optical polymers and dendrimers. Prog Polym Sci 2008;33:1013–58. https://doi.org/10.1016/j.progpolymsci.2008.07.007.

[12] Wu W, Qin J, Li Z. New design strategies for second-order nonlinear optical polymers and dendrimers. Polymer 2013;54:4351–82. https://doi.org/10.1016/j. polymer.2013.05.039.

[13] Cuétara-Guadarrama F, Vonlanthen M, Sorroza-Martínez K, González-Méndez I, Rivera E. Photoisomerizable azobenzene dyes incorporated into polymers and dendrimers. Influence of the molecular aggregation on the nonlinear optical properties. Dyes Pigments 2021:194. https://doi.org/10.1016/j. dyepig.2021.109551.

[14] Wu J, Li Z, Luo J, Jen AKY. High-performance organic second- and third-order nonlinear optical materials for ultrafast information processing. J Mater Chem C 2020;8:15009–26. https://doi.org/10.1039/d0tc03224g.

[15] Rutkis M, Tokmakovs A, Jecs E, Kreicberga J, Kampars V, Kokars V. Indanedione based binary chromophore supramolecular systems as a NLO active polymer composites. Opt Mater 2010;32:796–802. https://doi.org/10.1016/j. optmat.2010.01.006.

[16] Yesodha SK, Sadashiva Pillai CK, Tsutsumi N. Stable polymeric materials for nonlinear optics: a review based on azobenzene systems. Prog Polym Sci 2004;29: 45–74. https://doi.org/10.1016/j.progpolymsci.2003.07.002.

[17] Froehling PE. Dendrimers and dyes - a review. Dyes Pigments 2001;48:187–95.

[18] Zhang M, Xu H, Fu M, Yang M, He B, Zhang X, et al. Optimizing the molecular structure of 1,1,7,7-tetramethyl julolidine fused furan based chromophores by introducing a heterocycle ring to achieve high electro-optic activity. New J Chem 2019;43:15548–54. https://doi.org/10.1039/c9nj02309g.

[19] Huang H, Deng G, Liu J, Wu J, Si P, Xu H, et al. A nunchaku-like nonlinear optical chromophore for improved temporal stability of guest-host electro-optic materials. Dyes Pigments 2013;99:753–8. https://doi.org/10.1016/j.dyepig.2013.06.034.

[20] Ma H, Jen AK-Y. Functional dendrimers for nonlinear optics. Adv Mater 2001;13: 1201–5. https://doi.org/10.1002/1521-4095(200108)13:15<1201::AID-ADMA1201>3.0.CO;2-F.

[21] Wu W, Li C, Yu G, Liu Y, Ye C, Qin J, et al. High-generation second-order nonlinear optical (NLO) Dendrimers that contain isolation chromophores: convenient synthesis by using click chemistry and their increased NLO effects. Chem Eur J 2012;18:11019–28. https://doi.org/10.1002/chem.201200441.

[22] Wu W, Ye C, Yu G, Liu Y, Qin J, Li Z. New hyperbranched polytriazoles containing isolation chromophore moieties derived from AB4 monomers through click chemistry under copper(I) catalysis: improved optical transparency and enhanced NLO effects. Chem Eur J 2012;18:4426–34. https://doi.org/10.1002/chem.201102872.

[23] Wu W, Yu G, Liu Y, Ye C, Qin J, Li Z. Using two simple methods of Ar-ArF self-assembly and isolation chromophores to further improve the comprehensive performance of NLO dendrimers. Chem Eur J 2013;19:630–41. https://doi.org/10.1002/chem.201202992.

[24] Liao Y, Bhattacharjee S, Firestone KA, Eichinger BE, Paranji R, Anderson CA, et al. Antiparallel-aligned neutral-ground-state and zwitterionic chromophores as a nonlinear optical material. J Am Chem Soc 2006;128:6847–53. https://doi.org/10.1021/ja057903i.

[25] Luo J, Ma H, Haller M, Jen AK-Y, Barto RR. Large electro-optic activity and low optical loss derived from a highly fluorinated dendritic nonlinear optical chromophore. Chem Commun 2002:888. https://doi.org/10.1039/b200851c. –9.

[26] Traskovskis K, Mihailovs I, Tokmakovs A, Jurgis A, Kokars V, Rutkis M. Triphenyl moieties as building blocks for obtaining molecular glasses with nonlinear optical activity. J Mater Chem 2012;22:11268. https://doi.org/10.1039/c2jm30861d.

[27] Laipniece L, Kampars V. Synthesis, thermal and light absorption properties of push-pull azochromophores substituted with dendronizing phenyl and perfluorophenyl fragments. Main Group Chem 2015;14:43–58. https://doi.org/10.3233/MGC-140152.

[28] Traskovskis K, Zarins E, Laipniece L, Tokmakovs A, Kokars V, Rutkis M. Structure-dependent tuning of electro-optic and thermoplastic properties in triphenyl groups containing molecular glasses. Mater Chem Phys 2015;155:232–40. https://doi.org/10.1016/j.matchemphys.2015.02.035.

[29] Traskovskis K, Lazdovica K, Tokmakovs A, Kokars V, Rutkis M. Modular approach to obtaining organic glasses from low-molecular weight dyes using 1,1,1-triphenylpentane auxiliary groups: nonlinear optical properties. Dyes Pigments 2013;99: 1044–50. https://doi.org/10.1016/j.dyepig.2013.08.020.

[30] Hsu SM, Lin YC, Chang JW, Liu YH, Lin HC. Intramolecular interactions of a phenyl/perfluorophenyl pair in the formation of supramolecular nanofibers and hydrogels. Angew Chem Int Ed 2014;53:1921–7. https://doi.org/10.1002/anie.201307500.

[31] Bauer R, Liu D, Ver Heyen A, De Schryver F, De Feyter S, Müllen K. Polyphenylene dendrimers with pentafluorophenyl units: synthesis and self-assembly. Macromolecules 2007;40:4753–61. https://doi.org/10.1021/ma0625511.

[32] Kishikawa K, Oda K, Aikyo S, Kohmoto S. Columnar superstructures of non-disc-shaped molecules generated by arene–perfluoroarene face-to-face interactions. Angew Chem 2007;119:778–82. https://doi.org/10.1002/ange.200603594.

[33] Bacchi S, Benaglia M, Cozzi F, Demartin F, Filippini G, Gavezzotti A. X-ray diffraction and theoretical studies for the quantitative assessment of intermolecular arene-perfluoroarene stacking interactions. Chem Eur J 2006;12:3538–46. https://doi.org/10.1002/chem.200501248.

[34] Hori A, Shinohe A, Yamasaki M, Nishibori E, Aoyagi S, Sakata M. 1:1 Cross-assembly of two β-diketonate complexes through arene-perfluoroarene interactions. Angew Chem Int Ed 2007;46:7617–20. https://doi.org/10.1002/anie.200702662.

[35] Salonen LM, Ellermann M, Diederich F. Aromatic rings in chemical and biological recognition: energetics and structures. Angew Chem Int Ed 2011;50:4808–42. https://doi.org/10.1002/anie.201007560.

[36] Serrano-Becerra JM, Hernández-Ortega S, Morales-Morales D, Valdés-Martínez J. Bottom-up design and construction of a non-centrosymmetric network through π–π stacking interactions. CrystEngComm 2009;11:226–8. https://doi.org/10.1039/b816630g.

[37] Wu W, Wang C, Li Q, Ye C, Qin J, Li Z. The influence of pentafluorophenyl groups on the nonlinear optical (NLO) performance of high generation dendrons and dendrimers. Sci Rep 2014;4:6101. https://doi.org/10.1038/srep06101.

[38] Liu G, Liao Q, Deng H, Zhao W, Chen P, Tang R, et al. Janus NLO dendrimers with different peripheral functional groups: convenient synthesis and enhanced NLO performance with the aid of the Ar-ArF self-assembly. J Mater Chem C 2019;7: 7344–51. https://doi.org/10.1039/c9tc01724k.

[39] Li Z, Chen P, Xie Y, Li Z, Qin J. Ar-Ar F self-assembly of star-shaped second-order nonlinear optical chromophores achieving large macroscopic nonlinearities. Adv Electron Mater 2017:1700138. https://doi.org/10.1002/aelm.201700138.

[40] Kim T-D, Kang J-W, Luo J, Jang S-H, Ka J-W, Tucker N, et al. Ultralarge and thermally stable electro-optic activities from supramolecular self-assembled molecular glasses. J Am Chem Soc 2007;129:488–9. https://doi.org/10.1021/ja067970s.

[41] Zhou X-H, Luo J, Huang S, Kim T-D, Shi Z, Cheng Y-J, et al. Supramolecular self-assembled dendritic nonlinear optical chromophores: fine-tuning of arene-perfluoroarene interactions for ultralarge electro-optic activity and enhanced thermal stability. Adv Mater 2009;21:1976–81. https://doi.org/10.1002/adma.200801639.

[42] Kim T-D, Luo J, Jen AK-Y. Quantitative determination of the chromophore alignment induced by electrode contact poling in self-assembled NLO materials. Bull Kor Chem Soc 2009;30:882–6. https://doi.org/10.5012/bkcs.2009.30.4.882.

[43] Wu W, Fu Y, Wang C, Ye C, Qin J, Li Z. A series of hyperbranched polytriazoles containing perfluoroaromatic rings from AB2-type monomers: convenient syntheses by click chemistry under copper(I) catalysis and enhanced optical nonlinearity. Chem Asian J 2011;6:2787–95. https://doi.org/10.1002/asia.201100379.

[44] Wu W, Zhu Z, Qiu G, Ye C, Qin J, Li Z. New hyperbranched second-order nonlinear optical poly(arylene-ethynylene)s containing pentafluoroaromatic rings as isolation group: facile synthesis and enhanced optical nonlinearity through Ar-Ar F self-assembly effect. J Polym Sci Part A Polym Chem 2012;50:5124–33. https://doi.org/10.1002/pola.26345.

[45] Wu W, Wang C, Tang R, Fu Y, Ye C, Qin J, et al. Second-order nonlinear optical dendrimers containing different types of isolation groups: convenient synthesis through powerful "click chemistry" and large NLO effects. J Mater Chem C 2013;1: 717–28. https://doi.org/10.1039/C2TC00053A.

[46] Wu W, Ye C, Qin J, Li Z. Dendrimers with large nonlinear optical performance by introducing isolation chromophore, utilizing the Ar/ArF self-assembly effect, and modifying the topological structure. ACS Appl Mater Interfaces 2013;5:7033–41. https://doi.org/10.1021/am401299t.

[47] Deloncle R, Caminade A-M. Stimuli-responsive dendritic structures: the case of light-driven azobenzene-containing dendrimers and dendrons. J Photochem Photobiol C Photochem Rev 2010;11:25–45. https://doi.org/10.1016/j.jphotochemrev.2010.02.003.

[48] Alsantali RI, Alam Q, Alzahrani AYA, Sadiq A, Naeem N, Ullah E, et al. Dyes and Pigments Miscellaneous azo dyes : a comprehensive review on recent advancements in biological and industrial applications IR. Dyes Pigments 2022; 199:110050. https://doi.org/10.1016/j.dyepig.2021.110050.

[49] Wu W, Xu Z, Li Z. Using an orthogonal approach and one-pot method to simplify the synthesis of nonlinear optical (NLO) dendrimers. Polym Chem 2014;5: 6667–70. https://doi.org/10.1039/C4PY01058B.

[50] Wu W, Huang L, Song C, Yu G, Ye C, Liu Y, et al. Novel global-like second-order nonlinear optical dendrimers: convenient synthesis through powerful click chemistry and large NLO effects achieved by using simple azo chromophore. Chem Sci 2012;3:1256–61. https://doi.org/10.1039/C2SC00834C.

[51] Wu W, Huang Q, Xu G, Wang C, Ye C, Qin J, et al. Using an isolation chromophore to further improve the comprehensive performance of nonlinear optical (NLO) dendrimers. J Mater Chem C 2013;1:3226–34. https://doi.org/10.1039/c3tc00007a.

[52] Tang R, Zhou S, Xiang W, Xie Y, Chen H, Peng Q, et al. New "X-type" second-order nonlinear optical (NLO) dendrimers: fewer chromophore moieties and high NLO effects. J Mater Chem C 2015;3:4545–52. https://doi.org/10.1039/c5tc00182j.

[53] Wu W, Xu G, Li C, Yu G, Liu Y, Ye C, et al. From nitro- to sulfonyl-based chromophores: improvement of the comprehensive performance of nonlinear optical dendrimers. Chem Eur J 2013;19:6874–88. https://doi.org/10.1002/chem.201203567.

[54] Li Z, Wu W, Li Q, Yu G, Xiao L, Liu Y, et al. High-generation second-order nonlinear optical (NLO) dendrimers: convenient synthesis by click chemistry and the increasing trend of NLO effects. Angew Chem Int Ed 2010;49:2763–7. https://doi.org/10.1002/anie.200906946.

[55] Yokoyama S, Nakahama T, Otomo A, Mashiko S. Preparation and assembled structure of dipolar dendrons based electron donor/acceptor azobenzene branching. Chem Lett 1997;26:1137–8. https://doi.org/10.1246/cl.1997.1137.

[56] Yokoyama S, Nakahama T, Otomo A, Mashiko S. Intermolecular coupling enhancement of the molecular hyperpolarizability in multichromophoric dipolar dendrons. J Am Chem Soc 2000;122:3174–81. https://doi.org/10.1021/ja993569c.

[57] Zhang W, Xie J, Shi W, Deng X, Cao Z, Shen Q. Second-harmonic properties of dendritic polymers skeleton-constructed with azobenzene moiety used for nonlinear optical materials. Eur Polym J 2008;44:872–80. https://doi.org/10.1016/j.eurpolymj.2007.12.007.

[58] Li Z, Yu G, Wu W, Liu Y, Ye C, Qin J, et al. Nonlinear optical dendrimers from click chemistry: convenient synthesis, new function of the formed triazole rings, and enhanced NLO effects. Macromolecules 2009;42:3864–8. https://doi.org/10.1021/ma900471t.

[59] Park C, Lim J, Yun M, Kim C. Photoinduced release of guest molecules by supramolecular transformation of self-assembled aggregates derived from dendrons. Angew Chem Int Ed 2008;47:2959–63. https://doi.org/10.1002/anie.200705271.

[60] Ghosh S, Banthia AK, Chen Z. Synthesis and photoresponsive study of azobenzene centered polyamidoamine dendrimers. Tetrahedron 2005;61:2889–96. https://doi.org/10.1016/j.tet.2005.01.052.

[61] Lee J, Choi D, Shin EJ. Trans-cis isomerization of arylether dendrimers with azobenzene core and terminal hydroxy groups. Spectrochim Acta Mol Biomol Spectrosc 2010;77:478–84. https://doi.org/10.1016/j.saa.2010.06.022.

[62] Momotake A, Arai T. Water-soluble azobenzene dendrimers. Tetrahedron Lett 2004;45:4131–4. https://doi.org/10.1016/j.tetlet.2004.03.152.

[63] Jiang D-L, Aida T. Photoisomerization in dendrimers by harvesting of low-energy photons. Nature 1997;388:465–8. https://doi.org/10.1038/41290.

[64] Ray A, Bhattacharya S, Ghorai S, Ganguly T, Bhattacharjya A. Synthesis and trans-cis isomerization of azobenzene dendrimers incorporating 1,2-isopropylidenefuranose rings. Tetrahedron Lett 2007;48:8078–82. https://doi.org/10.1016/j.tetlet.2007.08.115.

[65] Junge DM, McGrath DV. Photoresponsive dendrimers. Chem Commun 1997: 857–8. https://doi.org/10.1039/A700292K.

[66] Grebel-Koehler D, Liu D, De Feyter S, Enkelmann V, Weil T, Engels C, et al. Synthesis and photomodulation of rigid polyphenylene dendrimers with an azobenzene core. Macromolecules 2003;36:578–90. https://doi.org/10.1021/ma021135n.

[67] Liao LX, Stellacci F, McGrath DV. Photoswitchable flexible and shape-persistent dendrimers: comparison of the interplay between a photochromic azobenzene core and dendrimer structure. J Am Chem Soc 2004;126:2181–5. https://doi.org/10.1021/ja036418p.

[68] Laipniece L, Kreicberga J, Kampars V. Divergent synthesis of polyester type dendrimers containing azobenzene in the core. Sci Proc Riga Tech Univ, Ser 1 2008;16:88–99.

[69] Seniutinas G, Laipniece L, Kreicberga J, Kampars V, Gražulevičius J, Petruškevičius R, et al. Orientational relaxation of three different dendrimers in polycarbonate matrix investigated by optical poling. J Opt Pure Appl Opt 2009;11: 034003. https://doi.org/10.1088/1464-4258/11/3/034003.

[70] Tokmakovs A, Rutkis M, Traskovskis K, Zarins E, Laipniece L, Kokars V, et al. Nonlinear optical properties of low molecular organic glasses formed by triphenyl modified chromophores. IOP Conf Ser Mater Sci Eng 2012;38:012034. https://doi.org/10.1088/1757-899X/38/1/012034.

[71] Seniutinas G, Tomašiūnas R, Czaplicki R, Sahraoui B, Kampars V. Third harmonic generation via dendrimers of four generations. In: 2009 3rd ICTON mediterranean winter conference. ICTON-MW 2009; 2009. p. 1–4. https://doi.org/10.1109/ICTONMW.2009.5385570.

[72] Navickaite G, Seniutinas G, Tomašiunas R, Petruškevičius R, Kampars V. Optical functionalism of azopolymers: photoinduced orientation and re-orientation of dendrimer structures of different generations. Phys Status Solidi Appl Mater Sci 2011;208:1833–6. https://doi.org/10.1002/pssa.201084044.

[73] Laipniece L, Kampars V. Synthesis and thermal properties of azobenzene core polyester dendrimers with trityl groups at the periphery. Key Eng Mater 2018;762: 171–5. https://doi.org/10.4028/www.scientific.net/KEM.762.171.

[74] Laipniece L, Kampars V, Belyakov S, Tokmakovs A, Nitiss E, Rutkis M. Dendronized azochromophores with aromatic and perfluoroaromatic fragments: synthesis and properties demonstrating Ar ArF interactions. Dyes Pigments 2019;162:394–404. https://doi.org/10.1016/j.dyepig.2018.10.035.

[75] Tokmakovs A, Rutkis M, Traskovskis K, Zarins E, Laipniece L, Kokars V, et al. Properties of EO active molecular glasses based on indandione and azobenzene chromophores. Book of abstracts of the 14-th international conference-school. Advanced materials and technologies. 2012. p. 96. Palanga, Lithuania.

[76] Dolomanov OV, Bourhis LJ, Gildea RJ, Howard JAK, Puschmann H. OLEX2: a complete structure solution, refinement and analysis program. J Appl Crystallogr 2009;42:339–41. https://doi.org/10.1107/S0021889808042726.

[77] Sheldrick GM. Shelxt - integrated space-group and crystal-structure determination. Acta Crystallogr Sect A Found Crystallogr 2015;71:3–8. https://doi.org/10.1107/S2053273314026370.

[78] Bourhis LJ, Dolomanov OV, Gildea RJ, Howard JAK, Puschmann H. The anatomy of a comprehensive constrained, restrained refinement program for the modern computing environment - olex2 dissected. Acta Crystallogr Sect A Found Crystallogr 2015;71:59–75. https://doi.org/10.1107/S2053273314022207.

[79] Vinczer P, Baán G, Juvancz Z, Novák L, Szántay C. Simple and stereocontrolled synthesis of an optimal isomeric mixture of 3,13-octadecadien-1-YL acetates. Synth Commun 1985;15:1257–70. https://doi.org/10.1080/00397918508077274.

[80] Brooke GM. The preparation and properties of polyfluoro aromatic and heteroaromatic compounds. J Fluor Chem 1997;86:1–76. https://doi.org/10.1016/S0022-1139(97)00006-7.

[81] Armstrong A, Brackenridge I, Jackson RFW, Kirk JM. A new method for the preparation of tertiary butyl ethers and esters. Tetrahedron Lett 1988;29:2483–6. https://doi.org/10.1016/S0040-4039(00)87913-7.

[82] Nakazato A, Sakagami K, Yasuhara A, Ohta H, Yoshikawa R, Itoh M, et al. Synthesis, in vitro pharmacology, Structure−Activity relationships, and pharmacokinetics of 3-Alkoxy-2-amino-6-fluorobicyclo[3.1.0]hexane-2,6-dicarboxylic acid derivatives as potent and selective group II metabotropic glutamate receptor antagonists. J Med Chem 2004;47:4570–87. https://doi.org/10.1021/jm0400294.

[83] Xiang Y, Hirth B, Kane JL, Liao J, Noson K, Yee C. Inhibitors of Sphingosine Kinase 1. WO2010033701 (A2). 2010.

[84] Hotchkiss P, Marder S, Giordano A, Anthopoulos TD. Electronic devices comprising novel phosphonic acid surface modifiers. WO2010115854A1; 2010.

[85] Chiu CS, Saha M, Abushamaa A, Giese RW. Chemical transformation/derivatization of O6-methyl- and O6-(hydroxyethyl)guanine for detection by GC-EC/MS. Anal Chem 1993;65:3071–5. https://doi.org/10.1021/ac00069a021.

[86] Hassner A, Alexanian V. Direct room temperature esterification of carboxylic acids. Tetrahedron Lett 1978;19:4475–8. https://doi.org/10.1016/S0040-4039(01)95256-6.

[87] Neises B, Steglich W. Simple method for the esterification of carboxylic acids. Angew Chem Int Ed Engl 1978;17:522–4. https://doi.org/10.1002/anie.197805221.

[88] Oudar JL, Chemla DS. Hyperpolarizabilities of the nitroanilines and their relations to the excited state dipole moment. J Chem Phys 1977;66:2664–8. https://doi.org/10.1063/1.434213.

[89] Herman WN, Hayden LM. Maker fringes revisited: second-harmonic generation from birefringent or absorbing materials. J Opt Soc Am B 1995;12:416–27. https://doi.org/10.1364/JOSAB.12.000416.

[90] Ohta K, Ishida H. Comparison among several numerical integration methods for Kramers-Kronig Transformation. Appl Spectrosc 1988;42:952–7.

[91] Alicante R. Photoinduced modifications of the nonlinear optical response in liquid crystalline azopolymers. Berlin, Heidelberg: Springer Berlin Heidelberg; 2013. https://doi.org/10.1007/978-3-642-31756-9.

L. Laipniece, V. Kampars, S. Belyakov, A. Tokmakovs, E. Nitiss, M. Rutkis. Dendronized azochromophores with aromatic and perfluoroaromatic fragments: Synthesis and properties demonstrating Ar-Ar^F interactions. *Dyes Pigm.*, **2019**, *162*, 394–404.

Publikācijas pielikums pieejams bez maksas *Science Direct* mājaslapā
The Supporting Information is available free of charge on the *Science Direct* website

Dendronized azochromophores with aromatic and perfluoroaromatic fragments: Synthesis and properties demonstrating Ar–ArF interactions

Lauma Laipniece[a,*], Valdis Kampars[a], Sergey Belyakov[a,b], Andrejs Tokmakovs[c], Edgars Nitiss[c], Martins Rutkis[c]

[a] Faculty of Materials Science and Applied Chemistry, Riga Technical University, P. Valdena 3/7, Riga, LV-1048, Latvia
[b] Latvian Institute of Organic Synthesis, Aizkraukles 21, Riga, LV-1006, Latvia
[c] Institute of Solid State Physics, University of Latvia, Kengaraga 8, Riga, LV-1063, Latvia

ARTICLE INFO

ABSTRACT

Syntheses of four new dendronized azochromophores were performed from 2-(2-amino-5-nitrophenoxy)ethanol, 2-[methyl(phenyl)amino]ethanol, 3,5-bis(benzyloxy)benzoic acid and 3,5-bis[(pentafluorophenyl)methoxy] benzoic acid using azo coupling reaction and ester formation reaction in presence of N,N′-dicyclohexylcarbodiimide and 4-(dimethylamino)pyridine. Arene-perfluoroarene (Ar–ArF) interactions are demonstrated in single crystal structure of dendronized azochromophore between pentafluorophenyl fragment and acceptor part of the azochromophore. The effect of Ar–ArF interactions becomes apparent in thermal and nonlinear optical properties of the chromophores. Glass transition temperatures of synthesized azochromophores are in the range from 37 to 60 °C. Nonlinear optical properties of synthesized azochromophores were characterized by second harmonic intensity measurements in corona poled thin films of pure amorphous solids. Nonlinear optical coefficient d_{33} values for molecular glasses containing single azochromophore were in the range from 20.2 to 50.5 pm·V^{-1}.

1. Introduction

Organic nonlinear optical (NLO) materials are promising for device applications in the communications and photonics industries [1,2] because they can be modified to have larger nonlinearity, better processability and faster response time than inorganic materials [2,3]. Main constituent of all organic NLO materials is a dipolar push-pull chromophore unit, which can be modified or processed to obtain host-guest polymers, chromophore containing linear, hyperbranched or cross-linked polymers, molecular glasses, dendrons and dendrimers [2]. Chromophore structure modifications are made to meet four main requirements: large NLO coefficients, good optical transparency, excellent temporal stability of noncentrosymmetrically aligned dipoles [2,4,5] and excellent photochemical stability at device application conditions [1–3,5].

The material needs to contain noncentrosymmetrically aligned chromophore dipoles to be able to demonstrate a second order NLO effect [1–4,6–8]. This can be achieved by various techniques of self-assembly or poling [2]. The relaxation process proceeds and dipolar chromophore units organize themselves back centrosymmetrically even below the glass transition temperature of the material, reducing or

cancelling out completely the NLO effect [2,4,6]. Thus to maintain the polar order, amorphous NLO material needs to have high glass transition temperature, and chromophores need to be isolated from each other to minimize the repulsion of ordered electric dipoles [2,4,6], or suitable interactions between some functional groups can be used to stabilize the orientation of chromophores after poling [2,4,5].

Aromatic-perfluoroaromatic (Ar–ArF) groups give favorable interring interactions, which organize molecules in single crystals [9–12], rigid superstructures in mesophases of liquid crystalline state [13], supramolecular nanofibers [14,15] and hydrogels [14]. Ar–ArF interactions are strong enough to be present even in solutions modifying reaction course [11]. Utilization of Ar–ArF self-assembly has been employed to obtain noncentrosymmetrically ordered amorphous structures and enhance their NLO properties [2,5,6,16–21]. Effects of Ar–ArF interaction on structure topologies and NLO properties have been investigated for dendrimers containing azobenzene throughout branches [22,23]. The authors proposed that pentafluorophenyl moieties have intramolecular interactions with donor part of azobenzene fragment [8,22,23]. Such effect has been suggested by quantum chemical calculations investigating dimer containing the same chromophore [24], although Ar–ArF interactions can be formed between

---

* Corresponding author.
E-mail address: lauma.laipniece@rtu.lv (L. Laipniece).

pentafluorophenyl moieties and aromatic group nearby [24,25]. The same statement was proposed in our previous work [26]. But till now, there were no experimental measurements proofing the Ar—Ar^F interaction in dendronized azochromophores, including arrangement and orientation of interacting rings.

Dendrimer or dendron synthesis is used to isolate the chromophore with large dipole moment in space and enhance thermal and chemical properties of the material [2,5,27–29]. Utilization of Ar—Ar^F interactions and introduction of dendrons in the molecule can be summed in one approach and dendrons with aromatic and pentafluorophenyl moieties utilizing Ar—Ar^F interactions can be used to increase NLO response and orientation stability of molecular glasses [16–18].

Azobenzene and dendrons or dendrimers can be connected in different ways [30]: azobenzene can be incorporated in dendron or dendrimer core, periphery or throughout dendrimer branches. Dendrimers containing simple azobenzene in the core have been synthesized to investigate their *cis-trans* isomerization [31–39]. Azochromophores of push-pull type were incorporated in dendrimer or dendron cores only in our previous works and NLO properties were reported [26,40–46]. Push-pull azobenzenes have been incorporated throughout dendrimer branches and their NLO properties also have been investigated [47–51], most extensive studies of push-pull azobenzene NLO dendrimers have been made in group of prof. Zhen Li [4,6,7,21–23,29,52–59]. They also investigated enhancement of NLO properties by Ar—Ar^F interactions for azobenzene dendrons, and dendrimers [21–23,55], and also polymers [19,20,24,25].

But single push-pull azobenzenes with dendritic aromatic and perfluoroaromatic substituents both at electron donor and electron acceptor parts have not been synthesized. Push-pull azobenzene with dendritic substituent and one pentafluorophenyl fragment is investigated in our recent paper [26], now we extend our research. Our aim was the synthesis of dendronized push-pull azochromophore substituted with 3,5-bis(benzyloxy)benzoic acid and 3,5-bis[(pentafluorophenyl)methoxy]benzoic acid fragments. The objective of this research was the investigation of the possible amorphous phase stabilization effects via Ar—Ar^F interaction and its influence on thermal, linear, and nonlinear optical characteristics of synthesized molecular glasses.

Investigation of holographic recordings is in progress [60,61] for symmetrically dendronized compounds and these results will be published elsewhere.

2. Results and discussion

2.1. Synthesis

Synthesis of dendronized azochromophores consisted of three stages: synthesis of dendronizing fragments, synthesis of azochromophore and link establishment between the former two. We started with known dendrimer synthesis method [62], where compound **1** was alkylated with benzyl bromide and ester **2** was obtained in 89% yield (Scheme 1). Hydrolysis of ester **2** in alkaline conditions gave dendronized acid **3** with excellent 92% yield.

Synthesis of fluorinated dendron was different, because of instability of fluoroaromatic compounds in strongly alkaline solutions [63]. 3,5-Dihydroxybenzoic acid (**4**) reacted with 1-(bromomethyl)-2,3,4,5,6-pentafluorobenzene to yield fully alkylated ester **5**, which was hydrolyzed in boiling H$_2$SO$_4$/dioxane solution for several days to yield 77% of dendronized acid **6**.

The first step of asymmetric azochromophore synthesis was dendronization of the electron donor part of the chromophore precursor (Scheme 2). Aniline **7** reacted both with dendronizing acids **3** and **6** using *N,N'*-dicyclohexylcarbodiimide (DCC) and 4-(dimethylamino) pyridine (DMAP), thus accordingly esters **8** and **9** were obtained.

Aniline **10** underwent diazotization and subsequent azo coupling reactions with esters **8** and **9** to form monodendronized

azochromophores **11** and **13** respectively (Scheme 3). Asymmetrical chromophores **12** and **14** with different dendronized moiety in every part of the molecule were obtained from azocompounds **11** and **13** in DCC and DMAP ensured reactions with dendronizing acids **6** and **3**.

Synthesis of symmetrical azochromophores with equal dendronized parts in the molecule was straightforward (Scheme 3). At first azocompound **15** was synthesized in azo coupling reaction from compounds **7** and **10**. Then symmetrical azochromophores **16** and **17** were synthesized in one DCC and DMAP ensured esterification step with either acid **3** or **6**.

2.2. Crystal structure

We obtained crystals of appropriate quality for X-ray analysis only for compound **14** (Fig. 1), although experiments were made to grow monocrystals for all four azochromophores **12**, **14**, **16** and **17**. Compound **14** is crystallized in triclinic system; space group of symmetry is $P\bar{1}$. Crystal unit cell consists of two molecules of compound **14** and they are arranged centrosymmetrically (Fig. 2). The crystal structure of compound **14** is stabilized by several different interactions: intramolecular Ar—Ar^F interaction and intermolecular CH⋯F, CH⋯O, π-π, and Ar—Ar^F interactions.

Intramolecular Ar—Ar^F interaction is observed between one pentafluorophenyl ring and azobenzene moiety in the acceptor side (Figs. 1 and 2), the ring C15—C20 is located over azobenzene atoms N2, N3 and C31. Planes C15—C20 and N2, N3, C31, C32, C36 are almost parallel, dihedral angle is 1.7(8)°, distance between centroid of ring C15—C20 and plane N2, N3, C31, C32, C36 is 3.290(9) Å. This Ar—Ar^F interaction has parallel-displaced geometry, which is more favorable among substituted phenyl rings [11,64], and the substituent with donor properties (in this case azo group) is located over pentafluorophenyl ring, this type of orientation is more stable [64].

Crystal structure of compound **14** has partial fragment disorder. Disordered fragment consists of O10, C46–48, C52, site occupancy *g*-factors are equal to 0.6 (respectively, *g* = 0.4 for other disordered atoms O10′, C46′, C47′, C48′, C52′). Only the atoms with maximal occupancy are shown on Fig. 1. Most abundant structure is stabilized by intermolecular hydrogen bonds of CH⋯F type [65,66] in two places: C46—H46A … F2(−1+*x*, *y*, 1 + *z*) (C⋯F = 3.310(9) Å, H⋯F = 2.63 Å, angle C—H⋯F = 127°) and C52—H52⋯F3(−1+*x*, *y*, 1 + *z*) (C⋯F = 3.331(9) Å, H⋯F = 2.42 Å, angle C—H⋯F = 170°). The other disordered atoms also have weak intermolecular CH⋯F interactions (C46′ both hydrogens with F6, distances 2.67 and 2.60 Å), and one of those hydrogens has also weak hydrogen bond (H-bond) with O2 (distance 2.58 Å).

Intermolecular π-π interaction is observed between dendronizing acid fragments of both molecules of compound **14** (Fig. 2). Central phenyl rings of two dendronizing fragments are stacking in parallel-displaced geometry. Corresponding planes of phenyl rings C8—C13 and C40—C45 are coplanar – dihedral angle is 0.9(7)°, distance between centroid of ring C40—C45 and plane C8—C13 is 3.445(8) Å.

Two Ar—Ar^F interactions are observed between pentafluorophenyl and phenyl rings. Ring C1—C6 is stacking with ring C54—C59, this interaction has parallel-displaced geometry, distance between ring centers is 3.979(8) Å and angle between corresponding planes is 22.0(7)°, which is slightly higher than observed in similar interactions [9]. Ring C15-20 is stacking with ring C47′, C48′, C49, C50, C51, C52′, this interaction has parallel-displaced geometry, distance between ring centers is 4.112(9) Å and angle between corresponding planes is 26.6(8)°. This angle is higher than observed in similar interactions [9], but we assume there is Ar—Ar^F interaction between those fragments.

It should be noted that in the crystal structure there are also disordered solvent molecules. Perhaps the disorder phenomenon in compound **14** and similar compounds promotes difficulties of growing of their monocrystals.
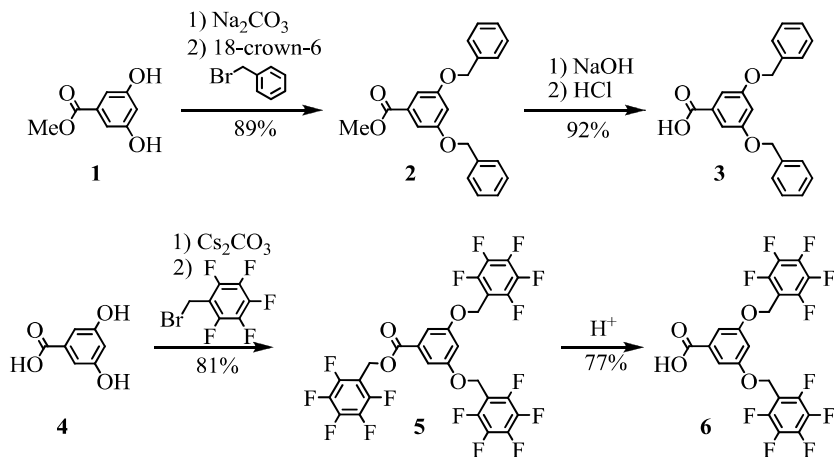
Scheme 1. Synthesis of dendronizing acids.
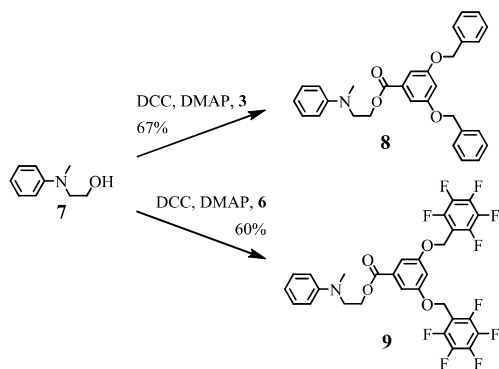
Scheme 2. Dendronization of chromophore precursor.

2.3. Thermal properties

Glass transition temperatures (T_g) of synthesized compounds were in the range from 37 to 60 °C (Table 1 and Fig. S3 in supporting information file). The azobenzene **15** which had no dendritic substituents had the lowest T_g (37 °C). Addition of first benzyl group containing dendritic substituent raised T_g for 7 °C in compound **11**, but addition of second substituent had no substantial change of T_g in compound **16**. Dendritic substituent with pentafluorophenyl fragments showed considerably greater effect on T_g: addition of first dendritic substituent raised T_g for 23 °C in compound **13**, but addition of second substituent did not change the T_g in compound **17**. Addition of dendritic substituent with pentafluorophenyl fragments to compound **11** also raised T_g for 9 °C in compound **12**. It is possible that compound **13** has favorable interactions between OH group and pentafluorophenyl fragment, because it has the highest T_g value amongst compounds with OH groups.

We expected that 3,5-bis(benzyloxy)benzoic acid and 3,5-bis[(pentafluorophenyl)methoxy]benzoic acid fragments in compounds **12** and **14** will have intermolecular Ar–Ar^F interactions between them similar to reported for mixture of pure acids [16] and this will give the highest T_g. But the real effect is different. Compounds **11**, **15**, **16** without pentafluorophenyl fragments have the lowest T_g, which is according to expectations. But compounds **13** and **17** with only pentafluorophenyl fragments had the highest T_g. This could be explained with Ar–Ar^F interactions between pentafluorophenyl fragments and azobenzene instead of benzyl fragments, which is clearly shown in crystal structure of compound **14** with the second highest T_g.

Two binary equimolar blends of azocompounds were prepared to further investigate Ar–Ar^F interactions: blend (**12** + **14**) was made from compounds **12** and **14**, and blend (**16** + **17**) was made from compounds **16** and **17**. Blends showed identical T_g which were about the average of their constituents (Fig. S4 in supporting information file). Blend (**12** + **14**) formed amorphous glass, but blend (**16** + **17**) crystallized. We expected, that both compounds of each blend will interact between them and T_g will be higher than individual components as in Jen's work [16], but the effect was not observed.

The highest T_g of 60 °C from our compounds is low compared to widely expected [3], but it has potential niche in cold climates. High T_g is needed for materials used in room temperature or higher, but materials with low T_g could be suitable for uses in Arctic or Antarctic temperatures [4].

Melting temperatures showed no trends and deducible effects of functional groups. Compounds **11** and **16** had two polymorphic modifications as indicated by two melting points (mp). Thermal stabilities (Table 1 and Fig. S5 in supporting information file) of all compounds were very good as showed by 5% weight loss temperatures (T_d). Benzyl and pentafluorophenyl fragments have similar influence on thermal stability.

2.4. Linear optical properties

Light absorption maxima and intensity of lowest frequency charge transfer transition band were investigated for all compounds in CHCl$_3$ and ethyl benzoate (EtOBz) solutions (Table 1). Absorption bands look very similar in CHCl$_3$ solutions (Fig. 3) for all fully dendronized azochromophores **12**, **14**, **16**, and **17**, most notable differences are in 250–350 nm range, this part of spectrum corresponds to dendronizing fragments, which holds the differences in these compounds.

Absorption maxima (λ_{max}) is bathochromic shifted of azochromophore **15** in both solutions compared to other synthesized chromophores. Molar absorptivity (ε) of compound **15** is the greatest in CHCl$_3$ solution, but the smallest in EtOBz solution. Azochromophore **15** and partially dendronized azocompounds **11** and **13** have bathochromic shift in CHCl$_3$ solution compared to all fully dendronized compounds. These differences could be explained by the presence of OH groups.

UV–Vis spectra of glassy solid were measured for thin films of
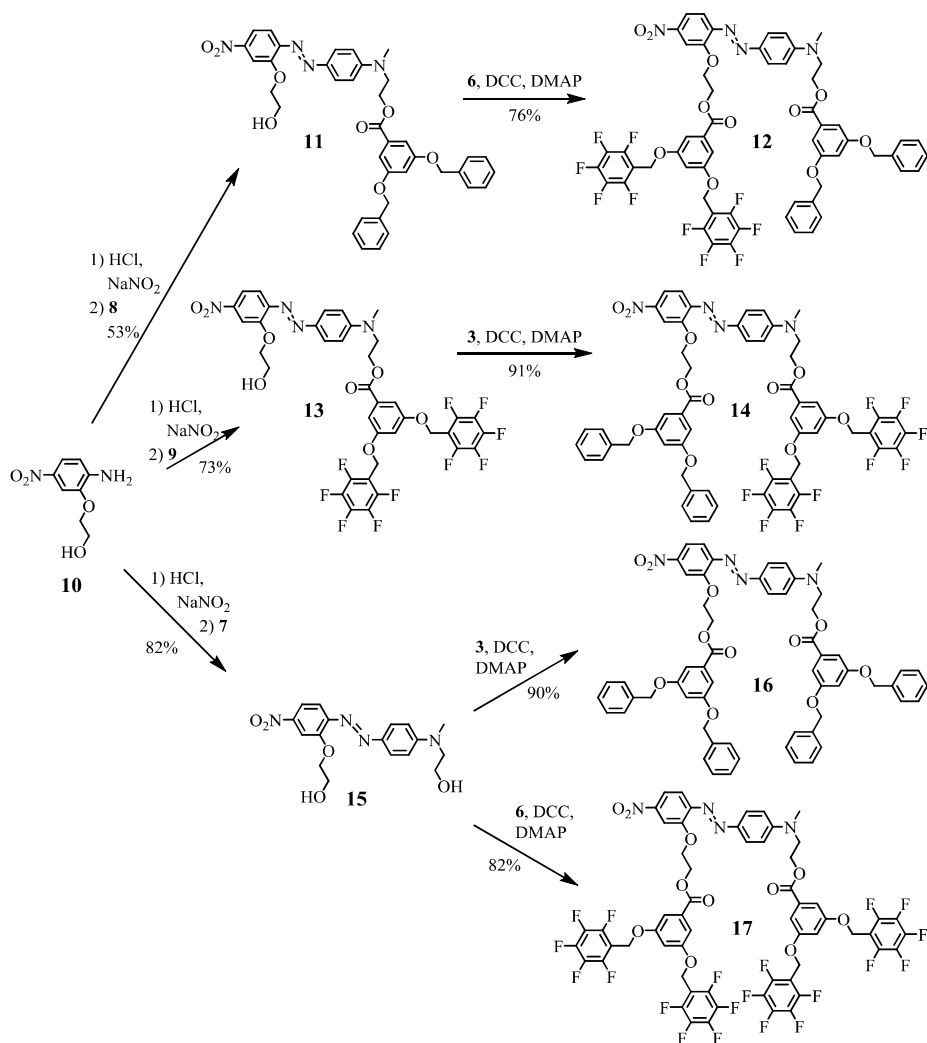
Scheme 3. Synthesis of dendronized azochromophores.

compounds which were used in NLO measurements (Fig. 4). All compounds show bathochromic shift in solid state for at least 11 nm compared to CHCl₃ solutions. Blends (**12** + **14**) and (**16** + **17**) exhibit absorption maximum identical to component which λ_{max} is in longest wavelength. No specific effect could be observed due to interactions between molecules of both compounds in the blends (**12** + **14**) and (**16** + **17**).

2.5. Nonlinear optical properties

NLO properties were tested for fully dendronized compounds **12**, **14**, **16**, **17** and both blends (**12** + **14**), (**16** + **17**). NLO properties were not tested for compounds with OH groups – **11**, **13**, and **15**, because they do not form stable amorphous films.

The second order NLO coefficients d_{33}, d_{31} and $d_{33}(0)$ were used to characterize the NLO properties of amorphous films of synthesized compounds, second harmonic intensity (SHI) in a Maker fringe

experiment was measured for poled spin-coated films of pure compounds. Fig. 5 shows typical example of Maker fringe for sample of compound **17**. The corona poling procedure using corona triode was employed to break centrosymmetric ordering inside previously prepared glassy films. It is necessary to determine the refractive index of the material at fundamental and second harmonic wavelengths (n_{1064} and n_{532} in Table 2) for evaluation of NLO coefficients d_{33} and d_{31} of thin films. Our film samples have absorption maxima around 500 nm and absorption band includes wavelength of 532 nm. Therefore direct measurement of refractive index was not possible, and we used numerical Kramers-Kronig transformation of absorption spectra suggested by Ohta et al. [67]. The experimentally measured NLO coefficients are frequency dependent and resonance enhancement of NLO efficiency was interfering at 532 nm. An extrapolation to zero frequency ($d_{33}(0)$) according to two-level model [68] was made to overcome this interference.

All investigated samples are NLO active, measured NLO coefficients
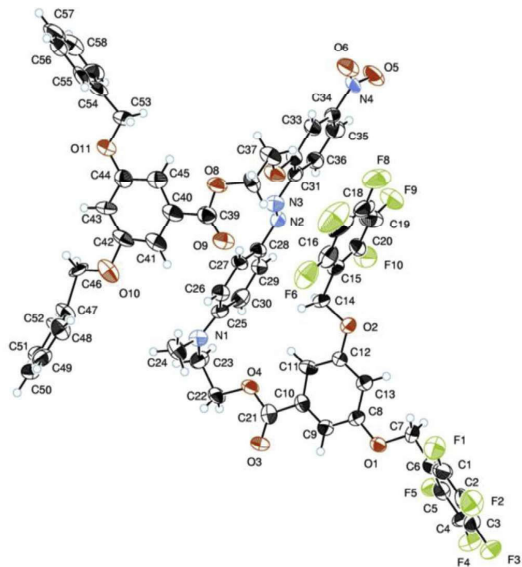
Fig. 1. ORTEP drawing of the molecule **14** with atomic labels and thermal ellipsoids at 50% probability.
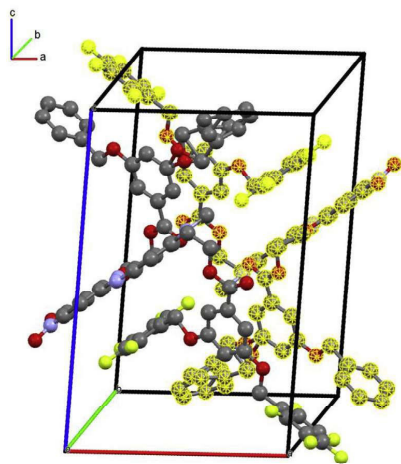
Fig. 2. Crystal unit cell with two molecules (one is highlighted) of compound **14**.

(Table 2) are similar in margins of experimental error. The order of obtained NLO coefficients are consistent with values of widely known azochromophore DR1 [70]. Response of NLO properties is dependent on chromophore content, molecular hyperpolarizability and extent of polar order. Ratio of NLO coefficients d_{33}/d_{31} show polar order of poled chromophore films. For all pure chromophore **12**, **14**, **16**, **17** samples this ratio is 3.2–3.7 and indicates high polar order [71]. Both blends (**12** + **14**) and (**16** + **17**) show noticeably lower ratio of 2.2 and 2.0, respectively, indicating poor alignment of chromophore molecules resulting to unexpectedly low NLO coefficient d_{33} and $d_{33}(0)$ values. Intramolecular interactions of both molecules in these blends may be in such a way to favor centrosymmetric ordering of chromophores leading

to decreased NLO coefficients. These results are opposite to literature findings where blend of complementary chromophores containing the same dendrons has more than two times higher r_{33} value than individual components [16].

We also used the SHI measurement for estimation of thermal properties of prepared thin films. The temperature T_{SHI50} (Table 2 and Fig. 6), when half of the initial SHI has faded, is in good agreement with T_g measurements. Differences between T_g and T_{SHI50} could arise from different packing of chromophore molecules in melted glass and in poled film, which was cast from solution, presence of trapped solvent molecules between dendritic fragments cannot be excluded. The highest T_{SHI50} has compound **14** and the reason of this could be ordering of molecules in poled glassy film due to intramolecular Ar—Ar^F interactions.

3. Conclusions

In summary, we have synthesized four new dendronized azochromophores using push-pull azobenzene as active chromophore moiety and adding benzyl and/or (pentafluorophenyl)methyl fragments containing dendrons to it. We demonstrated for the first time Ar—Ar^F interactions in crystal of large dendronized NLO active chromophore. Ar—Ar^F interactions are clearly present in crystal of compound **14**: both dendron fragments of two molecules are stacking and one pentafluorophenyl fragment is interacting with azobenzene moiety. The unexpected aspect was that interaction of pentafluorophenyl ring occurred with acceptor part of azobenzene moiety not donor part as could be expected considering electron density of the molecule. It is possible that some of these stable interactions are present in glassy state or in solution.

Connection of benzyl and pentafluorophenyl fragments containing dendrons to azobenzene chromophore donor or acceptor part gave very interesting and different results. In these chromophore series, the connection of pentafluorophenyl dendron fragment to donor part of azochromophore is most successful: compounds **14** and **17** both demonstrate high T_g, and T_{SHI50}, which is possibly due to Ar—Ar^F interactions, stabilizing overall conformation of molecular glass molecules in amorphous thin film. Connection of benzyl dendron fragment to donor part of azochromophore leads to lower T_g, and T_{SHI50}. The type of dendron connected to acceptor part of azochromophore has little influence on material properties.

Formation of complementary blends of chromophores did not give expected enhancement of thermal and NLO properties. We explain this with intermolecular interactions, but these interactions may be in such a way to favor centrosymmetric ordering of chromophores leading to decreased NLO coefficients.

4. Experimental section

4.1. Reagents and general procedures

Starting materials were purchased from Acros and Alfa Aesar. Solvents were dried by standard procedures. Starting materials were prepared according to the literature: methyl 3,5-dihydroxybenzoate (**1**) [40], 2-[methyl(phenyl)amino]ethanol (**7**) [26], 2-(2-amino-5-nitrophenoxy)ethanol (**10**) [26], 4'-[N-(2-hydroxyethyl)-N-methyl]amino-2-(2-hydroxyethoxy)-4-nitroazobenzene (**15**) [26]. Purity of all compounds was checked by TLC method on Merck F_{254} silica plates. The spots were visualized when necessary in UV light. Chromatographic separations were carried out on silica gel (ROTH Kieselgel 60, 60–200 μm). Melting points were measured on a Stuart SMP10 apparatus. The UV–Vis spectra of sample solutions were recorded with Perkin Elmer Lambda 35 spectrometer, sample concentrations were 10 μmol/L. The UV–Vis spectra of thin films were recorded with Ocean Optics HR4000CG-UVNIR spectrometer. NMR spectra were obtained on a Varian Mercury BB 200 MHz, Varian Mercury 400 MHz, Bruker

Table 1
Thermal and linear optical properties of synthesized compounds.

Compound	T_g, °C	mp, °C	T_d, °C	λ_{max}, nm CHCl$_3$	ε, M^{-1}·cm^{-1} CHCl$_3$	λ_{max}, nm EtOBz	ε, M^{-1}·cm^{-1} EtOBz	λ_{max}, nm thin film
11	44	132, 156	260	483.4	30000	482.3	30200	
12	53	147	282	478.9	28900	481.3	30800	492
13	60	166	287	482.2	32900	486.0	29800	
14	58	119	284	480.2	26600	486.6	31600	496
15	37	146	264	488.7	35200	498.7	24500	
16	46	130, 152	288	479.1	26800	482.1	29800	498
17	60	103	286	476.3	32100	484.1	31500	489
(12 + 14)	55	–						497
(16 + 17)	55	139						498
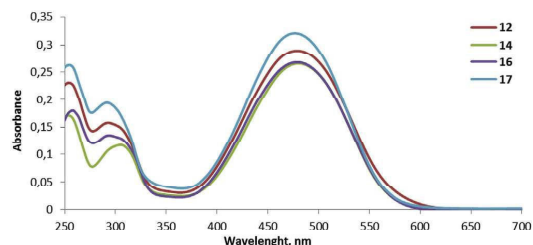
Fig. 3. Absorbance of CHCl$_3$ solutions of dendronized chromophores **12, 14, 16,** and **17**. Concentration is 10 μmol/L.
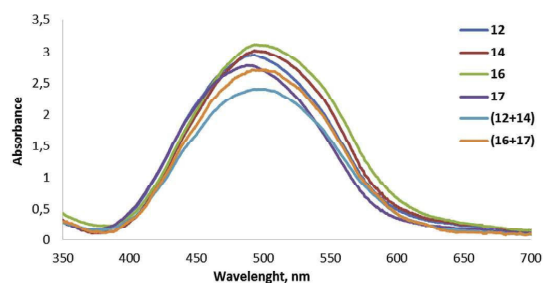
Fig. 4. Absorbance of thin films of dendronized chromophores **12, 14, 16,** and **17**, and blends (**12 + 14**) and (**16 + 17**). Absorbance values are normalized respective to film thickness of 1 μm.
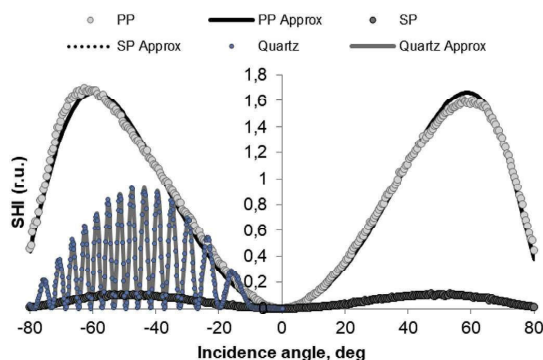
Fig. 5. Experimental Maker fringe SHI results for sample **17** as well as for thick x-cut quartz crystal indicated by points. The fit indicated by lines is done according to Herman-Hayden approach [69].

Avance 300 MHz spectrometers against solvent residue as internal reference, spin coupling constants are shown in Hz. The elemental analysis was carried out on a Carlo Erba EA 1106 automatic analyzer. Reaction mixture analysis was carried out on HPLC-MS system consisting of Waters Alliance 2695 chromatograph equipped with XTerra® MS C18 5 μm 2.1 × 100 mm column, Waters 2996 PDA detector, and Waters EMD 1000 (ESI) massspectrometer.

4.2. X-ray analysis

We obtained monocrystals of compound **14** slowly evaporating CH$_2$Cl$_2$/EtOAc solution. All measurements of single crystal X-ray analysis were made on a Bruker-Nonius KappaCCD imaging plate area detector with graphite monochromatic MoK radiation (λ = 0.71073 Å). The structures were solved by direct methods and refined by full matrix least squares with *SHELX* software package [72]. For further details, see crystallographic data for this compound deposited with the Cambridge Crystallographic Data Centre as Supplementary Publications of CCDC 1520858 number. Copies of the data can be obtained, free of charge, on application to CCDC, 12 Union Road, Cambridge CB2 1EZ, UK.

4.3. Thin film preparation

The glassy thin films used for measurements of NLO properties were prepared from chromophore solution in CHCl$_3$ (analytical grade) with a typical concentration of 100 mg/mL. The solution was spin-coated onto indium tin oxide (ITO) coated 1 × 1 inch glass slides with a Laurell WS-400B-6NPP/LITE spin-coater with total spinning time of 2.4 s, acceleration 800 rpm/s and rotation speed of 900 rpm. After spin-coating the samples dried at room temperature for 3 days. The thickness of the obtained films was measured with Dektak 150 profilometer and was in the range 0.7–1.3 μm.

Due to large absorption coefficients of the materials, absorption spectra were measured for specially prepared 40–85 nm thin samples. For preparation of 40–85 nm thin films on glass or quartz slides, the solution used in spin-coating was diluted 7 to 10 times. These samples were used only for absorption spectra measurements. The thickness of these thin films was determined by a Dektak 150 profilometer and white light interferometer Zygo NewView 7100.

4.4. Measurements of thermal properties

TG and DSC curves were measured on Perkin Elmer STA 6000 apparatus. All the samples were heated at 10 °C/min from 20 to 500 °C under nitrogen for the first time and T_d was measured where TG curve shows 5% weight loss. For determination of T_g all the samples were heated at 10 °C/min from 20 to 200 °C under nitrogen for the first scan, then cooled to 17 °C, and heated at 10 °C/min from 17 to 200 °C for the second scan.

The temperature corresponding to the 50% reduced NLO activity (T_{SHI50}) was evaluated from NLO activity decay measurements. The sample was put in a temperature controllable sample holder and

Table 2
Properties of thin films of compounds **12**, **14**, **16**, **17**, and blends (**12** + **14**), (**16** + **17**).

Sample	d_{33},[a] pm·V^{-1}	d_{31},[a] pm·V^{-1}	$d_{33}(0)$,[b] pm·V^{-1}	d_{33}/d_{31}	N,[c] %	T_{SHI50},[d] °C	n_{1064}[e]	n_{532}[e]
12	10	2.8	1.1	3.6	22	51	1.63	1.72
14	35	11	3.9	3.2	22	59	1.61	1.67
(**12** + **14**)	19	8.5	1.6	2.2	22	50	1.64[f]	1.72[f]
16	20	5.4	2.1	3.7	26	46	1.65	1.70
17	26	7.2	3.3	3.6	19	54	1.60	1.69
(**16** + **17**)	20	10	1.7	2.0	22	54	1.63[f]	1.70[f]

[a] NLO coefficients measured at 532 nm.
[b] NLO coefficient extrapolated to zero frequency.
[c] Loading density of the effective chromophore moiety.
[d] Temperature, at which second harmonic intensity is 50% from initial intensity.
[e] Refractive index at indicated wavelength.
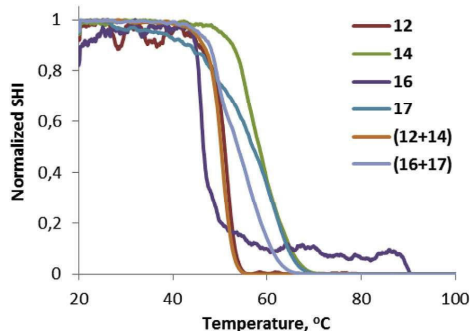[f] Estimated from Kramers-Kronig transformation of absorption spectra.

Fig. 6. Heat induced decay of SHI in poled amorphous films.

temperature was increased at 10 °C/min using setup described elsewhere [45]. SHI was simultaneously monitored and the temperature corresponding to the half vanished NLO activity was evaluated to be the T_{SHI50}. Here the second harmonic was excited using ns pulsed 1064 nm laser, and the SHI is recorded as a function of sample temperature.

4.5. Corona poling procedure

The corona poling procedure was applied to previously prepared glassy film. For this purpose, we used a custom-built corona triode setup [73–75]. The poling voltage was set to be 2.5 kV the entire poling process, when the samples were heated from room to poling temperature, which is equal to T_{SHI50}. The total poling time including heating of the sample was 15 min. After that the sample was cooled down to room temperature with poling field on. A PTFE mask with 8 mm diameter conical hole was used in the centre to limit the poled area.

4.6. Measurements of NLO properties

The refractive indexes at 1064 nm and 532 nm were measured by a prism-coupler Metricon 2010. Direct measurement of refractive index was not possible for materials with high absorption coefficients at 532 nm. Therefore numerical Kramers-Kronig transformation of absorption spectra was used suggested by Ohta et al. [67]. In the approach the dispersion spectra are obtained by numerical integration of absorption spectra via Maclaurin's formula according to Kramers-Kronig transformation rule. Since the approach requires knowing refractive index for at least one other point in the dispersion spectrum, the refractive index at either 633 nm or 1064 nm was measured with the prism-coupler.

The SHI were recorded as functions of the fundamental light (1064 nm) incidence angle and polarization (Maker fringe technique).

A scheme of the experimental SHI measurement setup is given in supporting information and literature [45]. To avoid electrical field induced second harmonic generation (EFISHG) signal caused by charges trapped on the film surface, the non-linear coefficients usually were measured two days after poling. For corona poled films the $C_{\infty v}$ symmetry was assumed and material could be characterized by three nonzero NLO coefficients – d_{33}, d_{31} and d_{15}. It was assumed that $d_{31} = d_{15}$ as it is done usually for poled polymer films according to Kleinman symmetry [69]. The NLO coefficients were obtained by least square fit of the experimental curves to theoretical approximation. Measurement error of a typical experiment does not exceed 15%.

The theoretical value of SHI was calculated using Herman – Hayden [69] approach, taking into account absorption of the film. The fitting was carried out in two steps: the value of d_{31} was evaluated from experimental s-p polarized SHI, then the d_{33} was calculated from the p-p polarized SHI. The x–cut quartz crystal was used as a reference (d_{11} = 0.3 p.m./V) to calibrate instrument response function [76]. An extrapolation to zero frequency ($d_{33}(0)$) according to two-level model [68] was made.

More detailed experimental setup for SHI measurements is described elsewhere [45,69,76,77].

4.7. Synthesis of methyl 3,5-bis(benzyloxy)benzoate (2)

Methyl 3,5-dihydroxybenzoate (**1**) (15.00 g, 0.089 mol) was dissolved in abs. acetone (120 mL), Na_2CO_3 (23.85 g, 0.23 mol) and solution of benzyl bromide (22.7 mL, 0.19 mol) in abs. acetone (90 mL) were added. Then the catalyst 18-crown-6 (0.34 g, 1.3 mmol) was added and resulting suspension was refluxed for 3 days. The reaction mixture was cooled, then filtered. Mother liquor was evaporated and recrystallized from MeOH. Yield 27.75 g (89%) of white crystals, *mp* 69–71 °C (lit. [62], 69–70 °C). Found: C, 75.56; H, 5.83%; $C_{22}H_{20}O_4$ requires C, 75.84; H, 5.79%. ^{1}H NMR (200 MHz, DMSO-d_6): δ = 7.40–7.25 (m, 10H), 7.23 (d, *J* = 2.2, 2H), 6.73 (t, *J* = 2.2, 1H), 5.00 (s, 4H), 3.83 (s, 3H) ppm. MS ESI+: *m/z* 349.1 [M+H]$^+$.

4.8. Synthesis of 3,5-bis(benzyloxy)benzoic acid (3)

Ester **2** (1.50 g, 4.3 mmol) was dissolved in EtOH (10 mL) and solution of NaOH (0.40 g, 10 mmol) in water (15 mL) was added, and resulting solution was refluxed for 5 h. The reaction mixture was cooled in a refrigerator, then precipitated sodium 3,5-bis(benzyloxy)benzoate was filtered off, dissolved in hot water, and acidified with solution of ~10% HCl. Crystals are formed overnight, which were filtered off and dried. Yield 1.33 g (92%) of white crystals, *mp* 212–214 °C (lit. [78], 208–209 °C). Found: C, 75.07; H, 5.31%; $C_{21}H_{18}O_4$ requires C, 75.43; H, 5.43%. ^{1}H NMR (300 MHz, DMSO-d_6): δ = 13.06 (s, 1H), 7.52–7.26 (m, 10H), 7.15 (d, *J* = 2.0, 2H), 6.92 (t, *J* = 2.0, 1H), 5.14 (s, 4H) ppm. ^{13}C NMR (75 MHz, DMSO-d_6): δ = 166.90, 159.41, 136.75, 132.89,

128.47, 127.92, 127.70, 107.98, 106.56, 69.49 ppm. MS ESI+: m/z 335.1 $[M+H]^+$.

4.9. Synthesis of (pentafluorophenyl)methyl 3,5-bis[(pentafluorophenyl) methoxy]benzoate (5)

3,5-Dihydroxybenzoic acid (**4**) (0.25 g, 1.6 mmol) was dissolved in abs. MeCN (10 mL), and Cs_2CO_3 (0.80 g, 2.5 mmol) was added. The mixture was heated for 1 h at 50 °C under Ar atmosphere, then solution of 1-(bromomethyl)-2,3,4,5,6-pentafluorobenzene (0.8 mL, 5.3 mmol) in abs. MeCN (2 mL) was added dropwise. Reaction mixture was heated for 3 days at 60 °C, then cooled and filtered. Solution was evaporated and recrystallized from hexanes. Yield 0.85 g (75%) of white crystals, *mp* 123–124 °C. Found: C, 48.54; H, 1.34%; $C_{28}H_9F_{15}O_4$ requires C, 48.43; H, 1.31%. ^1H NMR (200 MHz, CDCl$_3$): δ = 7.29 (d, $J = 2.3$ Hz, 2H), 6.76 (t, $J = 2.3$ Hz, 1H), 5.45 (t, $J = 1.3$ Hz, 2H), 5.13 (t, $J = 1.3$ Hz, 4H) ppm. MS ESI-: m/z 693.2 $[M - H]^-$.

4.10. Synthesis of 3,5-bis[(pentafluorophenyl)methoxy]benzoic acid (6)

Ester **5** (1.80 g, 2.6 mmol) was dissolved in dioxane (30 mL), conc. H_2SO_4 (8 mL) and water (15 mL) were added. The reaction mixture was refluxed for 10 days, then water (20 mL) was added and the solution was cooled in a refrigerator. Precipitated product was filtered. The crude product was recrystallized from EtOH. Yield 1.02 g (77%) of white crystals, *mp* 158–164 °C (lit. [79], 158–159 °C). Found: C, 49.39; H, 1.63%; $C_{21}H_8F_{10}O_4$ requires C, 49.05; H, 1.57. ^1H NMR (300 MHz, CDCl$_3$): δ = 7.39 (d, $J = 2.3$, 2H), 6.78 (t, $J = 2.3$, 1H), 5.14 (s, 4H) ppm. ^{13}C NMR (75 MHz, MeOD): δ = 168.84, 160.52, 147.03 (d, $J = 259$), 142.94 (d, $J = 252$), 138.80 (dt, $J = 250$, 15), 134.36, 111.58 (t, $J = 18$), 110.10, 107.81, 58.79 ppm. MS ESI-: m/z 513.0 $[M - H]^-$.

4.11. General procedure for ester formation with DCC and DMAP (DCC method)

To a solution of alcohol (1.0 mmol) and of acid (1.1 mmol) in dry CH_2Cl_2 (15 mL) was added DMAP (0.1 mmol) while stirring in ice bath, then a solution of DCC (1.1 mmol) in dry CH_2Cl_2 (4 mL) was added dropwise over 30 min. Reaction mixture was stirred for few days at room temperature until TLC analysis indicated the completion of the reaction. Flask was put in freezer for all *N,N'*-dicyclohexylurea to crystallize, then filtered and evaporated. The crude product was purified by appropriate method.

4.12. Synthesis of 2-[methyl(phenyl)amino]ethyl 3,5-bis(benzyloxy) benzoate (8)

DCC method was used. The crude product was purified by recrystallization from EtOAc. Yield 0.75 g (67%) of white crystals, *mp* 123–125 °C. Found: C, 76.66; H, 6.21; N, 3.01%; $C_{30}H_{29}NO_4$ requires C, 77.06; H, 6.25; N, 3.00%. ^1H NMR (300 MHz, CDCl$_3$): δ = 7.47–7.27 (m, 10H), 7.23–7.18 (m, 4H), 6.79–6.74 (m, 3H), 6.68 (t, $J = 7.3$, 1H), 5.01 (s, 4H), 4.46 (t, $J = 6.0$, 2H), 3.71 (t, $J = 6.0$, 2H), 2.99 (s, 3H) ppm. MS ESI+: m/z 468.1 $[M+H]^+$

4.13. Synthesis of 2-[methyl(phenyl)amino]ethyl 3,5-bis [(pentafluorophenyl)methoxy]benzoate (9)

DCC method was used. The crude product was purified by recrystallization from hexanes. Yield 0.53 g (60%) of white crystals, *mp* 103–105 °C. Found: C, 55.43; H, 2.83; N, 2.03%; $C_{30}H_{19}F_{10}NO_4$ requires C, 55.65; H, 2.96; N, 2.16%. ^1H NMR (300 MHz, CDCl$_3$): δ = 7.24–7.16 (m, 4H), 6.80 (d, $J = 7.4$, 2H), 6.72–6.60 (m, 2H), 5.05 (s, 4H), 4.49 (t, $J = 5.9$, 2H), 3.74 (t, $J = 5.9$, 2H), 3.02 (s, 3H) ppm. MS ESI+: m/z 648.2 $[M+H]^+$.

4.14. Synthesis of 4'-(N-{2-[3,5-bis(benzyloxy)benzoyloxy]ethyl}—N-methylamino)-2-(2-hydroxyethoxy)-4-nitroazobenzene (11)

2-(2-Amino-5-nitrophenoxy)ethanol (**10**) (0.25 g, 1.3 mmol) was dissolved in hot (80–90 °C) diluted HCl (2.0 mL dioxane and 0.54 mL conc. HCl). The solution was poured onto crushed ice (6 g). After additional cooling in an ice bath, a solution of $NaNO_2$ (0.089 g, 1.3 mmol) in water (1.2 mL) was added at such a rate as to prevent temperature from rising above +5 °C. After the addition was complete, stirring was continued for 1 h at 0–5 °C. This diazonium chloride solution was added dropwise at 0–5 °C to the emulsion of compound **8** (0.60 g, 1.3 mmol) in mixture of acetic acid (0.4 mL), water (0.4 mL), AcONa·3H$_2$O (0.4 g), dioxane (4 mL) and CH$_2$Cl$_2$, (4 mL). The reaction mixture was vigorously stirred 5 h in ice bath and another 14 h in room temperature. The mixture was filtered, washed with water till neutral pH and dried to afford crude product (0.68 g), which was recrystallized from EtOAc. Yield 0.36 g (53%) of deep red crystalline solid, *mp* 153–156 °C. Found: C, 66.96; H, 5.21; N, 7.87%. $C_{38}H_{36}N_4O_8$ requires C, 67.44; H, 5.36; N, 8.28%. ^1H NMR (300 MHz, CDCl$_3$): δ = 7.96–7.83 (m, 4H), 7.65 (d, $J = 8.7$, 1H), 7.46–7.30 (m, 10H), 7.23 (d, $J = 2.3$, 2H), 6.87 (d, $J = 9.3$, 2H), 6.80 (t, $J = 2.3$, 1H), 5.02 (s, 4H), 4.55 (t, $J = 5.7$, 2H), 4.35 (t, $J = 4.5$, 2H), 4.03–3.94 (m, 2H), 3.88 (t, $J = 5.7$, 2H), 3.19–3.06 (m, 4H) ppm. MS ESI+: m/z 677.3 $[M+H]^+$.

4.15. Synthesis of 4'-(N-{2-[3,5-bis(benzyloxy)benzoyloxy]ethyl}—N-methylamino)-2-(2-{3,5-bis[(pentafluorophenyl)methoxy]benzoyloxy} ethoxy)-4-nitroazobenzene (12)

DCC method was used. The crude product was purified by recrystallization from EtOAc/hexanes. Yield 0.35 g (76%) of brownish red crystals, *mp* 145–147 °C. Found: C, 60.68; H, 3.57; N, 4.89%; $C_{59}H_{42}F_{10}N_4O_{11}$ requires C, 60.41; H, 3.61; N, 4.78%. ^1H NMR (400 MHz, CDCl$_3$): δ = 7.97 (d, $J = 2.3$, 1H), 7.93–7.83 (m, 3H), 7.65 (d, $J = 8.8$, 1H), 7.43–7.29 (m, 12H), 7.21 (d, $J = 2.3$, 2H), 6.82–6.73 (m, 3H), 6.71 (t, $J = 2.4$, 1H), 5.03 (s, 4H), 5.01 (s, 4H), 4.84–4.75 (m, 2H), 4.64–4.57 (m, 2H), 4.52 (t, $J = 5.8$, 2H), 3.83 (t, $J = 5.8$, 2H), 3.13 (s, 3H) ppm. ^{13}C NMR (101 MHz, CDCl$_3$): δ = 166.10, 165.53, 159.79, 158.97, 154.92, 152.07, 148.10, 147.28, 145.59 (d, $J = 258$ Hz), 144.55, 137.52 (d, $J = 259$ Hz), 136.31, 132.16, 131.47, 128.57, 128.09, 127.50, 126.12, 117.58, 117.34, 111.43, 110.60, 109.52 (t, $J = 18$ Hz), 108.78, 108.33, 107.66, 107.49, 70.26, 68.56, 63.36, 61.99, 57.59, 50.70, 38.89 ppm.

4.16. Synthesis of 4'-[N-(2-{3,5-bis[(pentafluorophenyl)methoxy] benzoyloxy}ethyl)—N-methylamino]-2-(2-hydroxyethoxy)-4-nitroazobenzene (13)

2-(2-Amino-5-nitrophenoxy)ethanol (**10**) (0.19 g, 0.97 mmol) was dissolved in acetonitrile (1.5 mL) and conc. HCl (0.45 mL) was added. The solution was poured onto crushed ice (4 g). A solution of $NaNO_2$ (0.067 g, 0.97 mmol) in water (1.0 mL) was added at such a rate as to prevent temperature from rising above +5 °C. After the addition was complete, stirring was continued for 1 h at 0–5 °C. This diazonium chloride solution was added dropwise at 0–5 °C to the emulsion of compound **9** (0.63 g, 0.97 mmol) in mixture of acetic acid (0.32 mL), water (0.32 mL), AcONa·3H$_2$O (0.32 g), acetonitrile (4 mL) and CH$_2$Cl$_2$ (4 mL). The reaction mixture was vigorously stirred 4 h in ice bath and overnight in room temperature. CH$_2$Cl$_2$ (40 mL) was added and the mixture was separated in separatory funnel and organic phase was washed with satd. NaHCO$_3$ solution once and with water twice. The organic phase was dried over Na$_2$SO$_4$, filtered and evaporated. The crude product was purified by column chromatography eluted with EtOAc/hexanes (1:1). Yield 0.60 g (73%) of deep red crystalline solid, *mp* 165–167 °C. Found: C, 53.48; H, 2.89; N, 6.39%; $C_{38}H_{26}F_{10}N_4O_8$ requires C, 53.28; H, 3.06; N, 6.54%. ^1H NMR (300 MHz, CDCl$_3$): δ = 8.07 (d, $J = 8.6$, 2H), 7.89–7.97 (m, 2H), 7.70 (d, $J = 9.61$, 1H),

7.22 (d, $J = 2.07$, 2H), 7.00 (d, $J = 8.6$, 2H), 6.71 (t, $J = 2.07$, 1H), 4.99 (s, 4H), 4.49–4.69 (m, 2H), 4.26–4.45 (m, 2H), 3.92–4.11 (m, 4H), 3.27 (s, 3H) ppm. MS ESI+: m/z 857.2 $[M+H]^+$.

4.17. Synthesis of 4'-[N-(2-{3,5-bis[(pentafluorophenyl)methoxy] benzoyloxy]ethyl)−N-methylamino]-2-{2-[3,5-bis(benzyloxy)benzoyloxy] ethoxy}-4-nitroazobenzene (14)

DCC method was used. The crude product was purified by re-crystallization from EtOAc/EtOH. Yield 0.20 g (91%) of red crystals, *mp* 69–71 °C. Found: C, 60.20; H, 3.39; N, 4.55%; $C_{59}H_{42}F_{10}N_4O_{11}$ requires C, 60.41; H, 3.61; N, 4.78%. ^{1}H NMR (300 MHz, DMSO-d_6): δ = 8.05 (d, $J = 2.4$ Hz, 1H), 7.88 (dd, $J = 8.9$, 2.3 Hz, 1H), 7.73 (d, $J = 9.1$ Hz, 2H), 7.51 (d, $J = 8.9$ Hz, 1H), 7.23–7.41 (m, 10H), 7.19 (d, $J = 2.3$ Hz, 2H), 7.04 (d, $J = 2.2$ Hz, 2H), 6.94 (d, $J = 9.3$ Hz, 2H), 6.80–6.89 (m, 2H), 5.02 (s, 4H), 4.94 (s, 4H), 4.67–4.80 (m, 2H), 4.54–4.67 (m, 2H), 4.41 (t, $J = 4.8$ Hz, 2H), 3.87 (t, $J = 5.1$ Hz, 2H), 3.03 (s, 3H) ppm. ^{13}C NMR (75 MHz, DMSO-d_6): δ = 165.15, 164.97, 159.43, 158.71, 154.55, 152.89, 147.65, 145.83, 145.00 (d, $J = 247$), 143.33, 140.93 (d, $J = 248$), 136.71 (d, $J = 247$), 136.47, 131.72, 131.52, 128.33, 127.83, 127.53, 125.76, 116.61, 116.23, 111.61, 109.95, 109.65 (t, $J = 18$), 108.05, 107.94, 107.41, 106.68, 69.51, 67.95, 62.97, 62.86, 57.43, 49.00, 37.33 ppm.

4.18. Synthesis of 4'-(N-{2-[3,5-bis(benzyloxy)benzoyloxy]ethyl}−N-methylamino)-2-{2-[3,5-bis(benzyloxy)benzoyloxy]ethoxy}-4-nitroazobenzene (16)

DCC method was used. The crude product was purified by column chromatography eluted with CH_2Cl_2/hexanes (gradient from 10% to pure CH_2Cl_2). Yield 0.67 g (90%) of red crystals, *mp* 151–155 °C. Found: C, 71.22; H, 5.14; N, 5.66%; $C_{59}H_{52}N_4O_{11}$ requires C, 71.36; H, 5.28; N, 5.64%. ^{1}H NMR (300 MHz, DMSO-d_6): δ = 8.05 (d, $J = 2.3$, 1H), 7.88 (dd, $J = 8.8$, 2.3, 1H), 7.75 (d, $J = 9.1$, 2H), 7.53 (d, $J = 8.8$, 1H), 7.41–7.21 (m, 20H), 7.15 (d, $J = 2.2$, 2H), 7.05 (d, $J = 2.3$, 2H), 6.93–6.83 (m, 4H), 5.02 (s, 8H), 4.74–4.60 (m, 4H), 4.42 (t, $J = 4.3$, 2H), 3.84 (t, $J = 4.3$, 2H), 3.02 (s, 3H) ppm. ^{13}C NMR (75 MHz, DMSO-d_6): δ = 165.31, 165.18, 159.44, 159.41, 154.59, 152.43, 147.65, 146.38, 143.67, 136.48, 131.53, 131.40, 128.38, 127.88, 127.65, 127.63, 125.77, 116.95, 116.78, 111.63, 110.21, 108.05, 107.84, 107.10, 106.72, 69.53, 67.98, 63.16, 62.55, 49.78, 38.24 ppm. MS ESI+: m/z 993.9 $[M+H]^+$.

4.19. Synthesis of 4'-[N-(2-{3,5-bis[(pentafluorophenyl)methoxy] benzoyloxy}ethyl)−N-methylamino]-2-(2-{3,5-bis[(pentafluorophenyl) methoxy]benzoyloxy}ethoxy)-4-nitroazobenzene (17)

DCC method was used. The crude product was purified by re-crystallization from EtOAc/EtOH. Initially an oil was formed, which was heated with insufficient amount of EtOH to dissolve, but it facilitated crystallization. Yield 0.82 g (82%) of red crystals, *mp* 102–104 °C. Found: C, 52.74; H, 2.48; N, 3.91%; $C_{59}H_{32}F_{20}N_4O_{11}$ requires C, 52.38; H, 2.38; N, 4.14%. ^{1}H NMR (300 MHz, DMSO-d_6): δ = 8.05 (d, $J = 2.2$, 1H), 7.86 (dd, $J = 8.9$, 2.2, 1H), 7.68 (d, $J = 9.1$, 2H), 7.51 (d, $J = 8.9$, 1H), 7.24 (d, $J = 2.2$, 2H), 7.11–6.95 (m, 3H), 6.95–6.78 (m, 3H), 5.15 (s, 4H), 4.96 (s, 4H), 4.79–4.68 (m, 2H), 4.68–4.57 (m, 2H), 4.51–4.41 (m, 2H), 3.96–3.84 (m, 2H), 3.06 (s, 3H) ppm. ^{13}C NMR (75 MHz, DMSO-d_6): δ = 165.39, 165.24, 159.29, 159.21, 155.08, 153.22, 148.16, 146.41, 145.47 (d, $J = 246$), 143.79, 141.46 (d, $J = 251$), 137.39 (d, $J = 244$), 132.39, 132.17, 126.08, 117.10, 116.79, 111.98, 110.59, 110.26 (m), 109.16, 108.46, 107.79, 107.48, 68.48, 63.65, 63.21, 58.21, 57.99, 49.50, 37.85 ppm.

Acknowledgement

Appendix A. Supplementary data

Supplementary data to this article can be found online at https://doi.org/10.1016/j.dyepig.2018.10.035.

References

[1] Cho MJ, Choi DH, Sullivan PA, Akelaitis AJP, Dalton LR. Recent progress in second-order nonlinear optical polymers and dendrimers. Prog Polym Sci 2008;33:1013–58. https://doi.org/10.1016/j.progpolymsci.2008.07.007.

[2] Dalton LR, Sullivan PA. Electric field poled organic electro-optic materials: state of the art and future prospects. Chem Rev 2010;110:25–55. https://doi.org/10.1021/cr9000429.

[3] Dalton LR, Sullivan PA, Bale DH, Hammond S, Olbricht BC, Rommel H, et al. Organic photonic materials. Bellingham, USA: SPIE: Tutorials in Complex Photonic Media; 2007. p. 525–74. https://doi.org/10.1117/3.832717.ch16.

[4] Li Z, Li Q, Qin J. Some new design strategies for second-order nonlinear optical polymers and dendrimers. Polym Chem 2011;2:2723–40. https://doi.org/10.1039/c1py00205h.

[5] Jang S-H, Jen AK-Y. Electro-optic (E-O) molecular glasses. Chem Asian J 2009;4:20–31. https://doi.org/10.1002/asia.200800179.

[6] Wu W, Qin J, Li Z. New design strategies for second-order nonlinear optical polymers and dendrimers. Polymer 2013;54:4351–82. https://doi.org/10.1016/j.polymer.2013.05.039.

[7] Tang R, Li Z. Second-order nonlinear optical dendrimers and dendronized hyper-branched polymers. Chem Rec 2017;17:71–89. https://doi.org/10.1002/tcr.201600065.

[8] Li Z, Chen P, Xie Y, Li Z, Qin J. Ar-Ar^F self-assembly of star-shaped second-order nonlinear optical chromophores achieving large macroscopic nonlinearities. Adv Electron Mater 2017:1700138. https://doi.org/10.1002/aelm.201700138.

[9] Bacchi S, Benaglia M, Cozzi F, Demartin F, Filippini G, Gavezzotti A. X-ray diffraction and theoretical studies for the quantitative assessment of intermolecular arene-perfluoroarene stacking interactions. Chem Eur J 2006;12:3538–46. https://doi.org/10.1002/chem.200501248.

[10] Hori A, Shinohe A, Yamasaki M, Nishibori E, Aoyagi S, Sakata M. 1:1 Cross-assembly of two β-diketonate complexes through arene-perfluoroarene interactions. Angew Chem Int Ed 2007;46:7617–20. https://doi.org/10.1002/anie.200702662.

[11] Salonen LM, Ellermann M, Diederich F. Aromatic rings in chemical and biological recognition: energetics and structures. Angew Chem Int Ed 2011;50:4808–42. https://doi.org/10.1002/anie.201007560.

[12] Serrano-Becerra JM, Hernández-Ortega S, Morales-Morales D, Valdés-Martínez J. Bottom-up design and construction of a non-centrosymmetric network through π–π stacking interactions. CrystEngComm 2009;11:226–8. https://doi.org/10.1039/b816630g.

[13] Kishikawa K, Oda K, Aikyo S, Kohmoto S. Columnar superstructures of non-disc-shaped molecules generated by arene–perfluoroarene face-to-face interactions. Angew Chem Int Ed 2007;119:778–82. https://doi.org/10.1002/ange.200603594.

[14] Hsu SM, Lin YC, Chang JW, Liu YH, Lin HC. Intramolecular interactions of a phenyl/perfluorophenyl pair in the formation of supramolecular nanofibers and hydrogels. Angew Chem Int Ed 2014;53:1921–7. https://doi.org/10.1002/anie.201307500.

[15] Bauer R, Liu D, Ver Heyen A, De Schryver F, De Feyter S, Müllen K. Polyphenylene dendrimers with pentafluorophenyl units: synthesis and self-assembly. Macromolecules 2007;40:4753–61. https://doi.org/10.1021/ma0625511.

[16] Kim T-D, Kang J-W, Luo J, Jang S-H, Ka J-W, Tucker N, et al. Ultralarge and thermally stable electro-optic activities from supramolecular self-assembled molecular glasses. J Am Chem Soc 2007;129:488–9. https://doi.org/10.1021/ja067970s.

[17] Zhou X-H, Luo J, Huang S, Kim T-D, Shi Z, Cheng Y-J, et al. Supramolecular self-assembled dendritic nonlinear optical chromophores: fine-tuning of arene-per-fluoroarene interactions for ultralarge electro-optic activity and enhanced thermal stability. Adv Mater 2009;21:1976–81. https://doi.org/10.1002/adma.200801639.

[18] Kim T-D, Luo J, Jen AK-Y. Quantitative determination of the chromophore alignment induced by electrode contact poling in self-assembled NLO materials. Bull Kor Chem Soc 2009;30:882–6.

[19] Wu W, Fu Y, Wang C, Ye C, Qin J, Li Z. A series of hyperbranched polytriazoles containing perfluoroaromatic rings from AB2-type monomers: convenient syntheses by click chemistry under copper(I) catalysis and enhanced optical nonlinearity. Chem Asian J 2011;6:2787–95. https://doi.org/10.1002/asia.201100379.

[20] Wu W, Zhu Z, Qiu G, Ye C, Qin J, Li Z. New hyperbranched second-order nonlinear optical poly(arylene-ethynylene)s containing pentafluoroaromatic rings as isolation group: facile synthesis and enhanced optical nonlinearity through Ar-Ar^F self-assembly effect. J Polym Sci Part A Polym Chem 2012;50:5124–33. https://doi.org/10.1002/pola.26345.

[21] Wu W, Yu G, Liu Y, Ye C, Qin J, Li Z. Using two simple methods of Ar-Ar^F self-assembly and isolation chromophores to further improve the comprehensive performance of NLO dendrimers. Chem Eur J 2013;19:630–41. https://doi.org/10.

1002/chem.201202992.

[22] Wu W, Wang C, Tang R, Fu Y, Ye C, Qin J, et al. Second-order nonlinear optical dendrimers containing different types of isolation groups: convenient synthesis through powerful "click chemistry" and large NLO effects. J Mater Chem C 2013;1:717–28. https://doi.org/10.1039/C2TC00053A.

[23] Wu W, Wang C, Li Q, Ye C, Qin J, Li Z. The influence of pentafluorophenyl groups on the nonlinear optical (NLO) performance of high generation dendrons and dendrimers. Sci Rep 2014;4:6101. https://doi.org/10.1038/srep06101.

[24] Wu W, Huang Q, Zhong C, Ye C, Qin J, Li Z. Second-order nonlinear optical (NLO) polymers containing perfluoroaromatic rings as isolation groups with Ar/Ar^F self-assembly effect: enhanced NLO coefficient and stability. Polymer 2013;54:5655–64. https://doi.org/10.1016/j.polymer.2013.07.073.

[25] Wu W, Huang Q, Qiu G, Ye C, Qin J, Li Z. Aromatic/perfluoroaromatic self-assembly effect: an effective strategy to improve the NLO effect. J Mater Chem 2012;22:18486–95. https://doi.org/10.1039/c2jm33129b.

[26] Laipniece L, Kampars V. Synthesis, thermal and light absorption properties of push-pull azochromophores substituted with dendronizing phenyl and perfluorophenyl fragments. Main Group Chem 2015;14:43–58. https://doi.org/10.3233/MGC-140152.

[27] Luo J, Ma H, Haller M, Jen AK-Y, Barto RR. Large electro-optic activity and low optical loss derived from a highly fluorinated dendritic nonlinear optical chromophore. Chem Commun 2002:888–9.

[28] Ma H, Jen AK-Y. Functional dendrimers for nonlinear optics. Adv Mater 2001;13:1201–5. https://doi.org/10.1002/1521-4095(200108)13. 15 < 1201::AID-ADMA1201 > 3.0.CO;2-F.

[29] Wu W, Li C, Yu G, Liu Y, Ye C, Qin J, et al. High-generation second-order nonlinear optical (NLO) Dendrimers that contain isolation chromophores: convenient synthesis by using click chemistry and their increased NLO effects. Chem Eur J 2012;18:11019–28. https://doi.org/10.1002/chem.201200441.

[30] Deloncle R, Caminade A-M. Stimuli-responsive dendritic structures: the case of light-driven azobenzene-containing dendrimers and dendrons. J Photochem Photobiol C Photochem Rev 2010;11:25–45. https://doi.org/10.1016/j.jphotochemrev.2010.02.003.

[31] Park C, Lim J, Yun M, Kim C. Photoinduced release of guest molecules by supramolecular transformation of self-assembled aggregates derived from dendrons. Angew Chem Int Ed 2008;47:2959–63. https://doi.org/10.1002/anie.200705271.

[32] Ghosh S, Banthia AK, Chen Z. Synthesis and photoresponsive study of azobenzene centered polyamidoamine dendrimers. Tetrahedron 2005;61:2889–96. https://doi.org/10.1016/j.tet.2005.01.052.

[33] Lee J, Choi D, Shin EJ. *Trans-cis* isomerization of arylether dendrimers with azobenzene core and terminal hydroxy groups. Spectrochim Acta Mol Biomol Spectrosc 2010;77:478–84. https://doi.org/10.1016/j.saa.2010.06.022.

[34] Momotake A, Arai T. Water-soluble azobenzene dendrimers. Tetrahedron Lett 2004;45:4131–4. https://doi.org/10.1016/j.tetlet.2004.03.152.

[35] Jiang D-L, Aida T. Photoisomerization in dendrimers by harvesting of low-energy photons. Nature 1997;388:465–8.

[36] Ray A, Bhattacharya S, Ghorai S, Ganguly T, Bhattacharjya A. Synthesis and *trans–cis* isomerization of azobenzene dendrimers incorporating 1,2-isopropylidenefuranose rings. Tetrahedron Lett 2007;48:8078–82. https://doi.org/10.1016/j.tetlet.2007.08.115.

[37] Junge DM, McGrath DV. Photoresponsive dendrimers. Chem Commun 1997:857–8.

[38] Grebel-Koehler D, Liu D, De Feyter S, Enkelmann V, Weil T, Engels C, et al. Synthesis and photomodulation of rigid polyphenylene dendrimers with an azobenzene core. Macromolecules 2003;36:578–90. https://doi.org/10.1021/ma021135n.

[39] Liao LX, Stellacci F, McGrath DV. Photoswitchable flexible and shape-persistent dendrimers: comparison of the interplay between a photochromic azobenzene core and dendrimer structure. J Am Chem Soc 2004;126:2181–5. https://doi.org/10.1021/ja036418p.

[40] Laipniece L, Kreicberga J, Kampars V. Divergent synthesis of polyester type dendrimers containing azobenzene in the core. Sci Proc Riga Tech Univ 2008;16:88–99. Ser 1.

[41] Seniutinas G, Laipniece L, Kreicberga J, Kampars V, Gražulevičius J, Petruškevičius R, et al. Orientational relaxation of three different dendrimers in polycarbonate matrix investigated by optical poling. J Opt A Pure Appl Opt 2009;11:034003. https://doi.org/10.1088/1464-4258/11/3/034003.

[42] Tokmakovs A, Rutkis M, Traskovskis K, Zarins E, Laipniece L, Kokars V, et al. Nonlinear optical properties of low molecular organic glasses formed by triphenyl modified chromophores. IOP Conf Ser Mater Sci Eng 2012;38:012034. https://doi.org/10.1088/1757-899X/38/1/012034.

[43] Seniutinas G, Tomašiūnas R, Czaplicki R, Sahraoui B, Kampars V. Third harmonic generation via dendrimers of four generations. Mediterr. Winter conf. ICTON-MW 2009 2009 3rd Ict. p. 1–4. https://doi.org/10.1109/ICTONMW.2009.5385570.

[44] Navickaite G, Seniutinas G, Tomašiunas R, Petruškevičius R, Kampars V. Optical functionalism of azopolymers: photoinduced orientation and re-orientation of dendrimer structures of different generations. Phys Status Solidi Appl Mater Sci 2011;208:1833–6. https://doi.org/10.1002/pssa.201084044.

[45] Traskovskis K, Zarins E, Laipniece L, Tokmakovs A, Kokars V, Rutkis M. Structure-dependent tuning of electro-optic and thermoplastic properties in triphenyl groups containing molecular glasses. Mater Chem Phys 2015;155:232–40. https://doi.org/10.1016/j.matchemphys.2015.02.035.

[46] Laipniece L, Kampars V. Synthesis and thermal properties of azobenzene core polyester dendrimers with trityl groups at the periphery. Key Eng Mater 2018;762:171–5. https://doi.org/10.4028/www.scientific.net/KEM.762.171.

[47] Yokoyama S, Nakahama T, Otomo A, Mashiko S. Preparation and assembled structure of dipolar dendrons based electron donor/acceptor azobenzene

[48] branching. Chem Lett 1997;26:1137–8. https://doi.org/10.1246/cl.1997.1137.

[49] Yokoyama S, Nakahama T, Otomo A, Mashiko S. Intermolecular coupling enhancement of the molecular hyperpolarizability in multichromophoric dipolar dendrons. J Am Chem Soc 2000;122:3174–81. https://doi.org/10.1021/ja993569c.

[49] Yamaguchi Y, Yokomichi Y, Yokoyama S, Mashiko S. Theoretical study of solvent effects of first-order hyperpolarizabilities of nitro–azobenzene dendrimers. J Mol Struct: THEOCHEM 2002;578:35–45. https://doi.org/10.1016/S0166-1280(01)00691-1.

[50] Yamaguchi Y, Yokomichi Y, Yokoyama S, Mashiko S. Theoretical predictions of first-order hyperpolarizabilities of azobenzene dendrimers. J Mol Struct: THEOCHEM 2001;545:187–96. https://doi.org/10.1016/S0166-1280(01)00414-6.

[51] Zhang W, Xie J, Shi W, Deng X, Cao Z, Shen Q. Second-harmonic properties of dendritic polymers skeleton-constructed with azobenzene moiety used for nonlinear optical materials. Eur Polym J 2008;44:872–80. https://doi.org/10.1016/j.eurpolymj.2007.12.007.

[52] Li Z, Yu G, Wu W, Liu Y, Ye C, Qin J, et al. Nonlinear optical dendrimers from click chemistry: convenient synthesis, new function of the formed triazole rings, and enhanced NLO effects. Macromolecules 2009;42:3864–8. https://doi.org/10.1021/ma900471t.

[53] Wu W, Xu Z, Li Z. Using an orthogonal approach and one-pot method to simplify the synthesis of nonlinear optical (NLO) dendrimers. Polym Chem 2014;5:6667–70. https://doi.org/10.1039/C4PY01058B.

[54] Wu W, Huang L, Song C, Yu G, Ye C, Liu Y, et al. Novel global-like second-order nonlinear optical dendrimers: convenient synthesis through powerful click chemistry and large NLO effects achieved by using simple azo chromophore. Chem Sci 2012;3:1256–61. https://doi.org/10.1039/C2SC00834C.

[55] Wu W, Ye C, Qin J, Li Z. Dendrimers with large nonlinear optical performance by introducing isolation chromophore, utilizing the Ar/Ar^F self-assembly effect, and modifying the topological structure. ACS Appl Mater Interfaces 2013;5:7033–41. https://doi.org/10.1021/am401299t.

[56] Wu W, Huang Q, Xu G, Wang C, Ye C, Qin J, et al. Using an isolation chromophore to further improve the comprehensive performance of nonlinear optical (NLO) dendrimers. J Mater Chem C 2013;1:3226–34. https://doi.org/10.1039/c3tc00007a.

[57] Tang R, Zhou S, Xiang W, Xie Y, Chen H, Peng Q, et al. New "X-type" second-order nonlinear optical dendrimers: fewer chromophore moieties and high NLO effects. J Mater Chem C 2015;3:4545–52. https://doi.org/10.1039/c5tc00182j.

[58] Wu W, Xu G, Li C, Yu G, Liu Y, Ye C, et al. From nitro- to sulfonyl-based chromophores: improvement of the comprehensive performance of nonlinear optical dendrimers. Chem Eur J 2013;19:6874–88. https://doi.org/10.1002/chem.201203567.

[59] Li Z, Wu W, Li Q, Yu G, Xiao L, Liu Y, et al. High-generation second-order nonlinear optical (NLO) dendrimers: convenient synthesis by click chemistry and the increasing trend of NLO effects. Angew Chem Int Ed 2010;49:2763–7. https://doi.org/10.1002/anie.200906946.

[60] Laipniece L, Kampars V, Ozols A, Augustovs P. Synthesis of dendronized chromophores and holographic recording in the chromophores containing samples. Abstr. 32nd sci. Conf. Riga: Institute of Solid State Physics, University of Latvia; 2016. p. 120.

[61] Augustovs P, Ozols A, Kokars V, Zarins E, Traskovskis K, Kampars V, et al. Peculiarities of the holographic vector recording by circularly polarized beams in molecular glassy films of different type. Abstr. 33rd sci. Conf. Riga: Institute of Solid State Physics, University of Latvia; 2017. p. 91.

[62] Frechet JMJ, Tomalia DA, editors. Dendrimers and other dendritic polymers. Ld: Chichester: John Wiley & Sons; 2001.

[63] Brooke GM. The preparation and properties of polyfluoro aromatic and heteroaromatic compounds. J Fluorine Chem 1997;86:1–76. https://doi.org/10.1016/S0022-1139(97)00006-7.

[64] Gung BW, Amicangelo JC. Substituent effects in C_6F_6-C_6H_5X stacking interactions. J Org Chem 2006;71:9261–70.

[65] Desiraju GR, Steiner T. The weak hydrogen bond: in structural chemistry and biology. Oxford: Oxford Univ. Press; 2001. https://doi.org/10.1093/acprof:oso/9780198509707.001.0001.

[66] Reichenbächer K, Süss HI, Hulliger J. Fluorine in crystal engineering-"the little atom that could". Chem Soc Rev 2005;34:22–30. https://doi.org/10.1039/b406892k.

[67] Ohta K, Ishida H. Comparison among several numerical integration methods for Kramers-Kronig Transformation. Appl Spectrosc 1988;42:952–7.

[68] Oudar JL, Chemla DS. Hyperpolarizabilities of the nitroanilines and their relations to the excited state dipole moment. J Chem Phys 1977;66:2664–8. https://doi.org/10.1063/1.434213.

[69] Herman WN, Hayden LM. Maker fringes revisited: second-harmonic generation from birefringent or absorbing materials. J Opt Soc Am B 1995;12:416–27. https://doi.org/10.1364/JOSAB.12.000416.

[70] Traskovskis K, Kokars V, Tokmakovs A, Mihailovs I, Nitiss E, Petrova M, et al. Stereoselective synthesis and properties of 1,3-bis(dicyanomethylidene)indane-5-carboxylic acid acceptor fragment containing nonlinear optical chromophores. J Mater Chem C 2016;4:5019–30. https://doi.org/10.1039/c6tc00203j.

[71] Alicante R. Photoinduced modifications of the nonlinear optical response in liquid crystalline azopolymers. Berlin, Heidelberg: Springer Berlin Heidelberg; 2013. https://doi.org/10.1007/978-3-642-31756-9.

[72] Sheldrick GM. A short history of SHELX. Acta Crystallogr Sect A Found Crystallogr 2008;A64:112–22. https://doi.org/10.1107/S0108767307043930.

[73] Vilitis O, Fonavs E, Rutkis M. Chromofore poling in thin films of organic glasses. 1. Overview of corona discharge application. Latv J Phys Tech Sci 2011;48:53–65. https://doi.org/10.2478/v10047-011-0038-1.

[74] Vilitis O, Titavs E, Nitiss E, Rutkis M. Chromophore poling in thin films of organic glasses. 3. Setup for corona triode discharge. Latv J Phys Tech Sci 2013;50:66–75.

https://doi.org/10.2478/lpts-2013-0004.

[75] Nitiss E, Titavs E, Kundzins K, Dementjev A, Gulbinas V, Rutkis M. Poling induced mass transport in thin polymer films. J Phys Chem B 2013;117:2812–9. https://doi.org/10.1021/jp310961a.

[76] Jerphagnon J, Kurtz SK. Optical nonlinear susceptibilities: accurate relative values for quartz ammonium dihydrogen phosphate, and potassium dihydrogen phosphate. Phys Rev B 1970;1:1739–44.

[77] Rutkis M, Vembris A, Zauls V, Tokmakovs A, Fonavs E, Jurgis A, et al. Novel second-order non-linear optical polymer materials containing indandione derivativatives as a chromophore. Proc. SPIE 6192 Org. Optoelectron. Photonics II; 2006. p. 61922Q.

[78] Theodorou V, Skobridis K, Tzakos AG, Ragoussis V. A simple method for the al-kaline hydrolysis of esters. Tetrahedron Lett 2007;48:8230–3. https://doi.org/10.1016/j.tetlet.2007.09.074.

[79] Faccini M, Balakrishnan M, Diemeer MBJ, Hu Z, Clays K, Asselberghs I, et al. Enhanced poling efficiency in highly thermal and photostable nonlinear optical chromophores. J Mater Chem 2008;18:2141–9. https://doi.org/10.1039/b801728j.

L. Laipniece, V. Kampars. Synthesis and Thermal Properties of Azobenzene Core Polyester Dendrimers with Trityl Groups at the Periphery. *Key Eng. Mater.*, **2018**, *762*, 171–175.

Publikācijas pilnais teksts pieejams *Scientific.net* mājaslapā

Kopsavilkums

Mēs esam sintezējuši poliestera tipa dendrimērus līdz 3. paaudzei, kas satur azobenzola hromoforu kodolā un tritilgrupas perifērijā, izmantojot diverģentās sintēzes stratēģiju. Mēs analizējām dendrimēru paraugus, izmantojot KMR, AEŠH, TG, DSC un UV-Vis metodes. Noskaidrojām, ka dendrimēra perifērijas funkcionalizēšana nav pilnīga. Dendrimēriem ar tritilgrupām perifērijā stiklošanās temperatūra ir diapazonā no 73 līdz 87 °C.

The full text of the publication is available on the *Scientific.net* website.

Abstract

We have synthesized polyester type dendrimers containing azobenzene chromophore in the core and trityl groups at the periphery using divergent growth strategy up to 3rd generation. We analyzed dendrimer samples using NMR, HPLC, TG, DSC and UV-Vis techniques. We found out that functionalization of dendrimer periphery is not complete. Dendrimers with trityl groups at the periphery have glass transition temperatures in the range 73–87 °C.

L. Laipniece, V. Kampars. Synthesis, thermal and light absorption properties of push-pull azochromophores substituted with dendronizing phenyl and perfluorophenyl fragments. *Main Group Chem.*, **2015**, *14*, 43–58.

Synthesis, thermal and light absorption properties of push-pull azochromophores substituted with dendronizing phenyl and perfluorophenyl fragments

Lauma Laipniece* and Valdis Kampars
Institute of Applied Chemistry, Riga Technical University, Riga, Latvia

Abstract. 4′-[*N*-(2-Hydroxyethyl)-*N*-methylamino]-2-(2-hydroxyethoxy)-4-nitroazobenzene (**1**) has been synthesized in azo coupling reaction. Nine different analogues of **1** has been prepared symmetrically and alternately substituted with dendritic phenyl and perfluorophenyl moieties using standard methods for ester and ether bond formation and azo coupling reaction. Thermal and light absorption properties of the azochromophores have been examined. The effect of trityl, tetrahydropyranyl, hydroxyl, pentafluorophenyloxy and 2,3,4,5,6-pentafluorobenzyl propionate moieties on glass transition, melting point and thermal stability has been proposed.

Keywords: Azo compounds, fluoroaromatics, thermal properties, π interactions

1. Introduction

Organic nonlinear optical (NLO) materials have attracted increasing interest for many years due to their potential application in electro-optical devices [1–7]. A good NLO material is composed of non-centrosymmetrically oriented chromophores with parallel aligned dipoles [5–8] and must possess high thermal stability [4, 9]. A relatively new direction for obtaining such materials is the synthesis of molecular glasses [8], low molecular weight compounds which form a stable amorphous phase. The more interesting ones are molecular glasses based on dendrimers of chromophores and on the reversible self-assembly of chromophores [10]. The chromophore molecule modification by dendritic substituents [11–14] or simultaneously both phenyl and perfluorophenyl moieties [15, 16] improve material properties. These dendritic substituents increase solubility and macroscopic nonlinearity [4, 9, 11–14, 17] via stabilization of chromophore alignment in amorphous phase. Fluoroaromatic parts being together with aromatic moieties increase glass transition temperature and thermal stability [4, 9], because of the self-assembly in stacks owing to arene-perfluoroarene (Ar-Ar^F) π-π interactions [15, 18–22], and that can lead to increased electro-optical coefficients [18–20].

---

*Corresponding author: Lauma Laipniece, Institute of Applied Chemistry, Riga Technical University, Paula Valdena street 3, LV-1048, Riga, Latvia. Tel.: +371 28771841; E-mail: lauma.laipniece@rtu.lv.
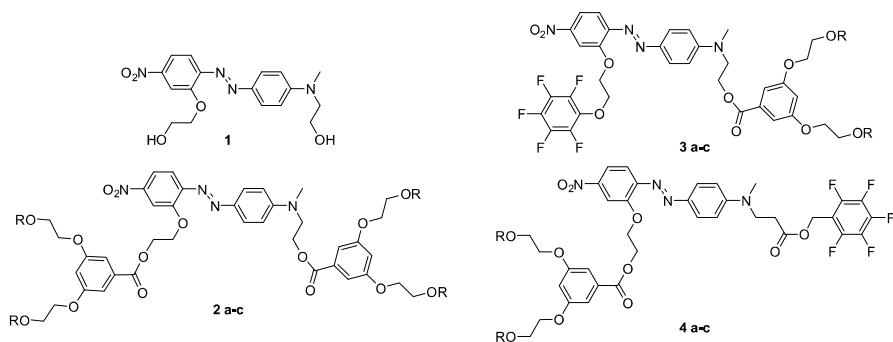
Fig. 1. Structures of the azochromophores. R = THP – tetrahydropyranyl (a), Trt – trityl (triphenylmethyl) (b), H (c).

Azobenzene chromophore containing materials have been investigated as components for NLO devices, lithography, all-optical switches and optical data storage [23, 24]. Dendrons have been attached to 4-position [25], 4,4′-positions [26–31], 2,2′-positions [32] or 3,3′,5,5′-positions [33, 34] of simple azobenzenes in order to investigate *cis-trans* isomerisation. Azochromophores of push-pull type have been incorporated in dendrimer branches [35–38] and their NLO properties also have been investigated [35–39]. But push-pull azobenzenes with dendritic substituents both at electron donating and electron withdrawing parts have not been synthesized till now.

The objective of this research was the investigation of the effect of molecular design on thermal and linear optical characteristics of molecular glasses obtained by symmetrically and alternately linking dendritic phenyl and perfluorophenyl moieties (compounds **2–4**) to the chromophore core **1** (Fig. 1). Thus to achieve this objective the methods of synthesis of nine new dendronized chromophores were elaborated using 3,5-bis(2-hydroxyethoxy)benzoic acid fragment with different end groups and pentafluorophenyl-substituent to strengthen the forces of the intramolecular attraction.

2. Experimental section

2.1. Reagents and general procedures

Starting materials were purchased from Acros and Alfa Aesar. DMF, CHCl$_3$ and CH$_2$Cl$_2$ were distilled from P$_2$O$_5$, dioxane was distilled from sodium. Starting materials were prepared according to the literature: methyl 3,5-dihydroxybenzoate [40], 3,5-bis(2-(tetrahydro-2*H*-pyran-2-yloxy)ethoxy)benzoic acid (**10a**) [40], methyl 3,5-bis(2-hydroxyethoxy)benzoate [40] and 3-(*N*-methylanilino)propionic acid (**13**) [41]. Purity of all compounds was checked by TLC method on Merck F$_{254}$ silica plates. The spots were visualized when necessary in UV light and in iodine vapour. Chromatographic separations were carried out on silica gel (ROTH Kieselgel 60, 60–200 µm) or using Biotage SP1 HPFC with Biotage silica gel cartridges. Melting points were taken on a Stuart SMP10 apparatus. The UV-Vis spectra were recorded with Perkin Elmer Lambda 35 spectrometer. IR spectra were recorded with Perkin Elmer Spectrum 100 FT-IR spectrometer using UATR accessory, NMR spectra were obtained on a Varian Mercury BB 200 MHz, Varian Mercury 400 MHz, Bruker Avance 300 MHz spectroscopes against solvent residue

as internal reference. The elemental analysis was carried out on an automatic analyzer EA 1106. Reaction mixture analysis was carried out on HPLC-MS system consisting of Waters Alliance 2695 chromatograph equipped with XTerra® MS C18 5 μm 2.1 × 100 mm column, Waters 2996 PDA detector, and Waters EMD 1000 (ESI) masspectrometer. TG and DSC curves were taken on Perkin Elmer STA 6000 apparatus. All the samples were heated at 10°C /min from 20 to 500°C under nitrogen for the first time and T_d was measured where TG curve shows 5% weight loss. For determination of T_g all the samples were heated at 10°C/min from 20 to 200°C under nitrogen for the first scan, then cooled to 15°C, and heated at 10°C/min from 15 to 180°C for the second scan.

2.2. Compound syntheses

2.2.1. 4-Nitrobenzenediazonium-2-olate (6)

2-Amino-5-nitrophenol (**5**) (4.00 g, 0.026 mol), NaNO$_2$ (1.60 g, 0.026 mol) and NaOH (1.04 g, 0.026 mol) were dissolved in water (14 mL) with heating. The obtained solution was added dropwise to ice (24 g) with conc. H$_2$SO$_4$ (5.2 mL) during period of 2 h, then reaction was stirred additional 30 min. Slurry was filtered and light sensitive betaine **6** was dried in dark place. Yield 3.48 g (81%). MS ESI+: *m/z* 165.9 [M+H]$^+$. ^{1}H NMR (300 MHz, DMSO-d$_6$): δ = 7.88 (d, *J* = 9.6, 1H), 7.25 (d, *J* = 2.2, 1H), 6.88 (dd, *J* = 9.6, 2.2, 1H) ppm. ^{13}C NMR (75 MHz, DMSO-d$_6$): δ = 175.05, 155.47, 129.69, 117.89, 106.02, 92.97 ppm.

2.2.2. 4'-(N-Methyl)amino-2-hydroxy-4-nitroazobenzene (7)

Diazonium betaine **6** (2.64 g, 16 mmol) as a suspension in water (52 mL) was added stepwise at 0–5°C to the solution of *N*-methylaniline (1.71 g, 16 mmol) in mixture of acetic acid (1 mL), water (40 mL) and AcONa·3H$_2$O (6.8 g). The reaction mixture was stirred 5 h at 5°C, then 2 days in room temperature. The mixture was extracted with EtOAc (3 × 50 mL), organics was washed with satd. NaHCO$_3$ and water, dried over Na$_2$SO$_4$, filtered and evaporated. Crude product was chromatographed with EtOAc/petroleum ether (gradient 1/6 to 1/1). Betaine **6** 1.37 g (52%) was recovered. Yield of product **7** 0.22 g (5%, based on recovered starting material 10%) as violet crystalline solid, *mp* 174–178°C. C$_{13}$H$_{12}$N$_4$O$_3$: calcd. C 57.35; H 4.44; N 20.58; found: C 57.14; H 4.32; N 20.10. MS ESI+: *m/z* 273.1 [M+H]$^+$. ^{1}H NMR (300 MHz, DMSO-d$_6$): δ = 11.32 (br. s, 1H), 7.87 (d, *J* = 9.1, 2H), 7.75 (m, 3H), 7.12 (q, *J* = 5.0, 1 H), 6.70 (d, *J* = 9.1, 2H), 2.82 (d, *J* = 5.0, 3H) ppm.

2.2.3. 2-(2-Hydroxyethoxy)-4-nitroaniline (8)

2-Amino-5-nitrophenol (**5**) (1.00 g, 6.5 mmol) was dissolved in abs. DMF (5 mL) and NaH (0.25 g, 6.5 mmol, 60% in mineral oil) was added stepwise. 2-Bromoethanol (0.50 mL, 7.0 mmol) was added after 30 min. and reaction mixture was stirred at 50°C for 10 h. Then 10% NaOH solution (20 mL) was added and extracted with MTBE (5 × 10 mL). Organics was dried over Na$_2$SO$_4$ and concentrated; the crude product was recrystallized from EtOAc/hexanes. Yield 0.57 g (44%) of yellow crystalline solid, *mp* 143–145°C. C$_8$H$_{10}$N$_2$O$_4$: calcd. C 48.48; H 5.09; N 14.14; found: C 49.27; H 5.28; N 13.70. MS ESI+: *m/z* 199.1 [M+H]$^+$. ^{1}H NMR (400 MHz, CDCl$_3$): δ = 7.78 (dd, *J* = 2.3, 8.7, 1H), 7.66 (d, *J* = 2.3, 1H), 6.61 (d, *J* = 8.7, 1H), 4.53 (br. s, 2H), 4.17 (t, *J* = 4.3, 2H), 4.06-3.92 (m, 2H), 1.79 (t, *J* = 5.5, 1H) ppm.

2.2.4. N-(2-Hydroxyethyl)-N-methylaniline (9)

N,N-Dimethylaniline (20.75 g, 0.17 mol) and 2-chloroethanol (20.13 g, 0.25 mol) was dissolved in *n*-BuOH (50 mL), and KI (1.66 g, 0.01 mol) was added, resulting solution was refluxed for 24 h. Reaction

mixture was cooled and filtered, filtrate concentrated and obtained blue crude product was distilled in vacuum at 137–145°C/10 mmHg, yield 11.36 g (44%) of yellowish liquid. MS ESI+: *m/z* 152.1 [M+H]$^+$. ^{1}H NMR (200 MHz, CDCl$_3$): δ = 7.16 (dd, *J* = 7.2, 8.3 Hz, 2H), 6.60–6.72 (m, 3H), 3.69 (t, *J* = 5.8 Hz, 2H), 3.34 (t, *J* = 5.8 Hz, 2H), 2.85 (s, 3H), 2.08 (s, 1H) ppm.

2.2.5. 4'-[N-(2-Hydroxyethyl)-N-methyl]amino-2-(2-hydroxyethoxy)-4-nitroazobenzene (1)

Aniline **8** (0.40 g, 2.0 mmol) was dissolved in hot (80–90°C) diluted HCl (1.5 mL water, 4 mL MeOH and 1.2 mL conc. HCl). The solution was poured onto crushed ice (12 g). After additional cooling in an ice bath, a solution of NaNO$_2$ (0.14 g, 2.0 mmol) in water (2.5 mL) was added at such a rate as to prevent temperature from rising above +5°C. After the addition was complete, stirring was continued for 1 h at 0–5°C. This diazonium chloride solution was added dropwise at 0–5°C to the solution of aniline **9** (0.32 g, 2.1 mmol) in mixture of acetic acid (1.2 mL), water (2 mL) and AcONa·3H$_2$O (0.6 g). If necessary a 10% solution of sodium acetate was added to hold pH 4-5. After 2 h the reaction mixture was refrigerated overnight. The mixture was filtered, washed with water till neutral pH and dried to afford of crude product (0.62 g), which was recrystallized from acetone/water, filtered crystals were dried in a desiccator with P$_2$O$_5$. Yield 0.59 g (82%) of violet crystalline solid, *mp* 144–146°C. C$_{17}$H$_{20}$N$_4$O$_5$: calcd. C 56.66; H 5.59; N 15.55; found: C 56.63; H 5.46; N 15.38. MS ESI+: *m/z* 361.2 [M+H]$^+$. ^{1}H NMR (300 MHz, DMSO-d$_6$): δ = 8.00 (d, *J* = 1.7 Hz, 1H), 7.89 (dd, *J* = 9.0, 2.4 Hz, 1H), 7.80 (d, *J* = 8.9 Hz, 2H), 7.62 (d, *J* = 8.7 Hz, 1H), 6.88 (d, *J* = 8.9 Hz, 2H), 4.97 (t, *J* = 5.5 Hz, 1H), 4.81 (t, *J* = 5.1 Hz, 1H), 4.31 (t, *J* = 4.7 Hz, 2H), 3.82 (q, *J* = 5.0 Hz, 2H), 3.54–3.65 (m, 4H), 3.11 (s, 3H) ppm. ^{13}C NMR (75 MHz, DMSO-d$_6$): δ = 154.91, 152.67, 147.60, 146.64, 143.43, 125.90, 117.11, 116.47, 111.55, 109.88, 71.74, 59.60, 58.30, 54.11, 39.07 ppm.

2.2.6. 2-(Trityloxy)ethyl chloride

Trityl chloride (7.81 g, 28 mmol), 2-chloroethanol (2.01 mL, 30 mmol) and NEt$_3$ (7.81 mL, 56 mmol) were dissolved in dry CHCl$_3$ (40 mL) and catalyst DMAP (0.36 g, 3 mmol) was added. Resulting solution was stirred for 24 h at room temperature. The reaction mixture was washed with brine (3 × 10 mL), dried over Na$_2$SO$_4$, filtered through thin layer of silica gel, then concentrated and recrystallized from EtOH. Yield 5.52 g (61%) of white crystalline solid, *mp* 130–133°C. IR: ν = 3061.6, 2919.3, 2873.9, 1595.3, 1492.5, 1447.7, 1295.9, 1218.2, 1180.2, 1152.1, 1098.4, 1051.5, 997.5, 899.6, 770.2, 761.9, 750.5, 700.2 cm^{-1}. ^{1}H NMR (300 MHz, CDCl$_3$): δ = 7.40 (d, *J* = 7.0 Hz, 6H), 7.26–7.14 (m, 9H), 3.51 (t, *J* = 5.9 Hz, 2H), 3.31 (t, *J* = 5.9 Hz, 2H) ppm.

2.2.7. Methyl 3,5-bis(2-(trityloxy)ethoxy)benzoate

Method A: NaH (0.46 g, 11 mmol, 60% in mineral oil) was added to a solution of methyl 3,5-dihydroxybenzoate (0.91 g, 5.4 mmol) in dry DMF (10 mL), and the mixture was heated at 110°C for 2 h, cooled to 60°C, and 2-(trityloxy)ethyl chloride (4.00 g, 12 mmol) in dry DMF (10 mL) was added while stirring. After 4 days at 60°C the mixture was cooled to room temperature, filtered through Celite, and concentrated in vacuum. CHCl$_3$ and water were added to the residue and it was washed with water. CHCl$_3$ solution was dried over Na$_2$SO$_4$, filtered and evaporated. Crude product was chromatographed with CH$_2$Cl$_2$/hexanes (gradient 0–60%). 2-(Trityloxy)ethyl chloride 2.28 g (57%) was recovered. Yield 1.06 g (27%, based on recovered starting material 54%) of white amorphous solid.

Method B: Methyl 3,5-bis(2-hydroxyethoxy)benzoate (0.20 g, 0.78 mmol), trityl chloride (0.48 g, 1,7 mmol) and DBU (0.30 mL, 2.0 mmol) were dissolved in dry CH$_2$Cl$_2$ (20 mL). Reaction mixture was stirred at room temperature for 4 days. Then solution was filtered through thin layer of silica eluted

with CH_2Cl_2 and product containing fractions were evaporated. Yield 0.40 g (69%) of white amorphous solid. $C_{50}H_{44}O_6$: calcd. C 81.06; H 5.99; found: C 81.47; H 5.90. MS ESI+: *m/z* 763.5 [M+Na]$^+$. ^{1}H NMR (300 MHz, DMSO-d$_6$): $\delta = 7.18–7.46$ (m, 30H), 7.15 (d, *J* = 2.3 Hz, 2H), 6.90 (t, *J* = 2.3 Hz, 1H), 4.26 (t, *J* = 4.4 Hz, 4H), 3.86 (s, 3H), 3.24–3.31 (m, 4H) ppm.

2.2.8. 3,5-Bis(2-(trityloxy)ethoxy)benzoic acid (10b)

General method was used [42]. Methyl 3,5-bis(2-(trityloxy)ethoxy)benzoate (0.70 g, 0.9 mmol) was dissolved in CH_2Cl_2/MeOH mixture in 9/1 ratio (20 mL) and solution of NaOH (0.15 g, 3.7 mmol) in MeOH (1.5 mL) was added. Resulting solution was stirred 2 days at room temperature. Solvent was evaporated and residue was dissolved in mixture of EtOH/H_2O/CH_2Cl_2. 5–8% HCl solution was added dropwise to it while vigorously stirring, when precipitate formed, addition of acid was stopped. Precipitate was filtered and washed with water, dried in vacuum. Yield 0.63 g (93%) of white amorphous solid. IR: $\nu = 1692.3, 1592.9, 1488.6, 1449.2, 1345.9, 1325.7, 1180.4, 1094.8, 1077.2, 1018.3, 984.9, 876.9, 818.4$ cm^{-1}. MS ESI-: *m/z* 726.0 [M-H]$^-$. ^{1}H NMR (300 MHz, DMSO-d$_6$): $\delta = 13.06$ (s, 1H), 7.21–7.44 (m, 30H), 7.15 (d, *J* = 2.4 Hz, 2H), 6.85–6.88 (m, 1H), 4.17–4.31 (m, 4H), 3.25–3.31 (m, 4H) ppm.

2.2.9. General procedure for ester formation with DCC and DMAP (DCC method)

To a solution of alcohol (1.0 mmol) and of acid (1.1 mmol) in dry CH_2Cl_2 (15 mL) was added DMAP (0.1 mmol) while stirring in ice bath, then a solution of DCC (1.1 mmol) in dry CH_2Cl_2 (4 mL) was added dropwise over 30 min. Reaction mixture was stirred for few days at room temperature until TLC analysis indicated the completion of the reaction. Flask was put in freezer for all *N,N'*-dicyclohexylurea to crystallize, then filtered and evaporated. The crude product was purified by appropriate method.

2.2.10. 4'-[N-(2-{3,5-Bis[2-(tetrahydro-2H-pyran-2-yloxy)ethoxy]benzoyloxy}ethyl)-N-methyl]amino-2-(2-{3,5-bis[2-(tetrahydro-2H-pyran-2-yloxy)ethoxy]benzoyloxy}ethoxy)-4-nitroazobenzene (2a)

DCC method was used. The crude product was purified by silica gel chromatography, eluted with EtOAc/hexanes (gradient 20–60%). Yield 0.22 g (70%) of red very viscous oil. $C_{59}H_{76}N_4O_{19}$: calcd. C 61.88; H 6.69; N 4.89; found: C 61.25; H 7.35; N 4.57. ^{1}H NMR (300 MHz, DMSO-d$_6$): $\delta = 8.07$ (d, *J* = 2.3 Hz, 1H), 7.92 (dd, *J* = 8.9, 2.3 Hz, 1H), 7.73 (d, *J* = 9.0 Hz, 2H), 7.65 (d, *J* = 8.9 Hz, 1H), 7.05 (d, *J* = 2.1 Hz, 2H), 6.97 (d, *J* = 2.1 Hz, 2H), 6.89 (d, *J* = 9.2 Hz, 2H), 6.73–6.80 (m, 2H), 4.63–4.76 (m, 4H), 4.51–4.61 (m, 4H), 4.47 (t, *J* = 5.1 Hz, 2H), 3.99–4.11 (m, 8H), 3.77–3.96 (m, 6H), 3.55–3.76 (m, 8H), 3.35–3.44 (m, 4H), 3.12 (s, 3H), 1.33–1.70 (m, 24H) ppm. ^{13}C NMR (75 MHz, DMSO-d$_6$): $\delta = 165.43$, 165.27, 159.70, 159.66, 154.68, 152.55, 147.71, 146.50, 143.70, 131.48, 131.33, 125.80, 116.99, 116.93, 111.61, 110.39, 107.73, 107.45, 106.54, 106.19, 98.11, 98.06, 68.09, 67.59, 65.13, 63.23, 62.61, 61.29, 61.24, 49.77, 38.24, 30.11, 24.99, 19.05, 19.00 ppm.

2.2.11. 4'-[N-(2-{3,5-Bis[2-(trityloxy)ethoxy]benzoyloxy}ethyl)-N-methyl]amino-2-(2-{3,5-bis[2-(trityloxy)ethoxy]benzoyloxy}ethoxy)-4-nitroazobenzene (2b)

DCC method was used. The crude product was purified by silica gel chromatography, eluted with CH_2Cl_2. Necessary fractions were evaporated and product was precipitated from EtOAc/EtOH. Yield 0.15 g (72%) of red glass. ^{1}H NMR (300 MHz, DMSO-d$_6$): $\delta = 8.03$ (d, *J* = 2.3 Hz, 1H), 7.81 (dd, *J* = 8.9, 2.3 Hz, 1H), 7.69 (d, *J* = 8.9 Hz, 2H), 7.49 (d, *J* = 8.9 Hz, 1H), 7.15–7.39 (m, 60H), 7.10 (d, *J* = 2.1 Hz, 2H), 7.03 (d, *J* = 2.1 Hz, 2H), 6.77–6.84 (m, 4H), 4.59–4.73 (m, 4H), 4.38–4.46 (m, 2H), 4.07–4.14 (m, 8H), 3.77–3.83 (m, 2H), 3.15–3.24 (m, 8H), 3.00 (s, 3H) ppm. ^{13}C NMR (75 MHz, DMSO-d$_6$): $\delta = 165.39$,

165.28, 159.72, 154.61, 152.28, 147.63, 146.47, 143.74, 143.60, 131.53, 131.36, 128.25, 127.83, 127.00, 125.76, 116.90, 116.82, 111.56, 110.33, 107.91, 107.73, 106.84, 106.41, 86.10, 68.09, 67.42, 63.19, 62.36, 49.92, 38.40 ppm.

2.2.12. 4'-(N-{2-[3,5-Bis(2-hydroxyethoxy)benzoyloxy]ethyl}-N-methyl)amino-2-{2-[3,5-bis(2-hydroxyethoxy)benzoyloxy]ethoxy}-4-nitroazobenzene (2c)

Compound **2a** (82 mg, 0.07 mmol) was dissolved in CH_2Cl_2 (1 mL), EtOH (15 mL) and PPTS (18 mg, 0.07 mmol) were added. Reaction mixture was refluxed for 5 h, then satd. $NaHCO_3$ solution in water and EtOAc were added. Aqueous phase was extracted 3 times with EtOAc. Combined organics were dried over Na_2SO_4, filtered and evaporated. Crude product was recrystallized from EtOAc. Yield 44 mg (77%) of red crystalline solid, mp 149.7°C. MS ESI+: m/z 809.6 [M+H]$^+$. ^{1}H NMR (300 MHz, DMSO-d$_6$): $\delta = 8.07$ (d, J = 2.3 Hz, 1H), 7.93 (dd, J = 8.9, 2.4 Hz, 1H), 7.74 (d, J = 9.0 Hz, 2H), 7.64 (d, J = 8.9 Hz, 1H), 7.04 (d, J = 2.3 Hz, 2H), 6.99 (d, J = 2.3 Hz, 2H), 6.90 (d, J = 8.9 Hz, 2H), 6.70–6.77 (m, 2H), 4.80–4.88 (m, 4H), 4.63–4.74 (m, 4H), 4.47 (t, J = 5.1 Hz, 2H), 3.88–3.97 (m, 10H), 3.61–3.70 (m, 8H), 3.13 (s, 3H) ppm. ^{13}C NMR (75 MHz, DMSO-d$_6$): $\delta = 165.48$, 165.32, 159.88, 154.58, 152.44, 147.72, 146.58, 143.67, 131.44, 131.35, 125.83, 117.16, 117.02, 111.65, 110.44, 107.53, 107.30, 106.48, 106.12, 69.93, 68.09, 63.22, 62.57, 59.43, 49.89, 38.58 ppm.

2.2.13. 2-(Pentafluorophenoxy)ethyl mesylate

2-(Pentafluorophenoxy)ethanol (2.00 g, 8.8 mmol) was dissolved in dry CH_2Cl_2 (15 mL) and diisopropylethylamine (1.5 mL, 9 mmol) was added. Solution was cooled to −15°C and mesyl chloride (0.69 mL, 8.9 mmol) was added dropwise while stirring. Reaction mixture was stirred for 24 h, and then washed with saturated soda solution and water. Solution was dried over Na_2SO_4, filtered, and evaporated. The crude product was purified by silica gel chromatography, eluted with EtOAc/hexane (gradient 10–50%). Yield 2.10 g (78%) of colourless liquid. MS ESI+: m/z 307.0 [M-H]$^+$. ^{1}H NMR (400 MHz, CDCl$_3$): $\delta = 4.51$–4.57 (m, 2H), 4.39–4.47 (m, 2H), 3.10 (s, 3H) ppm.

2.2.14. 2-[2-(Pentafluorophenoxy)ethoxy]-4-nitroaniline (11)

2-Amino-5-nitrophenol (**5**) (0.55 g, 3.6 mmol) was dissolved in dry DMF (3 mL), K_2CO_3 (0.25 g, 1.8 mmol) was added and resulting mixture was stirred at 30–40°C for 1 h. 2-(Pentafluorophenoxy)ethyl mesylate (1.20 g, 3.9 mmol) solution in dry DMF (5 mL) was added and resulting mixture was heated at 120°C. Water was added after 12 h and precipitate was filtered, washed with $NaHCO_3$ solution and water. Dried precipitate was dissolved in CH_2Cl_2 (3 mL) and filtered through layer of silica gel. Solvent was evaporated and yellow crystals were obtained. Yield 0.82 g (35%), mp 115–117°C. IR: $\nu = 3503.6$, 3399.5, 2933.3, 1613.9, 1510.1, 1497.2, 1455.87, 1299.2, 1268.7, 1243.2, 1228.9, 1157.8, 1148.8, 1100.5, 1056.5, 1005.7, 986.7, 893.1, 876.5, 861.5, 817.9 cm^{-1}. ^{1}H NMR (300 MHz, DMSO-d$_6$): $\delta = 7.75$ (dd, J = 8.8, 2.4, 1H), 7.63 (d, J = 2.4, 1H), 6.68 (d, J = 8.8, 1H), 6.26 (s, 2H), 4.73 − 4.49 (m, 2H), 4.49 - 4.30 (m, 2H) ppm.

2.2.15. 4'-[N-(2-Hydroxyethyl)-N-methyl]amino-2-[2-(pentafluorophenoxy)ethoxy]-4-nitroazobenzene (12)

Compound **12** was synthesized from nitroaniline **11** and compound **9** using the same method as for synthesis of the azochromophore **1**. Crude product was recrystallized from EtOAc. Yield 0.57 g (54%) of violet crystalline solid, mp 150–155°C. $C_{23}H_{19}F_5N_4O_5$: calcd. C 52.48; H 3.64; N 10.64; found: C 52.45; H 3.79; N 10.47. MS ESI+: m/z 527.1 [M+H]$^+$. ^{1}H NMR (200 MHz, CDCl$_3$): $\delta = 7.86$ (m, 2H), 7.72 (d,

$J = 9.0$, 2H), 7.63 (m, 1H), 6.73 (d, $J = 9.0$, 2H), 4.54 (m, 4H), 3.84 (q, $J = 5.4$, 2H), 3.60 (t, $J = 5.4$, 2H), 3.11 (s, 3H), 1.55 (t, $J = 5.4$, 1H) ppm.

2.2.16. 4′-[N-(2-{3,5-Bis[2-(tetrahydro-2H-pyran-2-yloxy)ethoxy]benzoyloxy}ethyl)-N-methylamino]-2-[2-(pentafluorophenoxy)ethoxy]-4-nitroazobenzene (**3a**)

DCC method was used. The crude product was purified by silica gel chromatography, eluted with MTBE/heptanes (gradient 50–75%). Yield 0.51 g (73%) of brown crystalline solid, *mp* 111.9°C. $C_{44}H_{47}F_5N_4O_{12}$: calcd. C 57.51; H 5.16; N 6.10; found: C 57.64; H 5.21; N 6.02. MS ESI+: *m/z* 919.3 $[M+H]^+$. ^{1}H NMR (300 MHz, DMSO-d_6): $\delta = 7.99$ (d, $J = 2.3$ Hz, 1H), 7.92 (dd, $J = 8.7$, 2.3 Hz, 1H), 7.71 (d, $J = 9.2$ Hz, 2H), 7.64 (d, $J = 8.7$ Hz, 1H), 6.99 (d, $J = 2.3$ Hz, 2H), 6.95 (d, $J = 9.4$ Hz, 2H), 6.75 (t, $J = 2.3$ Hz, 1H), 4.59–4.68 (m, 4H), 4.55–4.59 (m, 2H), 4.49 (t, $J = 5.0$ Hz, 2H), 4.06 (t, $J = 4.5$ Hz, 4H), 3.94 (t, $J = 4.8$ Hz, 2H), 3.84 (dt, $J = 11.7$, 4.2 Hz, 2H), 3.59–3.76 (m, 4H), 3.15 (s, 3H), 1.49–1.72 (m, 4H), 1.34–1.49 (m, 8H) ppm. ^{13}C NMR (75 MHz, DMSO-d_6): $\delta = 165.41$, 159.67, 154.33, 152.60, 147.75, 146.20, 143.66, 141.41 (d, $J = 236$ Hz), 137.31 (d, $J = 250$ Hz), 136.84 (d, $J = 233$ Hz), 133.53, 131.38, 125.60, 117.05, 116.76, 111.66, 109.32, 109.24, 107.54, 106.51, 98.11, 73.82, 69.31, 67.60, 65.12, 62.51, 61.29, 49.87, 38.37, 30.12, 24.97, 19.02 ppm.

2.2.17. 4′-[N-(2-{3,5-Bis[2-(trityloxy)ethoxy]benzoyloxy}ethyl)-N-methylamino]-2-[2-(pentafluorophenoxy)ethoxy]-4-nitroazobenzene (**3b**)

DCC method was used. The crude product was purified by silica gel chromatography, eluted with EtOAc/CH$_2$Cl$_2$ (gradient 0–20%). Necessary fractions were evaporated and product was precipitated from EtOAc/EtOH. Yield 0.25 g (78%) of red crystalline solid, *mp* 137.5°C. $C_{72}H_{59}F_5N_4O_{10}$: calcd. C 70.01; H 4.81; N 4.54; found: C 70.12; H 4.76; N 4.37. ^{1}H NMR (300 MHz, DMSO-d_6): $\delta = 7.96$ (d, $J = 2.3$ Hz, 1H), 7.84 (dd, $J = 8.9$, 2.3 Hz, 1H), 7.67 (d, $J = 9.0$ Hz, 2H), 7.49 (d, $J = 8.7$ Hz, 1H), 7.18–7.41 (m, 30H), 7.07 (d, $J = 2.3$ Hz, 2H), 6.93 (d, $J = 9.0$ Hz, 2H), 6.82 (t, $J = 2.0$ Hz, 1H), 4.55–4.63 (m, 4H), 4.47 - 4.55 (m, 2H), 4.11–4.18 (m, 4H), 3.91–3.98 (m, 2H), 3.19–3.26 (m, 4H), 3.14 (s, 3H) ppm. ^{13}C NMR (75 MHz, DMSO-d_6): $\delta = 165.40$, 159.72, 154.23, 152.47, 147.66, 146.12, 143.65, 143.59, 141.47 (d, $J = 240$ Hz), 137.28 (d, $J = 245$ Hz), 136.66 (d, $J = 250$ Hz), 133.46 (t, $J = 13.1$ Hz), 131.42, 128.22, 127.83, 127.00, 125.54, 116.92, 116.66, 111.64, 109.24, 107.69, 106.80, 86.08, 73.75, 69.21, 67.43, 62.52, 62.34, 49.96, 38.48 ppm.

2.2.18. 4′-[N-(2-{3,5-Bis[2-(hydroxy)ethoxy]benzoyloxy}ethyl)-N-methylamino]-2-[2-(pentafluorophenoxy)ethoxy]-4-nitroazobenzene (**3c**)

Compound **3c** was synthesized from compound **3a** using the same method as for synthesis of the azochromophore **2c**. Crude product was recrystallized from acetone/hexanes. Yield 90 mg (85%) of violet crystalline solid, *mp* 193.1°C. $C_{34}H_{31}F_5N_4O_{10}$: calcd. C 54.40; H 4.16; N 7.46; found: C 54.29; H 4.02; N 7.14. MS ESI+: *m/z* 751.3 $[M+H]^+$. ^{1}H NMR (300 MHz, DMSO-d_6): $\delta = 7.99$ (d, $J = 2.6$ Hz, 1H), 7.92 (dd, $J = 8.9$, 2.3 Hz, 1H), 7.70 (d, $J = 8.9$ Hz, 2H), 7.63 (d, $J = 8.7$ Hz, 1H), 7.00 (d, $J = 2.3$ Hz, 2H), 6.95 (d, $J = 9.2$ Hz, 2H), 6.72 (t, $J = 2.2$ Hz, 1H), 4.84 (t, $J = 5.4$ Hz, 2H), 4.60–4.67 (m, 4H), 4.49 (t, $J = 5.0$ Hz, 2H), 3.90–3.98 (m, 6H), 3.65 (q, $J = 5.1$ Hz, 4H), 3.16 (s, 3H) ppm. ^{13}C NMR (75 MHz, DMSO-d_6): $\delta = 165.46$, 159.86, 154.30, 152.45, 147.73, 146.25, 146.16, 143.66, 141.49 (d, $J = 245$ Hz), 137.33 (d, $J = 248$ Hz), 136.73 (d, $J = 248$ Hz), 133.51, 131.35, 125.63, 117.06, 116.79, 111.63, 109.33, 109.22, 107.34, 107.29, 106.41, 73.82, 69.93, 69.29, 62.51, 59.43, 49.94, 38.63 ppm.

2.2.19. 4'-[N-(2-Carboxyethyl)-N-methyl]amino-2-(2-hydroxyethoxy)-4-nitroazobenzene (14)

Compound **14** was synthesized from nitroaniline **8** and compound **13** using the same method as for synthesis of the azochromophore **1**. Crude product was recrystallized from EtOH. Yield 0.48 g (62%) of violet crystalline solid, *mp* 182–185°C. $C_{18}H_{20}N_4O_6 \cdot H_2O$: calcd. C 53.20; H 5.46; N 13.79; found: C 53.73; H 5.34; N 13.54. IR: $\nu = 3469.6$, 2923.7, 1709.5, 1596.0, 1519.2, 1427.2, 1360.0, 1332.9, 1305.4, 1293.9, 1261.4, 1238.9, 1142.2, 1086.8, 953.7 cm^{-1}. MS ESI+: *m/z* 389.1 [M+H]$^+$. ^{1}H NMR (400 MHz, DMSO-d_6): $\delta = 12.30$ (br. s, 1H), 7.94 (d, $J = 2.3$, 1H), 7.84 (dd, $J = 8.8$, 2.3, 1H), 7.76 (d, $J = 9.2$, 2H), 7.56 (d, $J = 8.8$, 1H), 6.83 (d, $J = 9.2$, 2H), 4.90 (t, $J = 5.6$, 1H), 4.25 (t, $J = 4.9$, 2H), 3.76 (m, 2H), 3.68 (t, $J = 7.1$, 2H), 3.01 (s, 3H), 2.50 (t, $J = 7.1$, 2H) ppm.

2.2.20. 4'-(N-[2-(2,3,4,5,6-Pentafluorobenzyloxycarbonyl)ethyl]-N-methyl)amino-2-(2-hydroxyethoxy)-4-nitroazobenzene (15)

Azochromophore **14** (0.70 g, 1.3 mmol) and DBU (0.37 mL, 2.5 mmol) were dissolved in abs. dioxane (10 mL), then 2,3,4,5,6-pentafluorobenzylbromide (0.33 mL, 2.2 mmol) in abs. dioxane (2 mL) was added dropwise. Reaction mixture was stirred at room temperature for 24 hours. Precipitate was filtered off, EtOAc (15 mL) was added to the filtrate and it was washed with satd. NaHCO$_3$ (3 × 5 mL). Organic solution was dried over Na$_2$SO$_4$, evaporated and recrystallized from EtOH to give deep red crystals. Yield 1.00 g (98%), *mp* 112–114°C. MS ESI+: *m/z* 569.1 [M+H]$^+$. ^{1}H NMR (400 MHz, CDCl$_3$): $\delta = 7.91$-7.84 (m, 2H), 7.78 (d, $J = 9.3$, 2H), 7.65 (d, $J = 8.5$, 1H), 6.68 (d, $J = 9.3$, 2H), 5.15 (s, 2H), 4.31 (t, $J = 4.4$, 2H), 3.93 (t, $J = 4.4$, 2H), 3.74 (t, $J = 7.0$, 2H), 3.03 (s, 3H), 2.61 (t, $J = 7.0$, 2H), 1.53 (s, 1H) ppm.

2.2.21. 2-(2-{3,5-Bis[2-(tetrahydro-2H-pyran-2-yloxy)ethoxy]benzoyloxy}ethoxy)-4-nitro-4'-{N-methyl-N-[2-(2,3,4,5,6-pentafluorobenzyloxycarbonyl)ethyl]amino}azobenzene (4a)

DCC method was used. The crude product was purified by silica gel chromatography, eluted with EtOAc/hexane (gradient 5–25%). Yield 0.90 g (76%) of deep red very viscous oil. MS ESI+: *m/z* 961.4 [M+H]$^+$. ^{1}H NMR (300 MHz, DMSO-d$_6$): $\delta = 8.06$ (d, $J = 2.4$ Hz, 1H), 7.92 (dd, $J = 8.9$, 2.4 Hz, 1H), 7.68 (d, $J = 9.0$ Hz, 2H), 7.62 (d, $J = 8.9$ Hz, 1H), 7.03 (d, $J = 2.3$ Hz, 2H), 6.78 (t, $J = 2.3$ Hz, 1H), 6.78 (d, $J = 9.2$ Hz, 2H), 5.18 (s, 2H), 4.62–4.75 (m, 4H), 4.54–4.62 (m, 4H), 4.07 (t, $J = 4.5$ Hz, 4H), 3.84 (dt, $J = 11.5$, 4.1 Hz, 2H), 3.57–3.78 (m, 6H), 3.38–3.45 (m, 2H), 2.99 (s, 3H), 2.67 (t, $J = 6.8$ Hz, 2H), 1.49–1.74 (m, 4H), 1.31–1.49 (m, 6H) ppm. ^{13}C NMR (75 MHz, DMSO-d$_6$): $\delta = 170.89$, 165.23, 159.66, 154.62, 151.79, 147.69, 146.56, 145.03 (d, $J = 250$ Hz), 143.67, 140.89 (d, $J = 250$ Hz), 136.86 (d, $J = 248$ Hz), 131.44, 125.61, 117.00, 116.91, 111.44, 110.41, 109.71 (td, $J = 17.4$, 3.1 Hz), 107.67, 106.15, 98.04, 68.10, 67.55, 65.10, 63.23, 61.22, 53.08, 47.31, 37.83, 31.31, 30.09, 24.96, 18.97 ppm.

2.2.22. 2-(2-{3,5-Bis[2-(trityloxy)ethoxy]benzoyloxy}ethoxy)-4-nitro-4'-N-methyl-N-[2-(2,3,4,5,6-pentafluorobenzyloxycarbonyl)ethyl]amino}azobenzene (4b)

DCC method was used. The crude product was purified by silica gel chromatography, eluted with EtOAc/CH$_2$Cl$_2$ (gradient 0–10%). Necessary fractions were evaporated and product was precipitated from EtOAc/EtOH. Yield 0.38 g (71%) of red glass. $C_{74}H_{61}F_5N_4O_{11}$: calcd. C 69.58; H 4.81; N 4.39; found: C 69.22; H 4.61; N 4.03. ^{1}H NMR (300 MHz, DMSO-d$_6$): $\delta = 8.05$ (d, $J = 2.6$ Hz, 1H), 7.88 (dd, $J = 8.8$, 2.4 Hz, 1H), 7.58–7.71 (m, 3H), 7.17–7.41 (m, 30H), 7.10 (d, $J = 2.3$ Hz, 2H), 6.82–6.87 (m, 1H), 6.67 (d, $J = 9.0$ Hz, 2H), 5.14 (s, 2H), 4.64–4.76 (m, 4H), 4.11–4.19 (m, 4H), 3.60–3.69 (m, 2H), 3.19–3.26 (m, 4H), 2.89 (s, 3H), 2.55–2.62 (m, 2H) ppm. ^{13}C NMR (75 MHz, DMSO-d$_6$): $\delta = 170.74$, 165.23, 159.68, 154.59, 151.68, 147.65, 146.56, 145.03 (d, $J = 259$ Hz), 143.67, 143.55, 140.83 (d, $J = 250$ Hz), 136.78 (d, $J = 246$, 13 Hz), 131.50, 128.19, 127.77, 126.93, 125.56, 116.95, 116.83, 111.37, 110.41,

109.63 (td, $J = 18.0$, 3.4 Hz), 107.87, 106.38, 86.05, 68.13, 67.40, 63.21, 62.33, 53.01, 47.21, 37.70, 31.26 ppm.

2.2.23. 2-{2-[3,5-Bis(2-hydroxyethoxy)benzoyloxy]ethoxy}-4-nitro-4'-{N-methyl-N-[2-(2,3,4,5,6-pentafluorobenzyloxycarbonyl)ethyl]amino}azobenzene (4c)

Compound **4c** was synthesized from compound **4a** using the same method as for synthesis of the azochromophore **2c**. Crude product was purified by silica gel chromatography, eluted with CH_2Cl_2, then EtOAc/hexanes 2/1. Necessary fractions were recrystallized from MeOH. Yield 0.16 g (91%) of violet crystalline solid, *mp* 100.3°C. $C_{36}H_{33}F_5N_4O_{11}$: calcd. C 54.55; H 4.20; N 7.07; found: C 54.07; H 3.91; N 6.66. MS ESI+: *m/z* 793.3 [M+H]$^+$. ^{1}H NMR (300 MHz, DMSO-d_6): $\delta = 8.06$ (d, $J = 1.3$ Hz, 1H), 7.93 (dd, $J = 9.0$, 2.1 Hz, 1H), 7.60–7.72 (m, 3H), 7.02 (d, $J = 1.7$ Hz, 2H), 6.69–6.77 (m, 3H), 5.19 (s, 2H), 4.84 (t, $J = 5.5$ Hz, 2H), 4.63–4.73 (m, 4H), 3.93 (t, $J = 4.6$ Hz, 4H), 3.74 (t, $J = 6.6$ Hz, 2H), 3.61–3.69 (m, 4H), 2.99 (s, 3H), 2.67 (t, $J = 6.6$ Hz, 2H) ppm. ^{13}C NMR (75 MHz, DMSO-d_6): $\delta = 170.96$, 165.32, 159.87, 154.58, 151.86, 147.72, 146.61, 145.07 (d, $J = 247$ Hz), 143.68, 140.92 (d, $J = 251$ Hz), 136.87 (dt, $J = 250$, 16.9 Hz), 131.45, 125.65, 117.10, 116.99, 111.50, 110.41, 109.73 (td, $J = 18.3$, 3.4 Hz), 107.51, 106.09, 69.91, 68.11, 63.24, 59.45, 53.12, 47.35, 37.86, 31.39 ppm.

3. Results and discussion

3.1. Synthesis of azochromophores

We have studied 2 pathways of synthesis of the chromophore core **1** from aminophenol **5** to get an optimal overall yield (Scheme 1) of this compound – the main precursor of all new chromophores **2–4**. Since it was known that aminophenol **5** forms azo compounds in diazotation and azo coupling reactions with hydroxycompounds in good yields [43–47] and reactions with 30 various dialkylanilines are also

Scheme 1. Synthesis of azochromophores **1**, **2a-c** and **3a-c**. Ms – methanesulfonyl, DCC - *N,N'*-dicyclohexylcarbodiimide, DMAP - 4-(dimethylamino)pyridine, PPTS – pyridinium *p*-toluenesulfonate.

Scheme 2. Synthesis of azochromophores **4a-c**. DBU - 1,8-diazabicyclo[5.4.0]undec-7-ene.

patented [48], one of the investigated pathways was done by the use of betaine **6**. Thus diazonium betaine **6** was isolated in good yield from aminophenol **5**. Betaine **6** is orange crystalline solid, which is stable in boiling EtOAc for short periods of time, but is light sensitive and therefore must be used soon after the obtaining. Azo coupling reaction between betaine **6** and *N*-methylaniline gave very low yield of azo compound **7** although several different reaction conditions were employed varying solvent and pH. Monoalkylated intermediate was partially formed at the beginning of the alkylation reaction of azo compound **7** with 2-chloroethanol as it could be seen from the HPLC-MS data of the reaction mixture, but after prolonged heating decomposition occurred and compound **1** could not be detected.

The other pathway was successful; sodium salt from compound **5** was treated with 2-bromoethanol and compound **8** was obtained in moderate yield. Azochromophore **1** was obtained in azo coupling reaction from compound **8** and aniline **9** in good yield.

3,5-Bis(2-hydroxyethoxy)benzoic acid was chosen as a dendronizing fragment with two different end groups: tetrahydro-2*H*-pyran-2-yl (THP) and trityl (Trt). THP is a well-known end group, and the synthesis of acid **10a** has been described in an earlier paper [40]. Trt end groups were used because of their promising positive effect on glass transition temperature and amorphous film formation [49, 50]. The synthesis of acid **10b** was accomplished at first in a similar manner than that of acid **10a**: alkylation of methyl 3,5-dihydroxybenzoate with 2-(trityloxy)ethyl chloride gave corresponding ester in 27% yield. Alkylation with 2-(trityloxy)ethyl chloride was little effective presumably due to trityl group induced steric hindrance of CH$_2$Cl moiety. Therefore another synthesis pathway was used to improve the yield of this ester: alkylation of known methyl 3,5-bis(2-hydroxyethoxy)benzoate [40, 51] with trityl chloride ensured by 1,8-diazabicyclo[5.4.0]undec-7-ene (DBU) gave the ester in 69% yield. Subsequent hydrolysis of the ester gave acid **10b** in 93% yield.

Symmetrically dendronized chromophores **2a-c** were synthesized from compound **1** (Scheme 1). The coupling between chromophore unit and dendronizing fragment was ensured with *N,N'*-dicyclohexylcarbodiimide (DCC) and 4-(dimethylamino)pyridine (DMAP) - DCC method [52]. The reactions of compound **1** with either acid **10a** or acid **10b** gave azochromophores **2a** and **2b** respectively in good yields. Azochromophore **2c** was obtained from chromophore **2a** removing THP groups with pyridinium *p*-toluenesulfonate (PPTS) in ethanol.

The compounds with fluoroaromatic fragment in the acceptor part of azochromophore **3a-c** were synthesized as shown in scheme 1. Diazotation of compound **11** and subsequent azo coupling reaction with aniline **9** afforded compound **12**. The attachment of the dendritic acids to compound **12** and THP removal were very similar to previously described, and we obtained azochromophores **3a-c** as crystalline solids in good yields.

Compounds with fluoroaromatic fragment in the donor part of azochromophore **4a-c** were synthesized as shown in scheme 2. Aniline **8** was diazotized and coupled with compound **13** to prepare derivative

14 possessing both acid and hydroxyl groups in the molecule needed to form two novel ester bonds with dendronizing fragments. At first we used DBU method [53] to form ester at the acid end of the compound **14** with 2,3,4,5,6-pentafluorobenzylbromide and obtained compound **15** in excellent yield without the need of protection of hydroxyl group. Compounds **4a** and **4b** were synthesized in good yields from compound **15** and acids **10a** and **10b** by using DCC method. But compound **4c** was obtained from compound **4a** in ethanol removing THP groups with PPTS.

3.2. Thermal properties and UV-vis spectra of synthesized azochromophores *1-4*

We investigated two very important properties of the synthesized azochromophores - thermal behavior and light absorption (Table 1); these characteristics are significant for the creation of useful devices. When various structurally different fragments are incorporated in one molecule, glass transition temperature (T_g) of such compound is dependant on the properties of all the various fragments included, and so called copolymer effect is observed [54, 55]. Influences of some fragments on T_g were elucidated analyzing T_g of the synthesized compounds **1-4**.

None of the THP group containing chromophores **2a, 3a, 4a** has glass transition in the range of used apparatus: compounds **2a** and **4a** are soft; therefore their T_g is certainly below the room temperature, although compound **3a** is crystalline. The experimentally obtained results show that the THP group strengthens the tendency to form amorphous phase thanks to its chirality and both four THP end groups in compound **2a**, and even two THP end groups in compound **4a** are sufficient to make the chromophore soft. Contrary to that the flat pentafluorophenyl group facilitates crystallization and only one group in the appropriate position of molecule **3a** causes it, leading to melting point (*mp*) at 111.9°C. It is also evident that the molecular design plays a crucial role and linking only the pentafluorophenyl group in the acceptor part allows us to see its influence in full capacity. In general it becomes clear that the state of aggregation of particular chromophore material can be varied together with its characteristics using two different substituents, one from which facilitate formation of amorphous but the other - the crystalline state.

Trt groups containing substances **2b, 3b, 4b** have higher T_g than their analogues without Trt groups. Chromophore **2b** has the highest value of T_g (78.4°C) from all synthesized compounds due to the double

Table 1
Physical properties of compounds **1–4**

Compound	T_g,°C	*mp*,°C	T_d,°C	Light absorption in $CHCl_3$			Light absorption in EtOBz		
				λ_{max}, nm	ν_{max}, cm^{-1}	ε, M^{-1}·cm^{-1}	λ_{max}, nm	ν_{max}, cm^{-1}	ε, M^{-1}·cm^{-1}
1	37.4	145.9	263.7	488.7	20462	35200	498.7	20052	24500
2a	–	–	268.6	478.2	20912	29600	483.5	20683	26100
2b	78.4	–	284.7	478.2	20912	25400	482.7	20717	27300
2c	59.6	149.7	267.5	479.1	20872	26400	484.9	20623	–
3a	–	111.9	239.2	481.1	20786	27700	483.3	20691	25500
3b	65.8	137.5	247.3	478.7	20890	31900	483.1	20700	29400
3c	44.8	193.1	241.6	480.3	20820	30500	483.1	20700	25100
4a	–	–	264.0	476.1	21004	25600	478.4	20903	29500
4b	54.6	–	281.9	474.4	21079	29700	480.9	20794	26600
4c	40.8	100.3	265.3	474.5	21075	30200	480.9	20794	28800

amount of Trt groups. The mass of the Trt group nearly three times exceed the mass of THP group, therefore the Van der Waals force must increase remarkably. It is very important, that the combination of Trt and pentafluorophenyl substituents in chromophore **3b** allows increasing the T_g till 65.8°C. Melting points are not observed for compounds **2b** and **4b** where bulky Trt groups are possibly responsible for difficult packing in crystalline structures. But the same as with compound **3a**, also compound **3b** is crystalline due to the pentafluorophenyl group.

Compounds **1, 2c, 3c, 4c** with OH groups possess higher T_g than compounds **2a, 3a** and **4a**, but lower than compounds **2b, 3b** and **4b**. Compound **2c** has higher value of T_g than compounds **3c** and **4c**, because it has double amount of OH groups. All compounds containing OH group - **1, 2c, 3c, 4c** have *mp* due to hydrogen bonding. Combined influence of pentafluorophenyl ether and OH group determine the highest *mp* for compound **3c** (193.1°C). There is no correlation between T_g and *mp*, which points to remarkable variations of the spatial structure at higher temperatures. The intermolecular forces increase in the case of compound **3c** but decrease in the case of compound **4c**, when temperature rises.

Probably the position of the planar electron-deficient pentafluorophenyl moiety influences on the dipole-dipole interaction between neighboring molecules. In the case of compounds **4a-c** the pentafluorophenyl moiety is connected with the donor part of the chromophore and can lower the dipole moment by formation of a weak π-π complex with the donor part of the chromophore. In the case of compounds **3a-c** the pentafluorophenyl moiety is connected with the acceptor part of the chromophore and can increase intermolecular interaction by complexion with the donor part of neighboring molecule. Increased intermolecular interactions determine higher T_g and *mp* for compounds **3a-c** compared with compounds **4a-c**.

Azochromophore **1** shows interesting behavior (Fig. 2) upon repeated heating, it has two endothermic peaks at 145.9 and 155.3°C in the first heating, with enthalpies (ΔH) 34.6 and 41.6 J/g. Second heating reveals T_g at 37.4°C and cold crystallization at 80.9°C, and only one melting peak at 145.0°C with $\Delta H = 75.9$ J/g, which is equal to sum of those two peaks from the first scan. Two peaks at *mp* also has compound **2c** (149.7 and 156.0°C) and compound **3a** (100.6 and 111.9°C), but in less clarity (Fig. 2). The appearance of those two peaks could be explained with the existence of two polymorphic modifications, liquid crystalline state or crystals of *cis* and *trans* isomers, but further research is needed to resolve this question.
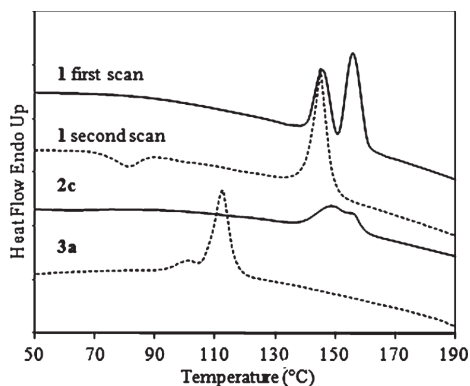

Fig. 2. Melting peaks of compounds **1**, **2c**, and **3a**.

Equally with compound **1** chromophore **3c** shows cold crystallization on the second scan at 102.2°C and subsequent melting. This tendency of ordering for OH groups containing compounds **1** and **3c** could be explained with hydrogen bonding and could lead to crystallization of amorphous materials over prolonged periods of time.

Thermal stabilities were evaluated using destruction temperature (T_d) where thermo gravimetric data slope shows 5% weight loss. All the synthesized compounds are stable at least up to 239°C, the highest T_d (284.7°C) has compound **2b**. Trt ether functionality increases thermal stability of the molecule, as could be seen - Trt groups containing substances **2b**, **3b** and **4b** have higher thermal stabilities than their analogues without Trt groups. THP and OH groups have about the same amount of influence on thermal stabilities. Compounds **4a-c** have higher thermal stability than compounds **3a-c**, which could be explained with higher thermal stability of ester bond which links the pentafluorophenyl moiety with the rest of the molecule compared to ether bond.

UV-Vis spectra were obtained for azochromophores **1–4** in CHCl$_3$ and EtOBz solutions (Table 1). EtOBz can interact with solute molecules via π-π interactions possibly excluding intramolecular π-π stacking of azobenzene chromophore moiety with dendronizing or pentafluorophenyl fragments of the molecule. Absorption maximum (λ_{max}) of azochromophore **1** is batochromic shifted in both solutions compared to other synthesized chromophores; likely it is because of different solvatochromic effects or intramolecular hydrogen bond.

Absorption maxima in both solutions does not differ more than 2.4 nm (104 cm^{-1}) inside each of the chromophore series, e. g., **2a-c, 3a-c** or **4a-c**. This means that the end groups of dendronizing fragment do not notably affect absorption energy of a chromophore regardless of the used solvent. Absorption intensity varies from chromophore to chromophore inside each of the chromophore series, although molar extinction coefficients (ε) are in the same order which is consistent with the use of the same azochromophore.

Position of pentafluorophenyl fragment has very weak effect on charge transfer energy and absorption intensity. We compared chromophores **3a-c** with their corresponding chromophores **4a-c**; hypsochromic shift (189–254 cm^{-1}) and hypochromic effect (300–2200 M^{-1}cm^{-1}) are observed in CHCl$_3$ solutions by changing connection of the pentafluorophenyl moiety from the acceptor part of the chromophore (compounds **3a-c**) to the donor part of the chromophore (compounds **4a-c**). EtOBz solutions show lesser hypsochromic shift (94–155 cm^{-1}) and no coherence in absorption intensity. Hypsochromic shift could arise from changes in electron density in donor or acceptor parts of the chromophore via electronic effects over chemical bonds or spatial interactions. Most likely the pentafluorophenyl moiety has intramolecular π-π interaction in CHCl$_3$ solutions with donor part of the azobenzene chromophores **4a-c** and lowers their donor strength. The pentafluorophenyl moiety can interact with solvent molecules in EtOBz solutions and does not affect absorption characteristics of the chromophores.

NLO properties of compound **2b** have been reported in two international conferences [56, 57].

4. Conclusions

Azochromophores of "push-pull" type substituted with dendronizing phenyl moieties and perfluorophenyl fragments alternating their position in the donor and the acceptor part of the chromophore have been synthesized and their structures approved. Structural fragments have following effects on thermal properties of synthesized compounds: trityl groups elevate glass transition temperature and thermal stability, tetrahydropyranyl groups decrease glass transition temperature, hydroxyl group and

pentafluorophenyl group in the acceptor part induce crystallinity, 2,3,4,5,6-pentafluorobenzyl ester function increases thermal stability. Further research should be focused on 2,3,4,5,6-pentafluorobenzyl ether formation, which could possess different thermal properties than 2,3,4,5,6-pentafluorobenzyl ester or pentafluorophenylether. We observed some property changes which could be explained with self-assembly resulting from arene-perfluoroarene π-π interactions. Intermolecular stacking elevated glass transition temperature and melting point of molecules where pentafluorophenyl group is connected to the acceptor part of the chromophore, but intramolecular stacking affected light absorption in the solution of molecules where pentafluorophenyl group is connected to the donor part of the chromophore.

Acknowledgments

References

[1]   M. Blanchard-Desce, V. Alain, P.V. Bedworth, S.R. Marder, A. Fort, C. Runser, M. Barzoukas, S. Lebus and R. Wortmann, Large quadratic hyperpolarizabilities with donor - acceptor polyenes exhibiting optimum bond length alternation: Correlation between structure and hyperpolarizability, *Chem Eur J* **3** (1997), 1091–1104.

[2]   F. Rizzo, M. Cavazzini, S. Righetto, F. De Angelis, S. Fantacci and S. Quici, A joint experimental and theoretical investigation on Nonlinear Optical (NLO) properties of a new class of push–pull spirobifluorene compounds, *Eur J Org Chem* (2010), 4004–4016.

[3]   Y. Yu, C. Cui, Y. Wu, Z. Yang, M. Wang, B. O'Keeffe and G. Chen, Qian, second-order nonlinear optical activity induced by ordered dipolar chromophores confined in the pores of an anionic metal–organic framework, *Angew Chem* **124** (2012), 1–5.

[4]   F. Bureš, H. Čermáková, J. Kulhánek, M. Ludwig, W. Kuznik, I.V. Kityk, T. Mikysek and A. Růžička, Structure-property relationships and nonlinear optical effects in donor-substituted dicyanopyrazine-derived push–pull chromophores with enlarged and varied π-linkers, *Eur J Org Chem* (2012), 529–538.

[5]   P.J.A. Kenis, E.G. Kerver, B.H.M. Snellink-Ruël, G.J. van Hummel, S. Harkema, M.C. Flipse, R.H. Woudenberg, J.F.J. Engbersen and D.N. Reinhoudt, High hyperpolarizabilities of donor-π-acceptor-functionalized calix[4]arene derivatives by pre-organization of chromophores, *Eur J Org Chem* (1998), 1089–1098.

[6]   M. Rutkis, A. Tokmakovs, E. Jecs, J. Kreicberga, V. Kampars and V. Kokars, Indanedione based binary chromophore supramolecular systems as a NLO active polymer composites, *Opt Mater* **32** (2010), 783–844.

[7]   J. Yu, Y. Cui, C. Wu, Y. Yang, Z. Wang, M. O'Keeffe, B. Chen and G. Qian, Second-order nonlinear optical activity induced by ordered dipolar chromophores confined in the pores of an anionic metal-organic framework, *Angew Chem* **124** (2012), 10694–10697.

[8]   Y. Liu, H. Pei, L. Zhang, J. Shi and S. Cao, Advances in organic all-optical photorefractive materials, *Macromol Symp* **317-318** (2012), 227–239.

[9]   J. Luo, H. Ma, M. Haller, A.K.-Y. Jen and R.R. Barto, Large electro-optic activity and low optical loss derived from a highly fluorinated dendritic nonlinear optical chromophore, *Chem Commun* **8** (2002), 888–889.

[10] S.H. Jang and A.K. Jen, Electro-optic (E-O) molecular glasses, *Chem Asian J* **4** (2009), 20–31.

[11] A. Herrmann, T. Weil, V. Sinigersky, U-M Wiesler, T. Vosch, J. Hofkens, F.C. De Schryver and K. Müllen, Polyphenylene dendrimers with perylene diimide as a luminescent core, *Chem Eur J* **7** (2001), 4844–4853.

[12] O.Y.-H. Tai, C.H. Wang, H. Ma and A.K.-Y. Jen, Wavelenght dependence of first molecular hyperpolarizability of a dendrimer in a solution, *J Chem Phys* **121** (2004), 6086–6092.

[13] O.D. Fominykh and M.Yu. Balakina, Modeling of structure and nonlinear optical activity of epoxy-based oligomers with dendritic multichromophore fragments, *Macromol Symp* **316** (2012), 52–62.

[14]   W. Wu, G. Xu, C. Li, G. Yu, Y. Liu, C. Ye, J. Qin and Z. Li, From nitro- to sulfonyl-based chromophores: Improvement of the comprehensive performance of nonlinear optical dendrimers, *Chem Eur J* **19** (2013), 6874–6888.

[15]   R. Bauer, D. Liu, A. ver Heyen, F. de Schryver, S. de Feyter and K. Müllen, Polyphenylene dendrimers with pentafluorophenyl units: Synthesis and self-assembly, *Macromolecules* **40** (2007), 4753–4761.

[16]   W. Wu, Y. Fu, C. Wang, C. Ye, J. Qin and Z. Li, A series of hyperbranched polytriazoles containing perfluoroaromatic rings from AB$_2$-type monomers: Convenient syntheses by click chemistry under copper(I) catalysis and enhanced optical nonlinearity, *Chem Asian J* **6** (2011), 2787–2795.

[17]   H. Ma and A.K.-Y. Jen, Functional dendrimers for nonlinear optics, *Adv Mater* **13** (2001), 1201–1205.

[18]   T.-D. Kim, J.-W. Kang, J. Luo, S.-H. Jang, J.-W. Ka, N. Tucker, J.B. Benedict, L.R. Dalton, T. Gray, R.M. Overney, D.H. Park, W.N. Herman and A.K.-Y. Jen, Ultralarge and thermally stable electro-optic activities from supramolecular self-assembled molecular glasses, *J Am Chem Soc* **129** (2007), 488–489.

[19]   W. Wu, Z. Zhu, G. Qiu, C. Ye, J. Qin and Z. Li, New hyperbranched second-order nonlinear optical poly(arylene-ethynylene)s containing pentafluoroaromatic rings as isolation group: Facile synthesis and enhanced optical nonlinearity through Ar-Ar^F self-assembly effect, *J Polym Sci Part A: Polym Chem* **50** (2012), 5124–5133.

[20]   W. Wu, G. Yu, Y. Liu, C. Ye, J. Qin and Z. Li, Using two simple methods of Ar-Ar^F self-assembly and isolation chromophores to further improve the comprehensive performance of NLO dendrimers, *Chem Eur J* **19** (2013), 630–641.

[21]   F. Ponzini, R. Zagha, K. Hardcastle and J.S. Siegel, Phenyl/pentafluorophenyl interactions and the generation of ordered mixed crysals: Sym-triphenethynylbenzene and sym-Tris(perfluorophenethynyl)benzene, *Angew Chem Int Ed* **39** (2000), 2323–2325.

[22]   T.-D. Kim, J. Luo and A.K.-Y. Jen, Quantitative determination of the chromophore alignment induced by electrode contact poling in self-assembled NLO materials, *Bull Korean Chem Soc* **30** (2009), 882–886.

[23]   K.G. Yager and C.J. Barrett, Novel photo-switching using azobenzene functional materials, *J Photochem Photobiol, A* **182** (2006), 250–261.

[24]   F.-K. Bruder, R. Hagen, T. Rölle, M.-St Weiser and T. Fäcke, From the surface to volume: Concepts for the next generation of optical–holographic data-storage materials, *Angew Chem Int Ed* **50** (2011), 4552–4573.

[25]   C. Park, J. Lim, M. Yun and C. Kim, Photoinduced release of guest molecules by supramolecular transformation of self-assembled aggregates derived from dendron, *Angew Chem Int Ed* **47** (2008), 2959–2963.

[26]   D.M. Junge and D.V. McGrath, Photoresponsive dendrimers, *Chem Commun* (1997), 857–858.

[27]   S. Ghosh and A.K. Banthia, Synthesis of photoresponsive polyamidoamine (PAMAM) dendritic architecture, *Tetrahedron Lett* **42** (2001), 501–503.

[28]   D. Grebel-Koehler, D. Liu, S. De Feyter, V. Enkelmann, T. Weil, C. Engels, C. Samyn, K. Müllen and F.C. De Schryver, Synthesis and photomodulation of rigid polyphenylene dendrimers with an azobenzene core, *Macromolecules* **36** (2003), 578–590.

[29]   L.X. Liao, F. Stelacci and D.V. McGrath, Photoswitchable flexible and shape-persistent dendrimers: Comparision of the interplay between a photochromic azobenzene core and dendrimer structure, *J Am Chem Soc* **126** (2004), 2181–2185.

[30]   S. Ghosh, A.K. Banthia and Z. Chen, Synthesis of photoresponsive study of azobenzene centered polyamidoamine dendrimers, *Tetrahedron* **61** (2005), 2889–2896.

[31]   J. Lee, D. Choi and E. Shin, Trans-cis isomerization of arylether dendrimers with azobenzene core and terminal hydroxy groups, *J Spectrochim Acta, Part A* **77** (2010), 478–484.

[32]   A. Momotake and T. Arai, Water-soluble azobenzene dendrimers, *Tetrahedron Lett* **45** (2004), 4131–4134.

[33]   D. Jiang and T. Aida, Photoisomerization in dendrimers by harvesting of low-energy photons, *Nature* **388** (1997), 454–456.

[34]   A. Ray, S. Bhattacharya, S. Ghorai, T. Gangulyb and A. Bhattacharjya, Synthesis and trans-cis isomerization of azobenzene dendrimers incorporating 1,2-isopropylidenefuranose rings, *Tetrahedron Lett* **48** (2007), 8078–8082.

[35]   S. Yokoyama, T. Nakahama, A. Otomo and S. Mashiko, Intermolecular coupling enhancement of the molecular hyperpolarizability in multichromophoric dipolar dendrons, *J Am Chem Soc* **122** (2000), 3174–3181.

[36]   Z. Li, W. Wu, Q. Li, G. Yu, L. Xiao, Y. Liu, C. Ye, J. Qin and Z. Li, High-generation second-order Nonlinear Optical (NLO) dendrimers: Convenient synthesis by click chemistry and the increasing trend of NLO effects, *Angew Chem Int Ed* **49** (2010), 2763–2767.

[37]   W. Wu, C. Ye, G. Yu, Y. Liu, J. Qin and Z. Li, New hyperbranched polytriazoles containing isolation chromophore moieties derived from AB$_4$ monomers through click chemistry under copper(I) catalysis: Improved optical transparency and enhanced NLO effects, *Chem Eur J* **18** (2012), 4426–4434.

[38] W. Wu, C. Li, G. Yu, Y. Liu, C. Ye, J. Qin and Z. Li, High-generation second-order Nonlinear Optical (NLO) dendrimers that contain isolation chromophores: Convenient synthesis by using click chemistry and their increased NLO effects, *Chem Eur J* **18** (2012), 11019–11028.

[39] Y. Yamaguchi, Y. Yokomichi, S. Yokoyama and S. Mashiko, Theoretical study of solvent effects of first order hyperpolarizabilities of nitro-azobenzene dendrimers, *J Mol Struct (Theochem)* **578** (2002), 35–45.

[40] L. Laipniece, J. Kreicberga and V. Kampars, Divergent synthesis of polyester type dendrimers containing azobenzene in the core, *Sci Proc Riga Tech Univ, Ser 1* **16** (2008), 88–98.

[41] X. Cui, J. Li, Z.-P. Zhang, Y. Fu, L. Liu and Q.-X. Guo, Pd(quinoline-8-carboxylate)$_2$ as a low-priced, phosphine-free catalyst for Heck and Suzuki reactions, *J Org Chem* **72** (2007), 9342–9345.

[42] V. Theodorou, K. Skobridis, A.G. Tzakos and V. Ragoussis, A simple method for the alkaline hydrolysis of esters, *Tetrahedron Lett* **48** (2007), 8230–8233.

[43] J. Griffiths and K.C. Feng, The influence of intramolecular hydrogen bonding on the order parameter and photostability properties of dichroic azo dyes in a nematic liquid crystal host, *J Mater Chem* **9** (1999), 2333–2338.

[44] H. Kocaokutgen and S. Ozkinali, Characterisation and applications of some o,o'-dihydroxyazo dyes containing a 7-hydroxy group and their chromium complexes on nylon and wool, *Dyes and Pigments* **63** (2004), 83–88.

[45] E. Luboch, E. Wagner-Wysiecka, Z. Poleska-Muchladoa and V.Ch. Kravtsov, Synthesis and properties of azobenzocrown ethers with π-electron donor, or π-electron donor and π-electron acceptor group(s) on benzene ring(s), *Tetrahedron* **61** (2005), 10738–10747.

[46] V.I. Ushkarov, K.I. Kobrakov, A.I. Alafinov, S.A. Shevelev and A.Kh. Shakhnes, Methylphloroglucinol as an available semiproduct for azo dye synthesis, *Theor Found Chem Eng* **41** (2007), 671–674.

[47] E. Luboch, E. Wagner-Wysiecka and T. Rzymowski, 4-Hexylresorcinol-derived hydroxyazo-benzocrown ethers as chromoionophores, *Tetrahedron* **65** (2009), 10671–10678.

[48] E. Robert and T. Grabenstein. Azo compounds. Pat. WO2006061438 (A1) (15.06.2006).

[49] A. Ozols, V. Kokars, P. Augustovs, K. Traskovskis, A. Maleckis, G. Mezinskis, A. Pludons and D. Saharov, Green and red laser holographic recording in different glassy azocompounds, *Opt Mater* **32** (2010), 811–817.

[50] K. Traskovskis, I. Mihailovs, A. Tokmakovs, V. Kokars, V. Kampars and M. Rutkis, Synthesis and nonlinear optical properties of novel *N,N*-dihydroxyethyl based molecular organic glasses using triaryl substitutes as amorphous phase formation enhancers, *Proc of SPIE* **811** (2010), 81130Z.

[51] H.W. Gibson, D.S. Nagvekar, Y. Delaviz and W.S. Bryant, Synthesis of a new class of difunctional tetraphenylene crown ethers, *Can J Chem* **76** (1998), 1429–1436.

[52] A. Hassner and V. Alexanian, Room temperature esterification of carboxylic acids, *Tetrahedron Lett* **46** (1978), 4475–4478.

[53] N. Ono, T. Yamada, T. Saito, K. Tanaka and A. Kaji, A convenient procedure for esterification of carboxylic acids, *Bull Chem Soc Jpn* **51** (1978), 2401–2404.

[54] K.L. Wooley, C.J. Hawker, J.M. Pochan and J.M.J. Fréchet, Physical properties of dendritic macromolecules: A study of glass transition temperature, *Macromolecules* **26** (1993), 1514–1519.

[55] H. Stutz, The glass temperature of dendritic polymers, *Polym Sci, Part B: Polym, Phys* **33** (1995), 333–340.

[56] A. Tokmakovs, M. Rutkis, K. Traskovskis, E. Zariņš, L. Laipniece, V. Kokars and V. Kampars, Nonlinear optical properties of low molecular organic glasses formed by triphenyl modified chromophores, *I IOP Conf Ser: Mater, Sci Eng* **38** (2012), 1–4.

[57] A. Tokmakovs, M. Rutkis, K. Traskovskis, E. Zariņš, L. Laipniece, V. Kokars and V. Kampars, Properties of EO Active Molecular Glasses Based on Indandione and Azobenzene Chromophores, *Book of Abstracts of the 14-th International Conference-School, Advanced Materials and Technologies*, Palanga, Lithuania, 2012, 96.

K.Traskovskis, E.Zarins, **L.Laipniece**, A.Tokmakovs, V.Kokars, M.Rutkis. Structure-dependent tuning of electro-optic and thermoplastic properties in triphenyl groups containing molecular glasses. *Mat. Chem. Phys.*, **2015**, *155*, 232–240.
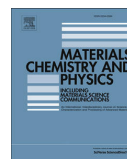
Structure-dependent tuning of electro-optic and thermoplastic properties in triphenyl groups containing molecular glasses

Kaspars Traskovskis [a], [*], Elmars Zarins [a], Lauma Laipniece [a], Andrejs Tokmakovs [b], Valdis Kokars [a], Martins Rutkis [b]

[a] Riga Technical University, Faculty of Materials Science and Applied Chemistry, 3/7 Paula Valdena Street, Riga LV-1048, Latvia
[b] Institute of Solid State Physics, University of Latvia, 8 Kengaraga Street, Riga LV-1063, Latvia

HIGHLIGHTS

- Triphenylmethyl groups can be used to reduce solid phase dipole interactions in organic molecular materials.
- NLO efficiency of a poled material is higher, if a number of present triphenyl groups increases.
- NLO efficiency of materials decreases, if polarity of used chromophores increases.
- Thermal stability of polar order up to 108 °C can be achieved in poled organic glasses.

ARTICLE INFO

ABSTRACT

The series of seven molecular compounds composed of D–π–A chromophores and triphenylmethyl auxiliary groups were characterized by UV–Vis spectroscopy, differential scanning calorimetry and quantum chemical calculations. Nonlinear optical (NLO) properties of compounds were determined by second harmonic generation measurements in corona poled thin glassy films. The results show that triphenylmethyl auxiliary groups are effective at shielding undesirable dipole interactions in solid phase thus increasing NLO efficiency of materials. Thermal stability up to 108 °C was achieved for a polar order in poled samples.

© 2015 Elsevier B.V. All rights reserved.

1. Introduction

During the last two decades the research of organic nonlinear optical (NLO) materials has resulted in a notable performance increase for organic NLO devices, making them viable for various practical applications [1,2]. For example, effective organic electro-optic modulators for fiber optical communication systems have been demonstrated [3].

A macroscopic NLO activity in an organic material can be observed if several structural requirements are met. At the microscopic level the material must contain molecules with large molecular hyperpolarizability (β) values. Such a property is common to donor-acceptor (D-A) dyes, and is to a great extent determined by a

donor or acceptor group strength [4], or by a length of π-electron chain in the D-A conjugation system [5]. Another important requirement for NLO materials is the noncentrosymmetric arrangement of NLO active structural elements. The molecules with large β values usually also have large dipole moment (μ), so in the solid state they tend to pack centrosymmetrically due to dipole–dipole interactions. The required polar order in the material is typically achieved by an electric field poling procedure. Unfortunately, dipole interactions limit the poling efficiency, and the achievable degree of polar order is low. To overcome this, the principle of site isolation is applied, modifying the molecule, so that polar interactions between molecules are shielded by bulky structural groups [6–9]. The known approaches are effective to just a certain degree and the intermolecular interactions still limit the attainable efficiency of organic NLO compounds. Therefore the search for materials with large structural noncentrosymmetry through means of molecular engineering is still one of the main

* Corresponding author.
E-mail address: kaspars.traskovskis@rtu.lv (K. Traskovskis).

challenges in the development of in NLO devices applicable organic materials.

Recently we have demonstrated a new structural approach to obtaining amorphous phase forming molecular materials, also known as molecular glasses, from different organic dyes [10,11]. The method is based on attaching triphenylmethyl-substituents to polar D-A organic dyes that otherwise would crystallize in the solid state. Such materials have potential in NLO [10,11], light emission [12] and holographic recording [13] applications. The structure of bulky and non-polar triphenylmethyl-substituents by concept could provide an effective sterical isolation of polar chromophores, falling within the idea of site isolation principle and making such materials particularly promising for use in NLO devices. In this study a series of triphenyl groups containing molecular glasses are investigated and structure-NLO performance relations are analysed. The acquired results could provide us with a better understanding of general structural requirements for a design of high-performance NLO materials.

2. Experimental

2.1. Materials and sample preparation

Chemical structures of the studied compounds are given in Fig. 1. The synthesis, spectral data and thermoplastic properties of materials **Azo-1** [14], **Pyr-1**, **Pyr-2** [12], **Pyr-3** [15] and **Iph-1**, **Iph-2** [16] are published in separate papers.

2.1.1. Synthesis of compound Azo-2

The synthesis of compound **Azo-2** is outlined in Scheme 1.

Starting materials were purchased from Acros and Alfa Aesar. Solvents, DMF and CH_2Cl_2, were dried over P_2O_5, MeCN and Py - over CaH_2. Compound **4** was prepared according a known procedure [17]. The UV—Vis spectra were recorded with Perkin Elmer Lambda 35 spectrometer. IR spectra were recorded with Perkin Elmer Spectrum 100 FT-IR spectrometer using UATR accessory, NMR spectra were obtained on a Bruker Avance 300 MHz or Varian 6 Unity Inova 600 MHz spectrometers using solvent residue as an internal reference. Reaction mixture analysis was carried out on HPLC-MS system consisting of Waters Alliance 2695 chromatograph equipped with XTerra® MS C18 5 μm 2.1 × 100 mm column, Waters 2996 PDA detector, Waters EMD 1000 (ESI) masspectrometer. The elemental analysis was carried out with Costech Instruments ECS 4010 CHNS–O Elemental Combustion System.

2.1.1.1. 4-[N-(2-hydroxyethyl)-N-(2-trityloxyethyl)amino]-4′-nitro-azobenzene (2). Compound **1** (3.00 g, 9.0 mmol) was dissolved in abs. Py (100 mL) and tritylchloride (2.53 g, 9.0 mmol) and NEt₃ (2.6 mL, 18 mmol) were added. Resulting solution was heated at 100 °C for 6 h, and water (400 mL) was added to the cooled reaction mixture. The next day a formed precipitate was filtered and dried, then it was mixed with CH_2Cl_2, unreacted insoluble starting material **1** was filtered off, filtrate was chromatographed on silica gel with CH_2Cl_2 then 10% EtOAc/CH_2Cl_2 as eluent. Yield 2.59 g (50%) of deep red crystals, *mp* 161—163 °C.

Elem. anal. calcd. for $C_{35}H_{32}N_4O_4$: C 73.41; H 5.63; N 9.78; found: C 73.27; H 5.87; N 9.56%.

MS ESI + *m/z* calcd. $C_{35}H_{33}N_4O_4$ 573.2 $[M+H]^+$, found 573.3 $[M+H]^+$.

^{1}H NMR (300 MHz, CDCl₃) δ 8.27 (d, *J* = 8.8, 2H), 7.86 (d, *J* = 8.8,
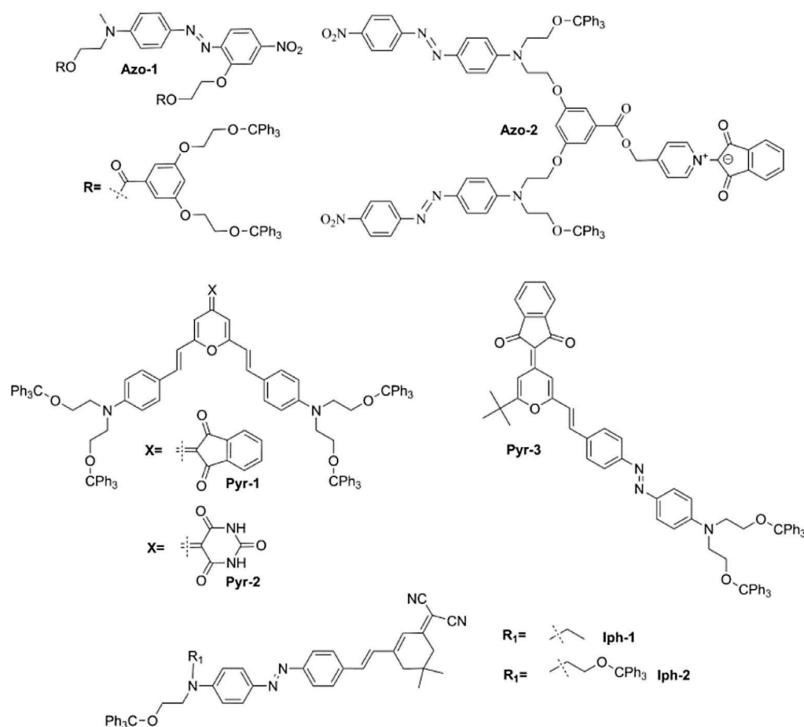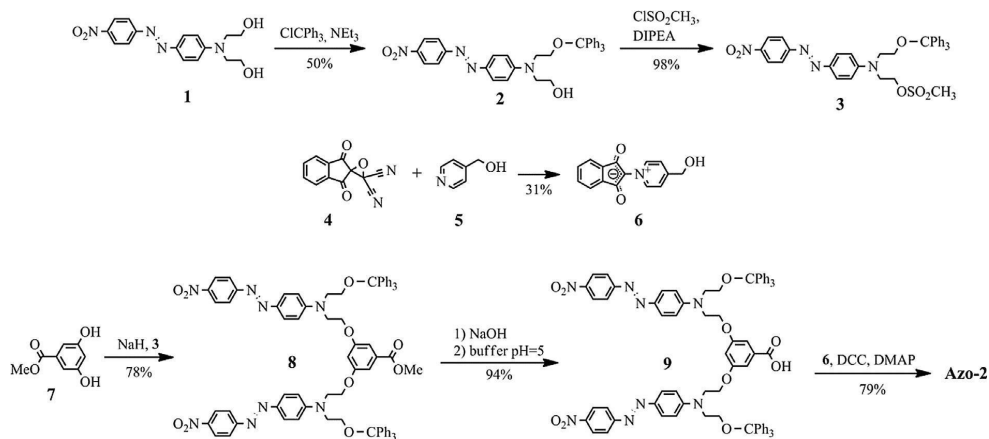

Fig. 1. Structures of the studied compounds.

Scheme 1. Synthesis of compound **Azo-2**.

2H), 7.78 (d, $J = 9.1$, 2H), 7.32 (m, 6H), 7.18 (m, 9H), 6.68 (d, $J = 9.1$, 2H), 3.79 (t, $J = 5.6$, 2H), 3.63 (t, $J = 5.6$, 4H), 3.37 (t, $J = 5.6$, 2H).

*2.1.1.2. 4-[N-(2-mesyloxyethyl)-N-(2-trityloxyethyl)amino]-4′-nitro-azobenzene (**3**).* Azocompound **2** (1.50 g, 2.6 mmol) was dissolved in dry CH$_2$Cl$_2$ (70 mL) and diisopropylethylamine (0.65 mL, 3.9 mmol) was added. The solution was cooled to −15 °C and mesyl chloride (223 μL, 2.9 mmol) was added dropwise over 40 min. The reaction mixture was stirred for 4 h and then washed with saturated sodium carbonate solution and water. The solution was dried over Na$_2$SO$_4$, filtered, and evaporated under reduced pressure. The crude product was crystallized from CH$_2$Cl$_2$/hexane. Yield 1.66 g (98%) of red crystals, mp 191–194 °C.

Elem. anal. calcd. for C$_{36}$H$_{34}$N$_4$O$_6$S: C 66.44; H 5.27; N 8.61; found: C 66.53; H 5.24; N 6.68%.

MS ESI + m/z calcd. C$_{36}$H$_{35}$N$_4$O$_6$S 651.2 [M+H]$^+$, found 651.3 [M+H]$^+$.

^{1}H NMR (300 MHz, DMSO-d_6) δ 8.38 (d, $J = 8.9$, 2H), 7.96 (d, $J = 8.9$, 2H), 7.83 (d, $J = 9.1$, 2H), 7.35–7.20 (m, 15H), 6.95 (d, $J = 9.1$, 2H), 4.40 (t, $J = 5.3$, 2H), 3.97 (m, 2H), 3.76 (m, 2H), 3.25 (t, $J = 5.3$, 2H), 3.15 (s, 3H).

*2.1.1.3. 1-(Indane-1,3-dion-2-yl)-4-(hydroxymethyl)pyridinium betaine (**6**).* 2-Dicyanomethylenindane-1,3-dione oxide (**4**) (1.00 g, 4.5 mmol) was dissolved in abs. MeCN (10 mL) and a solution of 4-hydroxymethylpyridine (**5**) (0.53 g, 4.9 mmol) in abs. MeCN (10 mL) was added. The resulting mixture was refluxed for 30 min, cooled and filtered. The obtained precipitate was crystallized from EtOH few times to separate 1-(indane-1,3-dion-2-yl)-4-(ethoxycarbonyloxymethyl)-pyridinium betaine. The mother liquor was collected, evaporated and the obtained solid residue was crystallized from acetone. Yield 0.35 g (31%) of deep yellow substance.

Elem. anal. calcd. for C$_{15}$H$_{11}$NO$_3$: C 71.14; H 4.38; N 5.53; found: C 71.24; H 4.51; N 5.55.

IR (cm^{-1}) 3320.8, 1614.3, 1569.4, 1505.9, 1459.8, 1396.9, 1365.9, 1322.3, 1215.3, 1064.3, 963.4, 880.3, 820.2.

UV-VIS (CHCl$_3$) $\lambda_{max} = 409.2$ nm, $\varepsilon = 43,800$ M^{-1} cm^{-1}.

MS ESI + m/z calcd. C$_{15}$H$_{12}$NO$_3$ 254.1 [M+H]$^+$, found 254.0 [M+H]$^+$.

^{1}H NMR (300 MHz, DMSO-d_6) δ 9.61 (d, $J = 7.0$, 2H), 7.93 (d, $J = 7.0$, 2H), 7.53–7.36 (m, 4H), 5.84 (t, $J = 5.2$, 1H), 4.74 (d, $J = 5.2$, 2H).

*2.1.1.4. Methyl 3,5-bis(2-((4-(-(4-nitrophenyl)diazenyl)phenyl) (2-(trityloxy)ethyl) amino)ethoxy)benzoate (**8**).* NaH (0.22 g, 5.4 mmol, 60% in mineral oil) was added to a solution of methyl 3,5-dihydroxybenzoate (**7**) (0.43 g, 2.6 mmol) in dry DMF (10 mL), and the mixture was heated at 70 °C for 2 h under Ar, then cooled to 50 °C. A suspension of compound **3** (3.50 g, 5.4 mmol) in dry DMF (50 mL) was then added, and the mixture was heated at 50 °C for 24 h. After cooling to room temperature the precipitated product was filtered. Mother liquor was filtered through Al$_2$O$_3$ and water (50 mL) and satd. NaCl solution (100 mL) were added. The resulting precipitate was filtered and dried. Both portions of product were crystallized separately from CHCl$_3$/hexanes. Yield 2.54 g (78%) of red crystals, mp 206–208 °C.

Elem. anal. calcd. for C$_{78}$H$_{68}$N$_8$O$_{10}$: C 73.34; H 5.37; N 8.77; found: C 73.27; H 5.42; N 8.82.

IR (cm^{-1}) 3100−2850, 1726.7, 1589.9, 1508.2, 1447.8, 1388.3, 1364.8, 1320.3, 1238.6, 1169.8, 1157.3, 1141.9, 1126.8, 1095.9, 1068.3, 999.3, 926.9, 899.0, 855.5, 819.2.

UV-VIS (CHCl$_3$) $\lambda_{max} = 471.5$ nm, $\varepsilon = 62,600$ M^{-1} cm^{-1}.

^{1}H NMR (600 MHz, CDCl$_3$): δ = 8.30 (d, $J = 9.1$, 4H), 7.90 (d, $J = 9.1$, 4H), 7.83 (d, $J = 9.2$, 4H), 7.37 (m, 12H), 7.22 (m, 12H), 7.17 (m, 6H), 7.11 (d, $J = 2.3$, 2H), 6.70 (d, $J = 9.2$, 4H), 6.49 (t, $J = 2.3$, 1H), 4.13 (t, $J = 5.6$, 4H), 3.91 (t, $J = 5.6$, 4H), 3.85 (s, 3H), 3.68 (t, $J = 5.8$, 4H), 3.40 (t, $J = 5.8$, 4H).

*2.1.1.5. 3,5-bis(2-((4-(-(4-nitrophenyl)diazenyl)phenyl) (2-(trityloxy) ethyl)amino) ethoxy)benzoic acid (**9**).* Compound **8** (1.00 g, 0.78 mmol) was dissolved in DMF (40 mL) and a solution of NaOH (0.31 g, 7.8 mmol) in water (1.5 mL) was added. The resulting mixture was heated at 50 °C for 90 min. The reaction mixture was cooled and buffer solution (12.0 g Na$_2$HPO$_4$·12H$_2$O, 40 mL H$_2$O, conc. HCl till pH = 5) was added while vigorously stirring. Precipitate was filtered, washed with water and dried under vacuum. The crude product was crystallized from CHCl$_3$/MTBE. Yield 0.93 g (94%) of red amorphous solid.

Elem. anal. calcd. for C$_{77}$H$_{66}$N$_8$O$_{10}$: C 73.20; H 5.27; N 8.87; found: C 71.71; H 5.30; N 8.85.

IR (cm^{-1}) 3100−2850, 1700.0, 1588.6, 1509.1, 1447.6, 1382.6, 1362.9, 1335.7, 1226.4, 1155.9, 1140.0, 1104.3, 1067.4, 999.5, 900.1, 855.9, 820.5.

UV-VIS (CHCl$_3$) $\lambda_{max} = 4736$ nm, $\varepsilon = 66,500$ M^{-1} cm^{-1}.

^{1}H NMR (600 MHz, CDCl$_3$): δ = 8.28 (d, $J = 8.8$, 4H), 7.88 (d,

$J = 8.8$, 4H), 7.82 (d, $J = 8.9$, 4H), 7.36 (d, $J = 7.4$, 12H), 7.21 (t, $J = 7.4$, 12H), 7.16 (t, $J = 7.4$, 6H), 7.14 (d, $J = 2.1$, 2H), 6.69 (d, $J = 8.9$, 4H), 6.51 (t, $J = 2.1$, 1H), 4.12 (m, 4H), 3.90 (m, 4H), 3.67 (m, 4H), 3.39 (t, $J = 5.4$, 4H).

*2.1.1.6. (4-(2-(3,5-bis(2-((4-(-(4-nitrophenyl)diazenyl)phenyl)   (2-(trityloxy)ethyl)amino) ethoxy)phenyl)-2-oxoethyl)pyridin-1-ium-1-yl)-1,3-dioxo-2,3-dihydro-1H-inden-2-ide (**Azo-2**).* To a solution of compound **9** (0.20 g, 0.16 mmol) and of indandione **6** (0.048 g, 0.19 mmol) in dry CH_2Cl_2 (5 mL) DMAP (0.011 g, 0.09 mmol) was added at 0 °C. Then a solution of DCC (0.0391 g, 0.19 mmol) in dry CH_2Cl_2 (3 mL) was added dropwise to the mixture over 30 min. The obtained solution was stirred for 24 h at room temperature. The flask was then put in freezer to fully crystallize *N,N*′-dicyclohexylurea, then the solution was filtered and evaporated. The obtained solid was mixed with MeCN (5 mL), heated and filtered to wash away unreacted compound **6**. The precipitate was chromatographed on neutral Al_2O_3, using CH_2Cl_2 then CH_2Cl_2/EtOAc as eluent. Yield 0.19 g (79%) of red amorphous solid.

Elem. anal. calcd. for $C_{92}H_{75}N_9O_{12}$: C 73.73; H 5.04; N 8.41; found: C 72.71; H 5.20; N 8.23.

IR (cm^{-1}): $\nu = 3100{-}2850$, 1728.3, 1586.1, 1508.2, 1447.8, 1384.3, 1333.7, 1216.3, 1155.7, 1139.8, 1102.5, 1063.5, 997.9, 855.5, 821.7.

UV-VIS $(CHCl_3)$ $\lambda_{max} = 429.3$ nm, $\varepsilon = 91{,}400$ M^{-1} cm^{-1}.

^{1}H NMR (600 MHz, $CDCl_3$): $\delta = 10.12$ (d, $J = 6.0$, 2H), 8.29 (d, $J = 9.1$, 4H), 7.89 (d, $J = 9.1$, 4H), 7.83 (d, $J = 9.2$, 4H), 7.53 (m, 4H), 7.45 (d, $J = 6.0$, 2H), 7.36 (d, $J = 7.4$, 12H), 7.21 (t, $J = 7.4$, 12H), 7.17 (t, $J = 7.4$, 6H), 7.15 (d, $J = 2.3$, 2H), 6.71 (d, $J = 9.2$, 4H), 6.56 (t, $J = 2.3$, 1H), 5.37 (s, 2H), 4.17 (t, $J = 5.6$, 4H), 3.95 (d, $J = 5.6$, 4H), 3.68 (t, $J = 5.8$, 4H), 3.39 (t, $J = 5.8$, 4H).

2.1.2. Thin film preparation

The glassy thin films used for measurements of NLO properties were prepared by dissolving compounds in analytical grade chloroform with a typical concentration 100 mg/mL, then covering indium tin oxide (ITO) coated glass slides with the prepared solution and spin-coating them with a *Laurell WS-400B-6NPP/LITE* spin-coater (starting speed − 0 rpm, terminal speed − 300 rpm, acceleration - 200 rpm/s, spinning time − 40 s). The thickness of the obtained films was in the range 0.7–1.3 μm. The samples prepared for obtaining thin film absorption spectra were 0.1–0.3 μm thick and were spin-coated from 2 to 3 times more diluted solutions.

2.2. Measurements of thermal properties

Glass transition temperatures of the compounds were determined by DSC thermograms using *Mettler Toledo DSC-1/200W* apparatus at a scanning rate 10 °C/min. The analysed samples initially underwent a cycle of heating above the melting temperature and cooling to room temperature. The temperature corresponding to the half vanished NLO activity (T_{SHI50}) was evaluated from NLO activity measurements with temperature scans at 10 °C/min.

2.3. Corona poling procedure

To break the symmetry of chromophores in the previously prepared glassy films, an external electrical field (corona) poling was used. The procedure and the custom build corona triode setup was identical to one described in our previous paper [10].

2.4. Measurements of linear and nonlinear optical properties of samples

The absorption and reflection spectra in spin-coated samples

were obtained with a setup based on *Ocean Optics HR4000CG-UV-NIR*spectrometer. The thickness of investigated thin films was determined by a *Dektac 150* profilometer and the refractive indexes were measured by a prism coupler *Metricon 2010*. In the separate cases refractive indices were evaluated by an interference fringe separation procedure in the sample reflection spectrum [18].

Second harmonic generation (SHG) measurements of the corona poled samples were carried out 1–2 days after the orientation to avoid an electric field-induced second harmonic generation (EFISHG) contribution caused by trapped charges. The NLO coefficients d_{ij} were obtained by a Maker fringe technique, i.e., by recording second harmonic intensities generated by a sample film as functions of the fundamental light incidence angle and polarization. A scheme of the used computer controlled measurement setup is given in Fig. 2.

The Q-switched DPSS Nd:YVO4 laser (NL640 by EKSPLA) was used as an excitation source. The typical pulse parameters were: repetition rate 40 kHz, duration ~15 ns and spot diameter ~200 μm. The SH intensity (SHI) generated by a sample and a reference KDP crystal was measured by a gated single photon counting. The laser pulse energy was kept at a level producing <0.5 counts per pulse, typically 1–10 μJ. The counting time window was synchronized with a laser pulse and kept <15 ns to eliminate the background noise and suppress non-coherent 532 nm signals. SHI from the sample channel used in the calculations was always normalized to the reference SHI obtained from frequency doubling KDP crystal that was kept at constant (30 °C) temperature. That allowed us to avoid an impact of laser pulse peak power variations during Maker fringe experiments. A filter system for both the sample and reference channels was used to isolate a 532 nm emission. Specifically, a negatively curved selective mirror (reflecting 1064 nm) is used to cut off the incidence exciting beam. The remains of 1064 nm radiation were removed with a low pass filter, and finally the SH light was passed to PMT via a 532 nm interference filter (full width at half maximum - 3 nm). The sample channel has a possibility to insert neutral density filters in the front of 532 nm IF.

SHI Maker fringes (typically −80 till +80° with a step 0.5; in the case of x-cut quartz with a step = 0.2) were recorded at 5-10 different spots of a sample film. Afterwards a response function of the setup was found by replacing an organic sample with a 2 mm thick x-cut quartz crystal, recording Maker fringe at the exact incidence angle and then fitting the data considering $d_{11} = 0.3$ pm/V [19]. ND filters were used to record quartz Maker fringes in the cases where SH signal from an organic film is weaker than from the x-cut crystal.

For corona poled films the $C_{\infty v}$ symmetry is assumed, therefore materials can be characterized by three nonzero NLO coefficients − d_{33}, d_{31} and d_{15}. As it is a common practice for poled organic films, we assume that $d_{31} = d_{15}$ [20] according to Kleinman symmetry. NLO coefficients were obtained by a least square fit of the experimental curves to a theoretical approximation. Theoretical values of SH intensity were calculated according to Herman and Hayden approach [20], using previously measured refractive indices at 532 nm and 1024 nm, absorption values and a thickness of the films. The fitting procedure was carried out in two steps: the s-p polarized SHG experimental data are used to calculate d_{31}, and then d_{33} was calculated from the p–p data, keeping into account that $d_{15} = d_{31}$. A typical experimental and approximation example is presented in Fig. 3.

3. Discussion

3.1. Chemical structures and quantum calculations

Generally the studied materials are designed utilizing a modular
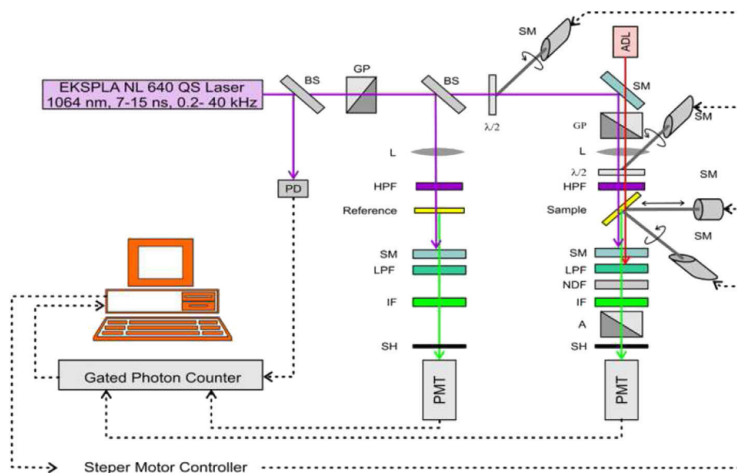
Fig. 2. Experimental set up for SHG investigations: BS - beam splitter; GP – Glan polarizer, L – lens, HPF – high past filter, SM - selective mirror, LPF – low past filter, IF -interference filter ($\lambda = 532$ nm), SH – shutter, $\lambda/2$ – half-wave plate ($\lambda = 1064$ nm), STM – step motor, ADL – alignment diode laser, NDF – neutral density filter, A -analyser, PMT – photo multiplier tube.

approach, where a polar chromophore is modified by attached triphenylmethyl-groups to ensure an amorphous phase formation in the solid state. Based on a structure of NLO active chromophore, the studied compounds can be classified in three categories. Materials **Azo-1,2** contain D-A azobenzene dyes. For **Azo-1** a branched dendritic molecular geometry is used, where the polar azochromophore is in the centre of molecule while isolating triphenylmethyl-groups are attached in the periphery. For compound **Azo-2** a three-arm, star-shaped structure is used. The two identical azochromophores present in the molecule are similar to in NLO studies well known *Disperse Red* dyes, but the third

chromophore is zwitterionic indanedione-1,3 pyridinium betaine (IPB). The dipole moment and hyperpolarizability directions in zwitterionic compounds are reversed in comparison with neutral ground-state chromophores, where they match. One could expect that the resulting structure formed by dipole–dipole interaction of such two (D-A and zwitterionic) chromophores can be characterized by a sum of individual hyperpolarizabilities and a difference of dipole moment values. The mentioned effect has been utilized to diminish a negative impact of dipole interactions in NLO materials [21,22]. The same intent was behind the chosen molecular design of **Azo-2**, where the configuration of dipoles in tree-arm structure
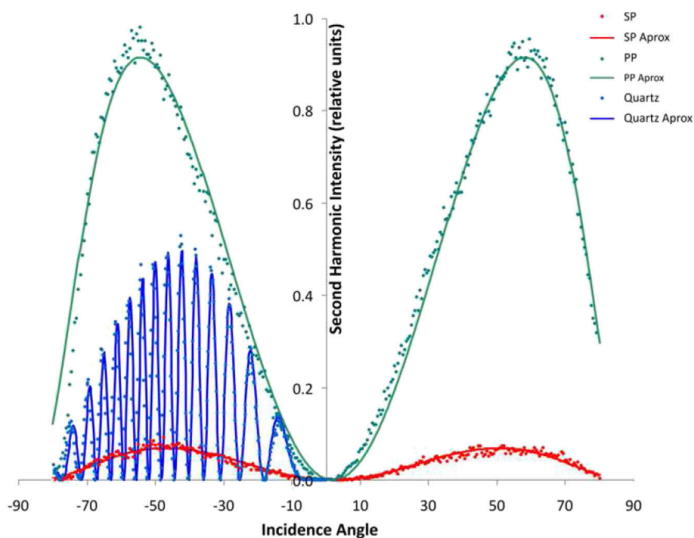
Fig. 3. Experimental Maker fringe SHI and approximation results for **Azo-1** and 2 mm thick x-cut quartz crystal. Dots represent experimental points, but solid lines our fit according to Herman–Hayden approach.

would result in decreased overall dipole moment value and increased hyperpolarizability.

Other two categories of compounds contain 4H-pyranilidene (**Pyr-1,2,3**) or isophorone-benzylidene-azobenzene (**Iph-1,2**) based chromophores. The molecular design of these materials is similar to that reported in our previous NLO studies [10,11], where triphenylmethyl-groups are attached to the oxygen atoms of N-phenyldiethanolamine fragment in the electron-donor part of the molecule (with the exception of compound **Iph-1** where a single bulky triphenyl isolating group is used instead of two). In the case of 4H-pyranilidene derivatives both the linear (**Pyr-3**) and V-shaped (**Pyr-1,2**) conjugation arrangements are used.

Several molecular properties of the synthesized compounds were predicted by the means of quantum chemical (QC) modelling in the vacuum by G09W software package. RHF (basis set 6-31G(p,d)) calculations are performed with default accuracy set by Gaussian. In particular, molecular hyperpolarizability $\beta_{(0)}$ and dipole moment (μ) values were calculated (see Table 1). Despite the fact that DFT B3LYP calculations have become increasingly popular in the field during the last decade, our more than ten years' experience using RHF method, as well as findings of other groups [23] suggest that both RHF and DFT QC modelling can be successfully used for experimental guidance.

The obtained hyperpolarizability (tensor element along the direction of the dipole moment) $\beta_{\mu(0)}$ and μ values are in good agreement with the corresponding chemical structures. Taking into account the empirical evidence that a hyperpolarizability of a D-A compound is expected to increase with the strength of electron acceptor and donor groups and with the length of conjugation chain [4,5], it is unsurprising that the highest β value is observed for compounds **Iph-1,2**, as the structure of the active chromophore in these molecules most closely meets the mentioned requirements. Significantly lower hyperpolarizabilities are calculated for 4H-pyranilidene derivatives **Pyr-1,2,3**. This observation can be attributed to several factors. For compounds **Pyr-1,2** the main cause is the shortened D-A conjugation chain length of the chromophores. While the chromophore in compound **Pyr-3** is structurally close to that in **Iph-1,2**, the lowered β in this case can be explained by the presence of 4-pyrone conjugation bridge fragment. Compared to simple polyenic fragments, pyran ring provides additional mesomeric forms that consequently lower the charge separation in a D-A charge transfer process, thus decreasing hyperpolarizability. The β values of V-shaped **Pyr-1,2** and linear **Pyr-3** are almost identical despite the latter molecule having a longer chromophore conjugation chain. This observation is in agreement with findings of Andreu et al. [24] that show that V-shaped 4H-pyranilidene chromophores have a higher NLO performance than linear structural analogues. Thus the lower overall efficiency of **Pyr-3** NLO-phore is compensated with a longer conjugation bridge, making the material comparable with **Pyr-1,2** in terms of calculated hyperpolarizability. It is worth mentioning that the compounds

containing 1,3-indandione acceptor fragment (**Pyr-1,3**) show reduced dipole moment values while retaining relatively high β, in agreement with other studies [25].

In the case of compound **Azo-2** the hyperpolarizability value is determined by the geometry of the molecule. One could roughly estimate the overall hyperpolarizability by a vectorial sum of hyperpolarizability tensor elements along the direction of the dipole moment of three chromophores. Two of them are D-A type dyes with calculated individual $\beta_{\mu(0)} = 31$ and the third is zwitterionic IPB with $\beta_{\mu}(0) = -11$. The calculated geometrical structure of **Azo-2** can be seen in Fig. 4, and it is apparent that the configuration of dipole directions of individual chromophores would result in a decreased overall μ value, as the dipoles of azochromophores and IPB are facing opposite directions. And as the QC results show, μ of **Azo-2** is by approximately a half lower than the sum of dipoles of individual NLO-phores. At the same time the hyperpolarizability of the molecule is relatively close to the sum of chromophore β values (~59 instead of the maximal value ~73).

The relatively low β value of compound **Azo-1** (compared to structural analogue *Disperse Red*; $\beta_{\mu(0)} = 31$) can be explained by the presence of an electron donating 2-ethoxy substituent in the acceptor part of the azochromophore.

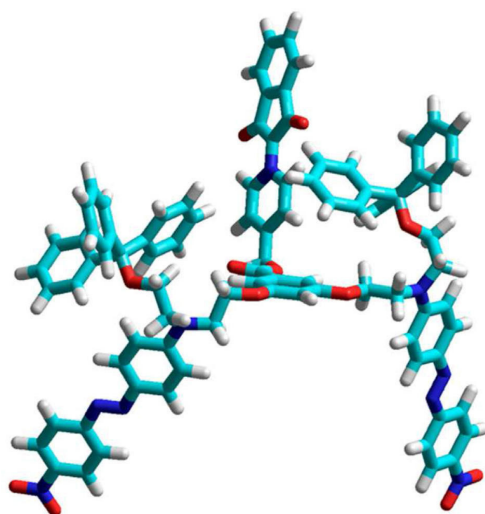### 3.2. Linear absorption in solutions and solid films

Solution and solid phase UV–Vis absorption spectra of the compounds are given in Fig. 5. All compounds have a strong absorption band in the visible light wavelength region. As it is expected, two overlapping absorption bands can be observed for compound **Azo-2**, the one with maxima at 420 nm corresponding to IPB [26] and the one at 495 nm-to *Disperse Red*. In the series of 4H-pyranilidene derivatives the V-shaped chromophores **Pyr-1,2** have batochromically shifted absorption bands if compared to linear **Pyr-3**. This is in agreement with the studies describing similar structures [24,27]. Generally, a widening of absorption bands is observed with an increase of conjugation chain length of chromophores (see **Pyr-3** and **Iph-1,2**).

Compared to the spectra taken in solutions, the UV-VIS

Table 1
The results of quantum chemical calculations.

Compound	$\beta_{\mu(0)}$, 10^{30} esu	μ, D
Azo-1	26.0	6.9
Azo-2	58.7	13.6
Pyr-1	35.4	8.0
Pyr-2	34.6	13.2
Pyr-3	32.1	6.2
Iph-1	59.0[a]	10.8[a]
Iph-2	59.0	10.8

[a] The calculated values of **Iph-2** are also used for **Iph-1**, as we assume, that the influence of slightly changed peripheral groups on the properties of chromophore is insignificant.

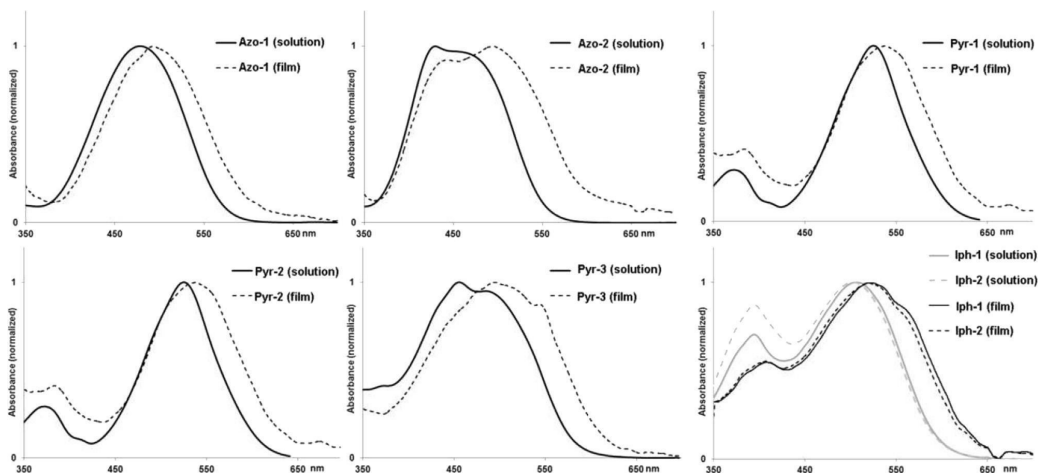**Fig. 4.** Calculated geometrical structure of **Azo-2**.

Fig. 5. UV–Vis absorption spectra in CH_2Cl_2 solutions and thin films.

absorption bands in solid phase for all compounds are broadened and bathochromically shifted. This observation indicates that intermolecular interactions between chromophores take place in glassy state due to a close packing of molecules. On the other hand, no notable splitting or shape variations are observed for absorption bands. This suggests that no ordered, crystal-like solid state molecular packing takes place [28]. A slight broadening can be seen in the solid phase absorption band of **Iph-1** in comparison with compound **Iph-2**. This observation can be explained by the chemical structures of these molecules. One could expect increased dipole–dipole interactions between chromophores in the case of **Iph-1**, where only one triphenylmethyl shielding moiety is present instead of two, causing the broadening of an absorption band.

3.3. Nonlinear optical properties

The NLO performance of the materials was evaluated by measured NLO coefficient-d_{33} (see Table 2). Since the experimentally measured NLO coefficients are frequency dependant, an extrapolation to zero frequency ($d_{33(0)}$) according to two-level model [29] was made for better comparison between different structures. However, in cases when measured SH frequency approaches the lowest charge–transfer transition, the precision of this model becomes unsatisfactory, because it overestimates the resonance enhancement of the measured signal [30]. An apt example of this is compound **Pyr-1**, where SH and absorption maxima values are almost coincident, resulting in an underestimated $d_{33(0)}$ value.

Table 2
Solid phase light absorption, thermal, and NLO properties of the materials.

Compound	λ_{max}, nm	α_{max}, cm^{-1}	T_g, °C	T_{SH50}, °C	RI_{532}	RI_{1064}	$d_{33(532)}$, $pm \times V^{-1}$	$d_{33(0)}$, $pm \times V^{-1}$
Azo-1	495	1.90	78	70	2.04	1.60	37.3	4.2
Azo-2	492	4.38	113	91	2.44	1.67	92.0	10.4
Pyr-1	533	4.93	118	108	2.20	1.60	106.0	0.3
Pyr-2	512	4.18	127	102	2.30	1.60	28.2	1.8
Pyr-3	493	4.63	122	103	2.36	1.66	66.2	7.3
Iph-1	517	3.60	91	74	2.21	1.73	62.8	2.8
Iph-2	515	3.67	105	87	2.53	1.71	125.7	6.1

Ignoring intermolecular interactions, the macroscopic NLO performance of a poled material is proportional to molecular parameters β and μ [1]. Based on this, for a purpose of data interpretation a correlation between molecular parameters and measured $d_{33(0)}$ coefficient was made (Fig. 6). An additional parameter-mass fraction of NLO-active chromophores ($w_{chr.}$) was used in the correlation to compensate large variations of chromophore mass concentration in different studied materials. Compound **Pyr-1** was excluded from the graph, as the extrapolation to zero frequency in this case gave undervalued $d_{33(0)}$.

The analysis of the acquired correlation graph reveals some important structure-NLO efficiency relations within the studied class of molecular glasses. A clear evidence of dipole shielding properties of the present triphenylmethyl groups is demonstrated in the case of compounds **Iph-1** and **Iph-2**. Despite the consequential drop in an active chromophore weight fraction for **Iph-2**, the attachment of an additional triphenylmethyl moiety to the chromophore core for this compound increases its NLO efficiency more than two times in comparison to **Iph-1**. Since the second order NLO efficiency of a poled organic material is proportional to the attainable degree of polar order, the increased non-linearity for **Iph-2** indicates more effective poling procedure and consequently-
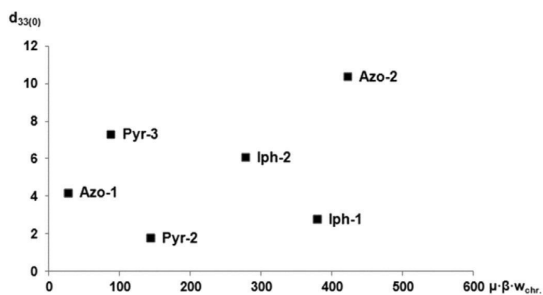

Fig. 6. Correlation between materials molecular properties and macroscopic NLO efficiency. Parameter $w_{chr.}$ was calculated as a ratio of the molecular weight of active chromophore to the molecular weight of the whole molecule.

decreased dipole interaction energy.

While dipole shielding properties of the triphenyl group is evident, Fig. 6 also shows that polar interactions still limit potentially attainable performance of the synthesized materials. In the case of non-interacting dipoles, there would be a clearly observable linear trend between molecular parameter $\beta\mu w_{chr.}$ and measured d_{33} values. Instead, it is evident that several compounds do not follow this tendency. In particular, taking into consideration the corresponding molecular parameters and the measured d_{33} values for other compounds, materials **Pyr-2**, **Iph-1** and **Iph-2** are less efficient than estimated. This observation can be easily explained, if dipole moment values of these compounds are taken into account. As the mentioned materials contain the most polar chromophores amongst the studied series ($\mu > 10$), it is unsurprising that the attainable poling efficiency for them are the lowest. Additionally to poling disrupting dipole–dipole interactions, a possible solid phase hydrogen bonding for compound **Pyr-2**, caused by the present barbituric acid acceptor fragment, cannot be excluded [31], making this material the least efficient.

In contradiction to previous observations, material **Azo-2** has the largest calculated dipole moment, but at the same time the highest NLO efficiency. However, it must be taken into consideration that the given calculated μ value represents the sum for three separate chromophores, and if they are characterized separately, these individual dipoles are relatively low polar. Assuming that the overall energy of solid phase dipolar interactions for compound **Azo-2** can be expresses as a sum of multiple low-polar interactions, it is plausible to predict that this sum would be lower than for materials that contain a single high-polar chromophore.

As mentioned, the highest nonlinearity was measured for star-shaped compound **Azo-2**. QC results showed that beneficial intramolecular interactions take place between D-A and zwitterionic NLO-phores positioning them in a way that total molecular hyperpolarizability is increased. However, the reduced number of dipole shielding triphenylmethyl-moieties (ratio of triphenylmethyl groups to NLO-phores in the molecule is 2/3 instead of 2/1 for the most other studied materials) most likely limit potential efficiency of the material. This is evident, if the NLO performance of **Azo-2** is compared to the performance of our previously synthesized materials. In particular, for a structurally similar N-phenyldiethanolamine based single *Disperse Red* chromophore containing molecular glass a slightly higher nonlinearity was achieved ($d_{33(0)}=$11.0 [11]).

Taking into account the studied structures and corresponding NLO efficiencies we propose that further improvements can be made on the presented molecular design. It is apparent that triphenylmethyl groups can be used as dipole shielding substituents; however, when high-polar chromophores are used a steep decrease in efficiency is still observed. We propose that an in advance modelling of molecular geometry can be applied to acquire more sterically isolated structures. Specifically, an attachment of additional triphenylmethyl-substituents in electron acceptor part of chromophores can be proposed.

3.4. Thermal properties

Thermal properties of the materials were characterized by two complementary parameters—glass transition temperature (T_g) and temperature at which 50% drop of NLO efficiency (second harmonic intensity — SHI) takes place (T_{SHI50}). The measured values are summarized in Table 2 and several examples illustrating a heat induced decay of SHI are given in Fig. 7. T_g and T_{SHI50} should match, as both measurements correspond to a start of a heat induced macroscopic molecular movement in a material. However, in the all cases the measured T_{SHI50} value is significantly lower than T_g
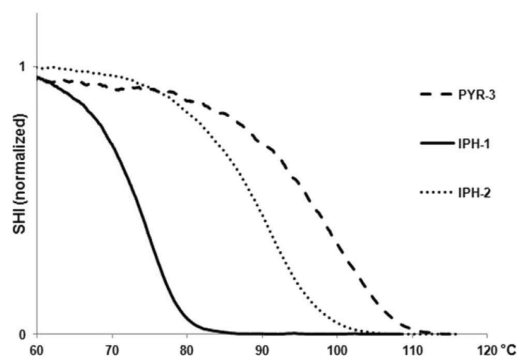

Fig. 7. A heat induced decay of SHI in several investigated materials.

indicating that thermal stability of materials in melted samples is higher than in poled spin-coated films. This observation can be explained by an increased free volume portion in solution-processed films compared to melts. Also a presence of residual solvent, trapped in an amorphous material, cannot be excluded.

The studies describing structural impact on glass transition temperatures in molecular glasses point out some clear relations that T_g of an amorphous material can be increased by synthesizing compounds with larger molecular weight or limiting a conformational freedom of a molecule [32]. This assumption is fully valid if it is applied to our compounds. The highest T_g values are measured for structurally rigid and large 4H-pyranilidene derivatives **Pyr-1,2,3**. The comparison of structurally similar **Iph-1** and **Iph-2** reveals clear influence of molecular weight as an addition of extra triphenylmethyl group increases T_g by 14 °C. The lowest T_g is measured for material **Azo-1**. While this compound has relatively large molecular weight, the low glass transition value can be explained by the presence of numerous structurally incorporated flexible alkyl chains that increases an overall conformational freedom of the molecule.

4. Conclusions

The analysis of NLO measurements of structurally different molecular glasses revealed clear evidence that triphenylmethyl groups can be used as effective dipole shielding structural fragments. The results also show that dipole interactions still take place and limit achievable efficiency of the studied materials, especially in the cases where NLO active chromophores have large dipole moment. The further structural improvements can be proposed with more pronounced encapsulation of polar chromophores. NLO efficiency of the studied corona poled materials (28–125 pm/V) close to a resonance conditions (1064 nm excitation) over performs widely used NLO materials like KDP (0.44 pm/V), KTP (13.7 pm/V) and LiNbO$_3$ (34.4 pm/V). At the same time it should be mentioned that, if being extrapolated to zero frequency, acquired NLO coefficient values (0.3–10.4 pm/V) are in the same range with above mentioned inorganic materials. The thermal stability of NLO effect in the materials is in the range of 70–108 °C and is mainly determined by molecular weight and conformational freedom of the molecules.

References

[1] L.R. Dalton, P.A. Sullivan, D.H. Bale, Chem. Rev. 110 (2010) 25–55.
[2] J. Luo, X.-H. Zhou, A.K.-Y. Jen, J. Mater. Chem. 19 (2009) 7410–7424.
[3] Y. Shi, C. Zhang, H. Zhang, J.H. Bechtel, L.R. Dalton, B.H. Robinson, W.H. Steier, Science 288 (2000) 119–122.
[4] L.T. Cheng, W. Tam, S.H. Stevenson, G.R. Meredith, J. Chem. Phys. 95 (1991) 10631–10643.
[5] M. Blanchard-Desce, V. Alain, P.V. Bedworth, S.R. Marder, A. Fort, C. Runser, M. Barzoukas, S. Lebus, R. Wortmann, Chem. Eur. J. 3 (1997) 1091–1104.
[6] J. Luo, H. Ma, M. Haller, A. Jen, R.R. Barto, Chem. Commun. (2002) 888–889.
[7] T. Liang, Y. Cui, J. Yu, W. Lin, Y. Yang, G. Qian, Thin Solid Films 544 (2013) 407–411.
[8] W. Wu, J. Qin, Z. Li, Polymer 54 (2013) 4351–4382.
[9] D.L. Elder, S.J. Benight, J. Song, B.H. Robinson, L.R. Dalton, Chem. Mater. 26 (2014) 872–874.
[10] K. Traskovskis, I. Mihailovs, A. Tokmakovs, A. Jurgis, V. Kokars, M. Rutkis, J. Mater. Chem. 22 (2012) 11268–11276.
[11] K. Traskovskis, K. Lazdovica, A. Tokmakovs, V. Kokars, M. Rutkis, Dyes Pigments 99 (2013) 1044–1050.
[12] A. Vembris, E. Zarins, J. Jubels, V. Kokars, I. Muzikante, A. Miasojedovas, S. Jursenas, Opt. Mater. 34 (2012) 1501–1506.
[13] A. Ozols, V. Kokars, P. Augustovs, K. Traskovskis, A. Maleckis, G. Mezinskis, A. Pludons, D. Saharov, Opt. Mater. 32 (2010) 811–817.
[14] L. Laipniece, V. Kampars, Main. Group Chem. 14 (2015) 43–58.
[15] E. Zarins, K. Siltane, E. Misina, V. Kokars, K. Lazdovica, A. Vembris, V. Kampars, I. Muzikante, M. Rutkis, Proc. SPIE 8435 (2012), 84351Q.
[16] E. Zarins, V. Kokars, M. Utinans, IOP Conf. Ser. Mater. Sci. Eng. 2 (2011) 012–019.
[17] I.K. Raiskuma, G.G. Pukitis, O. Ya Neiland, Chem. Heterocyc. Compd. 14 (1978) 714–717.
[18] E. Nitiss, R. Usans, M. Rutkis, Proc. SPIE. 8430 (2012), 84301C.
[19] J. Jerphagnon, S.K. Kurtz, Phys. Rev. B 1 (1970) 1739–1744.
[20] W.N. Herman, L.M. Hayden, J. Opt. Soc. Am. B 12 (1995) 416–427.
[21] Y. Liao, S. Bhattacharjee, K.A. Firestone, B.E. Eichinger, R. Paranji, C.A. Anderson, B.H. Robinson, P.J. Reid, L.R. Dalton, J. Am. Chem. Soc. 128 (2006) 6847–6853.
[22] M. Rutkis, A. Tokmakovs, E. Jecs, J. Kreicberga, V. Kampars, V. Kokars, Opt. Mater. 32 (2010) 796–802.
[23] C.M. Isborn, A. Leclercq, F.D. Vila, R. Dalton, J.L. Bredas, B.E. Eichinger, B.H. Robinson, J. Phys. Chem. A 111 (2007) 1319–1327.
[24] R. Andreu, L. Carrasquer, J. Garín, M.J. Modrego, J. Orduna, R. Alicante, B. Villacampa, M. Allain, Tetrahedron Lett. 50 (2009) 2920–2924.
[25] C.R. Moylan, R.J. Twieg, V.Y. Lee, S.A. Swanson, K.M. Betterton, R.D. Miller, J. Am. Chem. Soc. 115 (1993) 12599–12600.
[26] I. Muzikante, E. Fonavs, E.A. Silinsh, B. Yang, F. Ciuchi, B. Dubini, D. Hönig, Supramol. Sci. 4 (1997) 399–406.
[27] G. Koeckelberghs, L.D. Groof, J. Pérez-Moreno, I. Asselberghs, K. Clays, T. Verbiest, C. Samyn, Tetrahedron 64 (2008) 3772–3781.
[28] C. Uhrich, R. Schueppel, A. Petrich, M. Pfeiffer, K. Leo, E. Brier, P. Kilickiran, P. Baeuerle, Adv. Funct. Mater. 17 (2007) 2991–2999.
[29] J.L. Oudar, D.S. Chemla, J. Chem. Phys. 66 (1977) 2664–2668.
[30] S.D. Bella, New. J. Chem. 26 (2002) 495–497.
[31] F. Ramondo, A. Pieretti, L. Gontrani, L. Bencivenni, Chem. Phys. 271 (2001) 293–308.
[32] K. Naito, P. Miura, J. Phys. Chem. 97 (1993) 6240–6248.

A.Tokmakovs, M.Rutkis, K.Traskovskis, E.Zariņš, **L.Laipniece**, V.Kokars, V.Kampars. Nonlinear Optical Properties of Low Molecular Organic Glasses Formed by Triphenyl Modified Chromophores. *IOP Conference Series: Materials Science and Engineering*, **2012**, *38*, 012034.

Nonlinear optical properties of low molecular organic glasses formed by triphenyl modified chromophores.

A Tokmakovs[1], **M Rutkis**[1,3], **K Traskovskis**[2], **E Zarins**[2], **L Laipniece**[2], **V Kokars**[2], **V Kampars**[2]

[1]Institute of Solid State Physics, University of Latvia, Latvia

[2]Institute of Applied Chemistry, Riga Technical University, Latvia

E-mail: martins.rutkis@cfi.lu.lv

Abstract. The series of organic molecular glasses have been studied as possible candidates for nonlinear optical (NLO) applications. Amorphous phase formation of investigated materials is ensured by the presence of bulky triphenyl substituents in molecular structure of NLO chromophores. Linear optical properties as well as NLO coefficients and thermal stability of NLO activity for the 13 molecular materials in glassy thin solid films have been determined. For the benzylidene-1,3-indandione chromophore containing compound the highest d_{33} value equal to 280 pm/V was measured under the 1064 nm excitation. Among the investigated compounds uppermost achieved thermal sustainability of NLO response was 108 °C. The relationship between number of triphenyl substituents and increased thermal sustainability of nonlinear response was observed.

1. Introduction

Organic nonlinear optical (NLO) materials are a subject of interest in fields as data processing and transmission due to wide modification possibilities and increased performance characteristics compared to inorganic materials [1]. The progress in this field is very much dependent on the development and characterization of new functional materials exhibiting high NLO efficiency and good long term stability. Organic glasses, class of materials where amorphous phase formation is achieved in low molecular weight molecules [2-4], from practical point of view are good candidates for such applications. These compounds are easily obtained, purified and characterized. However, some of important for practical use properties like thermal stability of NLO efficiency are worse than that in the polymer materials. Enhancement of thermal stability is a key issue for the employment of such molecular glasses in practical applications. In the given study we present the values of the key characteristics, NLO coefficients and thermal stability, for a series of low molecular weight glasses where amorphous phase formation is achieved by introduction of triphenyl substituents [5]. The analyzed structures contain wide variety of chromophores, as well as shape and design of amorphous phase formation enhancers are different. Screening of these results could reveal the connections between the structural properties and NLO characteristics useful for further improvements of materials.

---

[3] To whom any correspondence should be addressed

2. Experimental

2.1. Materials and thin film sample preparation

The synthesis and characterization of the investigated compounds (figure 1) are given elsewhere: for **A1**, **A2**, **B2**, **B3**, **B5**, **B7** see [5], for **A3**, **B1**, **B4**, **B6** [6], **C1** [7], **C2** [8]. Azochromophore **B8** was synthesized from 4'-[N-(2-hydroxyethyl)-N-methyl]amino-2-(2-hydroxyethoxy)-4-nitroazobenzene and 3,5-bis(2-(trityloxy)ethoxy)benzoic acid in N,N'-dicyclohexylcarbodiimide and 4-(dimethylamino)pyridine mediated esterification [8]. To obtain thin film samples an appropriate amount of glass forming compound was dissolved in analytical grade chloroform or chlorbenzene at a typical concentration of 100 mg/ml. The films from solutions were spin-coated with a Laurell WS-400B-6NPP/LITE spin-coater on ITO covered glass slides.
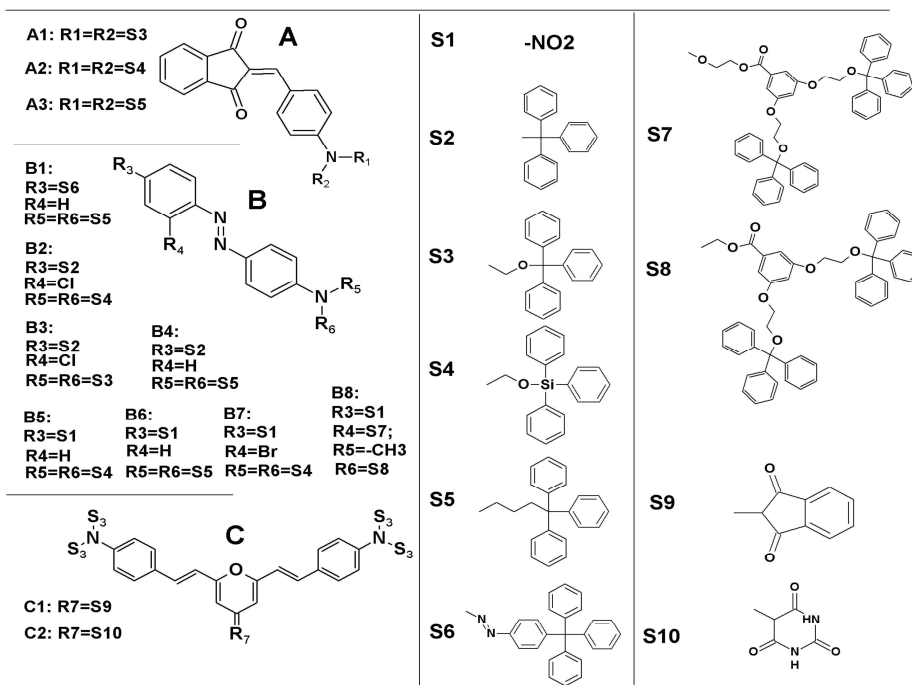
Figure 1. Structures of investigated glass forming compounds.

2.2. Corona poling procedure

To produce NLO active media thermo assisted electrical field poling procedure was applied to thin film samples via a custom built corona triode setup. The corona discharge was generated by a 9 kV voltage drop over a 15 mm gap between a tungsten wire needle (diameter 25μm) and a control grid. At a distance of 10 mm below the grid the ITO covered slide with spin coated glassy film was placed on a temperature controlled heater. All samples were poled through a mask with diameter of 0.8 cm by constant 2.7 kV grid to ITO layer potential. The corona discharge started in advance of heating the sample to poling temperature. At the point when the sample charging current reached an approximate steady state the poling was considered to be finished and the sample was cooled to room temperature under applied corona triode discharge. First of all samples where poled close to glass transition temperature ($T_{poling} \approx T_g$). For these samples the temperature corresponding to the half vanishing of NLO activity (T_{SHI50}) was evaluated from the SHI with temperature scans at 10 °C/min (see examples at figure 2). Finally fresh samples for further NLO coefficient measurements were poled at T_{SHI50}.

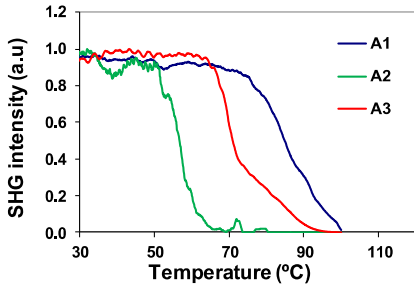**Figure 2.** SH intensity with temperature scans for **A1**, **A2** and **A3** compounds.
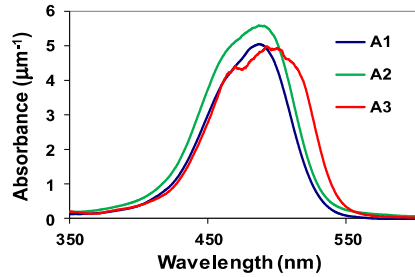

Figure 3. Absorption spectra of the thin films of **A1**, **A2** and **A3** compounds.

2.3. Measurements of linear and nonlinear optical properties of thin films

The absorption and reflectance spectra of the thin films were obtained with an *Ocean Optics HR4000CG-UV-NIR* based spectroscopic system. The thickness of investigated thin films was measured using a *Dektac 150* profilometer and refractive indexes were determined by a prism coupler *Metricon 2010*. In some cases thickness and refractive indices were evaluated by procedure described elsewhere [10] using interference fringe separation in the sample reflection spectrum. The experimental set-up for second harmonic generation is described elsewhere [11]. To avoid electric field-induced second harmonic generation (**EFISHG**) signal from charges trapped on the film surface the non-linear coefficients were usually measured 2 days after poling by Maker fringe technique. For corona poled films the $C_{\infty v}$ symmetry was assumed and the material could be characterized by three nonzero **NLO** coefficients − d_{33}, d_{31} and d_{15}. As it is usually done for the poled polymer films, we assume that $d_{31} = d_{15}$ [11] according to Kleinman symmetry. The **NLO** coefficients were acquired by a least squares fit of the experimental curves to the theoretical approximation. The theoretical value of second harmonic intensity (**SHI**) was calculated using the Herman − Hayden [12] approach, taking into account absorption of the film. The fitting was carried out in two steps: the value of d_{31} was evaluated from experimental *s-p* polarized **SHI**, then the d_{33} was calculated from the *p-p* **SHI**. An x–cut quartz crystal was used as reference ($d_{11} = 0.3$ pm/V) to calibrate the instrument response function [13]. The results of the measurements are given in table 1 where one could find also CT maxima wavelength (λ_{max}) and absorption coefficient (α_{max}) as well as refractive indexes at 532 and 1064 nm. Static field **NLO** coefficients $d_{33}(0)$ was obtained by extrapolation of experimental values to the zero frequency according to two level model.

Table 1. Linear and nonlinear optical properties of thin films.

Structure	λ_{max} (nm)	$\alpha_{max} \times 10^{-4}$ cm^{-1}	RI (532nm)	RI (1064nm)	T_{SHI50} (°C)	Orientation T(°C)	d_{33}(532) (pm/V)	d_{33}(0) (pm/V)
A1	489	5.56	1.90	1.60	84	85	22.7	2.8
A2	490	5.03	1.94	1.59	60	56	41.9	6.2
A3	504	4.69	2.24	1.61	71	73	280.0	22.3
B1	507	3.08	2.55	1.63	83	82	24.2	1.7
B2	440	2.09	1.79	1.62	58	56	5.8	1.5
B3	440	2.71	1.84	1.64	84	84	7.6	2.0
B4	435	3.58	1.71	1.59	73	74	8.6	2.4
B5	488	3.41	1.93	1.61	52	50	62.9	7.9
B6	500	5.40	2.15	1.61	72	72	88.3	8.0
B7	510	4.85	2.34	1.69	53	48	214.0	13.3
B8	495	1.93	2.04	1.60	90	92	37.6	5.7
C1	533	4.93	2.20	1.60	108	110	106.0	0.3
C2	512	4.18	2.30	1.60	102	105	28.2	1.8

3. Discussion

As it can be seen from table 1, T_{SHI50} values of the compounds vary from 52 to 108 °C. In figure 2 we have presented examples of SHI with temperature scans for three molecular glass systems based on same chromophore. The lowest value is met when a triphenylsilyl fragment (**S4**) is present in an **A2** molecule. As our previous research revealed [5] it can be attributed to the fact that the given functional fragment has increased conformational freedom compared to other modifying groups and thus lowers amorphous phase thermal stability. More conformational rigid glassy phase forming bulk substituent **S3** raises thermal stability by almost 25 °C. As one can see from figure 2, rise of system flexibility caused by replacement of oxygen by carbon in chain linking chromophore with triphenylmethyl group reduces T_{SHI50} by 13 °C. The increased flexibility allows different chromophore packing of the **A3** in comparison with **A1** and **A2** and therefore red shift of the absorbance band takes place (figure 3). The highest thermal stability of NLO activity among the all investigated systems is observed in the cases of compounds **B8**, **C1** and **C2**. From structural point of view this can be explained by increased number of triphenylmethyl groups present given molecules. Obtained NLO efficiency values d_{33} for investigated molecular glasses vary significantly (see table 1). In most of the cases it is due to different NLO properties of chromophores used in particular organic glass system. For some of the chromophores (**C1**) charge transfer (CT) absorbance band coincide with second harmonic wavelength, for some others (**B1**, **B7**, **C2**) CT wavelength values are close to it. In all these cases resonance enhancement of NLO efficiency takes place. At same time certain low d_{33} values (**B2**, **B3**, **B4**) can be explained by small molecular hyperpolarizabilities and off resonance conditions for employed chromophores. However, if one compares the results for benzylidene-1,3-indandione fragment containing compounds **A1**, **A2** and **A3** the acquired values still differ remarkably. The difference by an order of magnitude for d_{33} is observed among compounds **A1** and **A3,** although in the both cases the same chromophore is used. One of explanations could be the different level of acentric order achieved in the corona poled samples. In the case of compound **A3** chromophore core and triphenyl moiety are connected by flexible C-C bridge what can attribute to easier reorientation in the poling process.

4. Summary

The nonlinear optical properties of the series of organic molecular glasses have been studied. Correlation between chemical structure of investigated compounds and obtained NLO properties was observed. It is apparent that increased molecular weight and number of triphenyl substituents in the molecule increases the thermal sustainability of NLO response. Increased flexibility of chromophore to triphenyl substituent linking chain reduces thermal stability. On the other hand such flexibility increases chromophore core mobility during corona poling what results in the improved NLO efficiency. Therefore careful optimization of structure should be done to avoid trade-off between thermal stability and NLO efficiency.

References

[1]   Dalton L R, Sullivan P A and Bale D H 2010 *Chem. Rev.* **110** 25
[2]   Choi C S, Moon I K and Kim N 2009 *Appl. Phys. Lett.* **94** 053302
[3]   Kim T D *et al* 2007 *J. Am. Chem. Soc.* **129** 488
[4]   G. Seniutinas *et al* 2012 *Dyes Pigments* **95** 33
[5]   Traskovskis K *et al* 2012 *J. Mater. Chem.* DOI: 10.1039/C2JM30861D
[6]   Traskovskis K *et al* 2012 Proc. SPIE **8434** 8434-59
[7]   Zarins E, Jubels J and Kokars V 2011 *Adv. Mater. Res.* **222** 271
[8]   Vembris A *et al* 2012 *Opt. Mater*. DOI: 10.1016/j.optmat.2012.02.051
[9]   L.Laipniece, V.Kampars 2011 *Abstracts of the 52nd International Scientific Conference of Riga Technical University. Section: Material Science and Applied Chemistry* (Riga, Latvia) p 20
[10]   Nitiss E and Rutkis M 2012 *Proc. SPIE*, **8430**, 8430-49
[11]   Rutkis MA *et al* 2006 *Proc. SPIE* **6192** 61922Q
[12]   Herman W N, Hayden L M 1995 *J. Opt. Soc. Am. B* **12** 416
[13]   Jerphagnon J and Kurtz S K 1970 *Phys. Rev. B* **1** 1739

Lauma Laipniece dzimusi 1985. gadā Liepājā. Rīgas Tehniskajā universitātē (RTU) ieguvusi dabaszinātņu bakalaura grādu (2008) un maģistra grādu ķīmijā (2010). Kopš 2005. gada strādā RTU un nodarbojas ar nelineārās optikas materiāliem paredzētu azosavienojumu un dendrimēru sintēzi un īpašību pētījumiem, kopš 2017. gada pēta arī biodīzeļdegvielas iegūšanas reakcijas un rūpniecisko atkritumu izmantošanas iespējas jaunu produktu izveidē. Patlaban ir RTU Lietišķās ķīmijas institūta pētniece. Zinātniskās intereses saistītas ar rūpniecisko atkritumu valorizāciju, izmantojot tos biodegvielas un pārtikas piedevu ražošanā.

Lauma Laipniece was born in 1985 in Liepāja. She obtained a Bachelor's degree (2008) and a Master's (2010) degree of Natural Sciences in Chemistry from Riga Technical University (RTU). Since 2005, she has been working at RTU and is engaged in the synthesis and properties of azo compounds and dendrimers intended for nonlinear optical materials. Since 2017, she has also been researching biodiesel production reactions and the use of industrial waste as raw materials. Currently, she is a researcher at RTU Institute of Applied Chemistry. Her scientific interests are related to the valorization of industrial waste into biofuels and food additives.